Understanding the C_4 dicarboxylic acid metabolism in *Clostridium autoethanogenum*

Ronja Breitkopf, MSc

Thesis submitted to the University of Nottingham for the degree of Doctor of Philosophy

Synthetic Biology Research Centre, SBRC
University of Nottingham

October 2017

For my family

Declaration

Unless otherwise acknowledged, the work presented in this thesis is my own. No part has been submitted for another degree at the University of Nottingham or any other institute of learning.

Ronja Breitkopf

October 2017

Abstract

The acetogenic bacterium *Clostridium autoethanogenum* possesses the inherent ability to produce acetate and ethanol during growth on industrial waste gases such as carbon monoxide and carbon dioxide using the Wood-Ljungdahl Pathway (WLP) for carbon fixation. With the urgent need to reduce greenhouse gas emissions and produce chemicals and fuels in a more sustainable manner, autotrophic organisms such as *C. autoethanogenum* have received considerable industrial interest over recent years.

However, the metabolic pathways present in *C. autoethanogenum* and therefore its capability to produce industrial relevant carbon building-blocks and biofuels have not yet been sufficiently examined. Therefore, the investigation of pathways leading to the production of industrially relevant carbon building blocks is seen as a worthwhile undertaking at the interface of fundamental and applied research.

In this project, the metabolism of C_4 dicarboxylic acids in *C. autoethanogenum* in conjunction with the production of succinate was investigated. This analysis revealed a previously unrecognised carbon and energy source, fumarate, and unveiled the combination of the autotrophic WLP with reactions of the branched tricarboxylic acid (TCA), Krebs "cycle" using *in vivo* NMR techniques. Under the conditions employed, the reducing equivalents gained from the oxidative breakdown of fumarate to acetate were used to partially re-assimilate the CO_2 that was liberated during that process. Accordingly, inactivation of the fumarate hydratase led to a disruption of fumarate metabolism. Additionally, through the introduction of a fumarate reductase and

its overexpression in the organism, the resulting strain was able to produce succinate in amounts of up to 3.54 g l^{-1} and yields of up to 0.78 g g^{-1} fumarate. This study therefore presents an essential basis for the possible establishment of succinate production with *C. autoethanogenum* and a better understanding of its C_4 dicarboxylic acid metabolism.

List of publications

1. C. M. Humphrey, S. McLean, S. Schatschneider, T. Millat, A. M. Henstra, F. J. Annan, R. Breitkopf, B. Pander, P. Piatek, P. Rowe, A. T. Wichlacz, C. Woods, R. Norman, J. Blom, A. Goesman, C. Hodgman, D. Barrett, N. R. Thomas, K. Winzer, N. P. Minton, "Whole genome sequence and manual annotation of *Clostridium autoethanogenum*, an industrially relevant bacterium," *BMC Genomics*, vol. 16, 2015.

Acknowledgements

> I've heard it said, that people come into our lives for a reason, bringing something we must learn and we are led to those, who help us most to grow if we let them and we help them in return. Well, I don't know if I believe that's true but I know I'm who I am today, because I knew you...
>
> Stephen Schwartz, Wicked

A lot of effort has been put into this thesis and this work would not exist without the help and support of many people in both my professional and private life. First of all I would like to thank **Prof. Nigel P. Minton** for the opportunity to work on this project. In the same way, I would like to thank **LanzaTech** and the **BBSRC** for the funding of the project. I especially want to thank my supervisor **Dr. Klaus Winzer** for his consistent support, guidance and ideas throughout the years.

I also would like to thank **Dr. Huw E.L. Williams** for not just all the NMR time he has provided, but also his abilities to teach me in basic NMR and his contagious optimism. Additionally, I would like to thank **Dr. Philippa Strong** and **Dr. David Kirk** for their support in- and outside of the lab and their proof-reading abilities, and **Rupert Norman** for his model-predictions and our “thermodynamics-conversations”.

A very special thank you goes to my co-workers and very good friends **Alexander T. Wichlacz** and **Dr. Alexander Grosse-Honebrink**, for not just their highly appreciated friendship and mental encouragement throughout, but also their many tips and support whether with NMR analyses, statistics or in general scientifically stimulating conversations.

I further would like to thank all my colleagues and friends in the **SBRC**, the **Beeston Musical Theatre Group**, my amazing friends in Germany, who are still caring about keeping in touch - especially **Katrin Gärtner** - and everyone else that accompanied me on my way and stood by my side with either knowledgeable inputs and encouragements, or sometimes needed mind distractions. I could not have done this without you and I am very fortunate to have so many good friends in my life.

The greatest thank you, however, goes to my family. Mostly to my parents **Sabine** and **Thomas Breitkopf**, my grandparents **Elisabeth and Manfred Hauff**, and **Ruth Breitkopf** and my brother **Sven Breitkopf**, who understands exactly how much support is needed during a PhD. Each and every one of you supported me both financially and morally not just throughout my PhD, but my entire life. You taught me how to carry on and never give up, and I will be forever grateful for that.

Diese Arbeit ist euch gewidmet.

Table of contents

Abstract I
List of publications III
Acknowledgements IV
List of abbreviations X
Table of figures XV
List of tables XIX
1 Introduction 1
1.1 Acetogenic bacteria – a historical review 2
1.2 Metabolism of acetogens 3
1.2.1 Wood-Ljungdahl Pathway 3
1.2.2 Energy conservation 5
1.3 Industrial use of acetogens 7
1.4 *Clostridium autoethanogenum* 8
1.5 Tools for genetic engineering of *Clostridum* spp. 10
1.6 Succinic acid 16
1.6.1 Natural succinate producers 19
1.6.2 Genetically modified succinate producers 21
1.7 GASCHEM and PhD project 28
1.7.1 The GASCHEM project 28
1.7.2 Questions and goals for this PhD project 29
2 Materials and methods 31
2.1 Materials and suppliers 31
2.2 Bacterial strains, plasmids and oligonicleotides 34
2.3 Preparation of media and strain cultivation 39
2.3.1 Cultivation of *E. coli* 39
2.3.2 Cultivation of *C. autoethanogenum* 40
2.3.3 Media supplements 45
2.4 Stock cultures 46
2.5 Physiological parameters 47
2.5.1 Measuring optical density (OD) 47
2.5.2 Microscopy 47
2.5.3 Light microscopy 47
2.5.4 TEM 47
2.6 Growth experiments 49

2.7 Molecular biology methods 50
2.7.1 Treatment of devices and solutions 50
2.7.2 Isolation of nucleic acids 51
2.7.3 Agarose gel electrophoresis 53
2.7.4 Enzymatic modification of DNA 54
2.7.5 *In vitro* amplification of DNA *via* PCR 56
2.7.6 Sequencing 60
2.7.7 Generation of deletion and insertion mutants 60
2.7.8 Complementation of ClosTron mutants 64
2.7.9 Southern Blot 65
2.8 Generation of recombinant organisms 66
2.8.1 Transformation of *E. coli* 66
2.8.2 Transformation of *C. autoethanogenum via* conjugation 69
2.9 Protein tools 70
2.9.1 Cell harvesting and disruption 70
2.9.2 Standard protein methods 72
2.9.3 Enzyme assays 77
2.10 Metabolite analyses 84
2.10.1 Gas chromatography 84
2.10.2 High-performance liquid chromatography 85
2.10.3 Gas chromatography- mass spectrometry 86
2.10.4 Liquid chromatography–mass spectrometry 87
2.10.5 Nuclear magnetic resonance 87
2.10.6 *In vivo* NMR analyses 88
3 Growth of *C. autoethanogenum* on C_4 dicarboxylic acids 90
3.1 Introduction 90
3.2 Results 92
3.2.1 Genome investigation for existing C_4 dicarboxylic acid utilisation and production pathways in *C. autoethanogenum* 92
3.2.2 Utilisation of C_4 dicarboxylic acids 95
3.2.3 *In vivo* analyses of fumarate metabolism by *C. autoethanogenum* cultures grown in an NMR tube 107
3.2.4 Activity of key enzymes in *C. autoethanogenum* cells grown on fumarate and fructose 118
3.3 Discussion 122
3.3.1 C_4 dicarboxylic acid metabolism of *C. autoethanogenum* 122

3.3.2 Fumarate metabolism of *C. autoethanogenum* 124
3.3.3 Proposed fumarate fermentation pathway 126
3.3.4 Physiological behaviour of cells grown on fumarate and fructose 129
3.3.5 Summary 132
4 Construction and characterisation of mutants defective in fumarate metabolism 133
4.1 Introduction 133
4.2 Results 136
4.2.1 Allelic Exchange and ClosTron mutagenesis of the fumarate hydratase 136
4.2.2 Generation of an acetyl-CoA synthase deletion mutant 146
4.3 Discussion 152
4.3.1 Fumarate hydratase as the key enzyme of the fumarate fermentation pathway 152
4.3.2 CRISPR/Cas9 mutagenesis of *acsA* 155
4.3.3 Summary 157
5 Introduction of a soluble fumarate reductase into *C. autoethanogenum* 158
5.1 Introduction 158
5.1.1 Fumarate reductases 158
5.1.2 Expression of optimised FRD from *Trypanosoma brucei* in *Aspergillus* 159
5.2 Results 161
5.2.1 Construction of an expression plasmid containing an optimised FRD gene 161
5.2.2 Heterologous expression in *E. coli* 164
5.2.3 Heterologous expression in *C. autoethanogenum* 167
5.3 Discussion 182
5.3.1 Difficulties in the construction of the plasmid 182
5.3.2 Succinate production by *C. autoethanogenum* 184
5.3.3 Summary 189
6 Summary and general discussion 190
6.1 Key findings of this work 190
6.1.1 C_4 dicarboxylic acid metabolism of *C. autoethanogenum* 190
6.1.2 Fumarate metabolism of *C. autoethanogenum* 191
6.1.3 Production of succinate by *C. autoethanogenum* 194
6.2 Limitations of this study and future work 196

6.2.1 Limitations and challenges 196
6.2.2 Further analyses of the fumarate metabolism 197
6.2.3 Succinate production 197
6.3 Concluding remarks 201

7 Bibliography 202

Appendix XIX
a. Plasmid maps XIX
b. Codon optimised *frd* gene and protein sequence XXI
c. Intron sequences used for ClosTron mutants XXIV
d. Additional work during this thesis XXV
i. Inhibition of the acetate kinase of *C. autoethanogenum* XXV
ii. Isolation of teichoic acid from *C. autoethanogenum* cells XXVII
iii. Crystallisation of the PduL protein of *Moorella thermoacetica* XXVIII

List of abbreviations

µ	Micro; specific growth rate
A	Ampere, Adenine, Absorption, Alanine
A.	Aqua
AA	Amino acid(s)
ABE	Alcohol-Butanol-Ethanol
ACE	Allelic Coupled Exchange
ACK	Acetate kinase
ACS	Acetyl-CoA-Synthase
AcsA	CODH subunit of bi-functional CODH/ACS complex
ad	Top up to
ADH	Alcohol dehydrogenase
ADP	Adenosine-5-diphosphate
ALD	Acetolactate decarboxylase
ALDH	Aldehyde dehydrogenase
ALS	Acetolactate synthase
Amp	Ampicillin
AOR	Aldeyhde:ferredoxin oxidoreductase
AP	Alkaline phosphatase
APS	Ammoniumpersulfate
asRNA	Antisense RNA
ATCC	American Type Culture Collection
ATP	Adenosin-5-triphosphate
bla	*Beta*-Lactamase-Gen
Bp	Base pairs
BSA	Bovine serum albumin
c	Centi, concentration
C	Carbon
C-	Carboxy-
C.	*Clostridium*
°C	Degree Celsius
catP	Chloramphenicol acetyltransferase gene
CFE	Cell free extract
Cm	Chloramphenicol
CoA	Coenzyme A
CODH	Carbon monoxide dehydrogenase

CoFeSP	Corrinoid iro-sulfur protein
CRISPR	Clustered Regularly Interspaced Short Palindromic Repeat
CS	Citrate synthase
d	Layer thickness of cuvette, Deoxy-, day(s)
D	Aspartic acid
Da	Dalton
DMSO	Dimethylsulfoxide
DNA	Deoxyribonucleic acid
DNase	Deoxyribonuclease
dNTP	Deoxyribonucleoside-5-triphosphate
DSMZ	Deutsche Sammlung von Mikroorganismen und Zellkulturen
DSS	4,4-dimethyl-4-silapentane-1-sulfonic acid
DTE	Dithioerytrol
DTT	Dithiothreitol
E.	*Escherichia*
E	Glutamic acid
EDTA	Ethylenediaminetetraacetic acid
Ery	Erythromycin
et al.	*Et alteri* (and others)
F	Farad, phenylalanine
FAD	Flavinadenindinucleotide
Fd	Ferredoxine
FRD/FMR	Fumarate reductase
FH	Fumarate hydratase
FOA	5-Fluoroorotic acid
Fw	Forward
g	Gram
g	Gravitational acceleration
G	Guanine, Glycine
gDNA	Genomic DNA
h	Hour(s)
H^+	Proton
H/ His	Histidine
HMDB	Human metabolome database
$HO^{\cdot}$	Hydroxyl radical
HPLC	High-performance liquid chromatography
HSQC	Heteronuclear Single Quantum Coherence
I	Isoleucine

ICL	Isocitrate lyase
K	Lysine
k	Kilo
kb	Kilo base pair
kDa	Kilo Dalton
KEGG	Kyoto Encyclopaedia of Genes and Genomes
KO	Knockout
kPa	Kilo Pascal
kV	Kilo Volt
l	Litre, length
L	Leucine
LB	Luria-Bertani
LHA	Left homology arm
M	Molar (1 Molar = 1 mol/l), methionine
M.	*Moorella*
m	Milli
MCS	Multi cloning side
MDH	Malate dehydrogenase
MES	2-(*N*-morpholino)ethane sulphonic acid
min	Minute
ml	Millilitre
mod.	Modified
mRNA	Messenger RNA
MS	Malate synthase
MV	Methylviologen (1,1'-dimethyl-4,4'-bipyridiniumdichloride)
MW	Molecular weight
n	Nano
N	Nitrogen, normal
Na	Sodium
$NAD(P)^+$	Nicotinamidadenindinucleotide-(phosphate), oxidised form
NAD(P)H	Nicotinamidadenindinucleotide-(phosphate), reduced form
NMR	Nuclear magnetic resonance
OD	Optical density
Ω	Ohm
OH^-	Hydroxide
ORF	Open reading frame
ox	Oxidised
P	Proline

ppm	Parts per million
PAGE	Polyacrylamidgelelectrophoresis
PBS	Phosphate-buffered saline
PCR	Polymerase chain reaction
PduL	Propandiol utilization like protein
PEP	Phosphoenolpyruvate
PEPC	PEP carboxykinase
pers.	Personal (information)
PFL	Pyruvate formate lyase
PFOR	Pyruvate ferredoxine oxidoreductase
pH	Negative logarithm of the activity of hydrogen ions in an aqueous solution
pKa	Negative logarithm of the acid association constant
PTA	Phosphotransacetylase
PyrE	Orotate phosphoribosyl transferase
PYC	Pyruvate carboxylase
RBS	Ribosome binding side
RHA	Right homology arm
RNA	Ribonucleic acid
RNase	Ribonuclease
Rnf	Rhodobacter nitrogen fixation
rpm	Revolutions per minute
SDS	Sodium dodecyl sulfate
s, sec	Seconds
SNP	Single nucleotide polymorphism
SNV	Single nucleotide variation
SOE-PCR	Splicing by overlap extension polymerase chain reaction
TAE	Tris base-acetic EDTA
t_d	Doubling time
Tet	Tetracycline
TE	Tris-EDTA
TEM	Transmission Electron Microscopy
TEMED	N,N,N,N-Tetramethylethylendiamine
term.	Terminal
THF	Tetrahydrofolate
thl	Thiolase gene
Tm	Melting temperature, thiamphenicol
tRNA	Transfer RNA

UV	Ultraviolet
v/v	Volume per volume
w/v	Weight per volume
WLP	Wood-Ljungdahl Pathway
WT	Wild type

Table of figures

Figure 1.1: Wood-Ljungdahl Pathway. 4

Figure 1.2: Electron bifurcation. 6

Figure 1.3: *Clostridium autoethanogenum* visualised using transmission electron microscopy (TEM). 9

Figure 1.4: ClosTron mutagenesis. 11

Figure 1.5: Allelic exchange mutagenesis. 13

Figure 1.6: CRISPR mutagenesis. 15

Figure 1.7: Applications and products derived from succinate. 17

Figure 1.8: Succinate as C_4 building block. 18

Figure 1.9: Chemically production of succinic acid through maleic anhydride. 18

Figure 1.10: Succinate production pathways. 19

Figure 1.11: Metabolic engineering strategies to improve succinate production. 24

Figure 2.1: Principle of SOE-PCR. 59

Figure 2.2: Fumarate hydratase enzyme assay. 78

Figure 2.3: Reactions involved in the acetate kinase assay (physiological direction). 82

Figure 2.4: Reactions involved in the acetate kinase assay (non-physiologicaldirection) 83

Figure 3.1: Proposed pathway of a branch of the TCA cycle in *C. autoethanogenum*. 93

Figure 3.2: Putative route of succinate production by *C. autoethanogenum via* the reductive TCA pathway. 94

Figure 3.3: Fumarate feeding improves growth of *C. autoethanogenum*. 96

Figure 3.4: Growth of *C. autoethanogenum* on 15 mM 2,3-$^{13}C_2$-labelled fumarate and fructose. 97

Figure 3.5: Succinate concentration in culture supernatants following growth of *C. autoethanogenum* on fructose and fructose plus fumarate. 98

Figure 3.6: Analyses of succinate concentrations in different culture media. 98

Figure 3.7: ^{13}C NMR Carbon profile of unknown labelled compounds in supernatants of *C. autoethanogenum* cultures grown on fructose and 2,3-$^{13}C_2$ fumarate. 99

Figure 3.8: Thio-Michael Addition leading to the generation of succinyl-cysteine. 100

Figure 3.9: Growth of *C. autoethanogenum* on various carbon sources. 102

Figure 3.10: Optical density, pH, concentration of CO_2, gas pressure in the headspace, acetate and ethanol production of *C autoethanogenum* cultures during growth on fumarate and fructose, respectively. 104

Figure 3.11: NMR tube with *C. autoethanogenum* culture (A) and Bruker AV(III) 800 MHz spectrometer (B). 108

Figure 3.12: Plot of NMR spectra of *C. autoethanogenum* cultures using 2,3-$^{13}C_2$-labelled fumarate as carbon source taken over time. 109

Figure 3.13: Staggered plot of 2,3-$^{13}C_2$-labelled fumarate NMR peak over time. 110

Figure 3.14: Staggered plot of acetate and ethanol NMR peaks over time during growth on 2,3-$^{13}C_2$-labelled fumarate. 111

Figure 3.15: Alanine and ethanol NMR peaks with highlighted ^{13}C shouldering peaks. 111

Figure 3.16: Metabolite profile of a *C. autoethanogenum* culture grown on 2,3-$^{13}C_2$-labelled fumarate within an NMR tube. 113

Figure 3.17: Plot of NMR spectra of *C. autoethanogenum* cultures using $^{13}C_4$-labelled fumarate as carbon source taken over time. 115

Figure 3.18: Staggered plot of $^{13}C_4$-labelled fumarate and acetate NMR peaks over time. 115

Figure 3.19: Alanine (A) and ethanol (B) NMR peaks with highlighted ^{13}C shouldering peaks. 116

Figure 3.20: Metabolite profile of a *C. autoethanogenum* culture grown on $^{13}C_4$-labelled fumarate within an NMR tube. 117

Figure 3.21: Overview of analysed enzyme activities. 119

Figure 3.22: Proposed fumarate fermentation pathway of *C. autoethanogenum*. 128

Figure 4.1: PCR screening of putative ClosTron FH mutants. 138

Figure 4.2: Southern blot analysis of ClosTron FH mutants. 139

Figure 4.3: Growth of FH ClosTron mutants and WT on fructose (A), fumarate (B) and malate (C). 141

Figure 4.4: Growth of WT and ClosTron mutants on PETC-MES agar plates containing different carbon sources. 142

Figure 4.5: Growth of the FH_2_24 ClosTron mutant, complemented mutant and plasmid control 144

Figure 4.6: Growth of the FH ClosTron mutant, WT, complemented mutant and plasmid control on PETC-MES agar plates with 40 mM fructose (A) and fumarate (B). 145

Figure 4.7: PCR screening of putative acsA CRISPR/Cas9 mutants. 148

Figure 4.8: Growth of WT and acsA CRISPR mutants on fructose (A) and CO (B). 149

Figure 4.9: PCR reactions carried out to verify CRISPR mutagenesis of acsA. 151

Figure 4.10: CRISPR analyses. 151

Figure 4.11: Proposed pathway of fumarate fermentation in *C. autoethanogenum*. 155

Figure 5.1: Combined FRD fragment after PCR using ligation mix as template. 162

Figure 5.2: Control digest of putative pMTL8312_FRD clones. 163

Figure 5.3: SDS PAGE gel (A) and Western Blot (B) after attempted purification of *T. brucei* FRD produced in *E. coli*. 165

Figure 5.4: Anaerobic growth of E. coli DH5α, JW4114-1 and JW4114-1 pMTL8312_FRD on MM agar. 167

Figure 5.5: SDS PAGE gel (A) and Western Blot (B) after attempted purification of *T. brucei* FRD produced in *C. autoethanogenum*. 169

Figure 5.6: Growth and pH of *C. autoethanogenum* FRD strains, WT and plasmid control grown in PETC-MES on fructose. 171

Figure 5.7: Fructose consumption of *C. autoethanogenum* FRD strains, WT and plasmid control grown in PETC-MES medium. 171

Figure 5.8: Acetate (A) and ethanol (B) production of FRD strains, WT and plasmid control grown in PETC-MES on fructose 172

Figure 5.9: Succinate (A) and lactate (B) production of FRD strains, WT and plasmid control grown in PETC-MES on frcutose 173

Figure 5.10: Growth of FRD strains and WT grown in PETC-MES on fumarate (A) and fumarate + H_2 (B). 175

Figure 5.11: Acetate and ethanol production of FRD strains and WT in PETC-MES medium on fumarate (A) and fumarate + H_2 (B) 175

Figure 5.12: Succinate production of *C. autoethanogenum* FRD strains during growth on fumarate (A) and fumarate plus hydrogen (B). 177

Figure 5.13: Growth of WT and FRD strains on CO. 178

Figure 5.14: Acetate, ethanol (A) and succinate (B) production profile of WT and FRD strains in PETC-MES medium on CO..... 179

Figure 5.15: Growth (A) and product spectrum (B) of WT and FRD strains grown in PETC-MES on CO plus H_2. 181

Figure 5.16: Proposed scheme of energy conservation during the production of succinate from fumarate and hydrogen by *C. autoethanogenum* FRD1. 186

Figure 6.1: Proposed mechanism of electron bifurcation for a hypothetical ETF/FRD complex..... 200

Figure A.1: Plasmid map pMTL8315_FH..... XIX

Figure A.2: Plasmid map for pSBRCas9_ClauAscA XX

Figure A.3: pMTL8312_FRD.....XX

Figure A.4: Plasmid map of pTAck. XXVI

Figure A.5: Crystal structure of PduL2. XXX

List of tables

Table 2.1: Materials used during this study. 31

Table 2.2: Bacterial strains used in this study 34

Table 2.3: Plasmids used in this study 36

Table 2.4: Oligonucleotides used in this study 37

Table 2.5: Additional carbon sources 45

Table 2.6: Antibiotics 46

Table 2.7: Restriction enzymes 54

Table 2.8: Dilution scheme for GC standards 84

Table 3.1: Growth characteristics and products of 107

Table 3.2 Summary of enzyme activities 119

Table 4.1: Fumarate hydratase activities of FH ClosTron mutants and WT 140

Table 4.2: FH activities before and after complementation 146

Table A.1: Intron sequences used for ClosTron mutants XXIV

Table A.2: Mutated enzymes with one altered amino acid residue. XXX

Table A.3: PTA enzyme activities of mutated enzymes. XXX

1 Introduction

Ob mir durch Geistes Kraft und Mund
Nicht manch Geheimnis würde kund; Dass ich nicht
mehr mit sauerm Schweiß
Zu sagen brauche, was ich nicht weiß;
Dass ich erkenne, was die Welt
Im Innersten zusammenhält,
Schau' alle Wirkenskraft und Samen,
Und tu' nicht mehr in Worten kramen.

Johann Wolfgang von Goethe, Faust

The EIA (U.S. Energy Information Administration) projects world energy consumption will grow by 48 % by 2040 [1][2]. However, fossil raw materials, such as coal, gas and oil, are limited and the remaining oil resources are estimated to be around 700 gigatons [3][4]. Thus, if consumption remains at the same level as today, they will be running out within the forthcoming century [5][6]. Furthermore, the use of these fossil fuels leads to worldwide environmental problems in the form of global warming as a consequence of increasing concentration of carbon dioxide (CO_2) and other greenhouse gases in the atmosphere [7]. Thus, the need to access new carbon neutral resources for the future is high.

There are many microorganisms able to 'fix' inorganic CO_2 from waste, exhaust or syngas and their exploration has attracted a lot of interest lately, especially by biotech industries such as LanzaTech [8]. Specifically, anaerobic, autotrophic acetogenic bacteria, which can produce industrially relevant compounds from carbon monoxide (CO) and CO_2, present in exhaust fumes, received increased attention in recent years. The carbon fixation pathway that enables these organisms to grow under such conditions is called Wood-Ljungdahl or reductive acetyl-CoA pathway [9]. Industrially relevant products

currently focussed on especially, are ethanol and 2,3-butanediol (2,3-BD) due to their roles as biofuel and high-value chemical, respectively [10][11]. The production of so-called building-blocks for industrially interesting chemicals is being pursued with considerable determination. A list of the top value platform chemicals from biomass production published in 2015 included pyruvic acid, lactic acid, 3-hydroxypropionic acid, succinic acid and itaconic acid [12].

1.1 Acetogenic bacteria – a historical review

A total of six different pathways for autotrophic carbon fixation have been described in bacteria [13]. The Wood-Ljungdahl or reductive acetyl-CoA pathway is considered to be the most energy efficient [14] and is used by acetogenic bacteria (acetogens) to convert CO_2 or CO to acetyl-CoA. This can either be used to produce acetate and ethanol, or as a starting substrate for anabolic reactions required for growth [9][15]. The global importance of acetogens is well covered in Harold Drake's review 'Old acetogens, new light' [16]. In this it is stated that the acetyl-CoA pathway can be found in various organisms amongst bacteria and archea and therefore may have been the first autotrophic process on earth and important to the evolution of life [16][17].

The first acetogenic organism was discovered by Wieringa in 1936 and called *Clostridium aceticum* [18]. However, this bacterium was lost and only re-isolated in the early 1980s by Adamse (1980; [19]) and Braun (1981; [20]). Hence, *Clostridium thermoaceticum,* isolated by Fontaine in 1942 [21] and reclassified by Collins *et al.* in 1994 to *Moorella thermoacetica* [22], became the most important organism to solve the reactions taking place in the reductive acetyl-CoA pathway. This organism was able to convert one molecule of

glucose almost completely into three molecules of acetate as end product [21]. This new type of fermentation was therefore called 'homoacetogenesis' in analogy to homofermentative lactate fermentation [18]. However, this term disappeared over time and now those organisms are referred to as 'acetogens' rather than 'homoacetogens' [16].

1.2 Metabolism of acetogens

1.2.1 Wood-Ljungdahl Pathway

M. thermoacetica was used to resolve the biochemical reactions of the Wood-Ljungdahl Pathway (WLP; Figure 1.1) whereby CO and/or CO_2 feed both branches of the pathway, the methyl (eastern) branch and carbonyl (western) branch [23]. In the methyl branch, CO or CO_2 is reduced to a methyl group in a sequence of tetrahydrofolate (THF) and cobalamin-dependent reactions. This methyl group is combined with CO (either directly or after enzymatic reduction of CO_2) from the carbonyl branch to generate acetyl-CoA. This multifaceted reaction is catalysed by the carbon monoxide dehydrogenase/acetyl-CoA synthase (CODH/ACS) complex.

After more than half a century of research, the main pathway is reasonably well understood [24], although there are still new, contributing enzymes being found in these organisms. For example, a new type of phosphotransacetylases (PTA^{III}), PduL, experimentally proven to catalyse the reaction from acetyl-CoA to acetyl phosphate in *M. thermoacetica* was described as recently as 2016 [25].

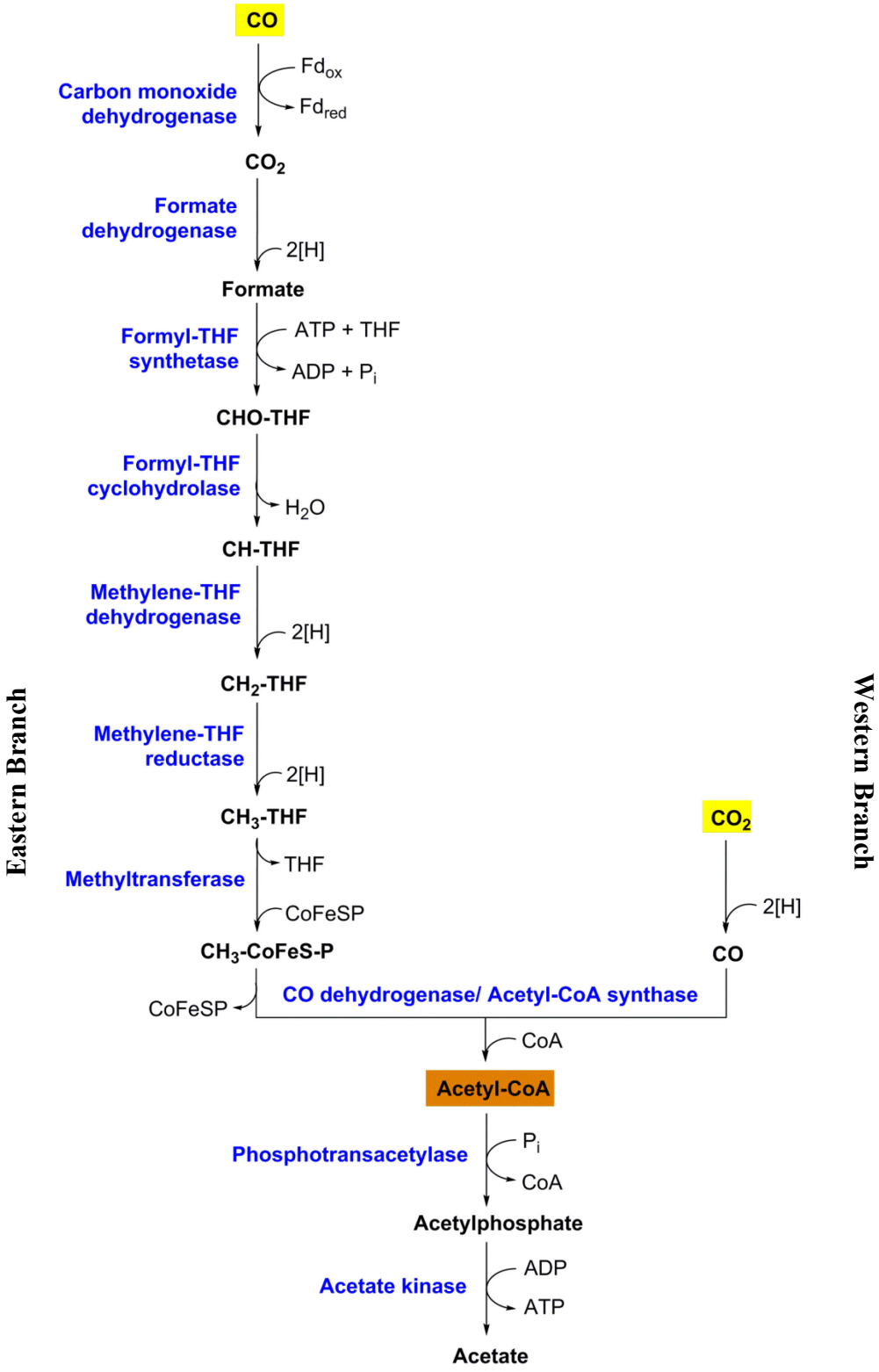


Figure 1.1: Wood-Ljungdahl Pathway.

Illustrated are the Eastern (Methyl) and Western (Carbonyl) branch, including all enzymes and cofactors required of the WLP. CoFeSP: corrinoid ironsulfur protein; THF: tetrahydrofolate. Modified after Müller *et al.* 2003 **[23]**.

1.2.2 Energy conservation

The conservation of energy in acetogens has been of considerable interest for many years. In 2003, Müller published a review in which different ways of energy conservations are described [23]. During the growth of those organisms on sugars like hexoses, the pathway of their consumption starts with the oxidation of the sugar *via* the Embden-Meyerhof-Parnas pathway to pyruvate. The pyruvate produced is then oxidised by pyruvate:ferredoxin oxidoreductase (PFOR) to acetyl-CoA which is subsequently converted to acetate *via* acetyl phosphate. The oxidative branch of the pathway is coupled to the synthesis of four molecules of ATP by substrate-level phosphorylation (SLP) [23]. The reducing equivalents produced during this first part of the reaction sequence are then used to reduce the two molecules of CO_2 liberated in the PFOR reaction to another molecule of acetate *via* the WLP. This demonstrates that during the growth on sugar the CO_2 can be regarded as an electron sink, which means that, in principle, there is no need for the WLP to be coupled with energy conservation [23].

However, this is different with respect to the autotrophic growth on CO_2 and H_2 or CO. Here, one molecule of ATP is produced by the acetate kinase reaction (production of acetate), but one molecule of ATP is also needed during the reduction of CO_2 in the eastern branch of the WLP for the formation of formyl-THF (see Figure 1.1). Therefore, under these conditions, the WLP must be coupled with energy conservation, which was found to be in form of an ion gradient-driven (F_1F_0-ATP synthase dependent) ADP phosphorylation [18][26]. Recent research has experimentally proven the existence of two main ways of energy conservation. One is sodium ion (Na^+) dependent (for example in *Acetobacterium woodii*) and another one is proton (H^+) dependent (for

example in *M. thermoacetica*) [27][28]. The proton dependent group contains cytochromes and a membrane-bound H^+ motive electron transport chain [23][26]. Before 2008 two ways of energy conservation had been identified: SLP and electron transport-linked phosphorylation were known as the two fundamental biological energy conservation mechanisms. However, in 2008 a new mechanism was found in *C. kluyveri*: electron bifurcation [29]. In 2012 this new way of energy conservation was also found in the acetogenic model organism *M. thermoactica* [30]. This was later proven as well for various other acetogens [31][32][33]. The mechanism of electron bifurcation simultaneously couples exergonic and endergonic oxidation-reduction processes to minimise the loss of energy [34]. Figure 1.2 explains schematically how electrons of one donor can be split to two acceptors; one of them having a lower energy potential than the donor, the other a higher one.

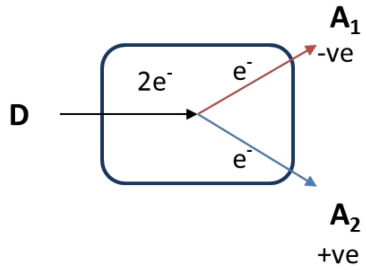


Figure 1.2: Electron bifurcation.

The scheme illustrates the principle of electron bifurcation during an electron transfer: a two-electron donor (D) of an intermediate reduction potential simultaneously provides electrons to acceptors (A) with a more positive (+ve) and more negative (-ve) potential. Modified after [34].

Since this mechanism has only recently been investigated in more detail, relatively little is known about the enzymes involved. Section 1.4 describes energy conservation of an acetogen during autotrophic growth in more detail.

1.3 Industrial use of acetogens

Many projects have been initiated with the aim of using acetogens and the WLP to convert exhaust fumes into industrially relevant products, such as ethanol, butanol and butanediol. For example in 1994 a new acetogenic organism was isolated, *Clostridium autoethanogenum*, which converted CO to ethanol, acetate and CO_2 using the WLP [35]. A very close relative of *C. autoethanogenum* is *C. ljungdahlii* which was isolated in 1993 [36]. In 2010, experiments with this organism showed that it was able to ferment CO_2/H_2 and synthetic gas (CO/H_2), also called syngas, besides sugars and other organic compounds [37]. This metabolism led to the production of ethanol, acetate, CO_2 and, after metabolic engineering, also small amounts of butanol and butyrate [37].

Just one year later Köpke *et al.* were able to produce 2,3-BD using industrial waste gas with the acetogenic organisms *C. autoethanogenum, C. ljungdahlii* and *C. ragsdalei* [11]. This study was aimed to gain insights into the genetic control of the carbon flow in these organisms. Thereby the potential to use these bacteria as a basis for the production of a broader spectrum of fuel or chemical products was investigated alongside [11]. Metabolic end products of acetate and ethanol were obtained using CO and steel-mill waste gas as a sole energy and carbon source. However, the study also revealed the synthesis of small amounts of 2,3-BD and traces of lactate during the stationary growth phase for all species.

These examples show that acetogenic bacteria may play a future role in the sustainable production of chemicals and fuels, as fossil resources are finite, and the need for alternatives and industrial bulk substrates is obvious. That is why several current Research Council UK and EU funded projects, like the

GASCHEM project (2013-2017) [38] (section 1.7.1), or SuPER-W as part of the EU-funded programme Horizon 2020 [39] (https://www.superw.ugent.be/ ; last accessed October 2017), focus on these organisms in an attempt to address environmental problems in a biotechnological way.

1.4 *Clostridium autoethanogenum*

C. autoethanogenum (Figure 1.3) was isolated by Abrini *et al.* in 1994 [35] and was described as strictly anaerobic, Gram-positive, spore-forming, rod-like, motile bacterium, which was enriched from rabbit faeces [35]. It is able to grow on CO and has ethanol and acetate as the main metabolic end products. This characteristic was unique at the time of its discovery and therefore this bacterium gained of lot of interest, especially with respect to chemical industry. In 2013 the partial genome sequence of this bacterium was published [40] and completed in 2014 [41]. However, after the whole genome sequencing of generated *pyrE* knockout strains by the GASCHEM group of the University of Nottingham (4.2.1.1), miss-callings of various genes were found caused by 250 insertions (consistent throughout the sequenced strains). Due to this, Humphreys *et al.* re-annotated the genome sequence of *C. autoethanogenum* in 2015 [42]. The differences in the genome sequence led to the discontinuing of various gene annotations, and the annotation of newly found genes.

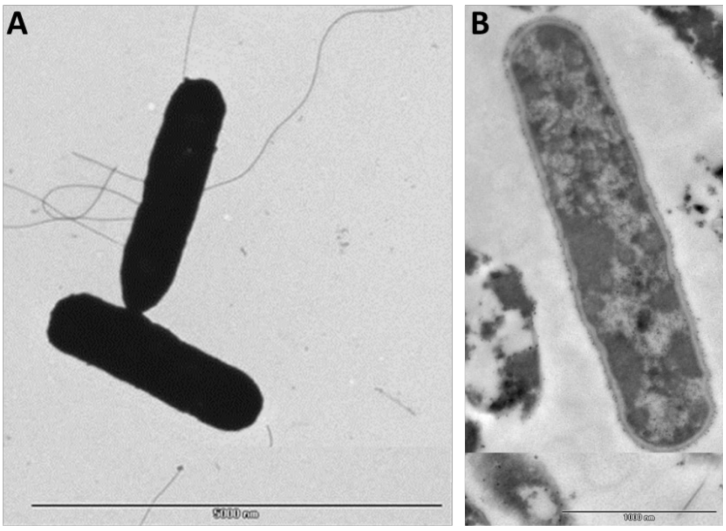


Figure 1.3: *Clostridium autoethanogenum* visualised using transmission electron microscopy (TEM).

TEM picture of *C. autoethanogenum.* A: negative staining, x 6,000 magnification. B: ultra-thin sectioning using resin to fix cells x 16,500 magnification. Breitkopf *et al.* (section 2.5.4).

As previously mentioned, the energy conservation of acetogenic bacteria is either Na^+- or H^+- dependent (section 1.2.2).

The energy conservation of *C. autoethanogenum* is H^+ dependent, but unlike in *M. thermoacetica*, it does not involve cytochromes. Instead, *C. autoethanogenum* uses a membrane-associated multi-subunit complex, the reduced ferredoxin:NAD^+ oxidoreductase (Rnf) to generate a proton gradient across the cell membrane. This mechanism also includes electron bifurcation for the generation of reduced ferreodoxin, which is described in section 1.2.2 [31][32]. In 2014 it was demonstrated that the energy conservation in acetogens when grown autotrophically, is close to "the thermodynamic limit of life" [43]. In 2015 the various metabolic variations and their coupled energy mechanisms when growing *C. autoethanogenum* at pH 5.3 on H_2 and CO_2 were described. It was stated that the highest ATP formation would occur when the generated acetic acid is reduced to ethanol *via* acetaldehyde by ferredoxin

dependent aldehyde oxidoreductase (AOR) and including the actions of Rnf and Nfn complexes [32].

1.5 Tools for genetic engineering of *Clostridum* spp.

The genus *Clostridium* includes not just several significant human pathogens like *C. difficile, C. botulinum,* and *C. tetani*, but also many species of biotechnologically important solvent-producers, such as *C. acetobutylicum*, and acetogens, like *C. autoethanogenum*.

Due to the importance and impact of these bacteria, tools for genetic engineering are needed to help investigating and changing their metabolic pathways. Minton *et al*. therefore proposed a roadmap in 2016 which provided a general framework for scientists when researching the modification of a new bacterium for biotechnological applications [44]. First the genome is to be sequenced to allow identification of restriction-modification systems against which plasmids can be protected by methylation. After this, a transformation system by either conjugation from an *E. coli* host, or electroporation can be implemented. Once a transformation system is in place, genetic tools can be developed to investigate gene functions.

One of those tools is the ClosTron system. The ClosTron system (Figure 1.4) developed by Heap *et al.* [45] is based on a group II Intron system, which is a rapid way of disrupting genes in bacteria and was developed several times independently in different *Clostridium* species [45]–[48].

As shown in Figure 1.4, the principle of the ClosTron system relies on the disruption of a target gene. A retrotransposition-activated marker (RAM), based on the *ermB* gene is used as selection marker. Thus, a successful

insertion can be selected for by screening for erythromycin resistance of the colonies. The re-targeted region is designed using an online re-targeting algorithm (www.clostron.com; last accessed October 2017).

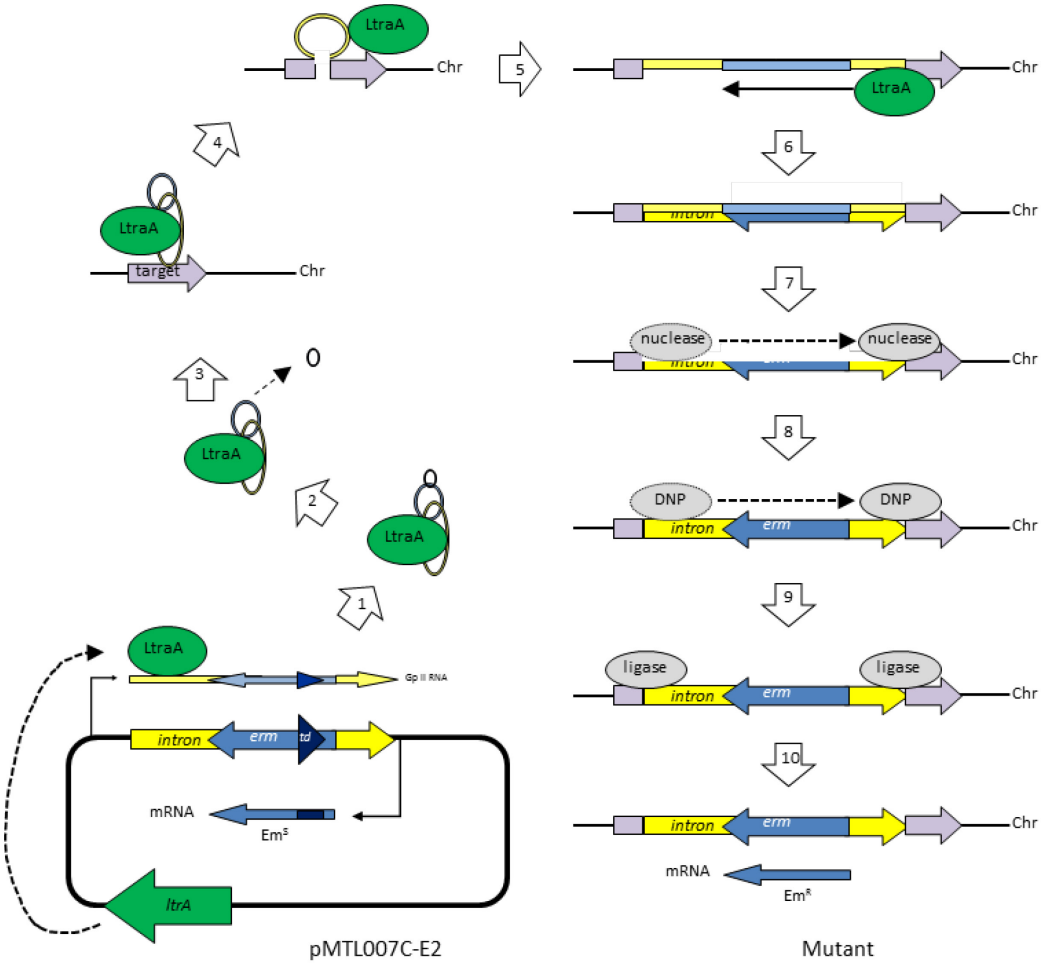


Figure 1.4: ClosTron mutagenesis.

Steps involved in the generation of ClosTron insertional mutants using the plasmid pMTL007C-E2 are shown. The *erm* marker (blue) on the group II intron (yellow) functions as a selection marker using antibiotics erythromycin or clarithromycin. The fragment within the *erm* marker is a small fragment of DNA containing the self-splicing phage td gene, a group I intron (dark blue), which is incorporated for inactivation purposes. However, this fragment is spliced out (self-catalysed) under the correct orientation during association with the LtrA protein to form a ribonuclear protein (RNP) complex (2). Following RNP recognition and binding to the target gene within the chromosome (3), the LtrA protein (green) cuts the DNA target (4), inserts the RNA and synthesises the complementary DNA strand *via* its reverse transcriptase activity with the help of a DNA polymerase (DNP) (5-8). Finally, the host ligases seal the gap which leads to a functional expression of the *erm* gene and antibiotic resistance (9-10). The figure was modified after Kuehne and Minton [49].

Although the ClosTron system seems to be suited for rapid gene disruptions, it has some disadvantages. Off-target and/or multiple insertions were observed, which makes Southern Blot analysis a necessity, in order to verify potential phenotypes were caused by the desired gene disruption and not by other insertions of the intron. Additionally, the ClosTron mediated gene disruption does not guarantee a complete gene inactivation depending on the insertion site within the gene [50]. The disruption of the gene might also have unforeseen polar effects [49] or can be reversed if the *ltrA* gene stays active in the host as reported in *L. lactis*, which is due to excision of the intron from the mRNA of the target gene [51].

Due to shortcomings with ClosTron, other mutagenesis techniques were employed to inactivate genes. One of those, called Allelic Exchange, allows for the removal of target DNA regions, replacing of genes, or knock-in of genes, while keeping gene reading frames intact [52]. This means that the technique should not interfere with neighbouring open reading frames (ORFs) and therefore not cause polar effects. Figure 1.5 shows the principle of this procedure using the example of an in-frame deletion. This is a method based on observed natural homologous recombination of two strands of DNA that show a certain degree of sequence similarity.

Several systems for counter selection have been developed, with the most common one making use of the orotate phosphoribosyltransferase (PyrE), which is involved in the *de novo* pyrimidine synthesis [53]. Given a fluorinated substrate, it generates fluorouracil which is then incorporated into RNA and DNA. As this is lethal for the cells, it can be used for counter selection purposes. Cells lacking the *pyrE* gene are uracil auxotrophs.

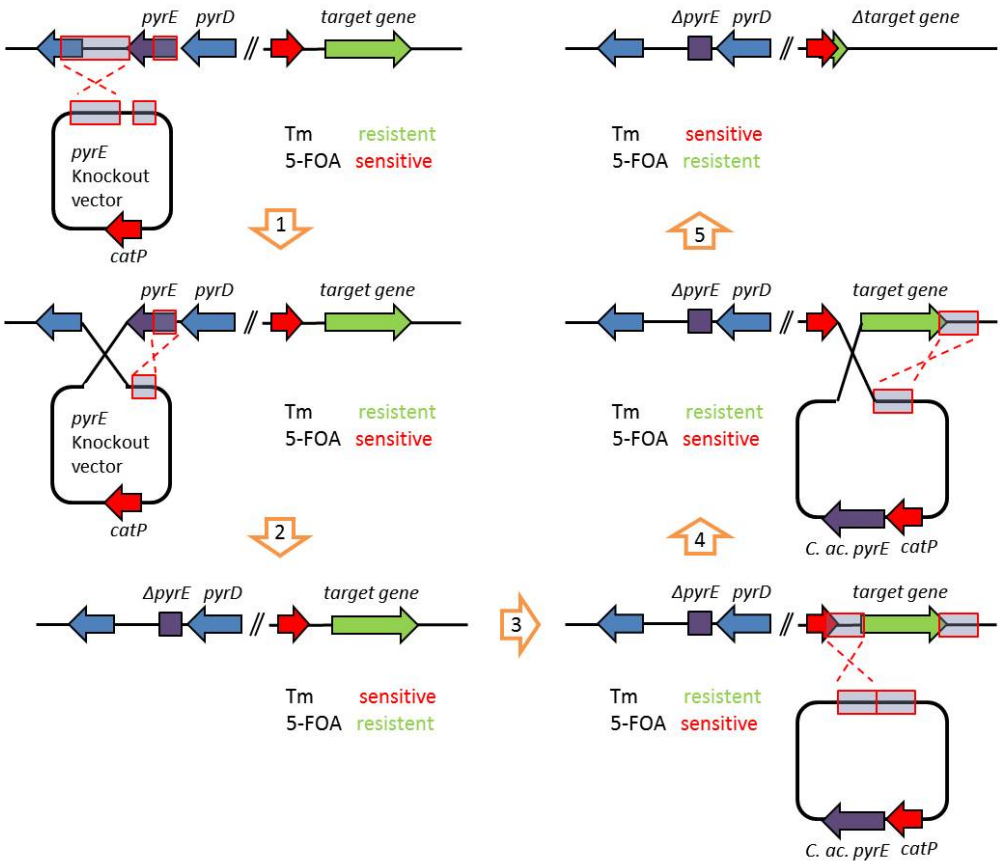


Figure 1.5: Allelic exchange mutagenesis.

Steps involved in the generation of an in-frame knockout mutant. (1) Single-crossover event of the *pyrE* knockout vector, incorporating the plasmid into the genome. (2) Double-crossover event causing the knock-out of the *pyrE* gene, giving 5-FOA resistance, screening for thiamphenicol (Tm) sensitivity confirming plasmid loss. (3) Transformation of the ACE knockout plasmid with for the target gene specific homology arms, introducing Tm resistance and 5-FOA sensitivity. (4): Single-crossover event, incorporating the plasmid into the genome (screen for fast growing colonies in the presence of Tm). (5) Double-crossover event causing the knockout of the target gene, and plasmid loss causing Tm sensitivity and 5-FOA resistance. Figure generated based on [52].

As convenient and clean as in-frame deletions are, they involve many time consuming and sometimes error prone steps. Not all colonies have had a single-crossover event, and sometimes the double-crossover event does not occur. Also, in order to obtain a clean knock-out mutant, the *pyrE* gene has to be repaired, which takes additional time and introduces more chances of errors.

A more recent method, clustered regularly interspaced short palindromic repeat (CRISPR) mediated genome editing, avoids some of the problems associated with Allelic Exchange. CRISPRs work with the CRISPR associated (Cas) proteins in bacterial adaptive immune systems [54]. The CRISPR system allows highly specific cleavage of DNA allowing targeting generation of mutants [55]. For *C. autoethanogenum*, a CRISPR/Cas9-based genome editing system was developed by Peter Rowe (University of Nottingham, unpublished) The principle of CRISPR is briefly described in Figure 1.6.

A further genetic tool for *Clostridia* is based on transposable elements (TE), also called transposons. These are sequences of DNA that move from one location of the genome to another, thereby often effecting gene functionalities. Transposons have been successfully used in *Clostridium* sp. A recent example includes derivatives of the mariner system [56] with a version recently being established for *C. autoethanogenum* (Craig Woods, University of Nottingham, unpublished). That is why transposons are great tools to identify and study genes that are important for an organism's phenotype.

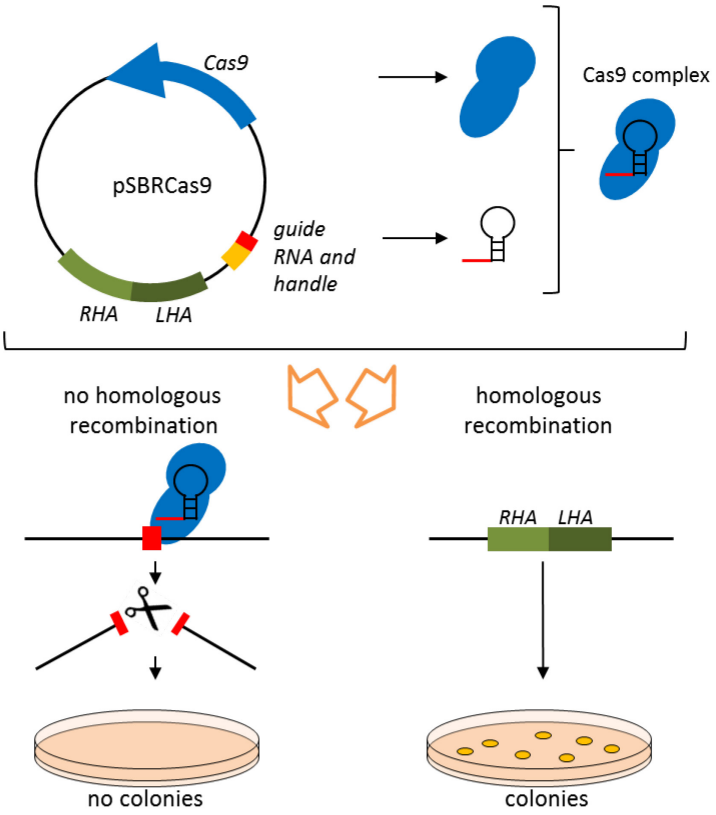


Figure 1.6: CRISPR mutagenesis.

Steps involved in the CRISPR mutagenesis in *C. autoethanogenum*. The pSBRCas9 plasmid contains the Cas9 gene, left and right homology arms for the target gene, target gene specific guide RNA (generated using Benchling® tools) and the RNA handle. The translated Cas9 and the guide RNA with the handle form the active Cas9 complex. The complex recognises the target gene and cuts the DNA. If no homologous recombination occurs, the DNA remains cut, no viable daughter cells can be generated and, thus, no colonies are able to grow. In case of a homologous recombination event, the homology arms repaired the break in the DNA, which allows colonies to grow.

1.6 Succinic acid

In 2004 succinic acid was highlighted by the US Department of Energy as one of 12 top value platform chemicals with special biotechnological manufacturing potential [57]. The anion of succinic acid that is formed in aqueous solution is succinate. From here on, the compound is referred to using that term as it is present in this form in the studied systems of this work. Succinate represents an important substrate, both in food and technical industries. In the European Union (EU) succinate is approved as a food additive (number *E 363*) functioning as a flavour enhancer for desserts, dry soups, in powders for drinks, and as an acidity regulator [57][58].

Even more important is the use of succinate in the industrial sector. Traditionally it is mainly produced by chemical processes from *n*-butane/butadiene *via* maleic anhydride in quantities of about 15,000 tons per year with a price range of about 6-9 USD per kg (effective 2008) [5]. In 2010 the succinate market was about 20,000 – 30,000 tons per year [60]. In 2017 it has been estimated that the global succinate market would steadily grow at a compound annual growth rate (CAGR) of around 27.4 % to reach 1.8 billion US dollars (USD) (768 megatons at 2.3 USD per kg) in 2025 [61].

Figure 1.7 shows an overview of applications and products derived from succinate.



Figure 1.7: Applications and products derived from succinate.

Figure modified after **[60]**.

As shown in Figure 1.7, succinate can be used as a basis for both commodity and speciality chemicals. It is used for the manufacturing of synthetic dyes and varnishes, and some esterified succinates are even used as solvents, plasticizer, and in the perfume industry [5][62]. Furthermore, succinate is utilised for the creation of biodegradable plastic based on polybutylene succinate. However, the most important industrial role of succinate is probably its function as C_4 building-block chemical. Hence, with succinate as a basis, industrially relevant products like 1,4-butanediol or tetrahydrofuran can be synthesised (Figure 1.8, [57]).

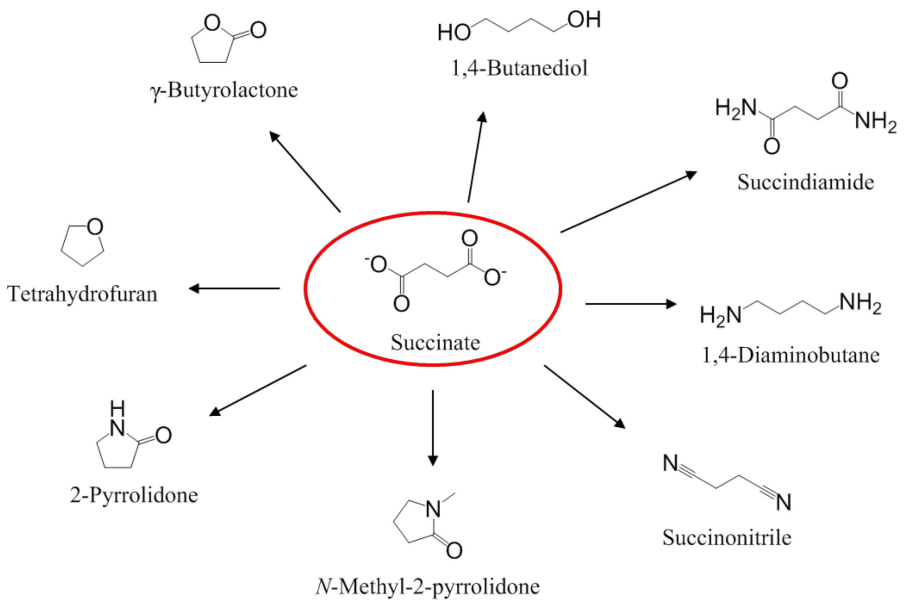


Figure 1.8: Succinate as C_4 building block.
Figure modified after [57].

Traditionally succinate is produced mainly by using butane as starting material (Figure 1.9) which is a chemical derived from fossil resources [62]. Other chemical routes are through paraffin, acetylene or acrylic acid as starting materials [63].

The chemical production of succinate from butane is not complicated as an overall process. However, the initial oxidation is performed in the vapour phase. Therefore, it has to be done *en masse* in industry due to it being gaseous [64].

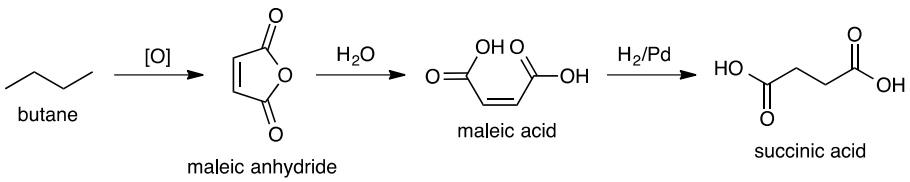


Figure 1.9: Chemically production of succinic acid through maleic anhydride.
Drawn based on information from [62][63].

1.6.1 Natural succinate producers

Succinate is an intermediate of the tricarboxylic acid (TCA) cycle and one of the fermentation end-products of some anaerobic bacteria [65]. Hence, the interest in microorganisms that can produce succinate has also greatly increased in the last few years [60], [62], [65], [66].

There are three main pathways of succinate production investigated so far (Figure 1.10; [65]).

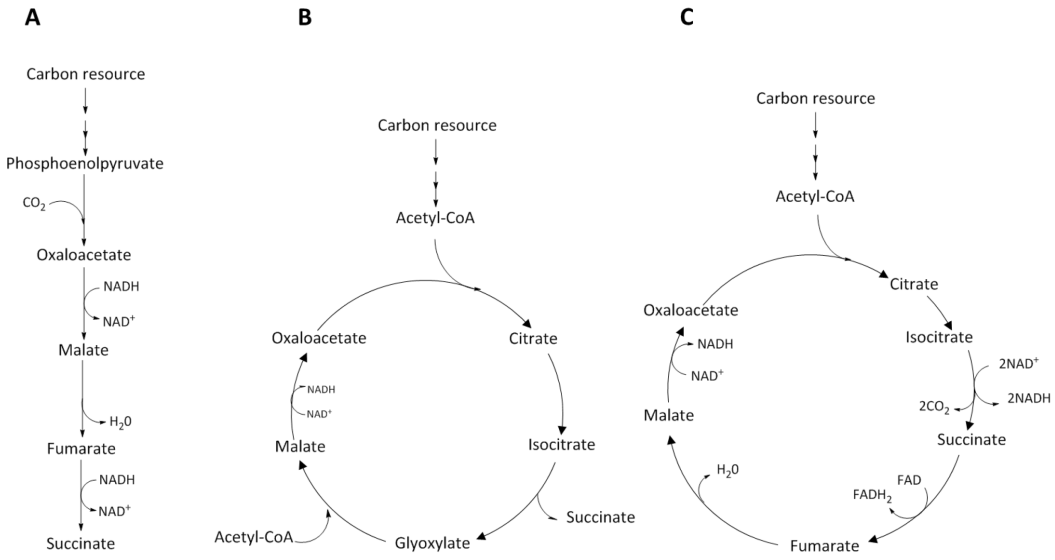


Figure 1.10: Succinate production pathways.

Image A represents the reductive branch of the TCA cycle; B, the glyoxylate pathway and C, the oxidative TCA cycle. In this last pathway the *sdhA* gene must be knocked out to block the conversion of succinate to fumarate. Figure modified after [65].

The first pathway is *via* the reductive branch of the TCA cycle (Figure 1.10A). Here, under anaerobic conditions, succinate represents the hydrogen acceptor instead of oxygen. Thus, succinate is derived from phosphoenolpyruvate (PEP), *via* oxaloacetate, malate and fumarate, whereby two molecules of NADH are required per molecule of succinate produced, based merely on the carbon balance.

A second route to succinate is via the glyoxylate pathway (Figure 1.10B), which is an anaplerotic reaction. The metabolic role of this reaction is to replenish the molecule pool of the TCA cycle [67]. This pathway operates as a cycle to convert two molecules of acetyl-CoA into one molecule of succinate. However, due to the production of NADH, this route alone is not redox balanced. Thus, during anaerobic cultivation and in the absence of an exogenous acceptor, the produced NADH could be used in parallel by the pathway shown in Figure 1.10A, and therefore gives the benefit of achieving higher succinate production [65].

However, formation of succinate can also be achieved through the oxidative TCA cycle under aerobic conditions (Figure 1.10C). Since succinate is an intermediate of the TCA cycle, the gene encoding succinate dehydrogenase (*sdh*) must be inactivated in potential production strains to block the conversion of succinate to fumarate [68]–[70]. As a consequence of the resulting disruption of the cycle, oxaloacetate must be formed *via* carboxylation of pyruvate as shown in Figure 1.10A to allow formation of citrate. Thus, one molecule of succinate can be generated from two molecules of pyruvate, with a net release of two molecules of CO_2.

So far three main natural succinate producers have been identified: *Actinobacillus succinogenes, Anaerobiospirillum succiniciproducens* and *Mannheimia succiniciproducens* [60]. All of them were isolated from the rumen [60], as the anaerobic conditions caused by carbon dioxide, methane and traces of hydrogen create an unique environment for microbial succinate production [71].

A. succinogenes was isolated from the bovine rumen in 1999 [72]. A specific strain $130Z^T$ produced more than 30 g l^{-1} of succinate. This production came

along with the production of acetic acid in high ratios (e.g. acetate: succinate; 5:1-8:1). Other by-products were formate, small amounts of pyruvate, oxaloacetate, and ethanol.

The second organism, *An. Succiniciproducens*, was isolated 1976 and is therefore the first natural succinate producer that has been isolated [73]. This bacterium was able to produce 32 g l^{-1} in 27 h with a yield of 0.99 g succinate g^{-1} glucose consumed [74] (including CO_2 fixation, contributing to succinate formation from phosphoenolpyruvate to oxaloactetate).

The third and the most recently isolated organism is *M. succiniciproducens*. It was isolated in 2002 by Lee *et al.* from bovine rumen [75]. Under an atmosphere of 100 % CO_2 it produced succinate, acetate and formate in a constant ratio of 2:1:1. It produced 13.5 g l^{-1} of succinate with 20 g l^{-1} glucose as carbon source.

For all three strains succinate is produced *via* the reductive TCA pathway under the extensive use of the PEP carboxykinase [75][76].

1.6.2 Genetically modified succinate producers

As described above, there are three species of bacteria that mainly produce succinate naturally. The easiest way to increase the production of a desirable compound is to genetically manipulate organisms already producing it. That is why all three of the earlier described bacteria have been optimised regarding succinate production.

Since only a few of the required genetic tools exist for *A. succinogenes*, the realisation of various modification ideas was not easily achieved.

Due to the by-product formation of formate, a formate dehydrogenase mutant of *A. succinogenes* strain FZ6 was created, however, this only increased pyruvate production instead of succinate [77]. An alternative method for growing *A. succinogenes* on glycerol was published by Carvalho *et al.* [66]. Here, dimethylsulfoxide (DMSO) was used as a new electron acceptor while growing the bacteria. When DMSO was added to the medium, glycerol consumption and succinate production were greatly stimulated. During fed-batch cultivation the measured concentrations of succinate reached 49.62 g l^{-1} with a product yield of 0.87 g g^{-1} glycerol and a maximum production rate of 2.31 g l^{-1} per h. This was the highest values reported for *A. succinogenes* using glycerol as carbon source.

M. succiniciproducens is a capnophilic, facultative anaerobic organism. In contrast to *A. succinogenes, M. succiniciproducens* has a complete TCA cycle and can efficiently grow under aerobic as well as anaerobic conditions [78]. The genome sequence for this organism proved advantageous for genetic tool development and therefore the generation of plasmids. The development of stable vectors opened up the possibility to overexpress certain genes for this bacterium [79][80]. Several *M. succiniciproducens* mutant strains have been generated. The target genes were *ldhA, pflB, pta* and *ackA*, encoding for lactate dehydrogenase, pyruvate-formate lyase, phosphotransacetylase and acetate kinase, respectively. Thus, in the strain LPK7 an optimal succinate production route was achieved by reducing acetate, lactate and formate formation. A fed-batch culture of that strain resulted in the formation of 52 g l^{-1} succinate with malate, acetate and pyruvate as by-products. This equated to 68 % of the maximal theoretical yield of 1.12 g g^{-1} [81]. In the same mutant strain malic enzyme was overproduced in an attempt to reduce pyruvate and malate

production [82][83]. However, although malate excretion was reduced by 37 %, pyruvate excretion increased. The pyruvate produced was finally metabolised after depletion of glucose, whereby acetate was created. Due to this, it was proposed that an efficient cofactor manipulating strategy is necessary to improve yield, reduce by-product formation and increase production rate [82]. This demonstrates the need to generate changes informed by accurate predictive models of metabolism.

An. succiniciproducens is able to ferment a broad spectrum of carbon sources, like wood hydrolysates and whey [75][84]. As a typical capnophilic organism, *An. succiniciproducens* requires high carbon dioxide concentrations for efficient growth and the supply of CO_2 affects the production of succinate significantly. Thus, an increase in CO_2 supply resulted in increased succinate yield and reduced lactate and ethanol concentrations [85]. Furthermore, addition of hydrogen to the sparging gas increased yield and production rate significantly, due to the increased availability of reducing equivalents. This may be caused by an increased activity of PEP carboxykinase and succinate formation which results in ATP generation, making that enzyme indispensable for growth coupled succinate production [86].

In addition to trying to improve succinate production in natural succinate producers, bacteria not naturally producing succinate were engineered by introducing relevant missing genes or entire metabolic pathways [65].

Due to the high variety of genetic tools available, its fast growth and simple culture medium, *Escherichia coli* became one of the most widely studied systems for succinate production.

In their review, Cheng *et al.* [65] classified the metabolic engineering strategies into four main methods that either had already been done or could be done in

future: improvement of substrate or product transport, enhancement of pathways directly involved in succinate production, deletion of pathways involved in by-product formation, and the combination of all of them (Figure 1.11).

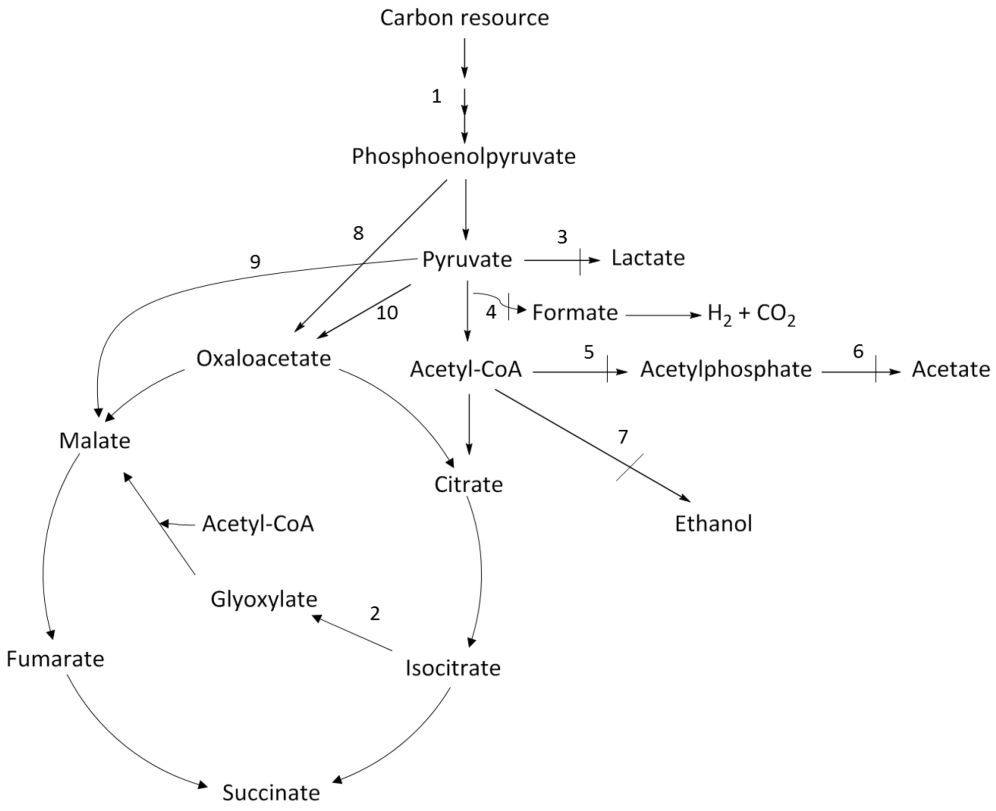


Figure 1.11: Metabolic engineering strategies to improve succinate production.

Vertical lines represent the inactivation of genes. Arrows show reactions that might be overexpressed. (1) PEP-dependent glucose uptake system is replaced with ATP-dependent phosphorylation; (2) activation of the glyoxylate pathway; (3) knockout of lactate dehydrogenase; (4) knockout of pyruvate formate-lyase; (5) knockout of acetate kinase; (6) knockout of phosphate acetyltransferase; (7) knockout of alcohol dehydrogenase; (8) overexpressed phosphoenolpyruvate carboxylase; (9) overexpressed malic enzyme; (10) overexpressed pyruvate carboxylase. Figure modified after [65].

To improve substrate or product transportation in *E. coli*, the phosphotransferase system (PTS) could be knocked out (*ptsG* gene) to avoid the simultaneous conversion of PEP to pyruvate with glucose uptake. The alternative uptake system is the galactose permease, glucokinase system. However, this system is not very efficient since it reduces growth rate but increases succinate yield [87]. The overproduction of the enzymes involved in the galactose permease, glucokinase system, led to a nearly wild type growth rate and was able to reduced by-product formation [88][89].

The import of succinate in *E. coli* is normally active under aerobic conditions whereas export proceeds under anaerobic conditions [65]. Beauprez *et al.* modified the dicarboxylic acid transport system to enhance production of succinate [90]. This approach comprised the elimination of succinate uptake and the enhancement of succinate export. The gene responsible for succinate import was knocked out and the gene encoding for export, was overexpressed. The combination of the thereby modified import and export systems increased the production rate of succinate by 55 % and the yield by 53 % [90].

The second strategy was to enhance the pathways directly involved in succinate production. Overexpression of genes involved in succinate production, such as pyruvate carboxylase, PEP carboxykinase, PEP carboxylase and malic enzyme, was reported in a number of publications. Millard *et al.* [91] were able to increase succinate production using *E. coli* JCL 1208 from 3 g l^{-1} to 10.7 g l^{-1} by overexpressing the native PEP carboxylase. However, overexpression of PEP carboxykinase had no influence on succinate production. Another attempt was to improve the pyruvate to succinate synthesis route through expression of pyruvate carboxylase, which converts pyruvate into oxaloacetate, but this enzyme is not present in *E. coli*. The

pyruvate carboxylase of *Rhizobium etli* was transferred into *E. coli,* which led to a succinate formation of 1.77 g l^{-1}, corresponding to a 50 % increased succinate formation compared to the parent strain. However, although the expression of pyruvate carboxylase had no effect on glucose uptake, it decreased the rate of cell growth [92].

A third option to improve succinate production was implemented by Stols *et al.* by developing genetically modified strains without lactate- and formate-forming routes [93]. By deleting by-product forming pathways, the NADH formerly used in these pathways was now available to improve succinate production. The *E. coli* NZN111 mutant, deficient in both the lactate dehydrogenase and pyruvate-formate lyase genes, accumulated pyruvate before metabolism terminated but did not show improvement of succinate production. However, with the additional introduction of the gene encoding for a NAD^+-dependent malic enzyme, *E. coli* NZN111 was able to consume all available glucose and thereby 12.8 g l^{-1} succinate was produced [94]. When this strain was transformed with the gene encoding for malic enzyme from *Ascaris suum,* succinate yield reached 0.39 g g^{-1} and productivity was 0.29 g l^{-1}.

Each of these methods for improving succinate production can be combined. The *E. coli* mutant NZN111 was screened by Donnelly *et al.* [95] for a spontaneous chromosomal mutation by growing on glucose in anaerobic conditions. This mutant was named AFP111. The succinate yield obtained for this mutant was 0.7 g g^{-1} glucose under 5 % H_2 and 95 % CO_2 flow. Moreover, when AFP111 was grown under aerobic conditions first for biomass formation and then shifted to anaerobic fermentation with CO_2 ventilation (dual-phase fermentation), higher succinate yields were achieved with 0.96 g g^{-1}. An obtained productivity of 1.21 g l^{-1} h^{-1} could be calculated [96][97]. Chatterjee *et*

al. [87] reported that the genetic difference between these strains (AFP111 and NZN111) was found to be in the glucose-specific PTS. Due to a PTS mutation, AFP111 relied mainly on glucokinase for glucose uptake. Vermuri *et al.* [97] showed that, furthermore, in both mutants the key glyoxylate shunt enzyme, isocitrate lyase, was not present under anaerobic conditions, but could be detected after 8 h of aerobic growth. Vermuri *et al.* also transformed the strain AFP111 with the pyruvate carboxylase form *Rhizobium etli*. A two-stage aeration strategy (first: aerobic fermentation, after oxygen concentrations decrease by 10 %, shift to anaerobic fermentation with oxygen free CO_2 sparged) was applied for higher succinate yield and productivity. Thus, a final succinate concentration of 99.2 g l^{-1} with a yield of 1.1 g g^{-1} and a productivity of 1.3 g l^{-1} h^{-1} was achieved [96]. Several more *E. coli* mutants were generated, but none of them got a higher succinate production compared to this [98][99][100][101].

Corynebacterium glutamicum has been used for amino acid production for several decades [102]. Although *Cb. glutamicum* cannot grow under anaerobic conditions, it is able to utilise glucose and excrete lactate and succinate after genetic modifications [103][104]. In 2013 Zhu *et al.* engineered a dual route for anaerobic succinate production into this bacterium [105]. The glyoxylate pathway was reconstructed by the overexpression of isocitrate lyase, malate synthase and citrate synthase. Thus, *Cb. glutamicum* produced 1.34 mol of succinate per mol glucose. After overexpression of the succinate exporter, succinate yield was increased to 1.43 mol per mol glucose. Using an anaerobic fed-batch fermentation process, the final strain produced 926 mM, which corresponds to 109 g l^{-1}, of succinate with a productivity of 9.4 mM h^{-1} and a

yield of 1.32 mol per mol glucose. This is the highest succinate concentration obtained for any microorganism, so far.

However, for all of these succinate productions achieved, heterotrophically grown bacteria were used so far. Until now, succinate could not be produced by bacteria grown autotrophically. Due to this, one focus of the GASCHEM project was to produce succinate from CO or CO_2/H_2, without the addition of other carbon sources. In order to do so, pathways involved in the succinate production had to be fully understood.

1.7 GASCHEM and PhD project

The organism of focus in the GASCHEM project, with which this PhD study is associated, was *C. autoethanogenum* due to its industrially interesting ability to grow on CO with the production of ethanol and acetate.

1.7.1 The GASCHEM project

The GASCHEM project had several main objectives. First was to understand and employ a systems biology approach to establish reliable models of *C. autoethanogenum* and its fermentation metabolism, based on both kinetic modelling and genome-scale network analyses. Second, metabolic engineering of the bacterium to improve and optimise ethanol and 2,3-BD production. Third, using a synthetic biology approach, the generation of novel production strains with a focus on implementing isobutanol- and succinate-producing pathways. A prerequisite for achieving these objectives was the development

and optimisation of genetic tools in order to manipulate and genetically modify the bacterium and to investigate the associated phenotypic changes.

1.7.2 Questions and goals for this PhD project

Considerable effort has been invested in the development of succinate overproducers through metabolic engineering. Most of these strains were grown anaerobically, due to the lower capital and operational costs when compared to aerobic fermentations [65]. Multiple studies have been dedicated to overcoming limitations in succinate production, such as introduction of an ATP-dependent glucose transport system, elimination of by-product formation by knockout of the NADH consuming enzymes lactate dehydrogenase (LDH), alcohol dehydrogenase (ADH), pyruvate formate lyase (PFL), or changes in the transport of carbon sources (import and export) (section 1.6.2).

An anaerobic autotrophic organism such as *C. autoethanogenum* may represent an alternative chassis for the production of succinate. It can grow on CO_2/H_2 and CO as the sole sources of carbon and energy. Additionally, it was reported that *C. autoethanogenum* can produce low amounts (0.002 g l^{-1}, equivalent to 17 µM) of succinate [106].

C. autoethanogenum is already seen as an industrially relevant microbe with numerous applications covered by patents [8][107][108]. It is mainly used for the production of ethanol and 2,3-BD while growing on steel mill waste gas as the sole carbon and energy source [109][110]. Therefore, succinate production during autotrophic growth with the help of this organism could be of considerable industrial interest.

To create an autotrophic succinate overproducer, the natural pathway(s) used for succinate production needed to be investigated, and genes that were assumed to be involved in this pathway were to be knocked out using commonly known *Clostridia* gene inactivation techniques like ClosTron, ACE and the newly developed CRISPR method (section 1.5). Additionally, the metabolism of C_4 dicarboxylic acids in the organism needed to be fully understood.

In summary, the overall objectives of this thesis were to (i) investigate the metabolism of the C_4 dicarboxylic acids in *C. autoethanogenum* using a combination of genetic, enzymatic and bioanalytical approaches, and (ii) to exploit the gained understanding to improve fermentative production of succinate.

2 Materials and methods

"This is insanity!"
"No, this is scholarship!"
Brandon Sanderson, Words of Radiance

2.1 Materials and suppliers

In order to conduct experiments, materials from various suppliers were used. The following table provides a list of the materials used in this work, including supplier and catalogue number.

Table 2.1: Materials used during this study.

Material	Supplier
3 mm Chromatography paper	Whatman (3030917)
Acetic acid	Fisher Scientific (A/0360/PB17)
Acetate, potassium salt	Sigma-Aldrich (P1147)
Acetly-CoA, sodium salt	Sigma-Aldrich (A2056)
Acetyl phosphate	Sigma-Aldrich (01409)
ADP	Sigma-Aldrich (A2754)
Agar bacteriological (Agar no. 1)	Oxoid (LP0011)
Agarose	Fisher Chemicals (BP/1356/500)
Amersham™ Hybond™ ECL membrane	GE Helathcare (RPN303D)
Ampicillin	AppliChem (A0839)
ATP	Sigma-Aldrich (A3377)
Bovine Serum Albumin (BSA)	Sigma-Aldrich (B2518)
Bradford Reagent	Sigma-Aldrich (B6916)
Casein acid hydrolysate, vitamin free (Casamino acids)	Sigma-Aldrich (C7970)
Chloramphenicol	Sigma-Aldrich (C0378)

Clarithromycin	AK Scientific, Inc. (H781)
Color Prestained Protein Ladder, Broad Range (11 - 245 kDa)	New England Biolabs (P7712S)
D-cycloserine	Acros Organics (68-41-7)
Deoxynucleotide (dNTP) Solution Mix	New England Biolabs (N0447)
DTE (dithioerytol)	Fisher Bioreagents (BP/173-5)
DTNB (5,5' dithionitrobenzoic acid)	Sigma-Aldrich (D8130)
DTT (dithiothreitol)	Sigma-Aldrich (D1532)
Erythromycin	Sigma-Aldrich (856193)
Ethanol	Fisher Scientific (G/0650DF/17)
Fluoroorotic acid (FOA)	Europa Biosciences (ML501A)
Fumarate, disodium salt	Acros Organics (215535000)
Fumarate, disodium salt, 2,3-$^{13}C_2$-labelled	Sigma-Aldrich (489468)
Fumaric acid, $^{13}C_4$-labelled	Cambridge Isotope Laboratories, Inc. (CLM-1529PK)
GenElute™ HP Plasmid MiniPrep Kit	Sigma-Aldrich (NA0160)
Glucose-6-phosphate dehydrogenase	Sigma-Aldrich (G8404)
Glycerol	Sigma-Aldrich (G7757)
Hexokinase	Sigma-Aldrich (H6380)
Hydrochloric acid	Fisher Scientific (A144)
Kanamycin	Sigma-Aldrich (K1377)
Lysozyme	Sigma-Aldrich (L6876)
Magnesium sulfate heptahydrate	Sigma-Aldrich (230391)
Malate, disodium salt	Merck (676-46-0)
Malic enzyme	Sigma-Aldrich (M5257)
Managenese sulfate monohydrate	Sigma-Aldrich (221287)
Milk Powder	The co-operative, Instant dried skimmed milk
MES (2-(*N*-morpholino)ethanesulfonic acid) hydrate	Sigma-Aldrich (PHG0003)
Methanol	Fisher Scientific (M/4056/17)
Microbank™ vials	Pro-Lab Giagnostics (PL.170)

NAD^+	Sigma-Aldrich (RES04101N-A101x)
NADH, disodium salt	AppliChemi (A1393-0001)
$NADP^+$	Fischer Scientific (BPE9744)
NBT/BCIP Stock solution	Roche (11-681-451-001)
NMR tube (aerobic); 507-PP-7	Wilmad-LabGlass (Z271993)
NMR tube (anaerobic); Screw cap; 5353-TR7	Wilmad-LabGlass (Z271950)
NuPAGE® MES running buffer (20x)	Fisher Scientific (NP0002)
NuPAGE™ 4-12% Bis-Tris Protein Gels, 1.0 mm, 10-well	Fisher Scientific (NP0321BOX)
NuPAGE™ LDS Sample Buffer (4x)	Fisher Scientific (NP0008)
O'GeneRuler 1 kb DNA Ladder, ready to use; 6 x Orange DNA Loading Dye	Fisher Scientific (SM1163)
Oxaloacetic acid	Sigma-Aldrich (07753)
Phosphate-buffered saline tablets	Sigma-Aldrich (P4417100TAB)
Phosphoenolpyruvate (PEP), monopotassium salt	AppliChem (4265-07-0)
Phusion® HF buffer (50x)	New England Biolabs (B0518)
Phusion® Polymerase	New England Biolabs (M0530)
Potassium chloride	Fisher Chemical (P/4280/53)
Potassium dihydrogen orthoposphate	Fisher Chemical (P/4800/53)
Potassium phosphate dibasic	Fluka (101807374)
Pyruvate, sodium salt	Sigma-Aldrich (P5280)
Pyruvate kinase / lactic dehydrogenase	Sigma-Aldrich (P0294)
Restriction Enzymes	New England Biolabs, Fisher Scientific
Resazurin, sodium salt	Sigma-Aldrich (R7017)
Sodium chloride	Sigma-Aldrich (S7653)
Sodium hydroxide	VWR Chemicals (28244-495)
Step-Tactin® AP conjugate	IBA (2-1503-001)
Strep-Tactin® Sepharose	IBA (2-1201-010)
Succinate, disodium salt	Fisher Chemical (S/6480/53)

Sulfuric acid	Sigma-Aldrich (320521)
SYBR® Safe	Fisher Scientific (S33102)
Syringe Needles, 0.5 x 25 mm	Henke Sass Wolf (4710005025)
Syringes (1 ml, 2 ml, 5 ml, 10 ml, 20 ml, 50 ml)	Terumo
T4 DNA Ligae Reaction Buffer	New England Biolabs (B0202)
T4 Ligase	New England Biolabs (M0202)
Thiamphenicol	Sigma-Aldrich (T0261)
Tris Base	Fisher Chemicals (BP152-1)
Tryptone	Sigma-Aldrich (T7293)
Tween® 20	Sigma-Aldrich (P9416)
Uracil	Sigma-Aldrich (U1128)
Yeast extract	Oxoid (LM0019)
ZymoClean™ Gel DNA recovery Kit	Zymo Research (D4002)

2.2 Bacterial strains, plasmids and oligonicleotides

Bacterial strains used for this study are listed in Table 2.2, plasmids in Table 2.3.

Table 2.2: Bacterial strains used in this study

Strain	Description / Genotype	Source / Reference
Escherichia coli BL21 DE3	Protein expression strain, F^- *ompT* hsdSB(rB^- mB^-) *galdcm* (DE3)	Studier and Moffat, 1986 [111]
Escherichia coli TOP10	Plasmid storage strain, F-*mcrA* Δ (*mrr-hsdRMS-mcrBC*)*φ80lacZΔM15* Δ*lacX74 deoR recA1 araD139* Δ*(ara-leu)7697 galU galK rpsL*(Str^R) *endA1 nupG*	Invitrogen Ltd
Escherichia coli DH5α	Plasmid storage strain, F^-, *φ8lacZΔM15*, *endA1, recA1, hsdR17, supE44, thi-1,* λ^-*, gyrA96, relA1,* Δ*(lacZYA-argF), U169*	Hanahan *et al*., 1983 [112]

Escherichia coli JW4114-1	FRD defect strain. *Δ(araD-araB)56, ΔlacZ4787(::rrnB-3), λ⁻, rph-1, Δ(rhaD-rhaB)568, ΔfrdB780::kan, hsdR514*	Baba *et al.*, 2006 [113]
Escherichia coli CA434 (HB101 + plasmid R702)	Conjugative transfer strain. *thi-I hsdS20* ($r_B m_B$) *supE44 recAB ara-14 leuB5proA2 lacYI galKl rpsL20* (Str^R) *xyl-5 mt1-1, dam⁺, dcm⁺*	Dong, H., M. Young UCW [114], Aberystwyth, UK
Escherichia coli Sexpress (NEBexpress + plasmid R702)	Conjugative transfer strain. *fhuA2 [lon] ompT gal sulA11 R(mcr-73::miniTn10--TetS)2 [dcm] R(zgb-210::Tn10--TetS) endA1 Δ(mcrC-mrr)114::IS10, dam⁺, dcm⁻*	NEB, Craig Woods and Peter Rowe, University of Nottingham
Clostridium autoethanogenum	Wildtype JA1-1	DSMZ 10061 [35]
Clostridium autoethanogenum Δ*pyrE*	*pyrE* truncation strain for ACE and allelic exchange	This thesis
Clostridium autoethanogenum1855::CT*ermB*-48s	Group II intron from plasmid pMTL007C-E2::FH directionally inserted at FH (Clau1855) gene locus	This thesis
Clostridium autoethanogenum1855::CT*ermB*-360s_2_24	Group II intron from plasmid pMTL007C-E2::FH directionally inserted at FH (Clau1855) gene locus	This thesis
Clostridium autoethanogenum1855::CT*ermB*-360s_2_24 pMTL83152_FH	*C. autoethanogenum1855*::CT*ermB*-360s with plasmid-based expression of the FH, pMTL83152 plasmid encoding the Clau1855 gene with a thioloase promotor from *C. acetobutylicum*.	This thesis
Clostridium autoethanogenumFH::CT*ermB*-360s_2_24 pMTL83152	*C. autoethanogenum1855*::CT*ermB*-360s containing plasmid pMTL83152	This thesis
Clostridium autoethanogenum FRD1	Contains plasmid pMTL83121 with codon-optimised fumarate reductase gene	This thesis
Clostridium autoethanogenum FRD2	Contains plasmid pMTL83121 with codon-optimised fumarate reductase gene	This thesis
Clostridium autoethanogenum FRD-*Strep*-TagII	Contains plasmid pMTL83121 with codon-optimised, *Strep*-tagged fumarate reductase gene	This thesis
Clostridium autoethanogenum pMTL83121	Contains plasmid pMTL83121	This thesis

Table 2.3: Plasmids used in this study

Plasmid	Size	Characteristics	Origin
pT::*hyd*A	5200 bp	Shuttle vector, carries ColE1 and repL origins of replication, *bla* and *ermB* resistance genes, $P_{thiolase}$, and C-term. *Strep*-TagII sequence	Girbal *et al.*, 2005
pANNE_ACE_del_pyrE	8464 bp	ACE plasmid for *pyrE* knockout, carries ColE1 and pCB102 origins of replication, *catP* resistance and *traJ* transfer gene, *pyrE* gene of *C.* $P_{thiolase}$, *Col*EI, pCB102, *cat*P, *tra*J, *C. acetobutylicum* and *pyrE* homology arms for *C. autoethanogenum*	Anne Meint-Henstra (SBRC, University of Nottingham)
pMTL83151	4476 bp	Conjugative shuttle vector, carries ColE1 and pCB102 origins of replication, *catP* resistance and *traJ* transfer gene, in addition to an MCS	Heap *et al.*, 2009 [115]
pMTL83152	4620 bp	Conjugative shuttle vector, carries ColE1 and pCB102 origins of replication, *catP* resistance and *traJ* transfer gene, in addition to a thiolase promoter from *C. acetobutylicum*	Philippa Strong (SBRC, University of Nottingham)
pMTL007C-E2::Clau1855_48s	9235	ClosTron plasmid retargeted for interruption of the sense strand of Clau1855	This thesis
pMTL007C-E2::Clau1855_360s	9235	ClosTron plasmid retargeted for interruption of the sense strand of Clau1855	This thesis
pMTL83121	4281 bp	Conjugative shuttle vector, carries p15 and pCB102 origins of replication, *catP* resistance and *traJ* transfer gene, in addition to an MCS	This thesis
pMTL8312_FRD	7605 bp	Plasmid pMTL83121 with *frd* gene (codon optimized from *Trypanosoma cruzi*) cloned using NotI and NheI	This thesis
pMTL8312_FRD *Strep*-TagII	7629 bp	Plasmid pMTL83121 with *frd* gene (codon optimized from *Trypanosoma cruzi*) including a C-terminal *Strep*-TagII, cloned using NotI and NheI	This thesis
pSBRCas9_Pbt_2	10174 bp	Conjugative shuttle vector, carries ColE1 and pCB102 origins of replication, *catP* resistance and	Peter Rowe (SBRC, University of

		traJ transfer gene, in addition to a thiolase promoter from *C. acetobutylicum* and a modified Cas9	Nottingham)
pSBRCas9_AcsA1	10452 bp	Plasmid pSBRCas9_Pbt_2, with guide sgRNA1* _AcsA, AcsA homology arms	This thesis
pSBRCas9_AcsA2	10452 bp	Plasmid pSBRCas9_Pbt_2, with guide sgRNA2* _AcsA, AcsA homology arms	This thesis
pSBRCas9_AcsA3	10452 bp	Plasmid pSBRCas9_Pbt_2, with guide sgRNA3* _AcsA, AcsA homology arms	This thesis

*guide RNA for CRISPR knockout, compare in Table 2.4

Table 2.4: Oligonucleotides used in this study

Name	5`- 3`Sequence*	T_m (°C)#
FRD_F1_NotI	CCCCGCGGCCGCACTAGC	57.0
FRD_R1_BamHI_overlap	GTCTTACTTTTGCCGGATCCCGTTTAATAAAACATGC	57.0
FRD_F2_BamHI_overlap	GCATGTTTTATTAAACGGGATCCGGCAAAAGTAAGAC	57.0
FRD_R2_NheI	GGGGGCTAGCTTAACTTCCACTAGGTTCAG	57.0
FRD_R2_NheI_*Strep*TagII	GGGGGCTAGCTTATTTTTCAAATTGAGGATGTGACCAACTTCCACTAGGTTCAG	60.0
FRD_Middle_Fw	AAACTACTATTTTAGCAGATGCAGTAA	53.0
FRD_Middle_Rev	TTACTGCATCTGCTAAAATAGTAGTTT	53.0
sgRNA1_AcsA	ATCTTAAGGAGGAGTTTTCGTCGACGCAGACATGAAGGTACAGTGGTTTTAGAGCTAGAAATAGCAAGTT	
sgRNA2_AcsA	ATCTTAAGGAGGAGTTTTCGTCGACGTAGCACCTCCAGTAACAGGGTTTTAGAGCTAGAAATAGCAAGTT	
sgRNA3_AcsA	ATCTTAAGGAGGAGTTTTCGTCGACGAACCCATATGAAGTACAGGGTTTTAGAGCTAGAAATAGCAAGTT	

Screening_F	GGAACTGACAGGAGTATGCATTCTCTT	60.0
Screening_R	CCTATATCCTTAGCTAATTTTTTAACATGCTTGAAC	57.0
LHAF_AcsA	ATATATATGCGATCGCAGTTGATAGAGCACGTGAAACAGG	57.0
LHAR_AcsA	GCTTGTCTTTATTATTAGATTTCCATTTTAATAATTCCCTCCTTAAAGAAATAACTTC	57.0
RHAF_AcsA	AGGGAATTATTAAAATGGAAATCTAATAATAAAGACAAGCAATTGCCATGC	57.0
RHAR_AcsA	ATATATATGGCGCGCCTACACCTTGTGCTGTTCCCCT	57.0
AcsA_fw	AGTATAGCACTTAGCTTGTATCA	50.8
AcsA_rev	CAAGTATCTATACCTGAAGTTACTAC	50.4
1855_Fw	CCCCATGAGAGAAGTAGATGTATCC	52.0
1855_Rev	GGGGTTACAATTCTATTTCCTTATGT	52.2
1855_comp_Fw	CATATGATGAGAGAAGTAGATGTATC	51.1
1855_comp_Rev	GCTAGCTTACAATTCTATTTCCT	51.1
M13_R	CAGGAAACAGCTATGACC	50.0
pCB102-R1	CTGTTATGCCTTTTGACTATC	51.0
P15 + tra-F2	CAAGAAGAGCGACTTCGC	50.0
CMHI	GAGCAAGGCAAGACC	60.0
ACE-pyrE FSP	GAGCTTATGCAATTCAAGTAGGTACTGCAAAC	50.0
ACE-pyrE RSP	CATCAAAGCTATACTATTTTCCGTATTTACATTTGGG	50.0
M13 FSP	TGTAAAACGACGGCCAGT	50.0
F1_FH_sacII	CCCCCCGCGGCAGCCCAATATTCC	49.8
R1_FH	GGGGATTACAATTCTCTCATAATTTAACACCAT	49.8
F2_FH	CCCCAATTATGAGAGAATTGTAATATTAAATTTCAA	50.3

R2_FH_ascI	GGGGGGCGCGCCGCCTGCCTTTGC	52.2
ColE1+tra F2	CCATCAAGAAGAGCGAC	55.0
pCB102 R1	CTGTTATGCCTTTTGACTATC	55.0

* Blue coloured letters imply *Strep*-tagII sequence, underlined letters imply restriction sides.
[#] Information obtained *via* Tm calculator from ThermoScientific.

2.3 Preparation of media and strain cultivation

Heat stable media and solutions were autoclaved for 20 min at 121 °C unless stated otherwise. Heat labile solutions were filter-sterilised (pore size 0.2 µm) using Minisart filters (Sigma-Aldrich).

2.3.1 Cultivation of *E. coli*

E. coli cells were grown over night in either liquid LB medium or on agar plates at 37 °C. If necessary, supplements listed in Table 2.6 were added (section 2.3.3).

LB medium after Bertani, 1951 [116][117]

Yeast extract		5	g
Tryptone		10	g
NaCl		10	g
dH_2O	*ad*	1000	ml

The pH of this medium was 7-7.5. For the generation of LB agar, 1.5 % [w/v] bacteriological agar (Table 2.1) was added to the liquid medium before autoclaving.

Additionally, *E. coli* was grown anaerobically on minimal medium according to Lambden and Guest (1976) [118].

Minimal medium

KH_2PO_4		5.44	g
K_2HPO_4		10.49	g
$(NH_4)_2SO_4$		2.00	g
$MgSO_4 \cdot 7\ H_2O$		0.05	g
$MnSO_4 \cdot 4\ H_2O$		5.00	mg
$FeSO_2 \cdot 7\ H_2O$		0.125	mg
$CaCl_2$		0.5	mg
dH_2O	*ad*	1000	ml

The medium was enriched with 0.5 g l^{-1} casamino acids, supplemented with 30 mg l^{-1} L-tryptophan and solidified with 1.5 % agar.

Subsequently the medium was autoclaved. Glycerol (40 mM) and sodium fumarate (40 mM) were added as required. Glycerol plus fumarate containing medium was called GF, and medium only containing fumarate was called F medium.

2.3.2 Cultivation of *C. autoethanogenum*

To cultivate *C. autoethanogenum,* either rich medium (YTF) or chemically more defined PETC medium was used. A variant of the latter, PETC-ljungdahlii, still contained yeast extract and was for later explained reason replaced by PETC-MES which contained casamino acids but no yeast extract. YTF medium was used in the anaerobic cabinets only, after incubating it for at least 4 h to obtain an anaerobic state before usage. PETC medium was used for growth experiments in serum bottles and Hungate-tubes.

The generation of anaerobic PETC medium was conducted according to Breznak and Costilow [119] in Hungate-tubes or serum bottles. After bringing the medium to boil in the microwave to expel dissolved oxygen, it was filled into tubes and bottles whilst being gassed with N_2 to avoid re-dissolving of oxygen, using a gas exchange station (GR Instruments BV, GW6400). The redox indicator resazurin (0.1 % [w/v]) was used as oxygen indicator.

The bottles were, after cooling down whilst gassing for about 10 min, closed airtight and autoclaved for 20 min at 121 °C.

A colour change due to the added resazurin after autoclaving from pink to colourless (faint yellow colour due to the presence casamino acids / yeast extract) indicated the anaerobic state of the medium.

Fructose and further media supplements were added after autoclaving from separate anaerobe and sterile stock solutions. Cysteine (50 µl in 50 ml of a 4 % stock solution) or sodium sulfide (50 µl in 50 ml of a 250 mM stock solution) was added to PETC medium variants prior to use, acting as reducing agent and additional sulfur source.

YTF medium

Yeast extract		10	g
Tryptone		16	g
Fructose		10	g
NaCl		0.2	g
1000 x Acidic trace element solution		1	ml
1000 x Base trace element solution		1	ml
1000 x Wolfe's vitamin solution		1	ml
0.1 % Resazurin (optional)		1	ml
dH_2O	*ad*	1000	ml

The pH was set to 5.8 using HCl. For YTF agar, 1.5 % bacterial agar was added to the liquid medium before autoclaving.

PETC-ljungdahlii (similar to ATCC medium 1754)

MES (2-(*N*-morpholino)ethanesulfonic acid)		5	g
Sodium formate		1	g
50 x Macronutrient solution		25	ml
1000 x Acidic trace element solution		1	ml
1000 x Base trace element solution		1	ml
1000 x Wolfe's vitamin solution		1	ml
Yeast extract		1	g
0.1 % Resazurin (optional)		1	ml
dH_2O	*ad*	1000	ml

The pH was adjusted to 5.7 with NaOH.

PETC-MES (according to LanzaTech [37]; ATCC medium 1754)

MES (2-(*N*-morpholino)ethanesulfonic acid)		20	g
50 x Macronutrient solution		20	ml
100 x Trace metal solution		10	ml
1000 x Wolfe's Vitamin solution		1	ml
Casamino acids (optional)		1.5	g
0.1 % Resazurin (optional)		1	ml
dH_2O	*ad*	1000	ml

The pH was adjusted to 5.7 with NaOH.

Wolfe's Vitamin solution (1000 x)

Biotin		20	mg
Folic acid		10	mg
Pyridoxine hydrochloride		100	mg
Thiamine-HCl		50	mg
Riboflavin		50	mg
Nicotinic acid		50	mg
Calcium D-(+)-pantothenate		50	mg
Vitamin B_{12}		1	mg
p-Aminobenzoic acid		50	mg
Thioctic acid		50	mg
dH_2O	*ad*	1000	ml

Trace metal solution (100 x)

Nitrilotriacetic acid		2	g (dissolve first, adjust to pH 6 by adding 3M KOH)
$MnSO_4 \cdot H_2O$		1	g
$Fe(SO_4)_2(NH_4)_2 \cdot 6\ H_2O$		0.8	g
$CoCl_2 \cdot 6\ H_2O$		0.2	g
$ZnSO_4 \cdot 7\ H_2O$		0.2	mg
$CuCl_2 \cdot 2\ H_2O$		0.02	g
$NaMoO_4 \cdot 2\ H_2O$		0.02	g
Na_2SeO_3		0.02	g
$NiCl_2 \cdot 6\ H_2O$		0.02	g
$Na_2WO_4 \cdot 2\ H_2O$		0.02	g
dH_2O	*ad*	1000	ml

Macronutrient solution (50 x)

NH_4Cl		25	g
NaCl		20	g
KCl		2.5	g
KH_2PO_4		2.5	g
$MgSO_4 \cdot 7\ H_2O$		5	g
$CaCl_2 \cdot 2\ H_2O$		1	g
dH_2O	*ad*	500	ml

The components of the macronutrient solution were added in order of appearance. Each component was completely dissolved before the next one was added.

Acidic trace element solution (1000 x)

HCl		50	mM
H_3BO_3		100	mg
$MnCl_2 \cdot 4\ H_2O$		230	mg
$FeCl_2 \cdot 4\ H_2O$		780	mg
$CoCl_2 \cdot 6\ H_2O$		103	mg
$NiCl_2 \cdot 6\ H_2O$		602	mg
$ZnCl_2$		78	mg
$CuSO_4 \cdot 5\ H_2O$		50	mg
$AlK(SO_4)_2 \cdot 12\ H_2O$		50	mg
dH_2O	*ad*	1000	ml

Base trace element solution (1000 x)

NaOH		10	mM
Na_2SeO_3		58	mg
Na_2WO_4		53	mg
$Na_2MoO_4 \cdot 2\ H_2O$		52	mg
dH_2O	*ad*	1000	ml

When growing *C. autoethanogenum* on carbon monoxide (CO), PETC-MES medium was used. For this 250 ml serum bottles containing 50 ml of medium were used and put into the anaerobic tent atmosphere over night. On the next day, after the addition of sodium sulfide (50 µl of a 250 mM stock solution) and the inoculation of the culture, CO was added to the bottles, with the help of a gassing station (GR Instruments BV, GW6400), to generate 1 bar overpressure. Bottles were incubated at 200 rpm and 37 °C.

2.3.3 Media supplements

If required, additional supplements including carbon sources (Table 2.5) or antibiotics (Table 2.6) were added to the media. All solutions were sterilised by either autoclaving, or, in case of antibiotic solutions and carbon sources, filtration. If antibiotic solutions were added to solid medium, the addition was made after the medium was cooled down to about 50 °C or lower.

Table 2.5: Additional carbon sources

Carbon source	Concentration of stock solution [mM]	Working concentration [mM]
D-Fructose	400	40
Sodium fumarate	400	15 or 40
Sodium fumarate (2,3-$^{13}C_2$)	No stock	40 – powder directly added into liquid medium
Fumaric acid ($^{13}C_4$)	400	40
Sodium pyruvate	400	40
Sodium malate	400	40
Sodium oxaloacetate	400	40
Sodium citrate	400	40
Sodium succinate	400	40

Table 2.6: Antibiotics

Supplement	Conc. Stock solution (mg/ml)	Dissolve in	Working concentration (µg/ml) (*E. coli*)	Working concentration (µg/ml) (*Clostridia*)	Storage Temp. [°C]
Ampicillin	50	Water	100		-20
Chloramphenicol	25	100 % Ethanol	25		-20
Erythromycin	50	100 % Ethanol	500	10	4
Clarithromycin	6	100 % DMSO		6	-20
Kanamycin	50	Water	50		-20
Spectinomycin	100	Water	250	250	-20
Thiamphenicol	15	50 % Ethanol / 100 % DMSO		15	4
Trimethoprim	10	100 % DMSO	10		fresh

2.4 Stock cultures

Stock cultures of *E. coli* were either made by adding 10 % DMSO (dimethylsulfoxide) to exponentially growing cultures or by using the Mikrobank® vial system, according to manufacturer's instructions.

Stock cultures of *C. autoethanogenum* were made anaerobically in either the anaerobic cabinet (Don Whitley Scientific) or Coy tent (Coy Lab. Inc.) by adding 10 % of DMSO to exponentially growing cells.

All stock cultures were stored at -80 °C.

2.5 Physiological parameters

2.5.1 Measuring optical density (OD)

The growth of bacteria cultures in liquid media was monitored by measuring the optical density at 600 nm. Distilled water was used as a blank control. For OD_{600} values of more than 0.5 the cell suspension was diluted until it was less than 0.5.

2.5.2 Microscopy

In order to visualize *C. autoethanogenum* cells and cultures two different methods of microscopy were used.

2.5.3 Light microscopy

To analyse physiology and morphology of cell cultures, a light microscope (Nikon Eclipse Ci) was used at 1000 fold magnification.

2.5.4 TEM

TEM images of *C. autoethanogenum* were taken in cooperation with Dr. Denise Mclean from the Advanced Microscopy Unit in the QMC, Faculty of Medicine & Health Sciences, University of Nottingham and two other SBRC members. Cells in the culture medium were centrifuged at 1000 *g* to form a cell pellet. The supernatant was removed, the pellet re-suspended in fixative (2 % glutaraldehyde and 2 % paraformaldehyde in 0.1 M phosphate buffer) and left

to incubate for 30 min. Afterwards the mix was centrifuged again to get a pellet, the fixative removed and the pellet re-suspended in 0.1 M cacodylate/phosphate buffer. The buffer wash step was repeated three more times. After the last washing step, the pellet was dissolved in 1 % aqueous osmium tetroxide and centrifuged again. Subsequently, the pellet was washed four times in 0.1 M cacodylate/phosphate buffer and afterwards washed for 5 min in distilled water. The washed pellet was dehydrated in graded ethanol series (2 x 15 min 50 % ethanol, 2 x 15 min 70 % ethanol, 2 x 15 min 90 % ethanol, 3 x 20 min 100 % ethanol, 2 x 15 min 100 % propylene oxide (propox)). The dehydrated pellet was infiltrated with resin which was generated as follows: 25 ml araldite CY212 resin, 15 ml agar 100 resin and 55 ml DDSA were stirred, then 2 ml dibutyl phthalate and 1.5 ml DMP 30 added. While stirring, the colour changed from red-orange to orange. The polymerisation took place for 48 h at 60 °C. The infiltration of the resin with the fixed and washed cell pellet was done in three varieties: 4 h in 1:3 resin:propox mix, over night in 1:1 resin:propox mix and in fresh bottles 3 x 2.5 h in pure resin. The embedded samples were taken in a BEEM® capsule and left in an oven at 60 °C for 2 days. For the imaging of *C. autoethanogenum* negative staining using uranyl acetate was used. The imaging was carried out on Tecnai Biotwin Transmission Electron Microscope with a digital camera system and an accelerating voltage of 100 kV.

2.6 Growth experiments

All growth experiments of *C. autoethanogenum* were performed at least in triplicate. The OD_{600} measurements of the triplicates was averaged and used for calculation of the standard deviation. Growth experiments were performed anaerobically in 250 ml serum bottles containing 50 ml PETC-MES medium, unless otherwise mentioned. In order to follow cell growth, 1 ml sample was taken in various steps to follow growth, usually every 12 to 24 h. However, the measurements were mainly dependent on cell growth. Samples were taken every 4-6 h during the exponential growth phase, and the waiting time between measurements was increased during stationary growth, until a decrease in OD, due to cell lysis, indicated the end of the growth experiment (usually after 90-120 h, in some experiments up to 200 h).

The 1 ml samples taken from the bottles were measured with regards to OD (600 nm) firstly (here, three technical replicates were performed and the average used). In case the absorption was higher than 0.5, the samples were diluted (2.5.1). If no dilution was necessary, samples were transferred from cuvettes into Eppendorf tubes and centrifuged at 4000 rpm for 5 min and 4 °C in order to sediment the cells. If dilution was needed, a fresh 1 ml sample was taken from the bottles and directly transferred into an Eppendorf tube for centrifugation. The supernatant was then transferred into a new Eppendorf tube and the pH measured. The supernatants were stored afterwards at -80 °C for later metabolic analyses.

To calculate growth rate and doubling time, the equations below were used [120][121]. The best approximation of the slope and intercept of the exponential growth phase in a logarithmic state was calculated [121]. From this two theoretical points N and N_0 with a time interval t could be determined,

which then led to the calculation of the specific growth rate μ using the following equation:

$$\mu = \frac{\ln(\frac{N}{N_0})}{t}$$

From this the doubling time (t_d) in hours could be calculated as:

$$t_d = \frac{\ln(2)}{\mu}$$

The dry weight of *C. autoethanogenum* was determined to be 0.34 ± 0.01 g l^{-1} OD^{-1} (Rupert Norman, University of Nottingham, 2017, unpublished data). The elementary composition for anaerobic bacteria $C_4H_{8.32}O_2N_{0.98}$ (Papoutsakis, 1984 [122]) was used for carbon balance calculations, which gives the molar mass μ of the bacterium (mass of a mole of bacterium) of 103.7937 g/mol.

2.7 Molecular biology methods

2.7.1 Treatment of devices and solutions

Devices and heat resistant solutions were autoclaved for 20 min at 121 °C to inactivate nucleases. Benches, worktops and non autoclavable devices were sterilised with 70 % (v/v) ethanol and dried. To filter-sterilise heat labile solutions, 0.2 μm syringe filters were used.

2.7.2 Isolation of nucleic acids

2.7.2.1 Isolation of genomic DNA

Genomic DNA from *E. coli* and *C. autoethanogenum* was isolated using either the genomic preparation kit (Sigma-Aldrich) or Phenol-Chloroform extraction.

For genomic DNA isolation, 1-10 ml of growing cells (OD_{600} ~ 1) were centrifuged at 10,000 *g* for 10 min and the supernatant discarded. The resulting cell pellets were processed as described below.

Isolation of genomic DNA using the Sigma-Aldrich kit

To isolate genomic DNA from *C. autoethanogenum* and *E. coli*, the genomic preparation Kit from Sigma-Aldrich was used according to the manufacturer's instructions. For the elution of the purified DNA 100 µl dH_2O were used.

Isolation of genomic DNA by Phenol-Chloroform extraction

Phenol-Chloroform extraction was used to obtain high quantity and high quality of genomic DNA (mainly for use in Southern Blots, 2.7.9).

For this, the following protocol was used:

1. 1-10 ml of culture was centrifuged (4 °C, 10 min, 4000 *g*) and the supernatant discarded
2. Cell pellets were re-suspended in 180 µl lysis buffer (10 mg/ml lysozyme in PBS)
3. Resulting cell suspensions were ncubated at 37 °C for 30 min – with occasional gentle agitation
4. 4 µl of RNase (Sigma) was added, followed by incubation at room temperature for 15 min

5. 25 µl proteinase K solution (Sigma) was added, together with 85 µl dH_2O and 110 µl 10 % (w/v) SDS solution, mixed by inversion and incubated at 65 °C for 30 min
6. 400 µl phenol/chloroform/isoamyl alcohol (25:24:1; saturated with 10 mM Tris, pH 8.0, 1 mM EDTA) were added and mixed thoroughly by inversion
7. The mix was transferred into phase-lock tube (Eppendorf: 0032 005.152) and spun at full speed for 3 min
8. The top layer was transferred into a fresh phase-lock tube and the phenol/chloroform/isoamyl alcohol extraction was repeated two more times
9. The top layer was transferred into a 1.5 ml Eppendorf tube containing 0.1 vol (40 µl) of 3 M sodium acetate and 2.0 vol (800 µl) of ice cold 100 % ethanol, gently mixed by inversion and placed on ice immediately
10. The sample was incubated at -80 °C for 30 min
11. The sample was centrifuged at full speed for 15 min
12. The supernatant was poured off quickly to avoid re-supension
13. The sample was washed by adding 1 ml of 70 % ethanol and spun at full speed for 3 min; the supernatant was poured off quickly, and the pellet spun for further 3 min, and all the liquid removed without touching the pellet
14. The DNA pellet was air dried for at least 45 min at room temperature in a sterile area (i.e. fume hood)
15. The pellet was re-dissolved in 50 µl dH_2O

The purity and concentration of DNA was monitored by using NanoDrop® (ND-1000) blanked with water.

2.7.2.2 Isolation of plasmid DNA

Plasmid DNA from *E. coli* was isolated using the Plasmid-Mini (or Midi) prep kit from Sigma-Aldrich according to manufacturer's constructions. For the elution of isolated DNA from the column, dH_2O was used instead of the supplied elution buffer.

Purity and concentration of DNA was monitored using NanoDrop® (ND-1000).

2.7.2.3 DNA extraction from agarose gels

DNA fragments were isolated from agarose gels using ZymoResearch's Zymoclean™ or Monarch® Gel DNA Recovery Kits according to the manufacturer's instructions. DNA was eluted form the columns with dH_2O instead of the supplied elution buffer.

The purity and concentration of DNA was monitored by using NanoDrop® (ND-1000).

2.7.3 Agarose gel electrophoresis

The separation of DNA *via* gel electrophoresis was used for both analysis and preparation of DNA molecules. For all gel electrophoreses carried out, 1 % [w/v] agarose in 1 x TAE was used. Before loading the gel, 0.2 volumes of 6 x loading dye (O'Gene, ThermoScientific) was added to the samples. To analyse DNA fragments sizes, the O'GeneRuler 1 kb DNA ladder was used. Gel electrophoresis was conducted at 80-100 V. The agarose gel was pre-stained with SYBR®Safe DNA gel stain (ThermoScientific) to visualise and document DNA under blue light afterwards.

50 x TAE

Tris		484	g
Glacial Acetic acid (ice cold)		114	ml
EDTA (0.5 M, pH 8.0)		200	ml
dH_2O	*ad*	2000	ml

The pH was adjusted to 7.5 using HCl.

2.7.4 Enzymatic modification of DNA

2.7.4.1 Restriction digestion of DNA

For the construction of all plasmids mentioned in this thesis, either FastDigest (ThermoFisher™) with buffer Green or plain FastDigest buffer, or (if available) high fidelity restriction enzymes of NEB in combination with CutSmart buffer were used. No more than 10 % (v/v) of enzyme was used in a digest. PCR fragments and plasmid DNA were usually incubated for 30 min up to 2 h at 37 °C. To stop the reaction, enzymes were heat inactivated or the mixture directly run on an agarose gel (2.7.3). Restriction sides and buffers of restriction enzymes used in this study are listed in Table 2.7.

Table 2.7: Restriction enzymes

Restriction enzyme	Manufacturer	Sequence	Buffer
BamHI	ThermoFisher	5'-G^GATCC-3' 3'-CCTAG^G-5'	1-times FastDigest®
HindIII	NEB	5'-A^AGCTT-3' 3'-TTCGA^A-5'	1-times CutSmart
NdeI	ThermoFisher	5'-CA^TATG-3' 3'-GTAT^AC-5'	1-times FastDigest®
NheI	ThermoFisher	5'-G^CTAGC-3' 3'-CGATC^G-5'	1-times FastDigest®

NotI	ThermoFisher	5'-G^CGGCCGC-3' 3'-CGCCGGC^G-5'	1-times FastDigest®
PmeI	NEB	5'-GTTT^AAAC-3' 3'-CAAA^TTTG-5'	1-times CutSmart
SbfI	NEB	5'-CCTGCA^GG-3' 3'-GG^ACGTCC-3'	1-times CutSmart
AsiSI	NEB	5'-GCGAT^CGC-3' 3'-CGC^TAGCG-5'	1-times CutSmart
SalI	NEB	5'-G^TCGAC-3' 3'-CAGCT^G-5'	1-times CutSmart

^cutting side

2.7.4.2 Dephosphorylation of DNA fragments

If DNA fragments were to be used for ligation (section 2.7.4.3) the DNA digest was followed by dephosphorylation of the free 5'- ends in order to avoid self-ligation of the plasmid. Only the backbone (plasmid part) of the final plasmid was dephosphorylated as the phosphate group is needed for the ligation for one of the ligation-partners. Dephosphorylation was carried out using "Shrimp Alkaline Phosphatase" (SAP, ThermoFisher, St. Leon-Rot) which could be completely inactivated by incubating the mixture at 80 °C for 10 min. Per 10 µg of linearized plasmid DNA 1 U SAP (1 U/µl) and 1 times SAP buffer was added to the digest mixture. Afterwards, the mix was incubated for further 20 min at 37 °C. To avoid residual activity of both restriction digest enzymes and phosphatase, the mixture was purified using ZymoResearch's Zymoclean™ Gel DNA Recovery kit according to manufacturer's instructions.

2.7.4.3 Ligation of DNA fragments

Backbone and insert were added into the ligation mixture in a ratio of 1:3. The volume of the mix was 20 µl including appropriate ligation buffer with a concentration of the T4-DNA-Ligase (ThermoFisher) of 0.25 U/µl. The mixture was incubated at 22 °C. After 20 min 5 µl were used for a transformation into chemically competent *E.* coli cells, the rest of the mix was incubated over night at 4 °C in case transformation did not work and longer incubation time was required.

2.7.5 *In vitro* amplification of DNA *via* PCR

Polymerase Chain Reaction (PCR) was mainly used to amplify fragments for cloning, but also as a control (colony PCR) after transformation and conjugation. The amplification was undertaken in thermocyclers with lid-heating (PCR-Cycler, Biometra).

By using the annotated genome of *C. autoethanogenum* [42] oligonucleotides needed for the PCR were constructed and ordered from Sigma. In order to clone fragments into specific plasmids, the addition of restriction enzymes (Table 2.7) on 5'- and 3'- sites was necessary. For primer design the predicted melting temperatures were taken into account. These were calculated using online software made available by ThermoFisher (https://www.thermofisher.com/uk/en/home.html), based on algorithms developed by Chester and Marshak [123]. The temperatures differed by no more than 1 °C for a given pair. Oligonucleotides used in this thesis are listed in Table 2.4.

The polymerase used in most of the PCR reactions was Phusion®DNA polymerase. The prepared master mix used for PCR reactions consisted of Phusion Polymerase Buffer, dNTPs (200 µM) and the specific primers (0.5 µM).

The PCR program varied according to the purpose of the PCR. PCR for amplifying fragments for cloning was carried out as follows:

Denaturation	98 °C	30	s	
Denaturation	98 °C	10	s	
Annealing	X-3 °C	30	s	10 x
Amplification	72 °C	30	s/kBp fragment	
Denaturation	98 °C	10	s	
Annealing	X °C			10 x
Amplification	72 °C	30	s/kBp fragment	
Completion of strands	72 °C	5	min	
Storage	15 °C	∞	until ready to use samples	

X stands for the calculated annealing temperature of the primers that were used.

Colony PCR

In order to identify mutants or plasmids directly from colonies, colony PCR was conducted. Colonies to be tested were re-suspended in 20 µl of dH_2O and 1 µl used as template. DreamTaq Polymerase (ThermoFisher) was used for colony PCR. The PCR protocol was as follows:

Denaturation	95 °C	5	min	
Denaturation	95 °C	30	s	35 x
Annealing	~ 60 °C	30	s	
Amplification	72 °C	60	s/kBp fragment	
Endsynthesis	72 °C	2	min	
Storage	15 °C	∞	until ready to use samples	

Splicing by overlap extension (SOE)-PCR

To combine two gene fragments, SOE-PCR was conducted. This process was carried out in two separate steps (Figure 2.1). The first step was the individual amplification of both fragments that are going to be combined. For the first fragment the reverse primer included about 10-15 bases of the start sequence of the second fragment. The second fragment's forward primer included about 10-15 bases of the first fragment's 3' sequence, thus resulting in a total overlap of 20-30 bases. The second step of the SOE-PCR was the combination of both fragments using the first fragment's forward and the second fragment's reverse primer. Due to the overlapping nucleotides that were amplified before, both fragments are combined during this step.

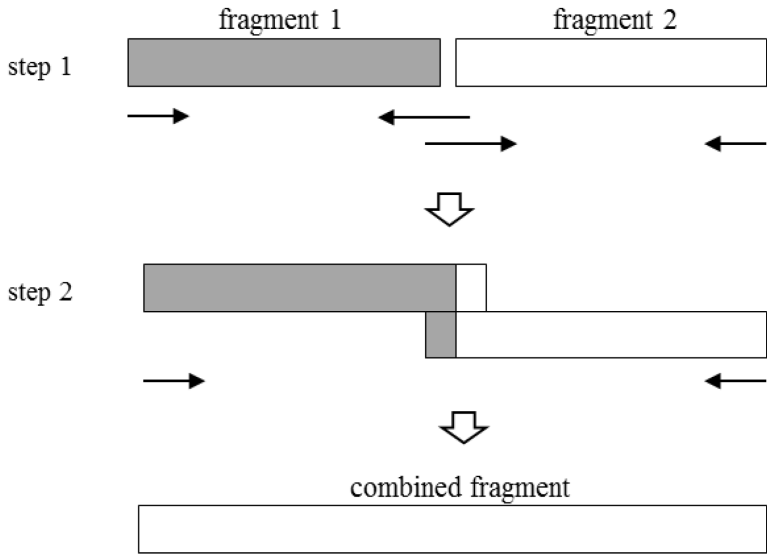


Figure 2.1: Principle of SOE-PCR.

In step 1 both fragments are amplified individually, whereby the reverse primer of fragment 1 and the forward primer of the fragment 2 overlap. In the second step, both fragments are combined. Initially, the ends of fragment 1 and 2 are extended, and then the resulting combined fragment is amplified.

The two steps were either carried out separately, by isolating the DNA from the agarose gels that were run after the first step PCR and using both fragment products in the second step PCR, or both steps were carried out in a single PCR tube.

To verify successful amplification, agarose gel electrophoresis (section 2.7.3) was conducted after every PCR.

2.7.6 Sequencing

In order to determine the sequence of plasmids or gene fragments amplified *via* PCR, samples were sent to a sequencing service (Eurofins, Germany) who sequenced these *via* Sanger sequencing.

2.7.7 Generation of deletion and insertion mutants

2.7.7.1 Generation of insertional mutants using the ClosTron system

ClosTron mutants were constructed according to the instructions given by Heap *et al.* [45].

Appropiate intron targeting regions within genes of interest were generated *in silico* at http://clostron.com/clostron3.php using the algorithm developed by Perutka *et al.* [124]. The introns (see Appendix for sequences, Table A.1) were synthesised by DNA 2.0 Inc. and provided already cloned into the ClosTron plasmid pMTL007C-E2 (Table 2.3).

The received ClosTron plasmids were electroporated into *E. coli* CA434 cells using spectinomycin and chloramphenicol (Table 2.6) as resistance markers, and stored as stock cultures at -80 °C for later conjugation (section 2.8.2).

After conjugation, colonies appearing on clarithromycin YTF plates were screened by colony PCR using flanking primers (Table 2.4). Wild type (WT) DNA was used as a negative control in these PCRs. Colonies that produced 1.8 kb larger amplicons than the WT were then re-streaked onto clarithromycin and thiamphenicol plus clarithromycin YTF plates. Colonies able to grow on clarithromycin but not on thiamphenicol showed plasmid loss and were used for further analysis. Final verification of the ClosTron mutants was conducted using Southern Blot analyses (section 2.7.9) to prove single insertion mutants.

2.7.7.2 Generation of CRISPR knockout mutants

A different mutagenesis system is provided by the CRISPR system, which is explained in more detail in section 1.5 and was used to inactivate *acsA*, encoding a key subunit of the CO dehydrogenase/Acetyl-CoA synthase complex. The guide RNAs (sgRNAs) chosen for this knockout were determined by utilising the Benchling® CRISPR sgRNA design tool (http://www.benchling.com; CRISPR generator). In order to include both the guide RNA and homology arms for the *acsA* gene, the pSBRCas9 plasmid (generated by Peter Rowe, University of Nottingham) was digested with SalI (Table 2.7) for 4 h at 37 °C and afterwards treated with antartic phosphatase to avoid re-circularisation for 2 h at 37 °C. The in that way generated backbone was run on an agarose gel and the DNA afterwards extracted and purified. It was then used for HiFi assembly to incorporate the *acsA* guide RNA encoding sequence: 10 µl 2x NEB HiFi MM, 40 ng linearized backbone, 2 µl sgRNA HiFi oligo (10 mM oligos diluted 1:20 in 1 x 2.1 NEB buffer), 6 µl dH_2O. The mixture was incubated for 1 h at 50 °C and afterwards 10 µl taken for transformation of chemically competent *E. coli* cells and plated onto LB agar plates containing chloramphenicol. Plasmids from the appearing colonies were extracted and sent for sequencing. Plasmids containing the guide RNA sequence were then used for cloning of the respective homology arms. These were cloned into the plasmid using the restriction enzymes AscI and AsiSI (Table 2.7). Colonies appearing after transformation of respective ligations were again used for plasmid preparation and plasmids sent for sequencing. The final plasmid (pSBRCas9_AcsA) was used for transformation into *E. coli* Sexpress cells (Table 2.2) and then conjugated with *C. autoethanogenum.* Colonies appearing on thiamphenicol containing YTF plates were used for

colony PCR using the screening primers (located outside of the homology arms in the genome; Table 2.4) in order to check for knockout mutants. Confirmed knock-out mutants were re-streaked onto YTF plates with and without thiamphenicol repeatedly. Colonies grown only on plates without thiamphenicol showed a plasmid-loss and were therefor used for further experiments.

2.7.7.3 Construction of in-frame deletion mutants using Allelic Exchange/ Allele-Coupled Exchange

Allele-Coupled Exchange (ACE) is a genetic tool developed by Heap *et al.* (2012, [52]). This system allows the selection of second recombination events without the use of counter-selectable markers. It can be used in order to generate Δ*pyrE* knockout strains which was done by all members of the GASCHEM project, to obtain a *pyrE*-negative version with a minimal number of second site mutations. The *pyrE* gene can be used as both a negative and positive selectable marker for genetic manipulation work.

To create a *pyrE* deletion strain, the plasmid pANNE Δ*pyrE* was electroporated into *E. coli* CA434 cells and then transferred into *C. autoethanogenum via* conjugation (section 2.8.2). Fast growing and larger colonies on thiamphenicol (Tm) YTF plates were selected to re-streak onto fresh Tm YTF plates. The single crossover event was verified *via* colony PCR, using the internal primer CMHI, annealing to a region located on the plasmid, and the downstream flanking primer ACE *pyrE* RSP (Table 2.4), generating a ~1800 bp fragment in the presence of a single crossover containing strain. To check for a double crossover event, those colonies with verified single crossover event were re-

streaked onto YTF plates containing 5-FOA (1 mg/ml) + uracil (20 µg/ml). Colonies appearing on these plates were then plated onto SDMM-C (semi-defined minimal media, containing casamino acids) plates with and without uracil, as colonies without functional *pyrE* gene are unable to grow on plates without uracil (uracil auxotroph). This procedure was repeated once and promising colonies (growing on plates with uracil but not without) were inoculated into liquid YTF medium for genomic DNA isolation. This DNA was then used for another PCR screening for a double crossover event using the primers ACE-*pyrE* FSP and M13 FSP (WT: no band, mutant 600 bp). Additionally, another PCR using ACE-*pyrE* FSP and ACE-*pyrE* RSP primers, was performed to isolate the deletion region (~ 2 kb) for sequencing. Once the gel purified fragments were sequenced and revealed the correct genomic sequence, the mutants were re-streaked onto unselective and Tm containing YTF plates to check for plasmid loss. The gDNA (phenol chloroform extraction - 2.7.2.1) of mutants with confirmed plasmid loss was then sent for whole genome sequencing. The one strain with the least single nucleotide polymorphisms (SNPs) or other changes in the genome was selected as the *pyrE* deletion strain for further use.

Using the created *pyre* knockout-strain, Allelic Exchange mutants can be generated in this background strain. To generate a fumarate hydratase (Clau1855) mutant, the left and right homology arm of the gene (~750 bp upstream and ~750 bp downstream of the gene) were amplified using the primers F1_FH_sacII, R1_FH, F2_FH and R2_FH_ascI and both homology arms combined *via* SOE-PCR (Figure 2.1) with the primers F1_FH_sacII and R2_FH_ascI (Table 2.4). Once both homology arms were combined, both the fragment and the plasmid pANNE_ACE_del_pyrE were digested with sacII

and ascI, and the plasmid additionally treated with antarctic phosphatase to avoid self-ligation. After ligation, the plasmid was transferred into *E. coli* DH5α cells *via* chemical transformation. The plasmid was isolated from growing colonies and sent for sequencing of the homology arms. After positive sequencing, the plasmid was cloned into *E. coli* CA434 cells for later conjugation into *C. autoethanogenum* (2.8.2).

2.7.8 Complementation of ClosTron mutants

To restore the wild type of and prove the influence of the mutation on the observed phenotype, complementation of the ClosTron mutants was necessary. Therefore, a plasmid-borne copy of the fumarate hydratase gene (Clau1855) was expressed in its corresponding ClosTron mutant. The gene was cloned into pMTL83152 using NheI and NdeI restriction sides, which were introduced *via* PCR (Table 2.4). For the complementation of Clau1855 the primers 1855_comp_Fw and 1855_comp_rev were used. Colonies that formed after conjugation of the plasmid, pMTL83152_FH, into *C. autoethanogenum* that had both antibiotic resistances (thiamphenicol for the plasmid and clarithromycin for the ClosTron) were selected and the phenotype analysed. In order to ensure that the restored phenotype was based on the introduction of the plasmid-borne gene rather than of the plasmid itself, a plasmid control strain containing pMTL83152 was generated.

2.7.9 Southern Blot

The final analysis of positive ClosTron mutants was done *via* Southern Blot. Here, 1 µg of DNA of each sample was digested over night with HindIII and EcoRV restriction enzymes, in two separate digests (Table 2.7) and run on a 1 % agarose gel (section 2.7.3). The DNA was transferred onto a nitrocellulose membrane (Amersham HYbond ECL, GE Healthcare) by pressure-driven capillary action using Whatman filter paper soaked with 0.4 M NaOH. After a 2-3 h transfer of DNA, the membrane was wrapped in cling film and exposed to UV light for 2 min on each side in order to crosslink the DNA (UVP CX-2000 UV Crosslinker). Afterwards, the membrane was rinsed in 2 x SSC buffer (300 mM sodium chloride, 30 mM sodium citrate, pH 7) to remove excess NaOH. The blot was then incubated in 10 ml DIG Easy Hyb (Roche) solution in a Techne Hybridiser oven (HB- 1D) at 42 °C for 1 h. Afterwards the Easy Hyb solution was replaced with 10 ml DIG Easy Hyb containing 1 µg DIG-labelled DNA probe (which had previously been boiled for 10 min and chilled on ice in order to get single stranded DNA). The probe was generated by PCR amplification of the Intron gene on the ClosTron plasmid using the primers EBP2 and Intron SalI R1 (Table 2.4). The labelling of the probe was achieved by incorporating DIG-labelled dUTPs using DIG High Prime (Roche). The probe solution was incubated over night at 42 °C.

After the incubation with the probe, the membrane was subjected to two low stringency washes (2 x SSC, 0.1 % (w/v) SDS) for 5 min at room temperature, followed by two high stringency washes (0.5 x SSC, 0.1 % (w/v) SDS) for 15 min at 68 °C. The equilibration of the membrane was conducted by incubating with washing buffer (0.1 M maleic acid, 0.15 M NaOH, pH 7, 0.3 % v/v tween 20) for 1 min at room temperature. The reaction was blocked by

incubating the membrane with 1 x blocking buffer diluted in 1 x maleic acid buffer (Easy Hyb kit) for 30 min at room temperature. This procedure was to block unspecific membrane binding sites for the later added antibody. The membrane then was incubated in blocking buffer containing 1:10,000 diluted anti-digoxigenin antibody (Roche) for 30 min at room temperature, followed by two washes with washing buffer for 15 min at room temperature. Afterwards the membrane was equilibrated in detection buffer (100 mM Tris HCl, pH 9.5, 150 mM NaCl) for 2 min at room temperature. For detection of bands, 1 ml of chemi-luminescent substrate CSDP Star (Roche) was added onto the membrane and the membrane sandwiched between two acetate sheets. Incubation was followed for 10 min at 37 °C. Finally, the membrane was both exposed to an Amersham Hyperfilm ECL (GE Healthcare) and documented in a LI-COR system using 'chemi' set up for 60 min.

2.8 Generation of recombinant organisms

2.8.1 Transformation of *E. coli*

The transformation of bacteria with plasmids was undertaken in two different ways. The first one was the transformation of chemically competent *E. coli* cells. This method was mostly used, especially to introduce plasmids into cells straight after a ligation. The transformation was conducted as follows:

1. 50 µl of chemically competent *E. coli* cells were thawed on ice
2. The cells were carefully mixed with 5 µl of plasmid solution or ligation mixture
3. The mixture was incubated for 20 min on ice
4. The mixture was at 42 °C for 90 s and 500 µl of LB added

5. The resulting suspension was incubated for 60 min at 37 °C whilst shaking
6. Aliquots of 50, 100 and 200 µl of transformation mixture were plated onto LB-agar plates with appropriate selection marker (Table 2.6)
7. Plates were incubated over night at 37 °C

The second way of transforming *E. coli* was *via* electroporation [125].

This method was mainly used to introduce confirmed plasmids into a second *E. coli* host (*E. coli* Sexpress) and was carried out as follows:

1. An electroporation cuvette (2 mm) was chilled on ice
2. 50 µl of electrocompetent cells were thawed on ice and mixed with 5 µl of plasmid
3. Electroporation was carried out using a Bio-Rad Micropulser electroporator and the following settings: 25µF, 200 Ω, 2.5 kV
4. 500 µl of LB medium were added to the cuvette and the resulting suspension transferred into an Eppendorf tube
5. The Eppendorf tube was incubated for 60 min at 37 °C whilst shaking, followed by the plating of 20, 30 and 50 µl aliquots onto LB agar plates with appropriate selection marker (Table 2.6)
6. Plates were incubated over night at 37 °C

Successful transformants were validated *via* plasmid mini-prep (section 2.7.2.2), control digest with appropriate restriction enzymes and sequencing.

Preparation of chemically competent *E. coli* cells

1. Cells were cultures over night (one colony or one bead from culture collection tube in 5 ml LB) and 0.5 ml used for the inoculation of 50 ml LB
2. The culture was incubated at 37 °C until it reached an OD_{600} of 0.4-0.6 (~3 h) and incubated on ice for 10 min
3. The chilled cultures were centrifuged at 4000rpm, 10 min, 4°C
4. The obtained cell pellet re-suspended in 10 ml (cold) 100 mM $CaCl_2$, 20 % v/v glycerol and incubated on ice for 15 min
5. The cell suspension was centrifuged at 4000rpm, 10 min, 4°C and re-suspended in 2 ml (chilled on ice) 100 mM $CaCl_2$, 20 % v/v glycerol and incubated on ice for 1-2 h
6. The suspension was aliquoted (50 – 100 µl) into 2 ml screw cap Eppendorf tubes and stored at -80 °C

Preparation of electrocompetent *E. coli* cells

1. Cells were cultures over night (one colony or one bead from culture collection tube in 5 ml LB) and 2 ml used for the inoculation of 200 ml LB
2. The culture was incubated at 37 °C until it reached an OD_{600} of 0.6-0.8 and incubated on ice for 10 min and subsequently aliquoted into 4 x 50 ml falcon tubes
3. The culture was centrifugated at 4 °C, 3000 *g* for 10 min, the supernatant discarded and the pellet re-suspended in 10 ml chilled 10 % glycerol
4. The mixture was centrifugated at 4 °C, 4000 *g* for 10 min, the supernatant discarded and the cell pellet re-suspended in 500 µl chilled 10 % glycerol
5. The cell mixture was aliquoted (50 µl) into each 2 ml screw cap Eppendorf tubes and stored at -80 °C

2.8.2 Transformation of *C. autoethanogenum via* conjugation

To introduce plasmids into *C. autoethanogenum* the method of conjugation was used, which is the transfer of genetic material between bacterial cells by either direct cell-to-cell contact or by a bridge-like connection between two cells. For conjugation into *C. autoethanogenum* a specific gene (*tra*J) was part of the vector backbone provided by the pMTL80000 modular vector system [115].

The protocol used for the conjugation into *C. autoethanogenum* was as follows:

1. One day prior to the conjugation, transformed *E. coli* Sexpress cells containing the plasmid of interest were inoculated into 5 ml LB containing 50 µg/ml kanamycin and the appropriate antibiotic for plasmid selection
2. Cells were incubated at 37 °C over night in a shaking incubator and YTF plates were prepared and left to equilibrate over night in the anaerobic cabinet
3. The following morning, 2 ml of Sexpress culture were gently pipetted into a microfuge tube and centrifuged for 2 min at 4000 rpm, and the supernatant was carefully removed
4. The cell pellet was gently re-suspended in 500 µl PBS buffer through aspiration with a pipette, and centrifuged for 2 min at 4000 rpm, followed by carefully removal of all supernatant
5. The washed cell pellet was transferred into the anaerobic cabinet, and the pellet left to equilibrate for 1 h
6. After equilibration, the cell pellet was gently re-suspended with 200 µl of *Clostridium* culture (24-36 h old) and the mixture spotted onto the

pre-reduced YTF agar plate without antibiotic selection and incubated for 24 h

7. Selection plates (YTF) containing 250 µg/ml of D-cycloserine to counter-select against the *E. coli*, and an appropriate antibiotic for selection of the plasmid of interest, were prepared and left over night to equilibrate in the cabinet
8. The next day, the conjugation mixture was harvested, using a 10 µl inoculation loop and re-suspended in 300 µl anaerobic PBS
9. The mix was divided over three plates containing antibiotic selection, spreading approximately 150 µl on to each plate
10. The plates were incubated anaerobically for 3-4 days, until discrete colonies were visible

2.9 Protein tools

In order to perform enzyme assays or purify tagged proteins, the proteins had to be isolated from the cells and, thus, cell free extract needed to be obtained. On the following pages the methods regarding the isolation and use of proteins are described.

2.9.1 Cell harvesting and disruption

To isolate tagged proteins from *E. coli*, 5 ml of LB medium supplemented with appropriate antibiotic was incubated with either one colony of a given strain or from -80 °C stocks and incubated over night at 37 °C. This pre-culture was then used to inoculate 200-250 ml of the main LB culture. This was grown up

to an OD_{600} of approximately 1.0, and subsequently divided into 50 ml Falcon tubes and centrifuged at 4 °C and 4000 rpm for 20 min to gain the cell pellet. This pellet could be either stored at -20 °C (for usually not longer than a week) or immediately re-suspended in 10 ml 1x BugBuster® reagent. After the addition of 0.2 mg of avidin (to avoid false-signals in SDS gel and Western Blot), 1 mg lysozyme and 0.5 mg DNase, the mixture was incubated at room temperature at 15 rpm for 20-30 min. Cell fragments were separated from the liquid by centrifugation (20 min, 7000 rpm, 4 °C). The protein concentration in the supernatant was analysed using Bradford reagent [126] (section 2.9.2.2). Subsequently affinity chromatography (section 2.9.2.1) SDS-PAGE (section 2.9.2.3) and/or Western Blot (section 2.9.2.5) and enzyme assays (section 2.9.3) could be conducted with the obtained cell extracts.

Additionally to the cell harvest and use of proteins from *E. coli* cells, the cell extract of *C. autoethanogenum* was needed for various enzyme assays and prepared as follows. *C. autoethanogenum* cells (200 ml) were grown anaerobically for 36-48 h. As the enzyme assays needed to be performed under anaerobic conditions, the disruption and extraction of the crude extract needed to be conducted anaerobically as well. Hence, the cultures were transferred into the anaerobic tent and centrifuged for 30 min at 4 °C and 4000 rpm. The cell pellet was either shock-frozen with liquid nitrogen and stored at -80 °C for not longer than a week, or immediately re-suspended in 1.5 ml 1x BugBuster® reagent supplemented with 3 mg lysozyme and 1 mg DNase and hand-shaken (slowly) for 20 min in the tent. Afterwards, the mixture was transferred into 2 ml screw cap tubes and centrifuged for 20 min at 4 °C and highest speed (7000 rpm). The supernatant was then transferred into 1.5 ml Eppendorf tubes

and stored on ice. Once the crude extract was obtained, it had to be used for enzyme assays on the same day.

2.9.2 Standard protein methods

2.9.2.1 Affinity chromatography using *Strep*-Tactin-Sepharose

To purify *Strep*-TagII fused proteins, affinity chromatography using *Strep*-Tactin-Sepharose (IBA, Göttingen) was conducted. For this 2 ml of 50 % (w/v) *Strep*-Tactin-Sepharose suspension were poured into an empty column (Poly-Prep, Chromatography Columns, BioRad). The liquid was allowed to flow out of the comlumn after an incubation of 5-10 min and the solid material equilibrated with 5 ml washing buffer (W). The prepared cell extract (section 2.9.1) was poured onto the column. Afterwards, the following steps were performed:

1. Washing of the column five times with 1 ml buffer W
2. Elution of the protein four times with 0.5 ml Buffer E
3. The column was regenerated by washing 3 times with 5 ml buffer R (colour turns red)
4. The column was stored with 2 ml buffer W at 4 °C

For the calculation of protein concentrations and preparation of an SDS-PAGE gel, 1 ml of each fraction was stored in 1.5 ml Eppendorf tubes at 4 °C, for same day use. All steps of the protein purification were performed on ice.

Buffer W (Washing and equilibration)

Tris-HCl (pH 8.0)	100	mM
NaCl	150	mM

Buffer E (Elution)

Buffer W + 2.5 mM desthiobiotin

Buffer R (Regeneration)

Buffer W + 1 mM HABA (4'-hydroxyazobenzene-2-carboxylic acid)

2.9.2.2 Determination of protein concentration after Bradford

The protein concentration of both crude extract and fractions of the protein purification was determined after Bradford [126]. For this, the Bradford-constant needed to be examined by creating a standard curve with different concentrations of BSA (50, 100, 200, 400, 600, 800 µg). Protein standard (50 µl) was mixed with 1 ml of Bradford solution, incubated for 5 min at room temperature and subsequently measured at 595 nm using a spectrophotometer. The obtained values were plotted using Excel and a linear regression line calculated. The hereby calculated Bradford constant was used to calculate unknown protein concentrations (as shown below). In order to do so, 50 µl of the given protein extracts were mixed with 1 ml of Bradford-reagent, incubated for 5 min at room temperature and the resulting absorption measured at 595 nm using a spectrophotometer. The washing buffer mixed with reagent was used as blank. The equation used to calculate protein concentrations was the following (ΔE: absorption at 595 nm; df: dilution factor):

$$x = \frac{\Delta E / 0.0011}{1000} \times df \qquad [mg/ml]$$

If the absorption was higher than 0.5, the liquid needed to be diluted in order to sustain an accurate measurement.

2.9.2.3 SDS-PAGE

SDS-Polyacrylamite gels were run in chambers from Analytik Jena and NuPAGE® gels (ThermoFisher) were used [127].

Before gels were loaded, protein samples were mixed with SDS buffer (loading dye) in a ratio of 4:1 and denatured by heating at 99 °C for 10 min.

The gels were run at 30 mA in 1x SDS running buffer (NuPAGE® MES running buffer) at room temperature until the blue colour of the loading dye reached the end of the gel. To distinguish different protein sizes a pre-stained protein weight marker (Color Prestained Protein Standard, Broad Range, NEB) was used.

2.9.2.4 Staining of proteins using colloidal coomassie

To visualise proteins, either colloidal coomassie or SimplyBlue SafeStain (ThermoFisher) was used. When colloidal coomassie was used, protein gels were gently shaken for 60 min in fixing buffer and afterwards stained with colloidal coomassie solution for up to 24 h at room temperature (shaking). De-staining of protein gels was conducted by using dH_2O. If SimplyBlue strain was used, the solution was poured onto the gel, after it had been washed briefly with dH_2O, and left for incubation for about 60 min (shaking). The de-staining was conducted using dH_2O.

The water was exchanged at regular intervals and the procedure continued until the gel was completely de-stained apart from stained protein bands.

Colloidal Coomassie solution

Orthophosphoric acid (85 % [v/v])		23.5	ml
Ammoniumsulfate		100	g
Coomassie stock		20	ml
Methanol (96 %)		200	ml
dH_2O	*ad*	1000	ml

Coomassie stock

Coomassie Brilliant Blue G250		50	g
dH_2O	*ad*	1000	ml

Fixing buffer

Glacial acetic acid		100	ml
Ethanol (96 %)		520	ml
dH_2O	*ad*	1000	ml

2.9.2.5 Transfer of proteins onto membranes (Western Blotting)

By using Western Blotting [128] it was possible to transfer proteins from SDS-PAGE gels onto nitrocellulose membranes. The binding of proteins is ensured *via* hydrophobic interaction and hydrogen bridge linkage. Tagging of proteins (*Strep*-TagII) makes it possible to verify and qualify proteins in the mixture. Building steps of the blot are summarised below:

1. 6x Whatman paper and membrane were cut to the size of the gel
2. The blot was set up as follows (bottom to top, positive (anode) to negative (cathode) plate)
    - 3 layers of Whatman paper (bottom)
    - Nitrocellulose membrane
    - SDS-gel
    - 3 layers of Whatman paper (top)

3. Air bubbles were eliminated by carefully rolling a glass tube after each layer that was added
4. Blotting chamber was closed and added transfer buffer added
5. The current was adjusted to 30 mA and the Blot was run for about 120 min
6. The blotting stock was dissembled

Once the blot was finished, verification of tagged proteins could proceed. For this, *Strep*-Tactin coupled alkaline phosphatase (*Strep*-Tactin AP conjugate, IBA) was used. The coupled alkaline phosphatase is able to transform the substrates NBT (Nitroblue-Tetrazolium chloride) and BCIP (5-Bromo-4-Chloro-3-Indolylphosphate). The complex formed can be seen as a blue-violet coloured complex. The following steps were carried out:

1. The membrane was incubated in 20 ml blocking buffer over night at 4 °C
2. The membrane was washed three times in 1x TGST buffer for 5 min and incubated in 50 ml 1x TGST buffer + 5 µl *Strep*-Tactin conjugate for 45 min at room temperature (slowly shaking)
3. The membrane was washed three times in 1x TGST for 10 min and treaded with 2 ml colouring solution (AP colouring solution) and incubated until signals were visible
4. The reaction was stopped by with dH_2O and the membrane dried for documentation purposes

Blocking buffer

1 x TGST buffer	50	ml
BSA	0.5	g
Milk powder	2.5	g

10x TGST buffer

Tris		1.21	g
NaCl		0.55	g
Tween 20		0.5	g
dH_2O	*ad*	100	ml

The pH was adjusted to 8.0 using HCl and the buffer stored at 4 °C.

10 x AP buffer

Tris		1.21	g
NaCl		5.7	g
$MgCl_2$		0.47	g
dH_2O	*ad*	100	ml

The pH was adjusted to 9.5 using HCl and the buffer stored at 4 °C.

AP colouring solution

NBT/BCIP-solution		5	µl
1x AP buffer	*ad*	2	ml

2.9.3 Enzyme assays

To demonstrate various enzyme activities in either cell free extracts or for purified proteins, the following enzyme assays were performed. Enzyme assays were either conducted under aerobic or anaerobic conditions, depending on assay requirements, at 37 °C. In all cases quartz cuvettes were used in order to measure absorption within the UV spectrum.

To calculate enzyme activities the following equation was used:

$$\text{Volume activity} = \frac{\Delta E/\text{min} \cdot V}{\varepsilon \cdot \delta \cdot \nu} \qquad [\frac{U}{ml}]$$

V: volume in cuvette [ml]; v: volume of used extract [ml]; ΔE: change in extinction per minute [min^{-1}]; ε: extinction coefficient [$cm^2/\mu mol$]; d: length of light path through the cuvette [cm]

Specific enzyme activity [U/mg] was calculated by dividing the volume activity by the protein concentration.

All enzyme assays were performed in 1 ml in 1 cm quartz cuvettes, using the Specord 250 photospectrophotometer (Analytik Jena) in combination with the WinASPECT program (version 2.4.0.0) to analyse the obtained data. As negative control both water as substrate and water instead of cell free extract were used.

2.9.3.1 Fumarate hydratase

Fumarate hydratase (FH), also known as fumarase, catalyses the reversible reaction of fumarate to malate. To measure its activity in the cell free extracts, the method after Hatch (1978) was used [129] (Figure 2.2). Enzyme activity was calculated as mentioned previously, using the extinction coefficient of NADP(H) at 340 nm of 6.3 x 10^3 mol^{-1} cm^{-1}(6.3 $cm^2/\mu mol$) [130].

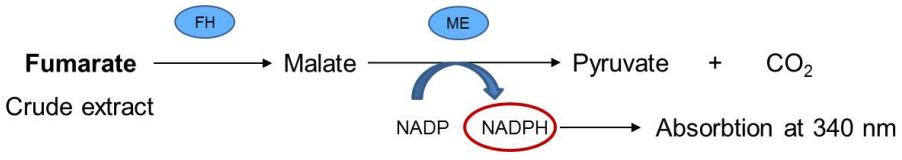


Figure 2.2: Fumarate hydratase enzyme assay.
FH: fumarate hydratase, ME: malic enzyme.

The pipetting scheme for 1 ml reaction solution was as follows:

1. 100 µl of 250 mM Hepes-KOH buffer (pH 7.5)
2. 40 µl of 10 mM $NADP^+$
3. 10 µl of 400 mM $MgCl_2$
4. 50 µl of 100 mM potassium phosphate buffer (pH 7.5)
5. 0.2 U NADP dependent malic enzyme (ME; Sigma-Aldrich)
6. 10 – 40 µl cell free extract
7. Start reaction by the addition of 10 mM sodium fumarate

The increase of absorbance due to the formation of NADPH was followed at 340 nm under aerobic conditions at 37 °C.

2.9.3.2 Alcohol Dehydrogenase

Alcohol dehydrogenase (ADH) catalyses the reversible reaction from acetaldehyde to ethanol. For both reaction directions, enzyme assays have been published. For clostridial ADHs, both assays had to be conducted under anaerobic conditions.

The assay for the forward reaction (acetaldehyde to ethanol) used in this work, was published by Hillmer *et al.* in 1972 [131]. Here, acetaldehyde was used as substrate to start the reaction. In 1 ml cuvette the following solutions and concentrations were present:

1. 940 µl of 70 mM potassium phosphate buffer (pH 7.6)
2. 10 µl of 50 mM NADH
3. 10 µl of 100 mM glutathione (reduced)
4. 10 – 40 µl cell free extract
5. 10 µl of 1 M acetaldehyde (start reaction)

The decrease in absorption due to the formation of NAD^+ from NADH was followed at 340 nm. The extinction coefficient used to calculate enzyme activities was 6.3 x 10^3 mol^{-1} cm^{-1}(6.3 cm^2/µmol) [130].

In order to measure the reverse reaction (ethanol as substrate) similar, but slightly modified method was used. In here the addition of ethanol started the reaction in which NAD^+ was converted into NADH and therefore an increase in absorbance was measured [132]. In the 1 ml cuvette the following solutions and concentrations were present:

1. 940 µl of 70 mM potassium phosphate buffer (pH 7.6)
2. 10 µl of 150 mM NAD^+
3. 10 µl of 100 mM glutathione (reduced)
4. 10 – 40 µl cell free extract
5. 10 µl of 50 % (v/v) ethanol (start reaction)

2.9.3.3 Acetaldehyde Dehydrogenase

Like the ADH, the acetaldehyde dehydrogenase (AlDH) catalyses both forward and reverse reaction from acetyl-CoA to acetaldehyde. Again, the enzyme assays were conducted under anaerobic conditions.

For the forward reaction the method described by Clark and Cronan in 1980 was used [133] which follows the increase in absorbance at 340 nm due to the formation of NADH from NAD^+. Hence, the extinction coefficient of 6.3 x 10^3 mol^{-1} cm^{-1}(6.3 cm^2/µmol) was used for activity calculations [130]. The pipetting scheme for this assay was as follows (1 ml cuvette):

1. 920 µl of 54 mM CHES buffer (pH 9)
2. 10 µl of 10 mM CoASH (Coenzyme A)
3. 10 µl of 100 mM DTE
4. 10 µl of 150 mM NAD^+
5. 10 – 40 µl cell free extract
6. 10 µl of 1 M acetaldehyde (start of reaction)

For the reverse direction, using acetyl-CoA as substrate, a similar method was used, modified after Hillmer *et al.* [131]. Here, the addition of acetyl-CoA started the reaction in which NADH was converted into NAD^+ and therefore the decrease in absorbance was measured at 340 nm. The pipetting scheme for this assay was as follows (1 ml cuvette):

1. 920 µl of 54 mM CHES buffer (pH 9)
2. 10 µl of 10 mM
3. 10 µl of 100 mM DTE
4. 10 µl of 50 mM NADH
5. 10 – 40 µl cell free extract
6. 10 µl of 13 mM acetyl-CoA (start of reaction)

2.9.3.4 Fumarate reductase

The fumarate reductase (FRD) catalyses the reaction of fumarate to succinate. This reaction is non-reversible as the energy barrier is too high to allow NADH formation. The method used, described in 2008 by Miura *et al.* [134], relies on the formation of NAD^+ from NADH and therefore a decrease in absorbance at 340 nm is detectable under aerobic conditions. For activity calculations the extinction coefficient of 6.3 x 10^3 mol^{-1} cm^{-1} (6.3 $cm^2/\mu mol$) was used [130]. The assay mixture contained the following:

1. 859 µl of 50 mM sodium phosphate buffer (pH 6.5)
2. 2 µl of 100 mM NADH
3. 10 – 40 µl cell free extract
4. 100 µl of 200 mM sodium fumarate (start reaction)

2.9.3.5 Acetate kinase

To measure acetate kinase (ACK) enzyme activity, enzyme assays in both the physiological [135], and non-physiological [132], direction were performed under aerobic conditions.

To measure enzyme activity in the physiological direction, a three-step coupled-assay was required, as described in Figure 2.3.

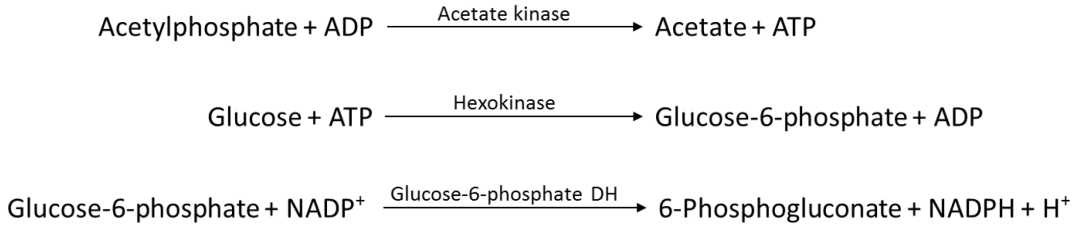


Figure 2.3: Reactions involved in the acetate kinase assay (physiological direction).

The increase in absorption at 340 nm (production of NADPH) was measured. For activity calculations the extinction coefficient of 6.3 x 10^3 mol^{-1} cm^{-1} was used. The assay mixture contained the following:

1. Imidazole-HCl (400 mM, pH 7.3)	50 µl
2. Glucose (80 mM)	50 µl
3. $MgCl_2$ (120 mM)	50 µl
4. $NADP^+$ (12.8 mM)	50 µl
5. ADP (40 mM)	50 µl
6. Acetyl phosphate (200 mM; stored at -70 °C)	25 µl

7. Hexokinase (2 mg/ml) 20 µl
8. Glucose-6-phosphate dehydrogenase (1 mg/ml) 20 µl
9. Cell free extract 40 µl
10. dH_2O 100 µl

After the addition of the sample, the mix was incubated for 1 min, then the reaction started with acetyl phosphate.

For the non-physiological direction, the following consecutive reactions were necessary:

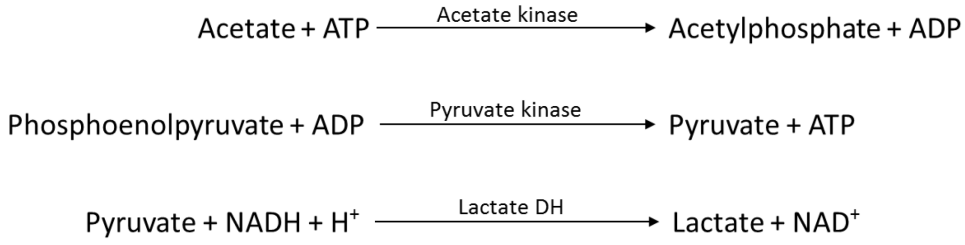


Figure 2.4: Reactions involved in the acetate kinase assay (non-physiologicaldirection)

The decrease of NADH was measured in this reaction (Figure 2.4).

Therefore, the following substances were needed:

1. Imidazole-HCl (400 mM, pH 7.3) 100 µl
2. $MgCl_2$ (100 mM) 100 µl
3. Phosphoenolpyruvate (15 mM) 50 µl
4. NADH + H^+ (14 mM) 20 µl
5. ATP (50 mM) 50 µl
6. Lactate dehydrogenase (5 mg/ml) 2 µl
7. Pyruvate kinase (10 mg/ml) 2 µl
8. Myokinase (1000 U/ml) 4 µl
9. Cell free extract 40 µl
10. Potassium acetate (3.2 M) 50 µl

The consumption of NADH after the addition of potassium acetate was followed at 340 nm. For activity calculations the extinction coefficient of 6.3 x 10^3 mol^{-1} cm^{-1} (6.3 $cm^2/\mu mol$) was used [130].

2.10 Metabolite analyses

In order to determine nature and concentration of metabolic products formed by *C. autoethanogenum*, various analytic methods were used.

2.10.1 Gas chromatography

For analysing samples by gas chromatography (GC), 1 M standards for Na-acetate and ethanol were prepared in 1 ml dH_2O (58.4 µl of 100 % ethanol; 82.03 mg of Na-acetate). Afterwards, standard concentrations were generated according to Table 2.8 using ELGA water (ultra-pure filtered).

Table 2.8: Dilution scheme for GC standards

Standard concentration [mM]	Volume from 1 M stock [µl]	Volume water [µl]
0	0	1000
1	1	999
3	3	997
5	5	995
10	10	990
30	30	970
50	50	950
100	100	900
150	150	850

Both standards and centrifuged culture supernatant samples (2.6) were treated as follows:

The samples (500 µl) were mixed with 5 µl 10 M H_2SO_4. To this mixture, 500 µl of propyl propionate containing 50 mM valeric acid (as internal standard) were added and the solutions mixed thoroughly by vortexing for 10 s. The extraction mix was afterwards centrifuged at >21 000 *g* for 1 min in order to remove possibly denatured protein. Afterwards, 300 µl of the top layer were pipetted into a GC sample vial containing and insert and screw cap.

The setup of the GC and determination of the peak values were undertaken by technicians Matthew Abbott and James Fothergill, University of Nottingham. Metabolite concentrations were calculated with the help of the internal standards.

2.10.2 High-performance liquid chromatography

Analysis of metabolic samples was also conducted *via* high performance liquid chromatography (HPLC). Standard solutions for this procedure were a 1 M stock mixture of 1 M ethanol, 1 M acetate, 1 M butyrate, and 1 M propanediol, and additionally 1 M solutions of sodium-fumarate, fructose, magnesium-aspartate and sodium-pyruvate. Those 1 M solutions were diluted to 100 mM, 50 mM, 25 mM, 10 mM and 1 mM solutions which were used to generate standard curves. Afterwards 300 µl of the standard solutions and samples were mixed with 300 µl of 5 mM H_2SO_4 plus 50 mM valerate as internal standard. The samples were filtered through 0.2 µm syringe filters directly into HPLC vials containing 300 µl inserts with split caps. The standards were filled into the HPLC vial directly without filtering.

Running of the instrument and all data analysis were carried out by Matthew Abbott, University of Nottingham.

2.10.3 Gas chromatography- mass spectrometry

Additionally to GC and HPLC analyses, Gas chromatography-mass spectrometry (GC-MS) was used for analysing samples. This was, bceause fumarate and some other C_3 and C_4 compounds cannot be traced by GC and the HPLC retention times for fumarate, acetate and aspartate were the same.

For the measurement of fumarate, pyruvate, aspartate, lactate and succinate standards were used in concentrations of 20, 10, 5, 2.5, 1.25 mM (dilution of 0.1 M solutions in ultrapure water). The samples and standards were prepared as follows:

1. Addition of 20 µl of standard/sample to a 2 ml screw cap centrifuge tube
2. Addition of 200 µl of 0.5 M sodium hydroxide solution
3. Additionof 200 µl of 4:1 1-propanol:pyridine
4. Addition of 10 µl of 10 mM benzoic acid
5. Addition of 20 µl of propyl chloroformate
6. The tube was closed, vortexed, the lid slowly opened in the fume cupboard and closed again
7. Vortexed for 30 s
8. Addition of 20 µl of propyl chloroformate
9. Vortexed for 30 s
10. Addition of 400 µl of chloroform
11. Vortexed for 10 s
12. Addition of 400 µl of 50 mM sodium bicarbonate
13. Vortexed for 10 s
14. 200 µl were transferred into a 300 µl glass insert in a vial, vial sealed using a snap cap

All GC-MS experiments were conducted with the help of James Fothergill, University of Nottingham, who set up GC-MS measurements and conducted the analyses.

2.10.4 Liquid chromatography–mass spectrometry

Liquid chromatography–mass spectrometry (LC-MS) analyses were performed by Dr. Sarah Schatschneider and Dr. Salah Abdelrazig, University of Nottingham. Supernatant and cell pellet samples, stored at -80 °C were handed over to either of the postdocs, who then ran the LC-MS and analysed generated data.

2.10.5 Nuclear magnetic resonance

All nuclear magnetic resonance (NMR) analyses were conducted in cooperation with Dr. Huw E.L. Williams and Alexander T. Wichlacz from the School of Chemistry, University of Nottingham, using a Bruker AV(III) 800 MHz spectrometer (equipped with a 5 mm QCI cryoprobe). NMR tubes used were Wilmad 535-PP-7 with screw top and Wilmad 507-PP-7. Before undergoing NMR analyses, the samples were thawed and concentrated *in vacuo*, before preparation using H_2O (540 µl), D_2O (55 µl) and DSS (10 mM, 5 µl). DSS was included as an internal standard to reference to 0.0 ppm in ^{1}H NMR in conjunction with the HMDB database to known metabolite standard NMR peaks [136]. The methods used to follow the metabolism of fumarate were: quantitative ^{1}H NMR, quantitative ^{1}H with ^{13}C decoupling, quantitative ^{13}C NMR and multiplicity edited ^{1}H-^{13}C-HSQC. Quantitative NMR experiments were acquired with solvent suppression, using a NOESY 1D

experiment with a recycling delay of 15 s to ensure complete relaxation of metabolites for determination of concentration. This value was calculated from a T1 relaxation experiment performed on the metabolites in culture, and the overall recycling delay was used as 5xT1 for the metabolite with the largest T1 value.

All data analyses were carried out by Alexander T. Wichlacz. All NMR acquisitions and analyses were performed with Bruker Topspin.

2.10.6 *In vivo* NMR analyses

In order to follow fumarate consumption over time, *in vivo* NMR analyses were conducted. *C. autoethanogenum* cells were grown on both $^{13}C_4$- and 2,3-$^{13}C_2$-labelled fumarate within in the NMR machine at 37 °C. NMR tubes used were Wilmad 535-PP-7 with screw top additionally sealed with PTFE tape. DSS and D_2O were added into the medium as standards for later data analysis. D_2O provided a convenient signal at the deuterium frequency that is a significant distance from other nuclei of interest present in the sample. Therefore, it was possible to monitor this frequency and use it as a reference (*via* the lock hardware) to correct for small field drifts in the main magnetic field without perturbing other signals. This increased the stability of the NMR measurement. A secondary effect was that the frequency of D_2O is known and the magnetic field is corrected in such a way as to reference the chemical shift scale [112][113].

Before the experiment was commenced, it was established that these chemicals were not toxic to the cells in the respective amounts.

The total amount of liquid in the anaerobic NMR tube was 650 µl: 540 µl PETC-MES medium (section 2.3.2), 55 µl D_2O and 5 µl 10 mM DSS. For inoculation, 50 µl of a 24 h pre-culture (grown on ^{12}C fumarate) were used.

For the experiments 4.2 mg of fumarate were dissolved in the PETC-MES medium in the anaerobic cabinet. For the partially labelled experiment 2,3-$^{13}C_2$-labelled disodium fumartae was obtained from Sigma-Aldrich. For the fully labelled experiment $^{13}C_4$ fumaric acid was obtained from GOSS Scientific. The disodium salt of the fumaric acid was generated by dissolving the compound in water, and adjusting the pH to 7 using sodium hydroxide. The mixture was then lyophilised by Alexander T. Wichlacz over night and resulted in sodium fumarate, which precipitated as white powder.

After inoculation, the tube was transferred into a Bruker AV (III) 800 MHz spectrometer. Methods used in order to analyse these samples were quantitative ^1H NMR, quantitative ^{13}C-decoupled NMR and ^{13}C-HSQC. All methods were programmed to measure the sample every hour. To ensure constant cell growth, the NMR tube was ejected every 8 h and cells mixed by inverting the NMR tube by hand. All data was analysed by Alexander T. Wichlacz. All NMR acquisitions and analyses were performed with Bruker Topspin.

3 Growth of *C. autoethanogenum* on C_4 dicarboxylic acids

If I seem to wander, if I seem to stray, remember that true stories seldom take the straightest way.

Patrick Rothfuss, Name of the Wind

3.1 Introduction

When Abrini *et al.* isolated *C. autoethanogenum* in 1994, the growth of the organism was tested on various carbon sources [35]. Not only could this bacterium grow on CO alone and H_2 plus CO_2, but also on pyruvate, xylose, arabinose, fructose, rhamnose and L-glutamate. Substrates tested but reported not to be utilised were formate, lactate, methanol, succinate, fumarate, melibiose, trehalose, citrate, glucose, starch, mannose, galactose, xylan, melezitose, saccharose, lactose, maltose, sorbitol, esculin and raffinose.

In 2013 it was stated in a patent, that *C. autoethanogenum* is able to produce succinate in quantities of 0.002 g l^{-1} (equivalent 17 µM) [106], and in 2016 it was found that this bacterium produces succinate as an "overflow" product [139]. Furthermore, for the very closely related *C. ljungdahlii* fumarate utilisation had been reported [36]. The pathways involved remained unknown, although it appears likely that succinate was produced from fumarate as a direct precursor. Thus, before any serious attempts could be made at engineering *C. autoethanogenum* to produce succinate, it was necessary to investigate the natural capacity of the organism to metabolise and produce C_4 dicarboxylic acids.

The specific aims of this study were therefore to

- Interrogate the genome of *C. autoethanogenum* to identify genes for putative enzymes involved in C_4 dicarboxylic acid metabolism.
- Investigate whether addition of exogenous fumarate would stimulate succinate production.
- Establish the capacity of *C. autoethanogenum* to utilise C_4 dicarboxylic acids as sole sources of carbon and energy, including succinate, fumarate, malate and oxaloacetate.
- Determine the activities of the encoded enzymes under different growth conditions.

3.2 Results

3.2.1 Genome investigation for existing C_4 dicarboxylic acid utilisation and production pathways in *C. autoethanogenum*

Before experimentally analysing the C_4 dicarboxylic acid metabolism of *C. autoethanogenum* and therewith the production pathway of succinate, the genome of the organism was studied with regards to its production pathways *in silico*.

Hereby, genes encoding for specific enzymes involved in the C_4 dicarboxylic acid metabolism (one branch of the TCA cycle; Figure 3.1) were found, as well as genes involved in succinate production *via* the reductive TCA pathway (Figure 3.2). Both analyses led to the assumption that *C. autoethanogenum* might be able to grow on various dicarboxylic acids (Figure 3.1).

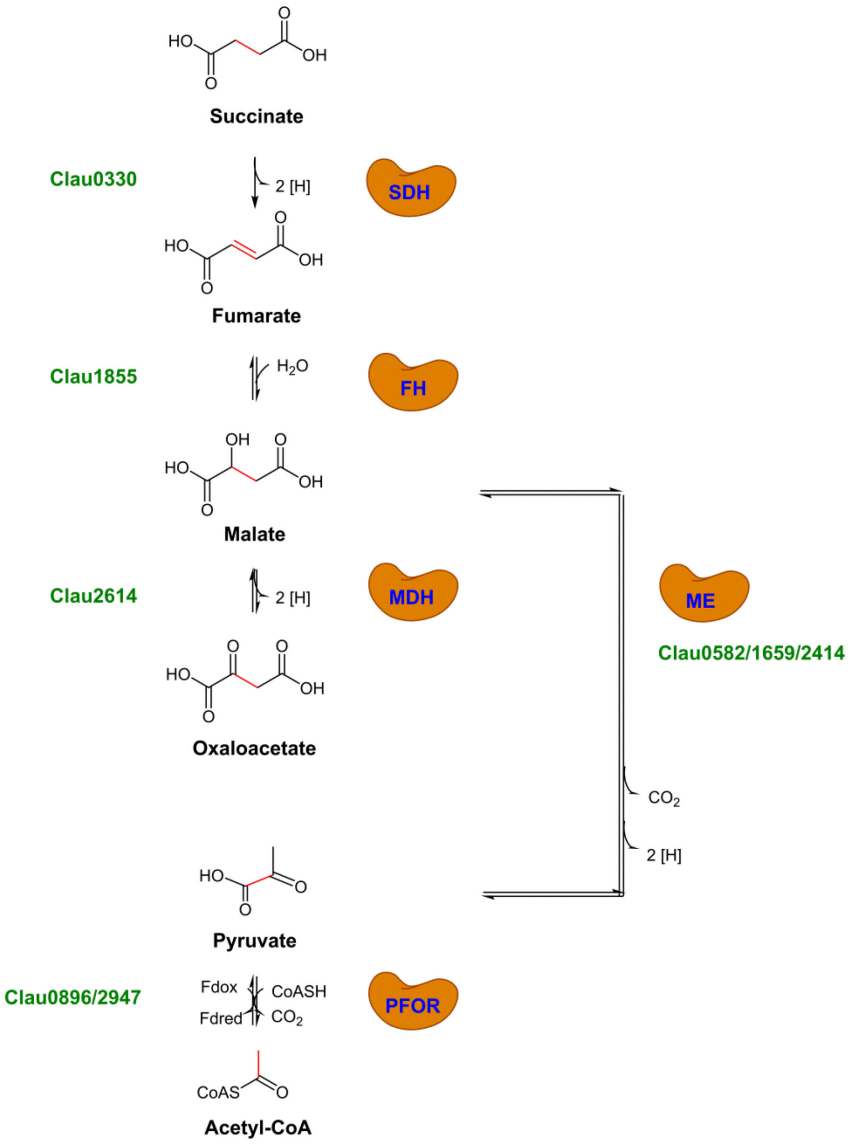


Figure 3.1: Proposed pathway of a branch of the TCA cycle in *C. autoethanogenum*.
Proposed utilisation of succinate and other C_4 carboxylic acids in *C. autoethanogenum*. Shown are all the intermediates and enzymes required together with their annotated locus tags from *C. autoethanogenum*. SDH: Succinate dehydrogenase; FH: Fumarate hydratase; ME: Malic enzyme; MDH: Malate dehydrogenase; PFOR: Pyruvate-ferredoxin oxidoreductase.

The enzyme converting fumarate to succinate, fumarate reductase, could be found in the genome sequence encoded by one gene, Clau0330, which was also annotated to encode for a succinate dehydrogenase. However, this protein only consists of 108 amino acids, which is very short compared to other succinate dehydrogenases and fumarate reductases [40][41].

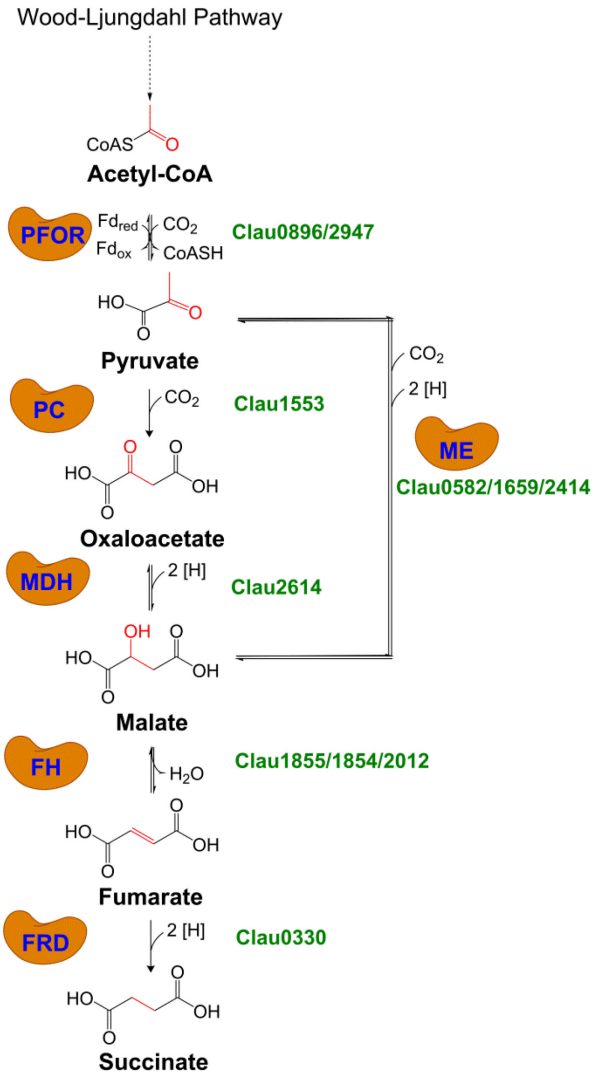


Figure 3.2: Putative route of succinate production by *C. autoethanogenum via* the reductive TCA pathway.

Acetyl-CoA, produced *via* the WLP, serves as starting metabolite. Shown are all the intermediates and enzymes required together with their annotated locus tags from *C. autoethanogenum*. PFOR: Pyruvate-ferredoxin oxidoreductase; PC: Pyruvate carboxylase; ME: Malic enzyme; MDH: Malate dehydrogenase; FH: Fumarate hydratase; FRD: Fumarate reductase.

3.2.2 Utilisation of C_4 dicarboxylic acids

3.2.2.1 Fumarate feeding experiments

To investigate whether provision of fumarate had any effect on succinate production of *C. autoethanogenum*, cultures were grown in the presence of various concentrations of fumarate (0 mM, 10 mM, 20 mM and 30 mM) and a fixed amount of fructose (40 mM). The medium used was PETC-ljungdahlii medium (section 2.3.2).

Figure 3.3 shows growth (OD_{600}) of *C. autoethanogenum* on fructose with and without additional fumarate. Interestingly, higher OD values were achieved in the presence of fumarate, even though previous studies had indicated that these bacteria should be unable to utilise fumarate as carbon source [35]. The observation that overall growth was dependent on fumarate concentration required further investigation.

To investigate fumarate uptake, metabolism and influence on growth, 2,3-$^{13}C_2$-labelled fumarate was used in a subsequent growth experiment. Metabolites were analysed *via* NMR and LC-MS.

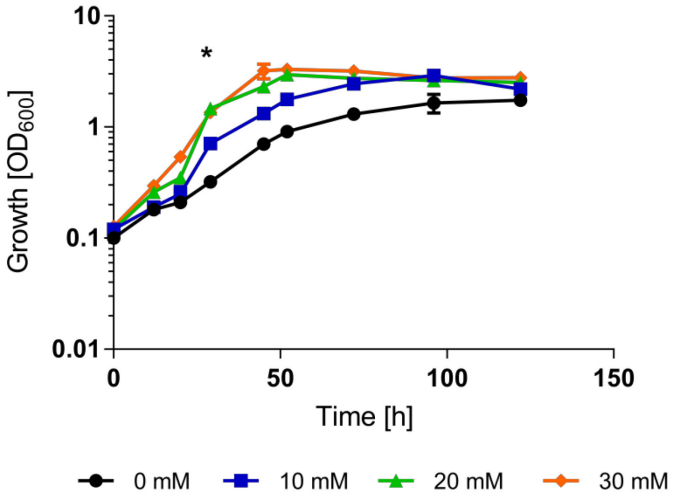


Figure 3.3: Fumarate feeding improves growth of *C. autoethanogenum*.
Growth (OD_{600}) of *C. autoethanogenum* on 40 mM fructose (black circles), fructose plus 10 mM fumarate (blue squares), fructose plus 20 mM fumarate (green triangles), and fructose plus 30 mM fumarate (orange diamonds). Differences in growth upon addition of fumarate were significant from time point at 29 h onwards. Significance determined using paired $t(4) = 7.16$, $p = 0.002$ (10 mM); $t(4) = 14.04$, $p = 0.000$ (20 mM); $t(4) = 10.52$, $p = 0.000$ (30 mM); at time point 29 h, respectively. Data shown as mean ± SEM (n = 3).

3.2.2.2 Growth of *C. autoethanogenum* on 2,3-$^{13}C_2$-labelled fumarate plus fructose

Since addition of fumarate to PETC-ljungdahlii growth medium had led to increased growth of *C. autoethanogenum*, the metabolic fate of fumarate was further investigated by using 2,3-$^{13}C_2$-labelled fumarate. Labelled fumarate, 15 mM, was added to PETC-ljungdahlii medium which was reduced using cysteine (0.33 mM).

As before, growth of *C. autoethanogenum* was higher with the additional fumarate than without (Figure 3.4). This was expected after the previous feeding experiments (section 3.2.2.1). However, LC-MS analyses of samples

taken at the end of the growth experiment showed the same concentration of succinate (Figure 3.5).

During these analyses, the pure medium (without inoculated culture) was also analysed regarding its succinate concentration. It was found that the concentration of succinate was the same in the pure medium as in the supernatant after growth of *C. autoethanogenum*. This led to the hypothesis that the undefined yeast extract in the medium supplied a specific amount of succinate. This assumption was proven *via* LC-MS analyses to be correct, as shown in Figure 3.6. Therefore, the medium used in all future growth analyses was changed to PETC-MES medium (section 2.3.2) which was without yeast extract and thus did not contain succinate.

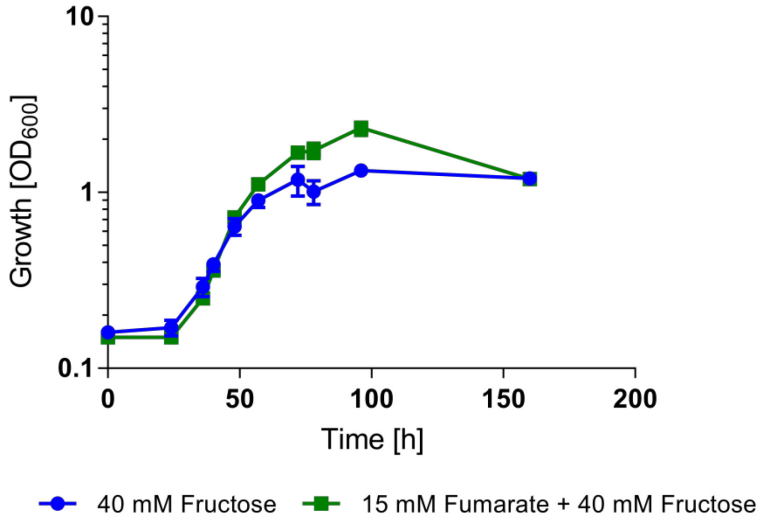


Figure 3.4: Growth of *C. autoethanogenum* on 15 mM 2,3-$^{13}C_2$-labelled fumarate and fructose.

Growth of *C. autoethanogenum* on 15 mM 2,3-$^{13}C_2$-labelled fumarate plus 40 mM fructose (green), compared to only 40 mM fructose (blue). Data shown as mean ± SEM (n = 3).

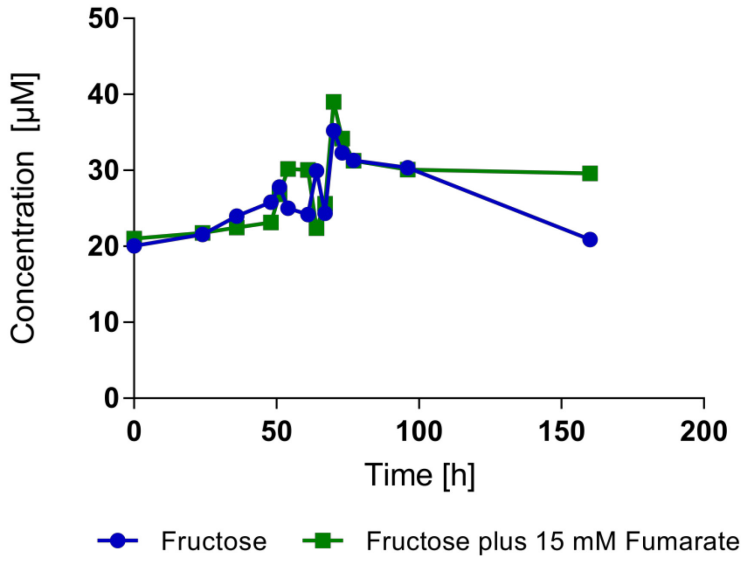


Figure 3.5: Succinate concentration in culture supernatants following growth of *C. autoethanogenum* on fructose and fructose plus fumarate.

Succinate concentrations [µM] in supernatants was measured by LC-MS following growth on 40 mM fructose (blue circles) and fructose plus 15 mM fumarate (green squares).

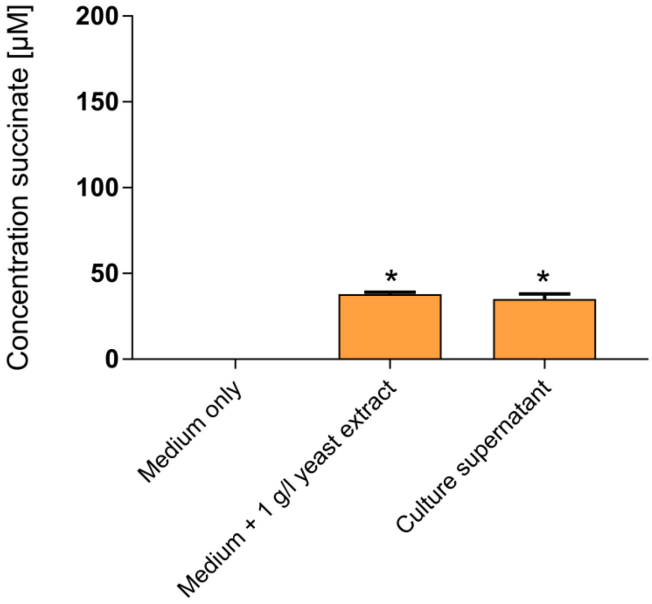


Figure 3.6: Analyses of succinate concentrations in different culture media.

Succinate concentrations were measured *via* LC-MS in samples of the following PETC medium variants: with and without yeast extract and the supernatant of a *C. autoethanogenum* culture after the growth on 40 mM fructose in PETC-ljungdahlii medium. Stars indicate significant difference to medium only, determined using paired t-test $t(8) = 77.04$, $p = 0.000$ (Medium plus yeast extract), $t(8) = 26.16$, $p = 0.000$ (Culture supernatant). Data shown as mean ± SEM ($n = 5$).

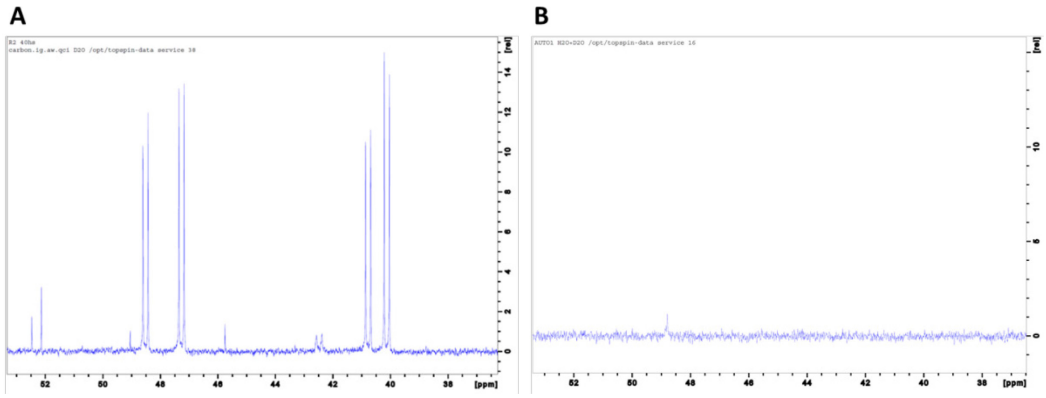


Figure 3.7: ^{13}C NMR Carbon profile of unknown labelled compounds in supernatants of *C. autoethanogenum* cultures grown on fructose and 2,3-$^{13}C_2$ fumarate.

A: ^{13}C NMR carbon profile of two ^{13}C-labelled compounds measured in the supernatant of a cell culture containing PETC-MES medium with 15 mM 2,3-$^{13}C_2$-labelled fumarate plus 40 mM fructose and 0.33 mM cysteine; B: ^{13}C NMR carbon profile of supernatants samples of a cell culture containing PETC-MES medium plus 40 mM 2,3-$^{13}C_2$-labelled fumarate and 0.25 mM sodium sulfide.

Samples of the 2,3-$^{13}C_2$-labelled fumarate growth experiment were also used for NMR analyses. Here, two unknown ^{13}C-labelled substrates in the supernatant of the cultures were revealed (Figure 3.7A). A search of literature revealed that fumarate can react with cysteine to form succinyl-cysteine [140], which was found to be one of the unknown compounds found in the ^{13}C NMR carbon profile. Thus, it was tested whether the chemical was also generated when fumarate (dissolved in water) and cysteine (dissolved in water) were combined without the influence of other chemicals or bacteria (data not shown). Thereby it was found that succinyl-cysteine was indeed generated spontaneously in a so-called Thio-Michael Addition (Figure 3.8) [141].

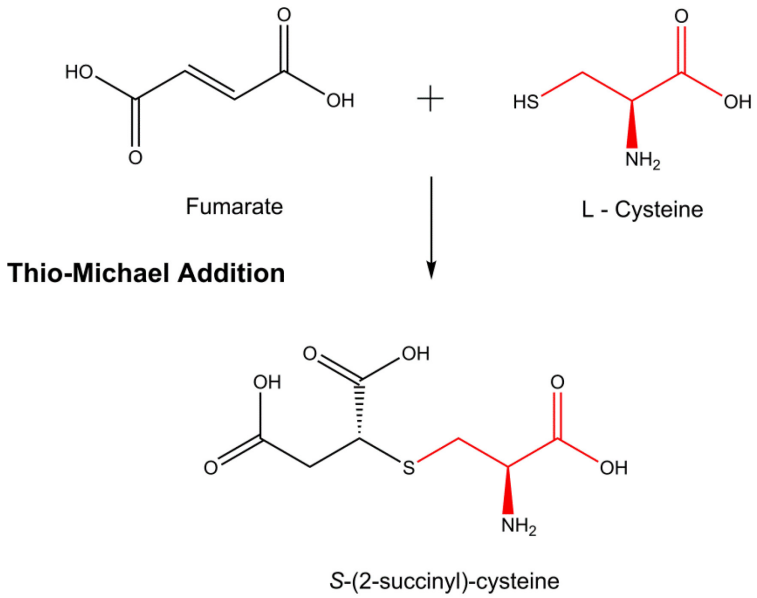


Figure 3.8: Thio-Michael Addition leading to the generation of succinyl-cysteine.
Thio-Michael Addition occurs as a result of a nucleophilic attack of a 1,4-conjugated system by a thiol group.

The second labelled compound was structurally very similar to the first and showed only a slight shift in the carbon spectrum. Most likely, this shift was caused by small changes in the succinyl-cysteine structure which could have been caused by another diastereomer. However, the exact structure of the second compound could not be determined with certainty.

Due to this undesirable reaction of cysteine, which was used in the medium as reducing agent and sulfur source, it was replaced by sodium sulfide (Na_2S) (sections 2.3.2 and 2.3.3). Using this chemical, none of the above mentioned ^{13}C-labelled compounds could be found in connection with 2,3-$^{13}C_2$-labelled fumarate (Figure 3.7B).

3.2.2.3 Growth of *C. autoethanogenum* on different carbon compounds

Following the above described changes to the growth media and in order to explain the observation that fumarate led to an increased growth but no increased succinate production, the ability of *C. autoethanogenum* to grow on various carbon compounds, including succinate and fumarate, was analysed. This was performed, to either corroborate or disprove previous work by Abrini *et al.* who stated that both fumarate and succinate were not used as (sole) carbon source [35].

A pre-culture after 40 h growth on fructose was used to inoculate serum bottles containing 50 ml PETC-MES medium and 40 mM succinate, fumarate, malate, oxaloacetate, pyruvate and citrate, respectively. All substrates were chosen due to their influence on, or their involvement in the TCA cycle.

It was found that *C. autoethanogenum* was able to grow on fumarate, malate, pyruvate and oxaloacetate with final OD_{600} values close to 1 or higher (Figure 3.9A). With regards to growth on succinate and citrate, after an initial growth up to OD_{600} 0.4, which was due to the remaining fructose of the pre-culture used for initial growth, there was a rapid decrease in OD, comparable to the control without added carbon source. After that, the provided carbon source could not be metabolised.

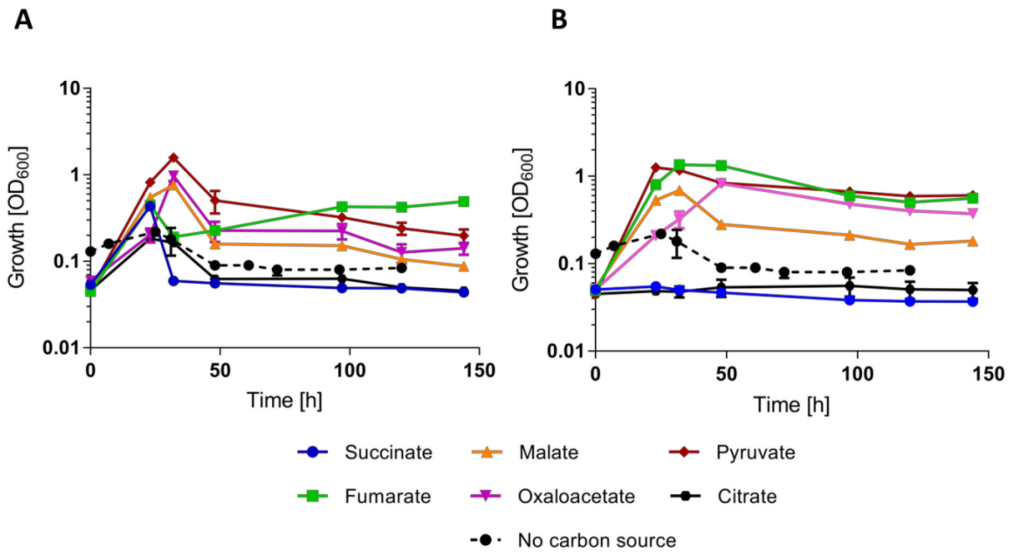


Figure 3.9: Growth of *C. autoethanogenum* on various carbon sources.

Growth of *C. autoethanogenum* on 40 mM succinate (blue circles), fumarate (green squares), malate (orange triangles), oxaloacetate (pink inverted triangles), pyruvate (dark red diamonds) and citrate (black hexagons), respectively, using, A: cells grown on fructose as pre-culture, and B: cells grown on fumarate. As control, cultures without added carbon source were used from fructose pre-cultures (black dashed line). Data shown as mean ± SEM (n = 3).

During the growth on fumarate, after initial growth followed by a slight decrease of the OD, the culture reached a final OD of 0.6. This culture (at OD_{600} of 0.8) was used to inoculate Hungate tubes containing 10 ml PETC-MES medium plus 40 mM fumarate. This fumarate adapted culture, devoid of contaminating fructose, reached ODs of higher than 1.

In order eliminate fructose from the pre-cultures, and to compare the ability of fumarate adapted cells to grow on the previous mentioned carbon sources, the above described growth experiment was repeated with pre-cultures grown on fumarate for 24 h. Under these conditions, *C. autoethanogenum* was able to grow on malate, oxaloacetate, pyruvate and fumarate, but did not show growth on succinate and citrate (Figure 3.9B). The initial growth on succinate and citrate seen with fructose grown pre-cultures was not detectable.

Due to the discovery of the ability of *C. autoethanogenum* to use fumarate as the sole source of carbon and energy, further experiments to compare the bacterium's growth on fructose with fumarate were conducted. The findings of these experiments are presented in the following section.

3.2.2.4 Growth of *C. autoethanogenum* on fumarate

As shown in Figure 3.9, it was possible to grow *C. autoethanogenum* on PETC-MES medium with 40 mM fumarate and achieve ODs of higher than 1 after adaptation. Subsequently, the growth characteristics of *C. autoethanogenum* grown on fructose and fumarate were being compared with regards to growth rate, pH and metabolic spectrum. The growth experiment was prepared as described in section 2.6 in 50 ml PETC-MES medium containing serum bottles in biological triplicates. As carbon sources 40 mM fructose and 40 mM fumarate were used respectively. Sodium sulfide was used as sulfur source and reducing agent. Cultures grown on fructose were inoculated from pre-cultures grown on fructose, and cultures grown on fumarate were inoculated from pre-cultures grown on fumarate.

The growth rate (using at least three data points within the exponential growth phase) of cells grown on fumarate was higher compared to fructose (Figure 3.10A) and the maximum OD during the growth on fumarate was lower. The pH of cells grown on fructose decreased over time by 1.5 units, whereas, when grown on fumarate, the pH slightly increased from 5.7 to 6.2.

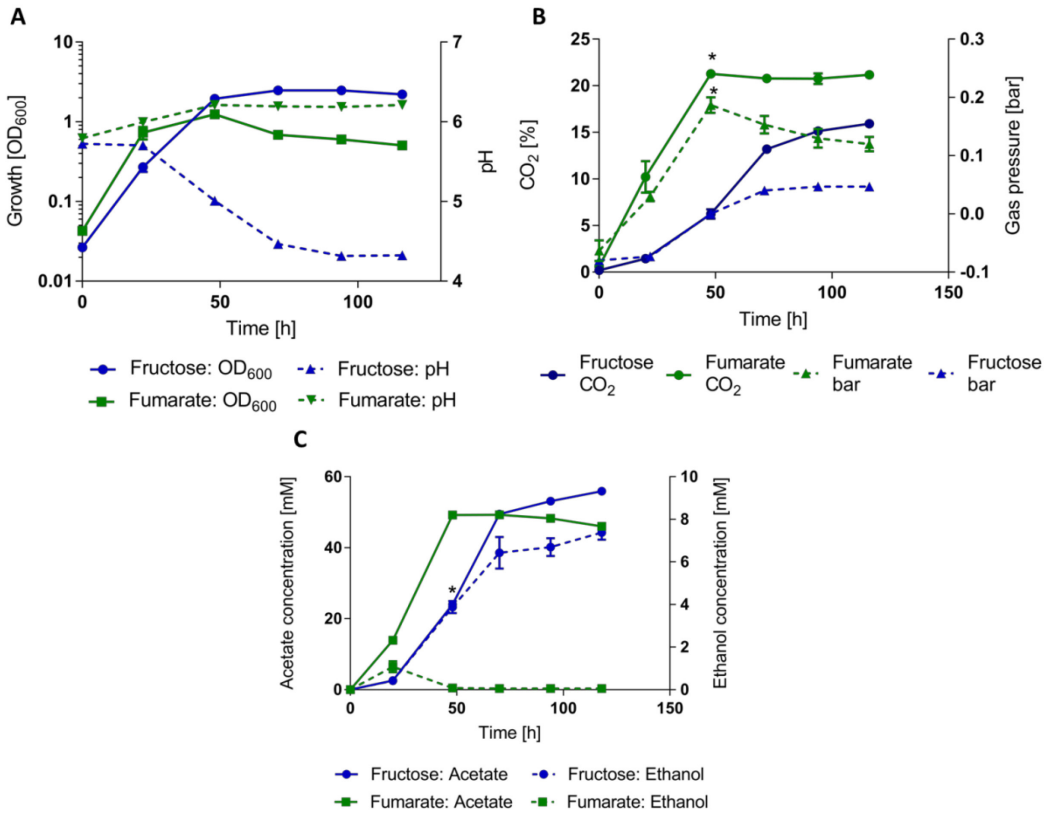


Figure 3.10: Optical density, pH, concentration of CO_2, gas pressure in the headspace, and acetate and ethanol production of *C. autoethanogenum* cultures during growth on fumarate and fructose, respectively.

A: OD_{600} and pH over time of cells grown on fructose (blue circles) and fumarate (green squares). Pre-cultures grown on fructose and fumarate, respectively. B: Concentration of CO_2 [%] (solid lines, circles) inside and the pressure [bar] (dashed lines, triangles) on the serum bottles were determined during the growth of *C. autoethanogenum* on fructose (blue) and fumarate (green). Significance for CO_2 data determined using paired t(4) = 21.74, p = 0.000; gas pressure significance determined using paired t(4) = 12.96, p = 0.000. From 20 h onwards, all data points were significantly different, shown is the specific analysis for 48 h, as example. C: Concentration in mM of acetate (solid lines) and ethanol (dashed lines) over time, measured *via* GC in the supernatant of *C. autoethanogenum* grown on fructose (blue) and fumarate (green). Ethanol significance determined using paired t(4) = 22.09, p = 0.000. From 20 h onwards, all data points were significantly different, shown is the specific analysis for 48 h, as example. Data shown as mean ± SEM (n = 3).

The cultures calculated specific growth rate (μ) was nearly twice as high for cells grown on fumarate with μ = 0.098 ± 0.001 (n = 3), compared to cells grown on fructose with μ = 0.050 ± 0.0004 (n = 3). This was reflected in the doubling time which was with 7.07 ± 0.09 h (n = 3) for cells grown on fumarate about half as long as for cells grown on fructose (13.78 ± 0.12 h (n = 3)). This is comparable to previous findings by Mock *et al.* in 2015, who determined a doubling time for *C. autoethanogenum* grown in a batch culture on fructose of 15 hours [32].

When cells were grown on fumarate, both gas pressure and CO_2 concentration were considerably increased in comparison to growth on fructose (Figure 3.10B). These differences were statistically significant. After 48 h of growth on fumarate, and therefore after the cells reached the end of the exponential growth phase (Figure 3.10B), the gas pressure in the serum bottles started to decrease again, although the CO_2 concentrations appear to remain unchanged. The ratio of CO_2 to nitrogen however, stayed constant (data not shown). The increase in CO_2 on fructose during stationary phase may be explained by a lack of reducing equivalents (H_2), which is most likely caused by ethanol formation.

The metabolic spectrum with focus on acetate, ethanol and succinate production was measured using HPLC and compared between cells grown on fructose and fumarate. However, it was found that the acetate and fumarate signal overlapped during HPLC analyses. Therefore, acetate and ethanol concentration were measured using GC. Fructose concentrations were measured using HPLC (data not shown). Succinate concentrations produced by *C. autoethanogenum* during growth on fructose and fumarate was under the detection limit of the HPLC (around 0.3 mM). Therefore, those measurements were repeated using LC-MS which can analyse lower concentrations.

However, the data obtained from these experiments were inconclusive due to wrong carbon balances in comparison with fructose and fumarate concentrations and questionable dilution rates.

As demonstrated in Figure 3.10C, the ethanol production of cells grown on fructose was significantly higher (7.4 mM) compared to cells grown on fumarate. It also appeared that, when cells grew on fumarate, ethanol was being produced during the first 24 h, albeit at very low amounts (1 mM, exponential growth phase), but was subsequently re-used. Acetate production reached the highest concentration (50 mM) when reaching the end of the exponential phase, when cells grew on fumarate. When grown on fructose, the highest concentration of acetate was reached after 118 h (end of experiment) with 56 mM.

Using data acquired during the GASCHEM project with regards to the cell composition of *C. autoethanogenum* (see Appendix d.ii) and data published [142][143][144], the carbon balance for *C. autoethanogenum* during the growth on both fructose and fumarate was calculated. Table 3.1 shows an overview of the differences observed in terms of growth characteristics and product formation. The concentrations of the used fumarate (and therefore the carbon recovery) were estimated using data provided from ^{13}C-labelled growth experiments (section 3.2.3) due to inconclusive LC-MS results for this experiment.

Table 3.1: Growth characteristics and products of *C. autoethanogenum* grown on fructose and fumarate.

Data for serum bottle fermentations in biological triplicates at time point of maximum OD_{600} (fructose: 94 h; fumarate 48 h). Data shown as mean ± SEM.

	Fructose	Fumarate
Growth characteristics		
Specific growth rate (μ) [h^{-1}]	0.05 ± 0.0004	0.098 ± 0.001
Doubling Time [h]	13.78 ± 0.12	7.07 ± 0.09
Max. OD_{600}	2.48 ± 0.11	1.24 ± 0.04
Carbon Recovery [%]	88.51 ± 3.68	84.29 (estimate)
Product concentrations [mM]		
Carbon source used	180 ± 1.65	128 (estimate)
Acetate	55.91 ± 2.92	45.03 ± 0.91
Ethanol	7.37 ± 0.34	-
Biomass	32.49 ± 1.46	16.31 ± 0.49
CO_2	0.27 ± 0.05	1.53 ± 0.13

3.2.3 *In vivo* analyses of fumarate metabolism by *C. autoethanogenum* cultures grown in an NMR tube

Following preliminary experiments of the growth of *C. autoethanogenum* on $^{13}C_4$-labelled sodium fumarate (data not shown), it was determined that a new approach to investigate *C. autoethanogenum* fumarate metabolism, was to grow cultures in a special anaerobic and sealed NMR tube (Figure 3.11A) within an NMR machine (Figure 3.11B). This allowed measuring substrate consumption and metabolite production of undisturbed cells *in vivo*. As substrates, both 2,3-$^{13}C_2$- and $^{13}C_4$-labelled fumarate were used. All NMR acquisitions and analyses were performed with Bruker Topspin by Alexander T. Wichlacz in collaboration with Dr. Huw E.L. Williams (University of Nottingham). The ability to reproducibly grow under these conditions was established in preliminary experiments, using unlabelled fumarate, first in anaerobic cabinets and then in the NMR machine.

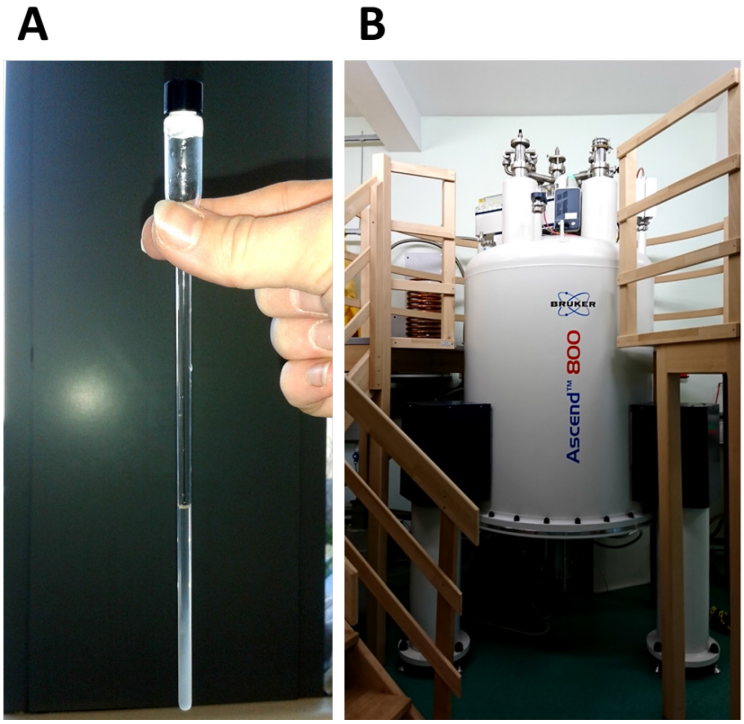


Figure 3.11: NMR tube with *C. autoethanogenum* culture (A) and Bruker AV(III) 800 MHz spectrometer (B).

A: sealed, anaerobic NMR tube with a growing *C. autoethanogenum* culture in PETC-MES medium plus Na_2S supplemented with 40 mM fumarate; B: NMR machine (Bruker AV(III) 800 MHz, equipped with a 5 mm QCI cryoprobe) used for *in vivo* NMR analysis of *C. autoethanogenum* cultures.

3.2.3.1 Growth of *C. autoethanogenum* on 2,3-$^{13}C_2$-labelled fumarate

C. autoethanogenum was grown at 37 °C in an NMR tube in the NMR machine and *in vivo* measurements undertaken every hour as described under 2.10.5 and 2.10.6. The culture volume used was 650 µl in total and contained 40 mM (calculated to be 4.2 mg) of 2,3-$^{13}C_2$-labelled fumarate (Sigma Aldrich) in 540 µl PETC-MES medium (plus Na_2S), as well as appropriate amounts of D_2O and DSS, the latter acting as a standard reference.

Every hour a quantitative ^{1}H NMR, quantitative ^{13}C-decoupled NMR and ^{13}C-HSQC NMR experiment were performed (section 2.10.6). In order to agitate

the samples and to ensure constant cell growth, the NMR tube was ejected every eight hours and cells mixed by inverting the NMR tube by hand. The MES, which was used to buffer the medium, unfortunately might have blocked some of the signals, as it showed three large peaks on the NMR spectrum (Figure 3.12). It was attempted to reduce the amount of MES used, however, this resulted in an inhibition of the bacterial growth (data not shown). Therefore, it was decided to continue using PETC-MES medium for the *in vivo* analyses, as the main compounds of interest (fumarate, acetate and ethanol) were still visible.

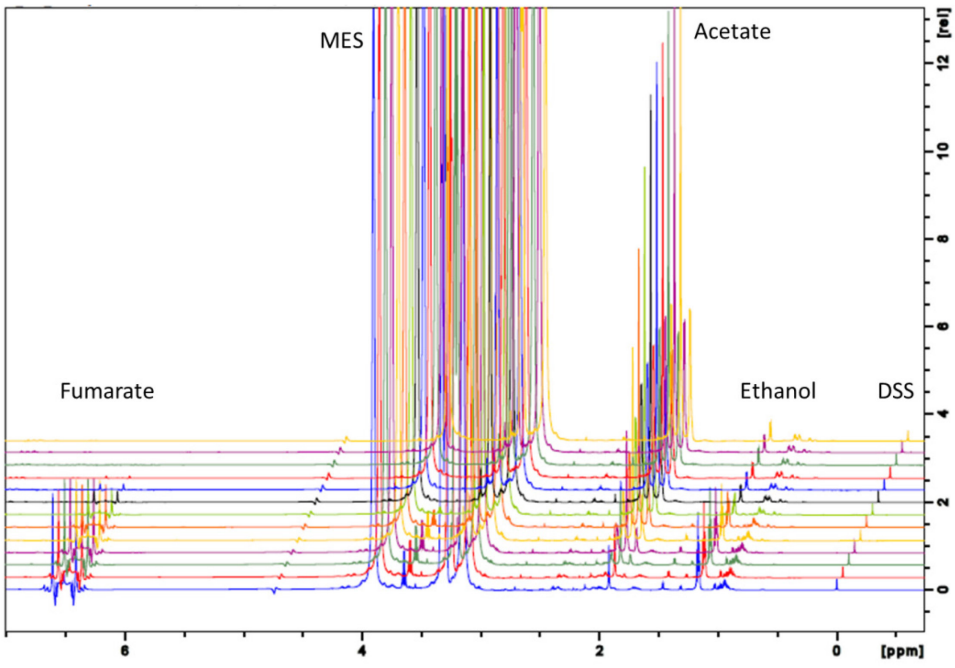


Figure 3.12: Plot of NMR spectra of *C. autoethanogenum* cultures using 2,3-$^{13}C_2$-labelled fumarate as carbon source taken over time.

Staggered plot of metabolites consumed and produced by *C. autoethanogenum* from 0 (front blue line) to 72 (last yellow line) h, for every 6 h. Fumarate, MES, acetate, ethanol and DSS peaks are highlighted.

Figure 3.12 shows a staggered plot of the metabolic spectrum of *C. autoethanogenum* over time in an overview. Labelled are fumarate, acetate, ethanol, MES and DSS.

The fumarate peak disappeared after 52 h of growth, whereas the acetate peak continued to increase. It can also be seen that the ^{13}C shoulders of the acetate peak did not overtake the ^{12}C peak of the acetate (this can be seen more clearly in Figure 3.14). The ethanol peak disappeared over time and an unknown, but unlabelled, compound was revealed under the ethanol peak (Figure 3.14).

Figure 3.13 shows a close-up of the fumarate peak, and Figure 3.14 displays both the acetate and ethanol peaks, by enlarging the respective ppm regions.

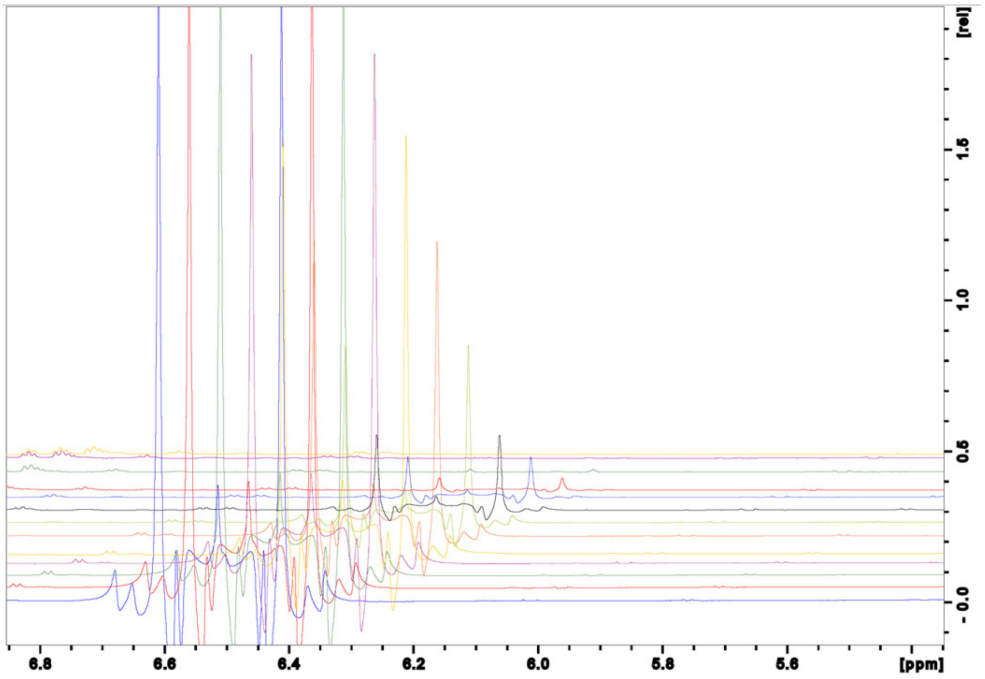


Figure 3.13: Staggered plot of 2,3-$^{13}C_2$-labelled fumarate NMR peak over time.

Staggered plot of NMR spectra showing fumarate consumption by *C. autoethanogenum* from 0 (front blue line) to 72 (last yellow line) h, for every 6 h. The enlarged area displays the fumarate peak at around 6.5 ppm.

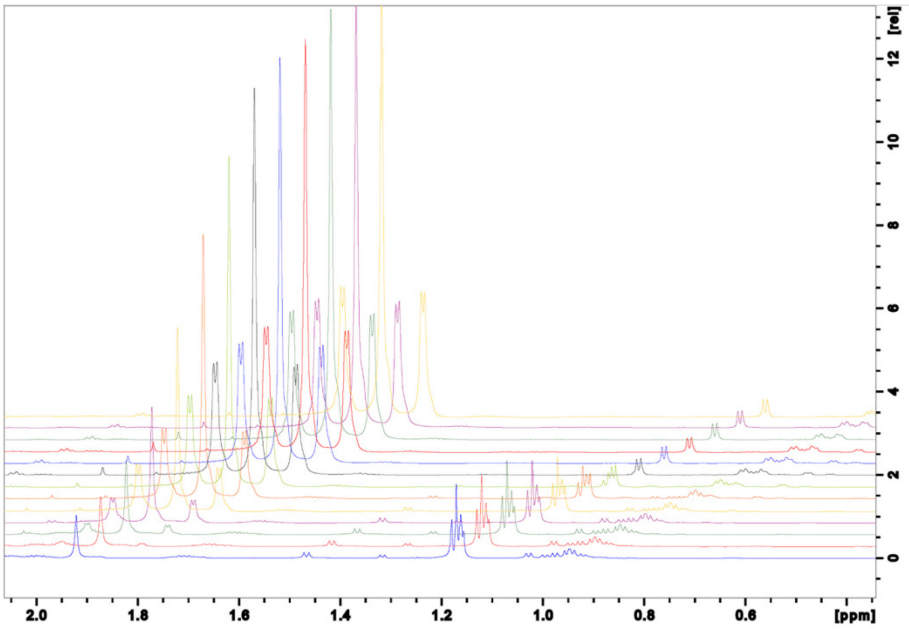


Figure 3.14: Staggered plot of acetate and ethanol NMR peaks over time during growth on 2,3-$^{13}C_2$-labelled fumarate.

Staggered plot of NMR spectra showing acetate and ethanol production (and consumption) by *C. autoethanogenum* from 0 (front blue line) to 72 (last yellow line) h, for every 6 h. The enlarged area displays the acetate (at 1.925 ppm) and ethanol (at 1.18 pm) peaks.

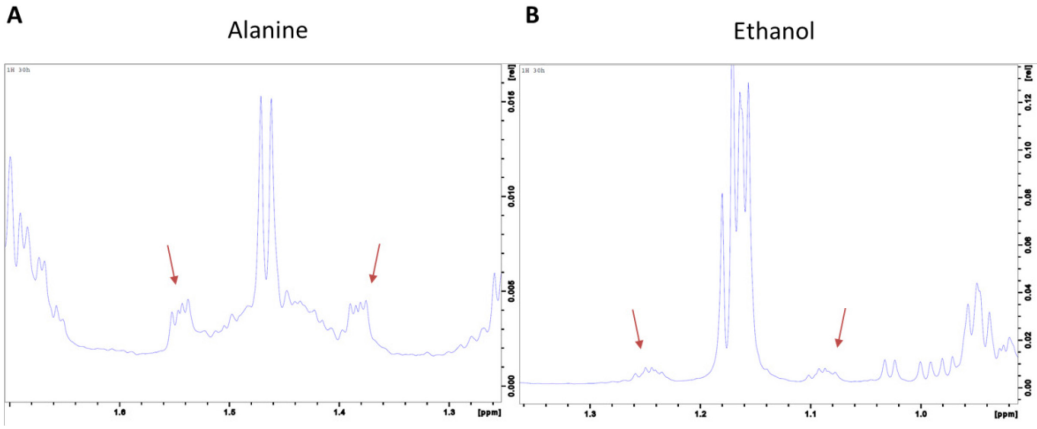


Figure 3.15: Alanine and ethanol NMR peaks with highlighted ^{13}C shouldering peaks.

^1H NMR pictures of (**A**): alanine (1.46 ppm) and (**B**): ethanol (1.18 ppm) peaks appearing, after 30 h of *in vivo* growth of *C. autoethanogenum* using 2,3-$^{13}C_2$-labelled fumarate as carbon source. The ^{13}C peaks appearing on the side of the ^{12}C peaks are highlighted with red arrows.

In these staggered plots, however, the ethanol peaks, and more importantly the appearing ^{13}C shoulders, are difficult to represent as the peaks are very low. In addition to the expected products acetate and ethanol, it was found that ^{13}C alanine was also generated in small amounts, and later re-consumed. However, this is also difficult to present in a staggered plot, for the same reason as for ethanol. Therefore, Figure 3.15A and B represent those peaks at a single time point, and the ^{13}C shouldering peaks are highlighted.

As can be seen for both alanine and ethanol, the characteristic ^{13}C peaks shouldering the ^{12}C peak do appear and therefore the quantity of ^{13}C can be calculated for these metabolites.

Using the provided DSS with its known concentration and number of protons, the concentrations of both the substrate used and products formed could be calculated. Additionally, the concentrations of ^{12}C and ^{13}C acetate was calculated separately, thus the exact amount of labelled fumarate that was used could be determined. The concentration of fumarate provided (11 mM) appeared to be lower than the previously calculated 40 mM (Figure 3.16). This was most likely due to the settings during the run of the NMR. The ^{13}C label causes a second order effect in the NMR, where the multiplet pattern becomes complex and non-trivial to analyse and interact with the solvent suppression routines to distort the singlet further. To overcome this problem, a change in the NMR setup was needed. This, however, only became obvious after the experiment had commenced. The new setup was used for later run as described in section 3.2.3.2.

As a consequence the actual concentration of the fumarate in this experiment could not be exactly calculated. However, it is clearly seen that the amount of ^{12}C and ^{13}C acetate differ slightly with a concentration of ^{13}C acetate of 18 mM

and 16 mM for ^{12}C acetate. Using later generated data (section 3.2.3.2; fully labelled experiment) it was calculated that the pre-culture used for inoculation, provided enough ^{12}C fumarate to generate around 7 mM ^{12}C acetate (compare Figure 3.20). The subtraction of those 7 mM from the measured 16 mM of ^{12}C acetate, led to a measured production of 9 mM ^{12}C acetate. Based on the resulting ratio of 2:1 for ^{13}C acetate to ^{12}C acetate, the assumption followed that all four carbons provided by 2,3-$^{13}C_2$ fumarate (labelled and unlabelled) were utilised, to some extent, for acetate formation.

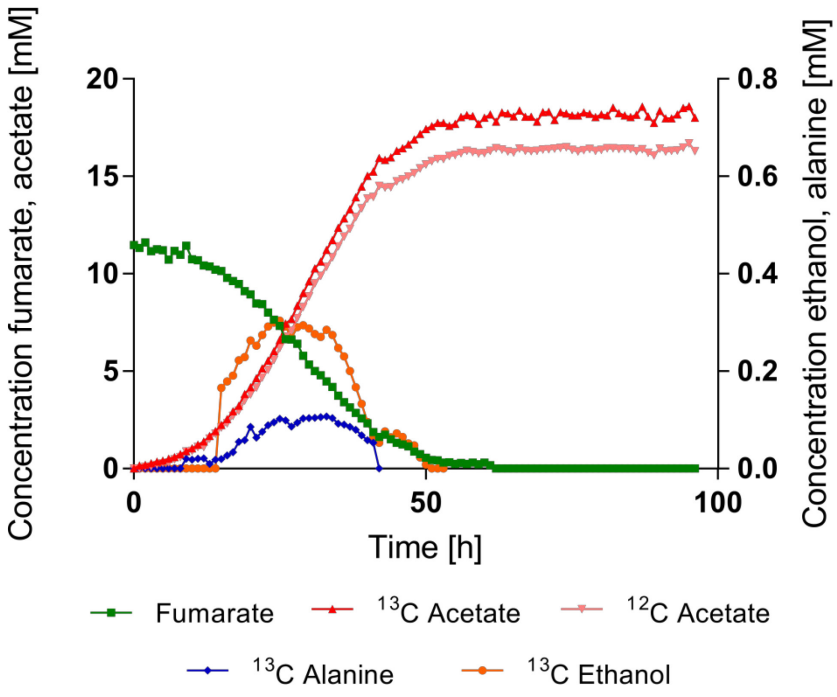


Figure 3.16: Metabolite profile of a *C. autoethanogenum* culture grown on 2,3-$^{13}C_2$-labelled fumarate within an NMR tube.

Shown are substrate and product concentrations over time during growth of a 650 µl *C. autoethanogenum* culture within an anaerobic NMR tube with 2,3-$^{13}C_2$-labelled fumarate as the sole source of carbon and energy. Green squares: fumarate; red upside triangles: ^{13}C acetate; pink downside triangles: ^{12}C acetate; blue circles: ^{13}C alanine; orange diamonds: ^{13}C ethanol. Please note that the estimated fumarate concentrations are too low, based on the solvent suppression used in this method. Metabolite concentrations were calculated from the NMR spectra shown in Figure 3.12.

The 2:1 ratio suggested that 1.5 molecules of acetate are made per 1 molecule of fumarate consumed. Hence, this was tested using fully labelled ($^{13}C_4$) fumarate to allow precise calculation of the ratio by allowing to eliminate unlabelled acetate generated from unlabelled material carried over from the pre-culture (section 3.2.3.2).

3.2.3.2 Growth of *C. autoethanogenum* on $^{13}C_4$-labelled fumarate

After the findings of the first *in vivo* growth experiment using partially labelled fumarate, a second study with fully labelled fumarate was undertaken using the same experimental setup, apart from the problems caused by the second order effect and solvent suppression which were resolved by adjusting the latter.

Figure 3.17 shows an overview of the obtained data of the $^{13}C_4$-labelled *in vivo* NMR experiment in a staggered plot. It can be seen that the peak intensity of fumarate decreased over time, whereas the peak intensity of acetate increased, as observed before. Figure 3.18 displays both peak areas in more detail. Here it can be noticed, that the fumarate peaks disappeared completely. After 60 h, the ^{12}C acetate peak remained at the same height. In contrast to the partially labelled experiment, in which the ^{13}C shouldering peaks never showed a higher peak intensity than the ^{12}C acetate peak, here the ^{13}C shouldering peaks of the acetate eventually did. In contrast to the previously explained partially labelled experiment, in the fully labelled one all peaks, caused by the second order effect, were above the base line, which allowed a more precise integration of the peaks and therefore calculation of the concentration.

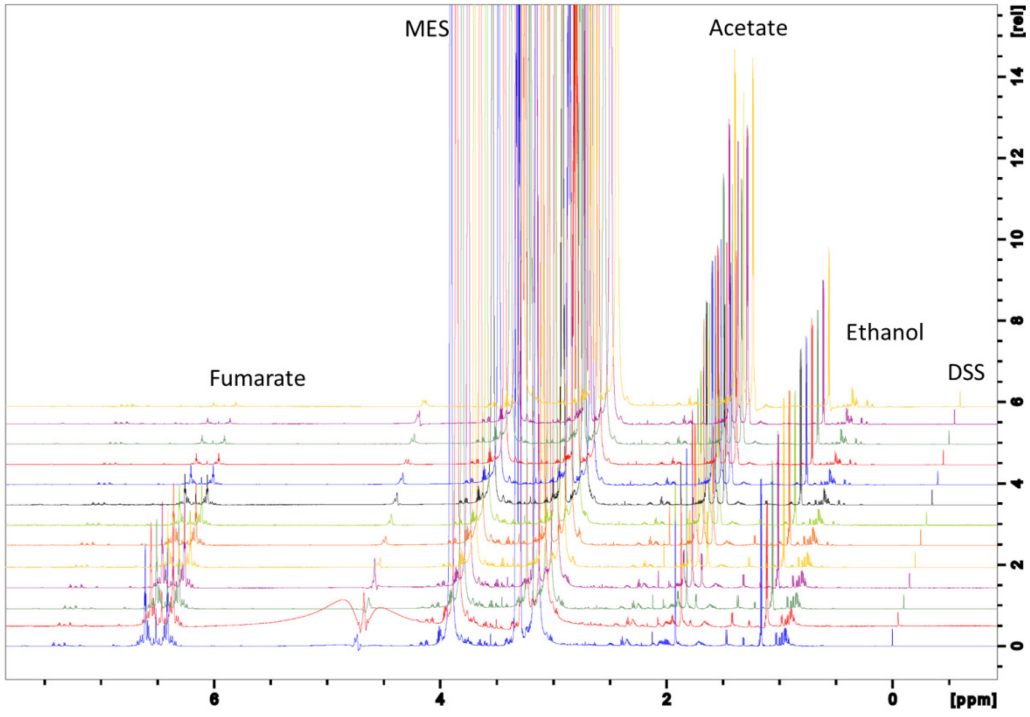


Figure 3.17: Plot of NMR spectra of *C. autoethanogenum* cultures using $^{13}C_4$-labelled fumarate as carbon source taken over time.

Staggered plot of metabolites consumed and produced by *C. autoethanogenum* from 0 (front blue line) to 72 (last yellow line) h, for every 6 h. Fumarate, MES, acetate, ethanol and DSS peaks are highlighted.

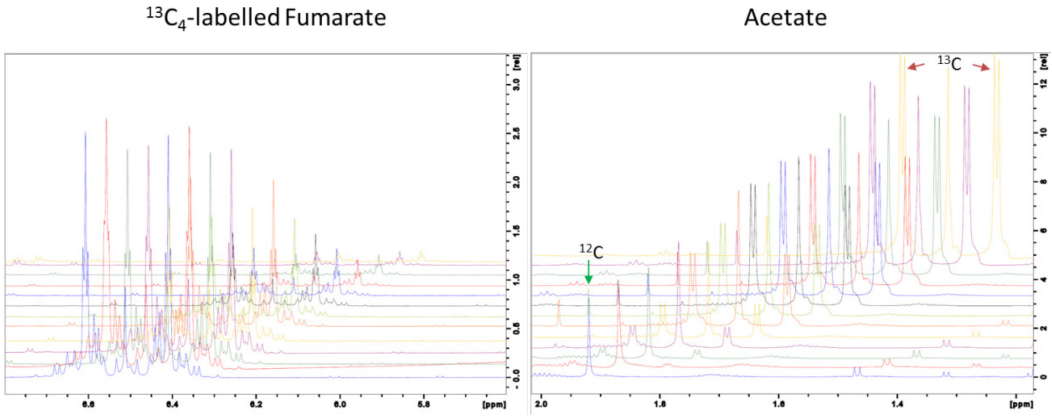


Figure 3.18: Staggered plot of $^{13}C_4$-labelled fumarate and acetate NMR peaks over time.

Shown are staggered plots of fumarate consumed and aceate produced by *C. autoethanogenum* from 0 (front blue line) to 72 (last yellow line) h, every 6 h. The ^{12}C and ^{13}C peaks of the acetate are highlighted with green and red arrows respectively.

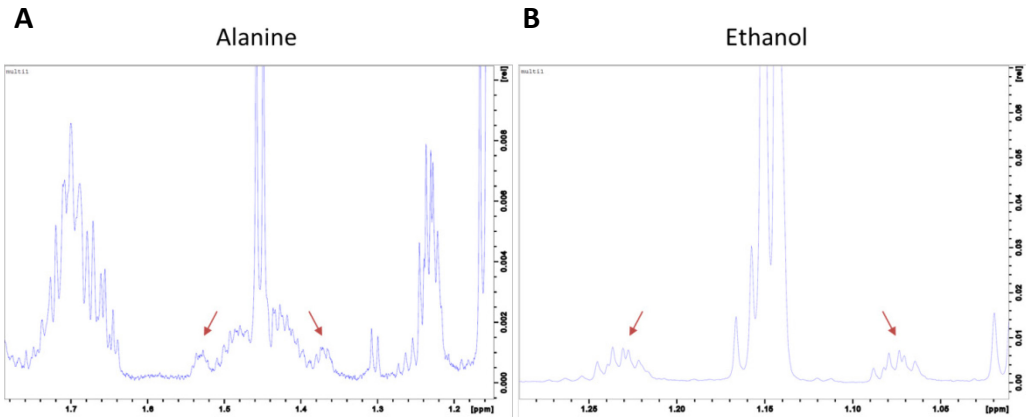


Figure 3.19: Alanine (A) and ethanol (B) NMR peaks with highlighted ^{13}C shouldering peaks.

^{1}H NMR pictures of A) alanine (1.46 ppm) and B) ethanol (1.18 ppm) peaks appearing, after 30 h of *in vivo* growth of *C. autoethanogenum* using $^{13}C_4$-labelled fumarate as carbon source. The ^{13}C peaks appearing on the side of the ^{12}C peaks are highlighted with red arrows.

In addition to the production of acetate, ^{13}C-labelled ethanol and alanine could be measured. Since both peaks were too small to be seen clearly in a staggered plot, only the enlarged spectra for the 30 h time point, are displayed in Figure 3.19. The characteristic ^{13}C shouldering peaks are highlighted with red arrows. As described in section 3.2.3.1 concentrations of the substrate and products could be calculated quantitatively. The following shows the concentrations of the substrate and products.

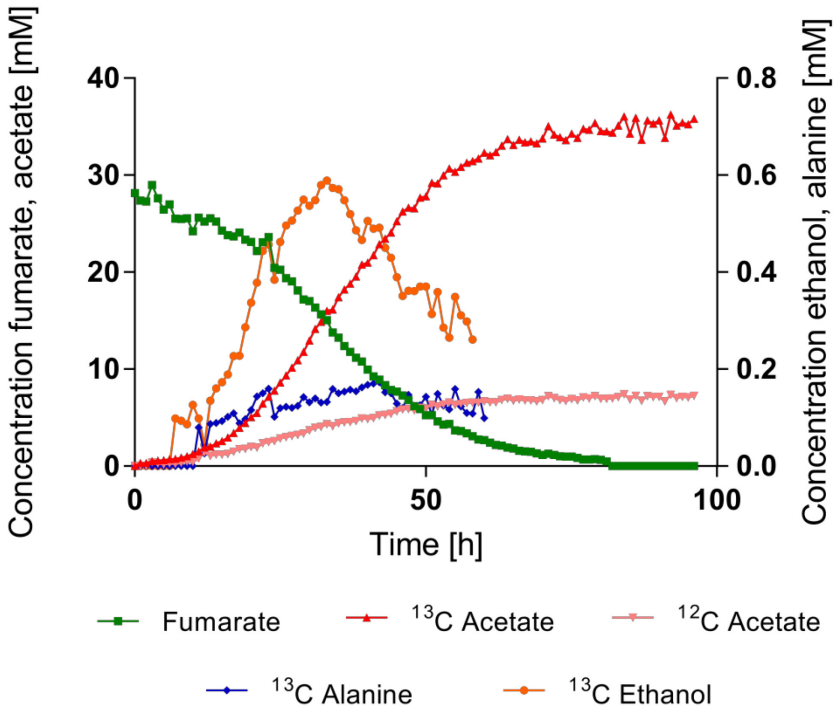


Figure 3.20 Metabolite profile of a *C. autoethanogenum* culture grown on $^{13}C_4$-labelled fumarate within an NMR tube.

Shown are substrate and product concentrations over time during growth of a 650 µl *C. autoethanogenum* culture within an anaerobic NMR tube with $^{13}C_4$-labelled fumarate as the sole source of carbon and energy. Green squares: fumarate; red upside triangles: ^{13}C acetate; pink downside triangles: ^{12}C acetate; blue circles: ^{13}C alanine; orange diamonds: ^{13}C ethanol. Metabolite concentrations were calculated from the NMR spectra shown in Figure 3.17.

In contrast to the partially labelled experiment, the measured total fumarate concentration (28 mM) was closer to the calculated one (Figure 3.20). The supplied fumarate completely disappeared at the end of the experiment, resulting in the production of 35 mM of ^{13}C acetate. Some ^{12}C acetate could still be measured (7 mM), which was most likely due to the left over ^{12}C fumarate from the pre-culture that was used for inoculation. The ^{12}C fumarate is not easily distinguishable from the ^{13}C fumarate due to its second order effect. Therefore the exact amount of the left-over ^{12}C fumarate could not be determined.

Having confirmed an approximate molar ratio of 1.5 between acetate formed and fumarate consumed, it was of interest to study the activity of known enzymes which take part in this fermentation. Therefore, the activity of key enzymes was determined in cell free extracts after the growth on fructose and fumarate, respectively. The findings are described in the following section.

3.2.4 Activity of key enzymes in *C. autoethanogenum* cells grown on fumarate and fructose

To shed light on the metabolic pathways involved in fumarate breakdown an conversion to acetate, the activity of potential key enzymes was analysed.

For this, the organism was grown on fructose and fumarate, respectively, in order to examine differences in specific enzyme activities. They assays for these enzymes were carried out as described in section 2.9.3.

Figure 3.21 shows the enzymes studied and their involvement in potential pathways of interest.

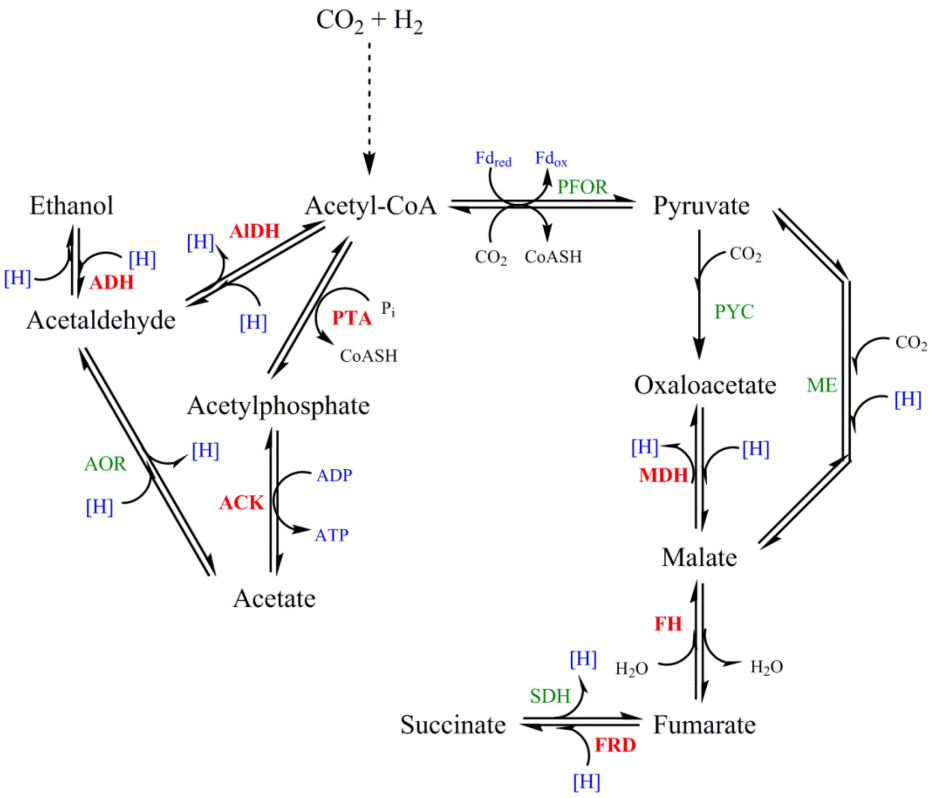


Figure 3.21: Overview of analysed enzyme activities.

Shown is an overview of known reactions present in *C. autoethanogenum* linking fumarate breakdown and acetate formation. Enzymes studied with regard to their activity in cell free extract of cells grown on fructose and fumarate are highlighted in red. ACK: Acetate kinase; ADH: Alcohol dehydrogenase; AlDH: Aldehyde dehydrogenase; FH: Fumarate hydratase; FRD: Fumarate reductase; MDH: Malate dehydrogenase; PTA: Phosphotransacetylase.

Table 3.2 Summary of enzyme activities

Shown are enzyme activities [U/mg] of various enzymes from cell free extract after growth on either fructose (after 48 h) or fumarate (after 24 and 48 h). ACK: acetate kinase, I: acetyl phosphate as substrate, II: acetate as substrate; ADH: alcohol dehydrogenase, I: acetaldehyde as substrate, II: ethanol as substrate; AlDH: aldehyde dehydrogenase, FH: fumarate hydratase; MDH: malate dehydrogenase; FRD: fumarate reductase; PTA: phosphotransacetylase. Bdl: enzyme activity was below detection limit. Nm: experimentally not measured.

	ACK	ADH	AlDH	FH	MDH	FRD	PTA
Fructose	I: 2.825 ± 0.035 (n = 2) II: 5.79 ± 2.08 (n = 2)	I: 0.098 ± 0.021 (n = 4) II: 0.003 ± 0.003 (n = 2)	0.033 ± 0.005 (n = 3)	0.15 ± 0.073 (n = 3)	bdl	bdl	bdl

Fumarate 24 h	I: nm II: 8.53 (n = 1)	I: 0.221 ± 0.065 (n = 2) II: 0.014 (n = 1)	nm	0.241 ± 0.115 (n = 5)	0.3 (n = 1)	bdl	bdl
Fumarate 48 h	I: 4.65 ± 1.23 (n = 2) II: 3.88 (n = 1)	I: 0.0434 ± 0.009 (n = 2) II: 0.0055 (n = 1)	0.0465 ± 0.018 (n = 3)	0.522 (n = 1)	0.79 (n = 1)	bdl	bdl

Enzyme activities for the cell free extract of cells grown on fructose differed compared to the activities for cells grown on fumarate (Table 3.2). The enzyme activities of the acetate kinase (ACK) were very similar when cells were grown on fumarate compared to fructose. When *C. autoethanogenum* was grown on fumarate for 24 h (mid-exponential phase), the alcohol dehydrogenase (ADH) activity was higher in both directions (using both acetaldehyde and ethanol as substrate) than when grown on fructose. The aldehyde dehydrogenase (AlDH) activity was similar for both cell free extracts. Regarding the activities of enzymes acting on C_4 dicarboxylic acids, cells grown on fumarate generally showed a higher activity. This applied to the fumarate hydratase (FH) which showed an up to 3.5 times higher activity after cells were grown on fumarate compared to cells grown on fructose. With respect to the malate dehydrogenase (MDH), which catalysed the subsequent reaction after the FH, no activity could be measured when *C. autoethanogenum* cells were grown on fructose. However, up to 0.79 U/mg were measured for the MDH activity for the cells free extract, after the bacteria were grown on fumarate. However, the MDH assays were only carried out once and findings need to be corroborated.

Phosphotransacetylase (PTA) activity, could not be detected using the assay and conditions described here, as the enzyme assay always showed background reaction (six independent assays). The activity for fumarate reductase (FRD) was measured as well (section 2.9.3.4). However, no activity could be measured due to similar problems as for the PTA activity. Therefore, presence of activity could neither be confirmed nor ruled out.

3.3 Discussion

When *C. autoethanogenum* was described by Abrini *et al.* in 1994, its ability to grow on various metabolites was tested [35]. Amongst these were also succinate and fumarate as C_4 metabolites. There it was found that this bacterium is not able to grow on either of these substrates. In this study, however, it was shown that *C. autoethanogenum* is indeed able to utilise fumarate and use it as carbon source. After these findings the C_4 dicarboxylic acid metabolism of this bacterium with focus on both the utilisation of fumarate and the production of succinate was of high interest. In the following section the findings of the general C_4 dicarboxylic acid metabolism and especially the fumarate pathway are being discussed.

3.3.1 C_4 dicarboxylic acid metabolism of *C. autoethanogenum*

The importance of C_4 compounds and the TCA cycle, also called the Krebs cycle, for plants, animals and bacteria is well established [145][146][147]. In the TCA cycle, C_4 compounds are part of the oxidative breakdown of acetyl-CoA, leading to the generation of reducing equivalents (NADH and $FADH_2$), and CO_2. They are also building blocks for important biosynthetic pathways, especially the synthesis for various amino acids [147]. Nevertheless, the classical (oxidative) TCA cycle is only relevant for respiring bacteria and eukaryotes as it generates the reducing equivalents required for aerobic (or anaerobic) respiration. However, in 1966 Evans *et al.* discovered a reductive TCA pathway [148], and found it to be used by a number of anaerobic organisms in order to fix carbon dioxide autotrophically [149][150].

Moorella thermoacetica, formerly known as *C. thermoaceticum*, represents perhaps the most thoroughly important acetogenic bacterium. In the past it was used to investigate the WLP and was analysed with regards to its ability to ferment C_6 and C_4 compounds. It was found that this organism was not able to utilise malate or fumarate [151]. However, when *C. ljungdahlii*, a close relative of *C. autoethanogenum*, was described in 1993 by Tanner *et al.* [36], it was stated that this organism was able to grow on fumarate as the sole source of carbon. Köpke *et al.* also reported that this bacterium may operate a branched TCA cycle [37]. For a strict anaerobe, generation of reducing equivalents *via* a fully operational TCA cycle is undesirable. However, as individual reactions of the cycle also serve to produce important metabolic intermediates, many anaerobic bacteria operate an incomplete "cycle", i.e. are able to carry out reaction sequences in the form of two branches, one leading from citrate to α-ketoglutarate, the other from oxaloacetate to fumarate and potentially succinate [152]. This shows that, even within the family of *Clostridiaceae*, and more specifically species of the genus *Clostridium* using the WLP, differences in their metabolic capabilities can occur. For example, *C. ljungdahlii* is closely related to *C. autoethanogenum*, and sometimes even said to be phylogenetically indistinguishable [153], as they have an average nucleotide identity (using BLAST) of 99.05 % [154]. However, as experienced in the GASCHEM group, there are clear physiological differences. Nevertheless, with respect to metabolic behaviours, especially ethanol and acetate production, both bacteria seem to share many characteristics [155].

Evidence produced in this study suggests that a branched TCA pathway also exists in *C. autoethanogenum* due to its ability to utilise fumarate, malate and oxaloacetate as carbon sources. The organism was not found to be able to use

succinate as carbon source, even though a gene encoding for a putative succinate dehydrogenase (SDH), which catalyses the reaction from succinate to fumarate, could be found in the genome (Clau0330). As stated in section 1.4, during the course of this study the genome of *C. autoethanogenum* had been re-sequenced and re-annotated [42], leading to changes in several gene annotations compared to the original study by Brown *et al.* [41]. Following re-annotation, the only remaining gene annotated to encode an SDH subunit was Clau0330 (designated locus tag Caethg0344 by Brown *et al.* [41] in 2014). Additional BLAST searches conducted as part of the current study did not reveal additional genes encoding SDH or FRD subunits. Furthermore, with 109 amino acids, the protein encoded by Clau0330 is far too small to encode a functional succinate dehydrogenase [156]. Thus, it can be concluded that the annotated succinate dehydrogenase subunit in *C. autoethanogenum* does not encode for an active SDH, which would explain the inability of *C. autoethanogenum* to utilise succinate as a carbon source.

3.3.2 Fumarate metabolism of *C. autoethanogenum*

Results obtained from the explained feeding experiments with fumarate led to a repeat of the carbon source analyses conducted by Abrini *et al.* [35]. In contrast to Abrini, however, it was found that *C. autoethanogenum* was able to use fumarate as carbon source. This was conclusively proven *via* various growth experiments where fumarate served as the sole source of carbon and energy, with the *in vivo* NMR experiments providing insight into the underlying metabolic pathways.

Here it was found that CO_2, released during the fumarate breakdown (as shown in Figure 3.10) was partially re-used by the bacteria as the carbon source and sink for the generated reducing equivalents. This is outlined below:

In the fully labelled experiment, the amount of ^{13}C-labelled acetate by far exceeds the amount of ^{12}C acetate, the latter being formed by unlabelled fumarate carried over from the pre-culture and CO_2 in the atmosphere of the anaerobic NMR tube. Ideally, washed cells would have been used for inoculation, but this generally resulted in irreproducible growth (data not shown).

When using 2,3-$^{13}C_2$ fumarate, however, a ratio of 2:1 was observed for the proportion of ^{13}C acetate to ^{12}C acetate. This agrees with the ratio calculated in equations **1-3,** which take into account the required balancing of reducing equivalents (see section 3.3.3). These calculations suggested that half of the CO_2 produced during the postulated conversion of fumarate to acetyl-CoA (see Figure 3.1) is being re-assimilated by *C. autoethanogenum via* the WLP, thereby using the NADH and reduced ferredoxin generated in the oxidative TCA branch and subsequent reactions. Assimilation of generated CO_2 *via* the WLP provides the only known route for generating ^{12}C acetate from 2,3-$^{13}C_2$ fumarate (see Figure 3.22). Thus, similar to what is observed during hexose catabolism, reducing equivalents are preferably used to generate more ATP *via* acetate generation, rather than reduction of acetyl-CoA to ethanol.

In 1978 Dorn *et al.* have shown that another organism of the genus *Clostridium*, *C. formicoaceticum*, is also able to use fumarate as carbon source [157] while producing acetate, CO_2 and succinate. However, this bacterium did not show an uptake of the produced CO_2 in contrast to *C. autoethanogenum*. *C. formicoaceticum* was also shown to oxidise CO and in 2017, after its whole

genome sequence was analysed, proven to possess genes encoding for enzymes of the WLP [158][159]. Still, during its growth on fumarate, this organism was not able to re-assimilate the CO_2 produced during its fumarate metabolism. Instead, it appears that the reducing equivalents formed during acetate formation were used to reduce part of fumarate to succinate. This illustrates how different bacteria have evolved different solutions for maintaining an even redox balance during fumarate fermentation.

3.3.3 Proposed fumarate fermentation pathway

A newly developed genome scale model of *C. autoethanogenum* (Rupert Norman, University of Nottingham, 2016, personal communication) was interrogated as part of a collaboration to investigate fumarate metabolism in *C. autoethanogenum*. Initially, this model predicted the formation of CO when growing the bacterium on fumarate. As it was shown in this chapter, no CO-formation could be measured, but release of CO_2. Thus, only after conducting the *in vivo* experiments, the involvement of the WLP was suggested and hence in-cooperated into the model. With the help of the improved model and the obtained experimental data, a pathway of fumarate degradation, including the energy conservation routes and predicted ATP yield, was proposed. Figure 3.22 shows this pathway including the in-cooperation of the energy conserving Rnf complex which was recently described for *C. autoethanogenum* [31][32].

According to the model developed by Rupert Norman, the maximal ATP yield (Y_{ATP}) from fumarate as sole carbon and energy source is 1.205. In this solution, the WLP (with bifurcating methylene-THF reductase) is used to fix CO_2 generated from malate decarboxylase, malic enzyme (MDH, ME) and

pyruvate:ferredoxin oxidoreductase (PFOR) during the conversion of fumarate to acetyl-CoA. The net stoichiometry for this solution is as follows:

(1) 2 fumarate ⟶ 2 acetate + 4 CO_2 + 4 [2 H]

(2) 2 CO_2 + 4 [2 H] ⟶ 1 acetate

---

(3) 1.0 fumarate ⟶ 1.5 acetate + 1.0 CO_2 (Y_{ATP} = 1.205)

Thus, for every fumarate molecule that is taken up, 1.205 ATP is yielded for use elsewhere (e.g. in biomass production or cellular maintenance). As the experiments in this chapter showed, during the growth of *C. autoethanogenum*, CO_2 is produced, and partially re-assimilated (Figure 3.10), in agreement with the above.

With regards to the differences of *C. autoethanogenum* cells grown on fructose and fumarate, it can be said that the production of acetate is very similar, however the production of ethanol differs significantly. As explained in section 3.2.2.4, when *C. autoethanogenum* was grown on fumarate, a small amount of ethanol was produced during the exponential growth phase, but re-assimilated when nearing stationary phase. Whereas for cells grown on fructose, a constant increase of ethanol could be measured. Additionally it was found that when cells were grown on ^{13}C fumarate, small amounts of ^{13}C alanine could be measured *via* NMR during the first 24 h. However, alanine disappeared again, similar to the observation with ethanol. Alanine is most likely formed *via* pyruvate by the use of an alanine-glyoxylate transaminase, a putative gene which can be found in the genome (Clau2157), which explains the appearance of the ^{13}C-labelled peaks of alanine in the NMR. Interestingly, alanine

production and consumption has also been observed for two other *Clostridia* possessing genes for the WLP, *C. difficile* and *C. sticklandii* [160][161].

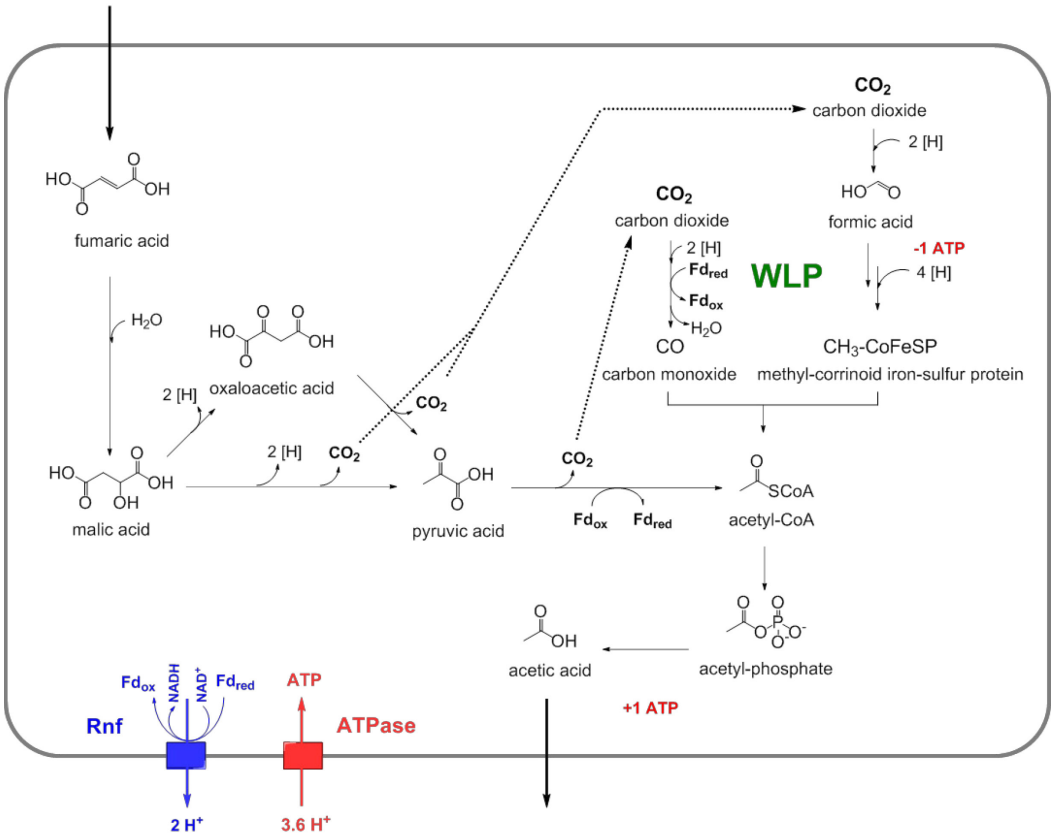


Figure 3.22: Proposed fumarate fermentation pathway of *C. autoethanogenum*.

Fumarate breakdown occurs *via* a branch of the incomplete TCA cycle and two consecutive decarboxylation reactions. The produced CO_2 is in part being re-assimilated *via* the WLP. ATP is generated *via* the Rnf complex, ATPase and acetate production. The calculated stoichiometry is: 1.0 fumarate → 1.5 acetate + 1.0 CO_2, providing an ATP yield of 1.205.

3.3.4 Physiological behaviour of cells grown on fumarate and fructose

Another difference between growth on fumarate and fructose was in the pH values measured over time in the supernatants of the cultures. When *C. autoethanogenum* was grown on fructose, the pH constantly decreased, with the most rapid decrease during the exponential growth phase, correlating with the production of acetate. However, when cells were grown on fumarate, a slight increase of the pH was determined. This can be explained by the relative pKa values of the product acetic acid and the substrate fumaric acid. Acetic acid and fumaric acid have pKa values of 4.76 and 3.03/4.44 (pKa_1 and pKa_2 of fumaric acid) respectively, meaning that fumaric acid is the stronger acid. Thus, as the concentration of the stronger fumaric acid decreases, and weaker acetic acid increases, the pH changes accordingly resulting in a less acidic environment.

Enzyme assays comparing the enzyme activities of the ADH, AlDH, ACK, FH and MDH were conducted with cells grown on either fumarate or fructose.

When cells grew on fumarate, during the exponential phase, ethanol was first produced (up to around 1 mM) and then re-assimilated (Figure 3.10), whereas ethanol produced during growth on fructose ethanol was continuously produced (up to 7.4 mM). This is in agreement with the measured ADH activities, which were high during exponential growth on fumarate, i.e. at the peak of ethanol production (0.221 U/mg; 24 h), but much lower during stationary phase when ethanol had been re-metabolised (0.0434 U/mg; 48 h). It may be worth noting that measured ADH activity during exponential growth on fructose was lower (0.098 U/mg) than on fumarate.

In 2013 Wang *et al.* analysed enzyme activities of enzymes involved in the WLP of *C. autoethanogenum* [31]. It was found that, when grown on CO, the

bacterium shows an enzyme activity for the ADH of 0.15 – 0.2 U/mg [31]. Similarly, another dataset published in 2015 by Mock *et al.* [32], for growth on fructose, showed an activity of 0.1 U/mg [32]. Thus, both studies found very similar ADH activities compared to what was shown in this work.

With respect to AlDH, it was found that for both fructose (0.033 U/mg) and fumarate (0.0465 U/mg; 48 h) grown cells, values were comparable to the previously measured activities by Wang (0.06 – 0.08 U/mg) and Mock (0.03 – 0.08 U/mg) *et al.* [31], [32].

The acetate kinase (ACK) is presumably one of the most important enzymes in *C autoethanogenum* as it is directly coupled to ATP generation *via* substrate level phosphorylation. The determined enzyme activities in the physiological direction were slightly higher for cells grown on fumarate (4.65 U/mg) compared to cells grown on fructose (2.825 U/mg). Literature values for *C. acetobutylicum* of 3.7 U/mg [162] compare with the findings for *C. autoethanogenum*. For another acetogen, *Acetobacterium woodii*, ACK activities up to 9.98 U/mg could be measured [163].

With regards to the enzymes involved in the fumarate pathway, it was expected to find higher fumarate hydratase (FH) and malate dehydrogenase (MDH) activities for cells grown on fumarate, compared to cells grown on fructose. Indeed, FH activities of 0.241 U/mg and 0.522 U/mg were determined for cells grown on fumarate after 24 and 48 h, respectively. When grown on fructose, FH was considerably lower (0.15 U/mg). With regards to the activity of the malate dehydrogenase (MDH), no activity could be seen for cells grown on fructose, whereas 0.3 – 0.79 U/mg where measured for cells grown on fumarate.

Additionally, it was attempted to analyse phosphotransacetylase (PTA) activity. However, an interfering background reaction of the enzyme assay resulted in too low ΔE values compared to the control (enzyme without substrate) to calculate enzyme activity with certainty. Unfortunately, this issue could not be resolved in time for this study. Previously measured PTA activity in cell free extracts (non-physiological reaction; formation of acetyl-CoA) of *C. acetobutylicum* showed an enzyme activity of 1.4 U/mg [164]. In another study in which acetyl-CoA was used as substrate (physiological direction), 0.30 U/mg PTA activity were reported [165]. The PTA reaction precedes the ACK reaction. As mentioned above, ACK activity of *C. acetobutylicum* was around 3.7 U/mg [162] and thus twelve times of that measured for PTA in physiological direction. Therefore it might be possible that PTA activity in cell free extracts is in general lower compared to the ACK activity (data obtained during studies in 2013 for PTA and ACK activity of *M. thermoacetica* resulted in the same observation [166]). This could explain the results found in this study.

With respect to FRD activity, a recent patent application [106] claimed to have measured activity of 17.3 nmol min^{-1} mg $protein^{-1}$ (17.3 nU/mg, or 0.0000173 U/mg), whereas no activity could be measured in the *C. autoethanogenum* cell free extracts studied here. Apart from this patent, no other work is currently available that provides data on FRD activity of *C. autoethanogenum.* In [106] it was also stated that genes encoding for putative succinate dehydrogenase/fumarate reductase could be found. However, during the GASCHEM re-annotation of the genome of *C. autoethanogenum* in 2016 [42], these genes were found most likely encode

for different proteins (see section 3.3.1). This would explain why no FRD activity for *C. autoethanogenum* could be determined in this work

3.3.5 Summary

In this chapter, the C_4 dicarboxylic acid metabolism of *C. autoethanogenum* was analysed. A branch of the TCA cycle could be verified for this organism, comprising fumarate hydratase and malate dehydrogenase. Activities for these enzymes were increased in fumarate grown cells. Accordingly, it was found that *C. autoethanogenum*, in contrast to its first description, was able to utilise fumarate as the sole carbon and energy source.

With the help of *in vivo* NMR analyses, it was revealed that fumarate metabolism is linked to the WLP, providing an interesting example for the interaction between reducing equivalent producing and consuming pathways in acetogenic bacteria. Although *in vivo* NMR analyses have been described in bacteria and eukaryotes [67], [167], [168], the growth of anaerobic, acetogenic bacteria in an NMR machine has not been described until now. This method therefore presents a new way of analysing those organisms.

In the next chapter the fumarate metabolism was investigated, by inactivating, and later complementing, a predicted key enzyme of the pathway. Additionally, the inactivation of the whole WLP was attempted to study its influence on fumarate metabolism.

4 Construction and characterisation of mutants defective in fumarate metabolism

Must it all be either less or more, either plain or grand?
Is it always 'or'? Is it never 'and'?

Stephen Sondheim, Into the Woods

4.1 Introduction

To analyse the process of fumarate fermentation in more detail, it was decided to create mutations both within and outside of the pathway. These mutants would provide information about their effect on the pathway with respect to metabolism, growth behaviour, and key enzyme activities. In this chapter the creation of these mutants and their phenotypic characterisation is described.

A common approach to elucidate metabolic pathways is mutagenesis. The acetone-butanol-ethanol (ABE) fermentation pathway, for example, was understood in more detail after inactivating twelve fermentation pathway genes using insertional mutagenesis (ClosTron) [169]. Additionally, the involvement of the Rnf complex in *C. ljungdahlii*'s energy conservation had only been confirmed, after the disruption of the *rnf* operon led to an inhibition of autotrophic growth [170]. This demonstrates how important the manipulation of genes is, when describing new metabolic behaviour in organisms.

For this study of particular interest, was the inactivation of the gene encoding fumarate hydratase (Clau1855). This enzyme is thought to be key for growth on fumarate, according to the pathway proposed in Figure 3.22. Hence, it was expected that without this specific enzyme the organism would not be able to grow on fumarate. The inactivation of the fumarate hydratase was to be

attempted both *via* insertional mutagenesis, using the ClosTron system [45], and *via* in-frame deletion [52].

Another mutation of interest was the acetyl-CoA synthase complex (*acsA*). As explained in the previous chapter (section 3.2.3.1), there is strong evidence that, when growing on fumarate, the released carbon is taken up and re-assimilated, using the Wood-Ljungdahl Pathway (WLP). In 2016 Liew *et al.* demonstrated that the *acsA* gene complex (Clau1578 and Clau1579) is crucial for the fixation of, and therefore growth on, CO and CO_2 [171], as the knockout of this gene resulted in an inactivation of the WLP. Therefore, in this study, it was assumed that growth on fumarate would either be restricted or entirely inhibited, due to the *acsA* mutant's inability to utilise CO_2 as an electron sink, i.e. for the recycling of NAD^+ and oxidised ferredoxin.

The metabolic flexibility of the organism has recently been shown by Mock *et al.* where it was determined that acetate and ethanol production differed when grown under different pH conditions. When *C. autoethanogenum* was grown at pH 4.7 mainly ethanol was produced [172], whereas when grown at a pH of 6.0 the ratio of formed ethanol to acetate was almost 1:1 [173]. Furthermore, when the *acsA* was inactivated by Liew *et al.* it was found that under heterotrophic conditions (growth on fructose), the mutant strain abolished acetate production in favour of increased ethanol, butanediol and lactate production [171]. Thus, it was assumed, that during heterotrophic growth on fumarate, if growth is not completely inhibited, the *acsA* mutant's product spectrum would be similar to findings of Liew *et al*. (increased ethanol, lactate or/and butanediol production).

From the work outlined above, the following specific aims emerged:

- To generate a fumarate hydratase mutant and investigate whether or not it can grow on fumarate.
- To generate an acetyl-CoA synthase mutant and investigate whether or not it can grow on fumarate.
- If mutant generation is successful, complement the mutation and investigate whether or not changes compared to the wild type occur.

4.2 Results

4.2.1 Allelic Exchange and ClosTron mutagenesis of the fumarate hydratase

After different growth experiments on fumarate (chapter 3) a putative fumarate fermentation pathway had been proposed in Figure 3.22. Following fumarate uptake, fumarate hydratase (FH) (encoded by a gene carrying the locus tag Clau1855) catalyses the first step in this pathway. It was thus considered key enzyme required for growth on fumarate. To test this hypothesis, a knockout mutant, leading to inactivation of this enzyme was required. For this, it was necessary to first inactivate the native *pyrE* gene to enable its use as selectable marker, as explained in section 2.7.7.3.

4.2.1.1 Generation of a Δ*pyrE* mutant

To create an in-frame deletion mutant of fumarate hydratase *via* Allelic Exchange, a *pyrE* knockout mutant, was created. This was also performed because it could serve as the starting point for other mutants and the use of Allele-Coupled Exchange (ACE) [52] (section 2.7.7.3). As described in 2.8.2, the plasmid pANNE_ACE_del_pyrE (constructed by Dr. Anne Meint Henstra) was conjugated from *E. coli* CA434 cells into *C. autoethanogenum*. The screening for a *pyrE* knockout mutant was performed according to section 2.7.7.3. The strain with, *via* sequencing, confirmed *pyrE* knockout and confirmed plasmid loss, was sent for whole genome sequencing. The analysis of the whole genome sequencing was carried out by Dr. Chris Humphreys (University of Nottingham) and revealed a single SNP (1 bp; Caethg2406: Phosphatidylserine synthase) for the created strain. This strain was designated

Δ*pyrE* and later used for Allelic Exchange mutagenesis by the entire GASCHEM group.

4.2.1.2 Generation of fumarate hydratase mutants

The fumarate hydratase knockout Allelic-Exchange plasmid was constructed accordingly to section 2.7.7.3. Once the sequence of the homology arms was confirmed, the plasmid was electroporated into *E. coli* CA434 cells. The resulting *E. coli* cells and the earlier generated Δ*pyrE* strain of *C. autoethanogenum* were then used for conjugation according to section 2.8.2. However, after several attempts, the conjugation resulted in either no colonies, or colonies that had the entire plasmid integrated *via* single crossover event; no double crossover event could be confirmed (data not shown). A major problem was the low conjugation success. Therefore, to obtain a FH mutant, the generation of a ClosTron mutant was attempted.

Two ClosTron plasmids pMTL007C-E2::FH48s (termed FH_1) and pMTL007C-E2::FH360s (termed FH_2), were designed and obtained from DNA2.0 as described in section 2.7.7.1, were conjugated into *C. autoethanogenum* according to 2.8.2. Again, problems with the conjugation efficiency were encountered when using *E. coli* CA434 donor cells, but the change to *E. coli* Sexpress (designed by Craig Woods, University of Nottingham, in the meantime) resulted in a great improvement in conjugation success.

Clarithromycin resistant *C. autoethanogenum* colonies were subjected to PCR screening using the primer pairs 1855_Fw and 1855_Rev, to confirm integration of the ClosTron in the fumarate hydratase gene. Clones 10, 12, 21,

22, 24 of FH_1 and 16, 24 of FH_2 showed the expected, larger fragments (due to the insert) (Figure 4.1) and were confirmed to have the expected sequence *via* Sanger Sequencing.

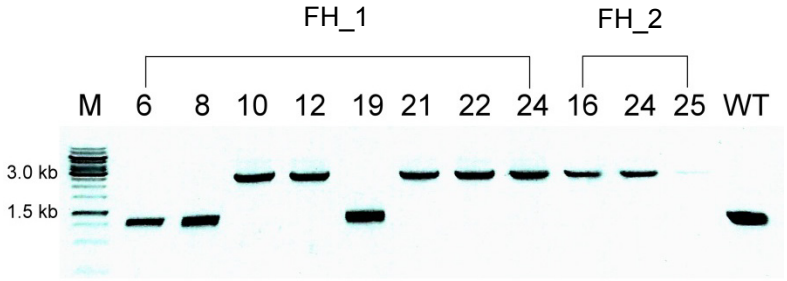


Figure 4.1: PCR screening of putative ClosTron FH mutants.
PCRs were carried out using exon-spanning primers (1855_Fw and 1855_Rev) to screen clarithromycin resistant clones for the presence of FH insertional mutants. M: O'GeneRuler 1 kb DNA Ladder (ThermoScientific); FH_1 ClosTron colonies; FH_2 ClosTron colonies; WT: wild type DNA template. Numbers are the respective clone numbers. Expected band size of ClosTron mutant was 2.4 kb. WT band without intron was 843 bp.

These ClosTron mutants were streaked onto plates with either clarithromycin or thiamphenicol antibiotic, to confirm plasmid loss (no growth on thiamphenicol). As a final validation, Southern blot analysis was conducted to verify single insertion of the ClosTron according to section 2.7.9. The enzymes used for restriction digest of chromosomal DNA (EcoRV and HindIII) did not cut within the ClosTron itself and hence insertions should show up as single bands in a Southern blot when using a ClosTron specific probe. As shown in Figure 4.2 only FH_1 21 and FH_2 24 showed no double insertion on both digests. However, since the band sizes of the intron in FH_1 21 varied compared to the other mutants, it was decided to exclude this strain from further analyses (excluding the plate growth experiments, see Figure 4.4). For complementation, only FH_2 24 was used.

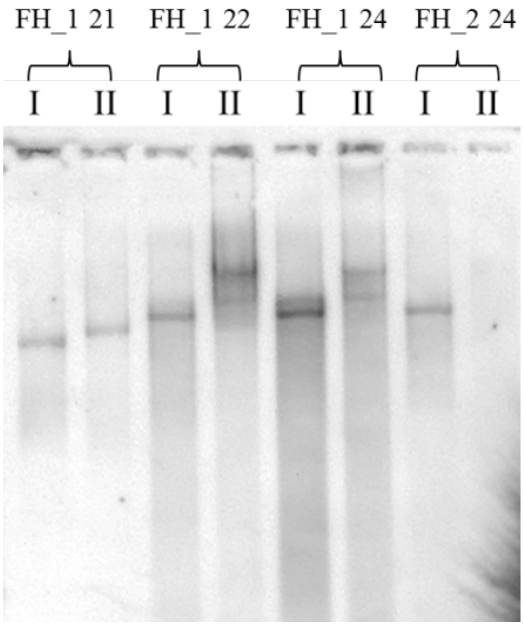


Figure 4.2: Southern blot analysis of ClosTron FH mutants.
Southern Blot analysis of EcoRV (I) and HindIII (II) digested chromosomal DNA of FH::CTermB-48s (FH_1) and FH::CTermB-360s (FH_2) clones. As probe, the *ermB* gene fragment was used.

4.2.1.3 Characterisation of ClosTron FH inactivation mutants

Determination of fumarate hydratase (FH) activity in WT and FH mutants

Following the inactivation of the FH gene it was important to establish whether the activity of the encoded enzyme had been completely abolished. For this, the fumarate hydratase enzyme assay by Hatch was used (section 2.9.3.1).

Table 4.1 lists measured FH activities for the WT grown on fructose and fumarate, and for all investigated ClosTron strains cultured on fructose. In all three ClosTron strains no FH activity of could be measured.

Table 4.1: Fumarate hydratase activities of FH ClosTron mutants and WT

Strain	U/mg
WT (on fructose)	0.15 ± 0.073 (n = 3)
WT (on fumarate)	0.241 ± 0.115 (n = 5)
FH_1 22 (on fructose)	0 (n = 2)
FH_1 24 (on fructose)	0 (n = 2)
FH_2 24 (on fructose)	0 (n = 2)

Growth experiments

To examine the impact of FH inactivation and to test the hypothesis of the enzymes role in fumarate metabolism, both the mutants and WT were grown in 250 ml serum bottles containing 50 ml PETC-MES medium (section 2.3.2). Figure 4.3A displays the growth of selected mutant strains and wild type on fructose. Despite a slightly longer lag-phase and lower final ODs for all FH mutants tested, all strains showed the same overall growth behaviour. As shown in Figure 4.3B, none of the FH ClosTron grew on fumarate in contrast to the WT. In order to compare the ability of the different *C. autoethanogenum* strains to grow on the remaining fructose from the pre-cultures (10 ml Hungate tubes), controls with no added carbon source were carried out. All mutants and the WT showed very little growth in this control (Figure 4.3B and data not shown).

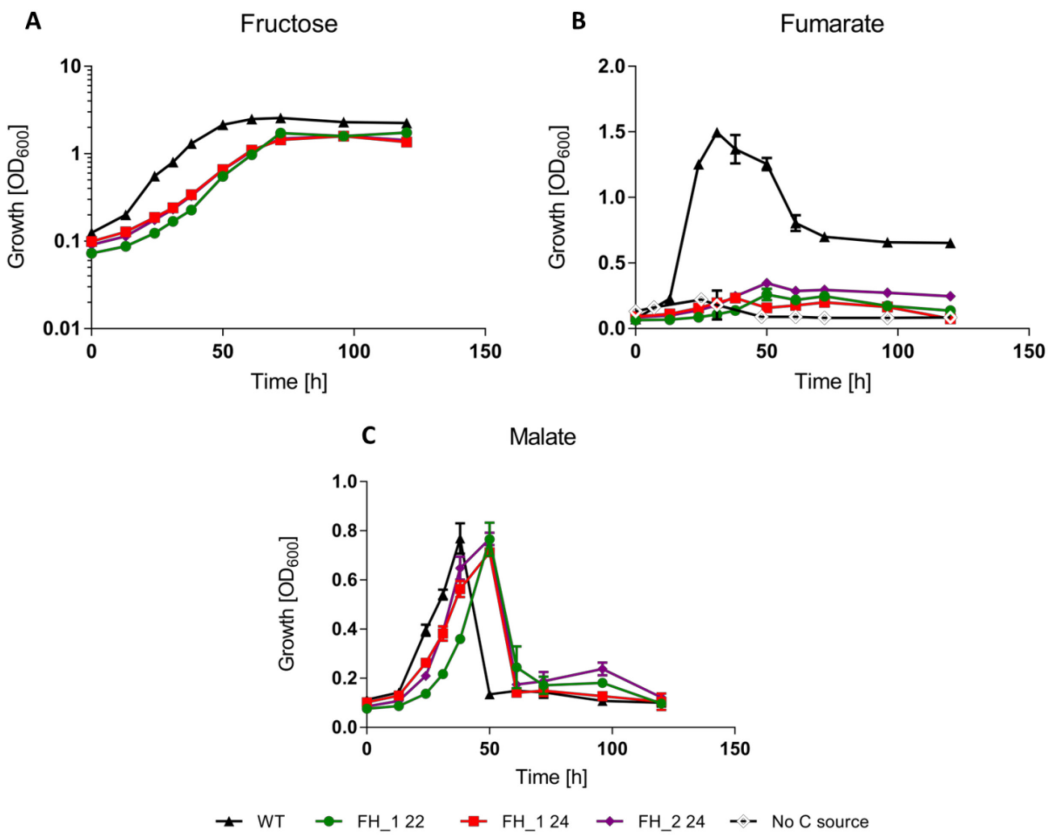


Figure 4.3: Growth of FH ClosTron mutants and WT on fructose (A), fumarate (B) and malate (C).

FH ClosTron mutants FH_1 22 (green), FH_1 24 (red) and FH_2 24 (purple). WT (black) and a negative control (WT) with no carbon source (dashed line) were used as references. A) Growth on fructose; B) Growth on fumarate; C) Growth on malate. Data shown as mean ± SEM (n = 3).

Even though the growth on fumarate was abolished for all FH mutants tested, the growth on malate was not influenced. All strains showed the overall same growth behaviour on this carbon source (Figure 4.3C), although the lag phase appeared to be slightly increased for the FH mutants. In addition to the growth experiments in liquid medium, plate experiments were carried out on PETC-MES agar plates. As Figure 4.4 shows, all strains grew on fructose and pyruvate, but only the WT strain showed growth on fumarate. The growth on

malate was tested and verified for those strains as well, however, the colonies formed were too small to capture on a photograph of the plate.

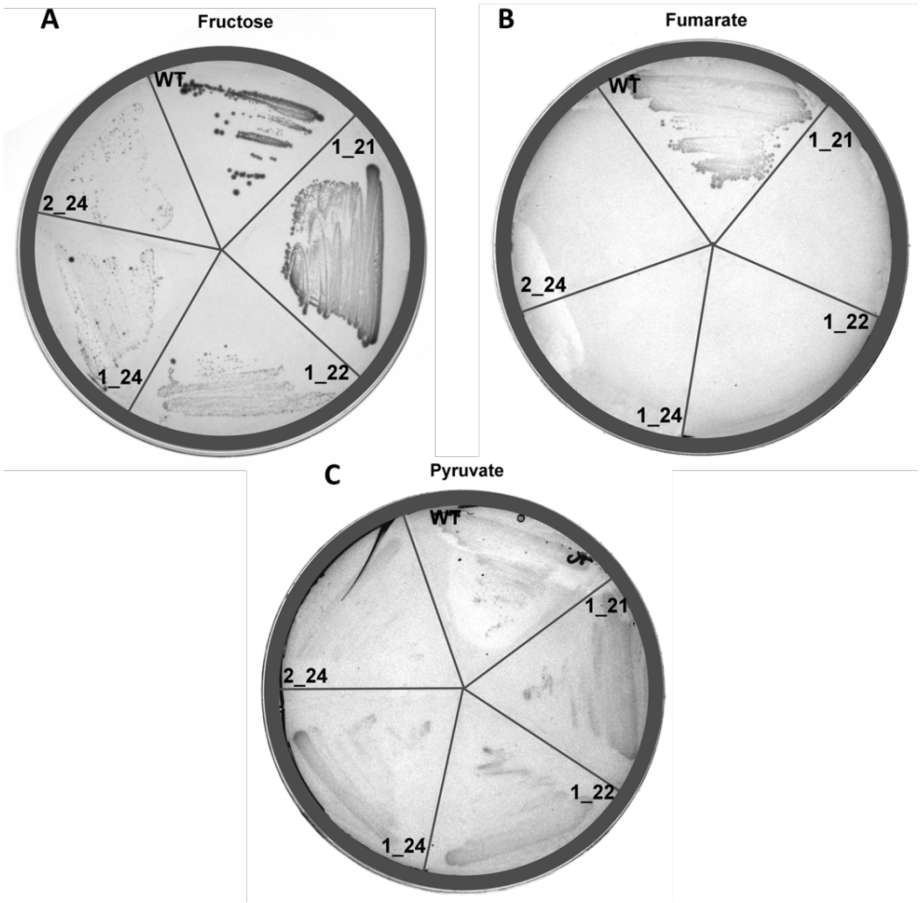


Figure 4.4: Growth of WT and ClosTron mutants on PETC-MES agar plates containing different carbon sources.

Shown are PETC-MES agar plates with A) fructose, B) fumarate, and C) pyruvate as carbon source. WT and all four ClosTron mutants (1_21; 1_22; 1_24; 2_24) were plated and plates incubated anaerobically for 48-72 h at 37 °C. The plates did not contain antibiotics to allow growth of the WT control.

4.2.1.4 Complementation of ClosTron mutants

To confirm that the loss of the ability to grow on fumarate was due to the inactivation of the FH (Clau1855), a complementation assay was undertaken by expressing a plasmid-borne copy of the FH gene in the FH ClosTron mutant FH_2 24 (section 2.7.8). The FH gene was amplified from chromosomal DNA using the primers 1855_comp_Fw and 1855_comp_Rev (Table 2.4) and cloned into plasmid pMTL83151 as described in section 2.7.8. Sanger sequencing of the region using primers ColE1+TraJ F2 and pCB102 R1 (Table 2.4) was carried out to verify successful cloning.

Both the plasmid containing the FH gene (pMTL8315_FH) and the plasmid without (pMTL83512) were conjugated into *C. autoethanogenum FH::*CTermB-360s (FH_2 24), generating the strains *C. autoethanogenum FH*::CTermB-360s pMTL83152_FH (FH_2_24 FHcomp) and *C. autoethanogenum FH::*CTermB-360s pMTL83152 (FH 2_24 P). The presence of both plasmids in the resulting Tm-resistant transconjugants was verified by plasmid rescue, PCR amplification using ColE1+tra F1 and pCB102 R1 primers and sequencing.

Strains were grown in 250 ml serum bottles containing 50 ml PETC-MES medium supplemented with fructose or fumarate (40 mM respectively). In addition to the respective carbon source, all bottles containing the complementation and plasmid control strains were supplemented with 15 µg/ml thiamphenicol (final concentration) to prevent plasmid loss.

As Figure 4.5 shows, after the complementation with the plasmid-borne FH gene, the capability for growth on fumarate was restored for the ClosTron FH_2_24 mutant, even though the lag phase was considerably increased compared to the WT. The plasmid control without the FH gene however, was

not able to grow on fumarate. The growth behaviour on fructose was similar for all three strains.

In addition to growth experiments in liquid medium, growth experiments on plates were carried out (Figure 4.6).

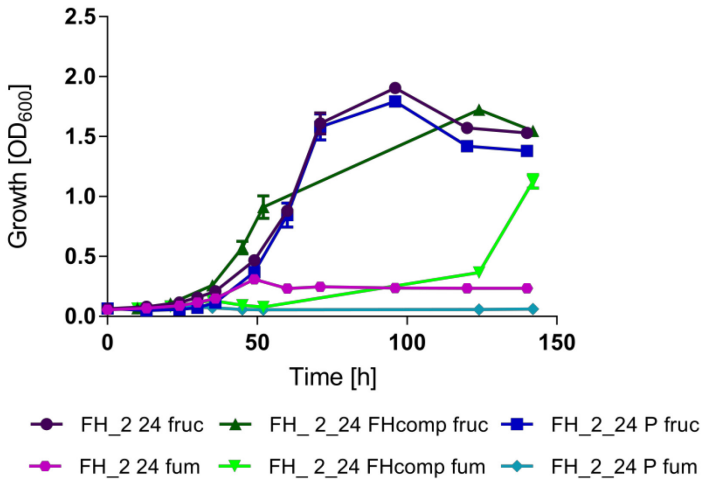


Figure 4.5: Growth of the FH 2 24 ClosTron mutant, complemented mutant and plasmid control

Growth is shown for the following strains and conditions: ClosTron mutant FH_2 24 on fructose (dark purple circles) and fumarate (lilac hexagons); complemented strain FH_2_24 FHcomp on fructose (dark green, triangles) and fumarate (bright green inverted triangles); and the plasmid control FH_2_24 P on fructose (dark blue squares) and fumarate (bright blue diamonds). Data shown as mean ± SEM (n = 3).

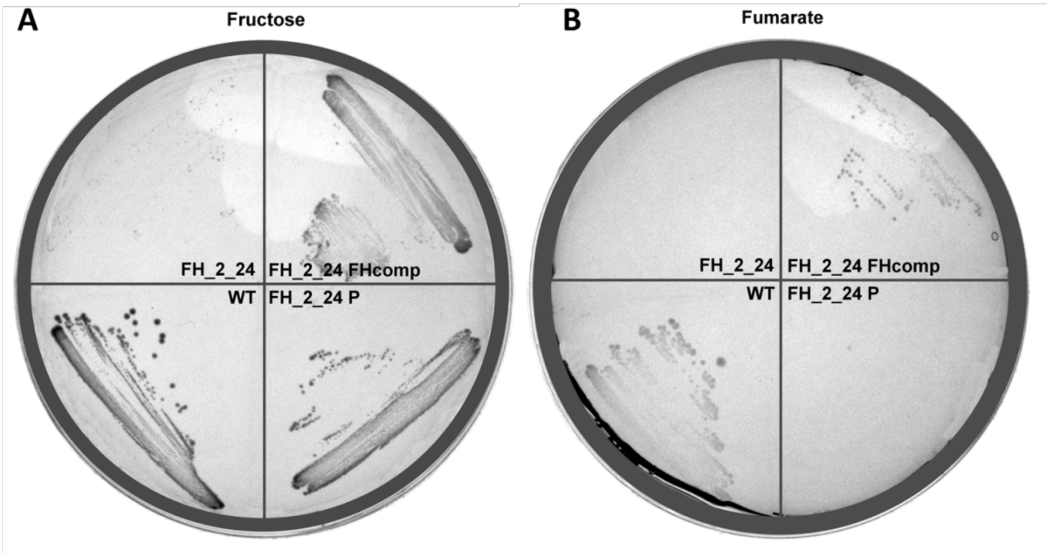


Figure 4.6: Growth of the FH ClosTron mutant, WT, complemented mutant and plasmid control on PETC-MES agar plates with 40 mM fructose (A) and fumarate (B), respectively.

PETC-MES agar plates supplemented with A) fructose and B) fumarate as carbon source. Plated were the FH_2 24 ClosTron mutant (FH_2_24), the complemented FH_2_24 FH mutant (FH_2_24 FHcomp), WT and the FH_2_24 plasmid control (FH_2_24 P). Plates did not contain antibiotics to allow growth of the WT and were incubated anaerobically for 48-72 h at 37 °C.

Whereas all strains were able to grow on fructose, only the wild type and the complemented FH mutant strain showed growth on fumarate (Figure 4.6).

As a final experiment to verify successful complementation of the FH_2_24 mutant, fumarate hydratase assays were conducted. The aforementioned strains were grown on PETC-MES medium supplemented with fructose and fumarate as appropriated (40 mM), and cells extracts prepared after 48 h as described in section 2.9.1.

Table 4.2: FH activities before and after complementation

Strain	U/mg
WT fumarate	0.241 ± 0.115 (n = 5)
WT fructose	0.15 ± 0.073 (n = 3)
FH_2 24 (on fructose)	0 (n = 2)
FH_2_24 FHcomp (on fumarate)	1.99 (n = 1)
FH_2_24 FHcomp (on fructose)	0 (n = 2)
FH_2_24 P	0 (n = 1)

Only when the complementation strain was grown on fumarate was FH activity restored (Table 4.2). Interestingly, when the strain was grown on fructose, no activity could be measured. The plasmid control (previously shown not to grow on fumarate and therefore only tested on fructose) showed no activity.

4.2.2 Generation of an acetyl-CoA synthase deletion mutant

As described in the introduction of this chapter, Liew *et al.* wer able to prove that the genes Clau1578 and Clau1579 encoding the AcsA subunit of the acetyl-CoA synthase complex, are crucial for the fixation of, and therefore growth on, carbon dioxide [171]. The knockout of this gene resulted in an inactivation of the WLP.

Using partially and fully labelled fumarate for *in vivo* NMR experiments demonstrated that during growth on fumarate the released CO_2 was re-assimilated in part *via* the WLP. Therefore, it was hypothesised that a knockout of this pathway might impact the ability of *C. autoethanogenum* to grow on fumarate. Since the previously engineered *acsA* knockout mutant generated by Eric Liew could not be used (the rights are owned by a company), it was decided to generate CRISPR mutants of these two genes.

4.2.2.1 CRISPR/Cas9-based inactivation of *acsA*

The plasmid pSBRCas9_Pbt_2 (Table 2.3) was constructed by Peter Rowe (University of Nottingham) as a part of the GASCHEM project. The plasmid was used to construct three derivative CRISPR plasmids for the inactivation of *acsA*, each containing a different guide RNA. In order to create these plasmids, the gene specific guide RNAs (sgRNAs) had to be synthesised. Utilising the Benchling® CRISPR sgRNA design tool (section 2.7.7.2), three promising guide RNA sequences were identified; sgRNA1_AscA, sgRNA2_AcsA and sgRNA3_AcsA (Table 2.4). These oligonucleotides were synthesised by Sigma-Aldrich. The construction of the plasmids, pSBRCas9_AcsA1, pSBRCas9_AcsA2 and pSBRCas9_AcsA3, including the in-frame deletion cassette, was undertaken as described in 2.7.7.2. After the plasmids were verified *via* sequencing, all three were transferred into *E. coli* Sexpress cells (section 2.8.1) and into *C. autoethanogenum via* conjugation (section 2.8.2). Growing colonies were first re-streaked onto a fresh YTF plate with added thiamphenicol. Colonies growing on this plate were then used for colony-PCR using the screening primers Screening_F and Screening_R (Table 2.4). However, no positive PCR result could be obtained, not even for the WT DNA which was used as negative control. Since various attempts including the change of temperatures and times in the PCR did not lead to an improvement, colonies were inoculated into liquid YTF containing thiamphenicol, and the gDNA isolated using the Sigma gDNA isolation kit (section 2.7.2.1). The obtained DNA was then used for PCR amplification.

However, even after several re-streaks, the PCR showed only bands of the size expected for WT DNA (3.7 kb instead of 1.8 kb). It was decided to perform

new conjugations with all plasmids. Again, after several attempts and re-streaks, finally two positive PCR amplicons could be obtained (Figure 4.7).

Clones 2_5 (guide RNA2, number 5) and 3_2 (guide RNA 3, number 2) showed a 1.9 kb shortened fragment compared to the WT, which corresponds to the size of the combined deleted genes Clau1578 and Clau1579 (Figure 4.7). As the PCR confirmed an *acsA* knockout, the respective colonies were tested for plasmid loss. Both colonies were inoculated into liquid without antibiotics and the growing cultures plated onto a plain YTP plate. Growing colonies were picked and replica-plated onto plates with and without thiamphenicol. Only colonies not growing on thiamphenicol were approved for plasmid loss and used for further analyses.

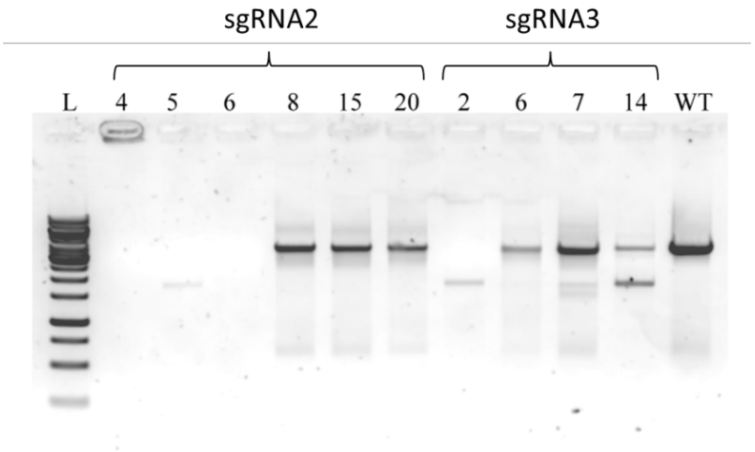


Figure 4.7: PCR screening of putative *acsA* CRISPR/Cas9 mutants.

PCR amplification of the *acsA* gene region from gDNA, isolated from re-streaked putative *acsA* knockout mutants. WT gDNA was used as a negative control. L: O'GeneRuler 1 kb DNA Ladder (ThermoScientific); sgRNA2: 4, 5, 6, 8, 15 and 20 indicate screened clones for guide RNA2 mediated gene inactivation; sgRNA3 2, 6, 7 and 14 indicate screened clones for guide RNA3 mediated gene inactivation. WT band size: 3.7 kb; CRISPR knockout: 1.8 kb.

4.2.2.2 Growth experiments

To analyse the growth of the two obtained *acsA* CRISPR mutants in comparison to the WT, all three strains were grown heterotrophically on fructose and autotrophically on CO, respectively.

When grown on fructose, all three strains showed the same growth behaviour (Figure 4.8). When grown on CO, all strains were still able to grow. CRISPR mutant strain 3_2 reached approximately WT OD levels after an extended lag phase, whereas mutant strain 2_5 started to grow only towards the end of the experiment. However, since those strains based on current understanding should not be able to grow on CO, the pureness of the strains was doubted, despite the results of the screening PCRs.

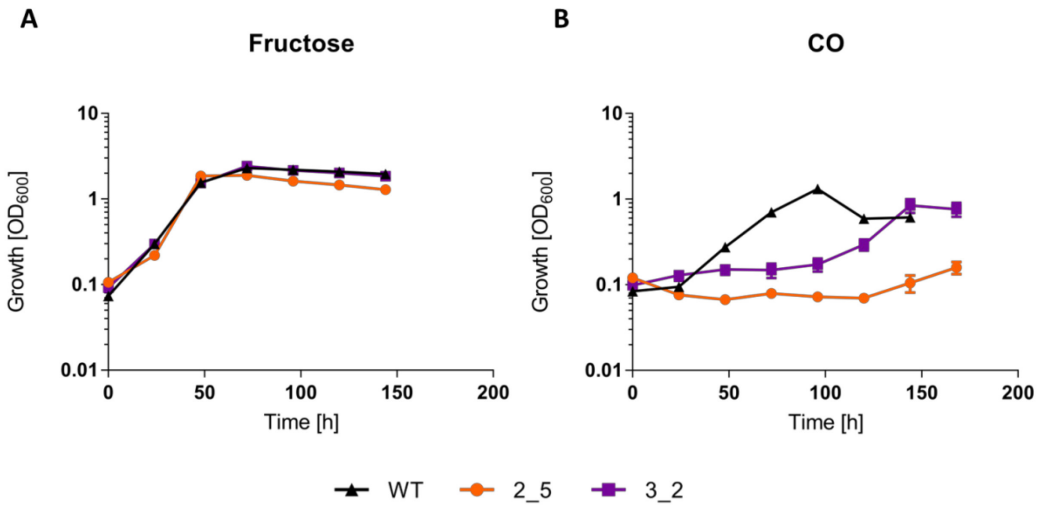


Figure 4.8: Growth of WT and *acsA* CRISPR mutants on fructose (A) and CO (B).
Growth [OD_{600}] of *C. autoethanogenum* WT (black triangles), *acsA* knockout strains 2_5 (orange circles) and 3_2 (lilac squares) on A) fructose and B) CO. Data shown as mean ± SEM (n = 3).

4.2.2.3 CRISPR verification

To clarify whether the *acsA* gene complex has indeed been knocked out, further PCR reactions were set up with different primer combinations, for all three strains (2_5 and 3_2 mutants and WT). Figure 4.9 shows the four different PCR reactions that were performed.

The result of these different PCR reactions is shown in Figure 4.10. The screening PCR using primers outside of both homology arms (PCR 1), again showed a 1.8 kb band size, which correlated with knocked out genes. However, apart from the PCR 2 reaction, both mutants showed the same banding pattern as the WT. This proved that, even though the initial screening PCR had suggested a successful knockout of the gene region, the gene was still present. This explains the ability of the mutants to grow on CO. In the second PCR set up (PCR 2), however, the gel showed unspecific bands in addition to the WT band. In case of the 3_2 mutant, a reduced band size was detectable, at around 1.5 kb. For the mutants in both PCR 3 and 4 (Figure 4.9), no band should have been detectable, as for both, one of the primers would have bound in the deleted gene region. Therefore, it can be concluded that the first screening PCR (Figure 4.7) led to a false positive result. The same result was obtained after a second, independent conjugation (data not shown). However, due to time constraints, it was not possible to undertake a third attempt to obtain a CRISPR *acsA* knockout mutant or to change the knockout strategy.

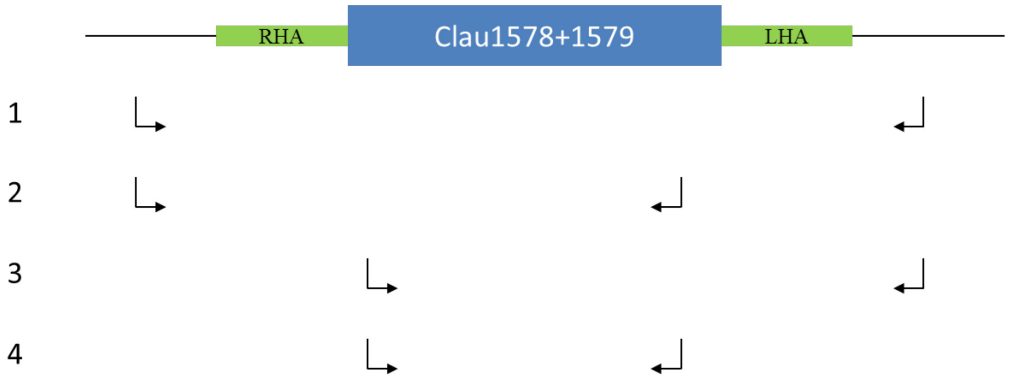


Figure 4.9: PCR reactions carried out to verify CRISPR mutagenesis of *acsA*.

Four different PCR reaction (1-4) that were set up, to verify the CRISPR/Cas mediated deletion of the *acsA* gene complex in *C. autoethanogenum*, consisting of the Clau1578 and Clau1579 locus. LHA and RHA: left and right homology arm sequence, respectively, used for the CRISPR plasmid (pSBRCas9_AcsA1/2/3) generation. Primer combinations: 1: Screening_F and Screening_R; 2: Screening_F and AcsA_rev; 3: AcsA_fw and Screening_R; 4: AscA_fw and AcsA_rev.

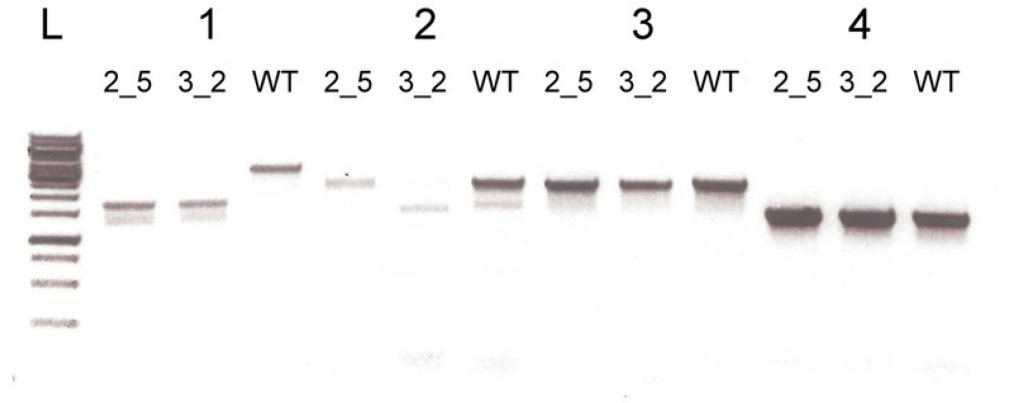


Figure 4.10: CRISPR analyses.

1 % agarose gel after PCR amplifications of the *acsA* gene and flanking regions, using the primer combinations described in Figure 4.9. Chromosomal DNA of CRISPR mutants 2_5 and 3_2 and the WT were used. L: O'GeneRuler 1 kb DNA Ladder (ThermoScientific), 1: PCR amplification using Screening_F and Screening_R primers; 2: PCR amplification using Screening_F and AcsA_rev; 3: PCR amplification using the primers AcsA_fw and Screening_R; 4: PCR amplification using the primers AscA_fw and AcsA_rev.

4.3 Discussion

The previous chapter proposed metabolic pathways and enzymes involved in fumarate fermentation in *C. autoethanogenum*. In this chapter, mutants unable to produce key enzymes of these pathways were generated and their physiological behaviour analysed. The findings that were made are discussed in the following section.

4.3.1 Fumarate hydratase as the key enzyme of the fumarate fermentation pathway

In section 4.2.1 the generation of an FH (fumarate hydratase) inactivation mutant was described. Due to disadvantages associated with insertional mutagenesis [49][50], it was initially attempted to generate an in-frame deletion mutant, after the generation of the required *pyrE* knockout strain. Even though the generation of the strain proved to be successful and resulted in a fully sequenced strain, which was used by the whole project group to generate knockout mutants, it was not possible to generate the FH deletion mutant. Reasons for this were poor conjugation success rates and the unsuccessful second homology recombination event. Consequently, it was decided to attempt generation of the FH knockout mutant using the ClosTron system. This system, despite its disadvantages like possible polar effects (influences of the genes up-/or downstream of the target gene caused by the inserted intron) [50], the possibility of multiple insertions and, occasionally, incomplete gene inactivation [50], is simple, fast and generally successful and therefore often used in *Clostridia* [165][174][175].

With respect to the FH inactivation mutants generated in this thesis, the ClosTron mutagenesis was successfully verified *via* PCR. Southern Blot analysis proved that the intron was only inserted once into the genome for the mutant FH2_24 used for later analyses and complementation.

As shown in this chapter, inactivation of the fumarate hydratase gene (Clau1855), abolished the ability to metabolise fumarate. The mutants lost the ability to grow on fumarate and no FH enzyme activity could be detected in the fructose grown cell free extracts.

As found in chapter 3, the fumarate metabolism pathway is based on several TCA cycle reactions. Fumarate is converted by the FH to malate, which is further metabolised to pyruvate and, in the end, acetate. The inactivation of FH led to the inactivation of the fumarate utilisation pathway. The mutants were unable to use fumarate as carbon source, but were still able to utilise malate. However, after re-introducing a plasmid-based copy of the encoding gene, both the FH activity and fumarate growth could be restored, although a considerably increased lag-phase was observed (Figure 4.5).

The reasons for the extended lag phase remain unknown. Presence of antibiotic in the cultures of plasmid containing strains did not seem to extend the lag phase, as can be seen from the complemented FH mutant growing on fructose. Furthermore, whilst fumarate grown cultures had been inoculated from pre-cultures grown on fructose (as the not-complemented FH mutant strains would otherwise not have been able to grow), lag phases for these conditions had been considerably shorter on previous occasions (Figure 3.9). It is possible that activity of the heterologous thiolase promoter driving FH gene expression is growth phase dependent and that it was too low to permit a fast transition into log phase.

In contrast to the FH complementation strain, the plasmid control did show neither growth on fumarate nor fumarate hydratase enzyme activity. This proves that the fumarate hydratase is a key-enzyme for *C. autoethanogenum*'s fumarate metabolism.

After these findings it was debated whether the inactivation of the malic enzyme (ME) and/or the malate dehydrogenase (MDH) might also lead to the loss of ability to grow on fumarate or malate. However, the malate to pyruvate conversion required either MDH and ME, or ME alone (Figure 4.11), as no gene encoding for an oxaloacetate decarboxylase was found in the genome. Although there was only one copy of the MDH within the genome, three putative encoding genes were found for ME. Consequently, it would require multiple gene inactivations (up to 4) to verify MDH/ME dependency. This was seen as too ambitious to be achieved within the timeframe of this project.

Pyruvate-ferredoxin oxidoreductase (PFOR) is another key enzyme of the proposed fumarate fermentation pathway. However, PFOR is essential for *Clostridia* and other anaerobic bacteria, as it plays a major role in the energy metabolism, using ferredoxin as an electron acceptor [176] and also required for gluconeogenesis. Therefore a knockout of this gene would most likely be lethal.

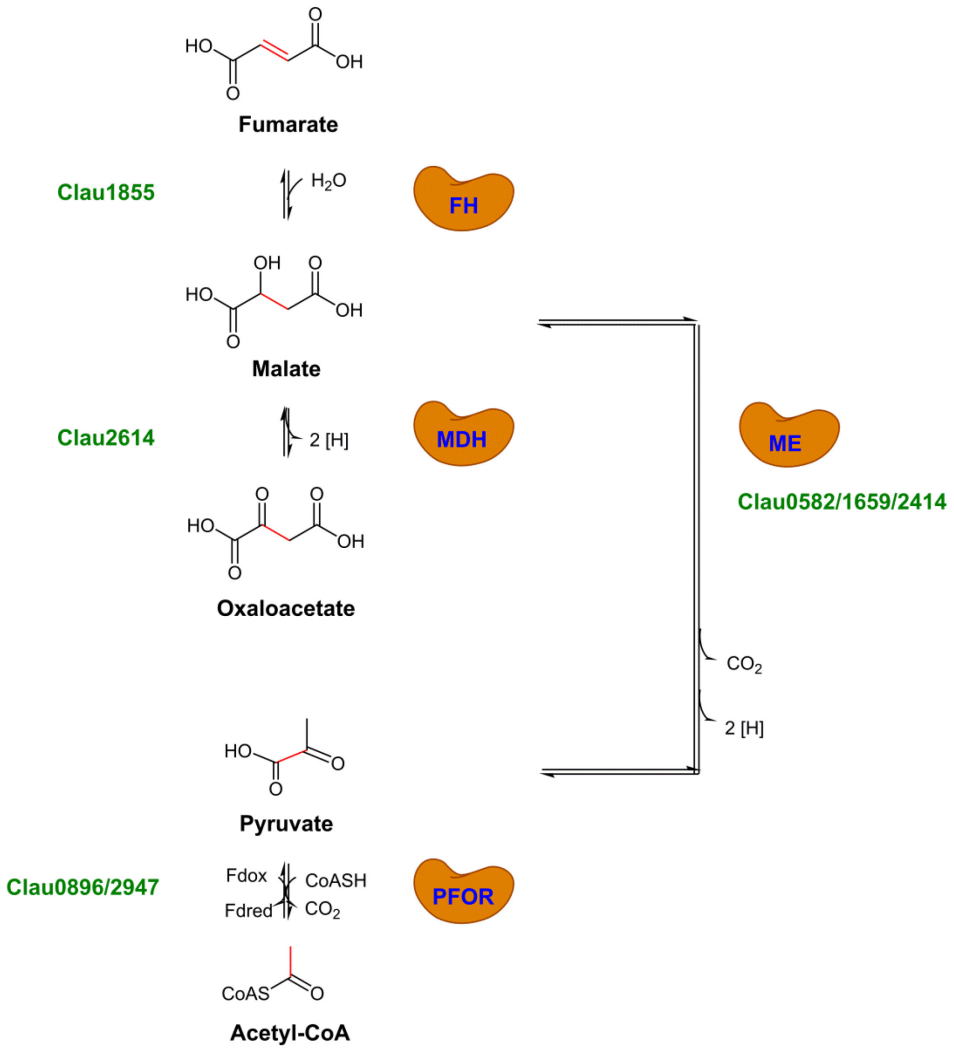


Figure 4.11: Proposed pathway of fumarate fermentation in *C. autoethanogenum*.
Pathway for fumarate utilisation and conversion to acetate in *C. autoethanogenum* including enzymes and their predicted encoding genes. FH: fumarate hydratase; MDH: malate dehydrogenase; ME: malic enzyme; PFOR: pyruvate-ferredoxine oxidoreductase. Not included is the contribution made by the WLP.

4.3.2 CRISPR/Cas9 mutagenesis of *acsA*

As reported previously, the knockout of the *acsA* complex (two genes with the locus tags Clau1578 and Clau1579) led to the inactivation of the WLP in *C. autoethanogenum* and thus loss of the ability to grow autotrophically [171]. In chapter 3 it was noted that during growth on fumarate *C. autoethanogenum* re-assimilated the released CO_2 *via* the WLP and produced acetate. Therefore,

the effects of an inactivated WLP on fumarate metabolism were of high interest. It was assumed that growth would be significantly reduced, the bacterium would start producing ethanol to recycle oxidised electron carriers, or the bacterium would lose the ability to metabolise fumarate entirely.

To investigate this further, it was decided to create a CRISPR knockout mutant, deleting the genes for *acsA*, encoding a subunit of the acetyl-CoA synthase complex. The CRISPR system was chosen, as it was newly established in the group for *C. autoethanogenum* by Peter Rowe (University of Nottingham) and was meant to be a straight forward system lacking the disadvantages of ClosTron mutagenesis. However, even though positive results and knockout mutants were obtained within the GASCHEM and SBRC group using this system, the deletion of the *acsA* gene complex was not successful, despite many attempts. The generation of false positive mutants, as described in this chapter, was highly unfortunate, as a lot of time was lost within this process. Since the original screening PCR of the suspected mutants showed clearly smaller amplicons compared to the WT, it was assumed that the deletion was successful. It was only during the growth experiments that the ability of these mutants to grow on CO led to questioning of the results.

The PCR conducted for verification of the mutants showed, that the *acsA* gene itself, however, was still present in both mutant strains. Due to the results of this PCR it was assumed that during the second recombination event (happening predominantly after the Cas9 has cut the gene), in which the plasmid is lost and the in-frame deletion region replaces the gene to be deleted, had undergone unanticipated recombination. The loss of the plasmid was confirmed through the inability of the strains to grow on the antibiotic thiamphenicol. False positive screening results when using primers outside of

the homology arms have been observed previously in the group using the ACE mutagenesis system (Baker, 2017, personal communication). After a second attempt showed the same results, due to time constrains, a third attempt of generating a CRISPR (or ClosTron or Allelic Exchange) mutant could not be conducted.

4.3.3 Summary

In this chapter the generation of a *pyrE* knockout strain of *C. autoethanogenum* was described. Additionally, it was proven that the generation of a fumarate hydratase inactivation mutant abolished the ability of *C. autoethanogenum* to utilise fumarate as carbon source. Since the plasmid-borne complementation restored this ability, it can be stated that the fumarate hydratase is a key enzyme in the fumarate metabolism for *C. autoethanogenum*. Therefore it can be excluded, that polar or other effects of the ClosTron intron have led to the described phenotype.

The knockout of the *acsA* gene cluster would have been a very interesting mutant to characterise, with regards to the growth on fumarate, but also malate and oxaloactetate as those substrates are most likely metabolised *via* the same pathway (see chapter three for references). However, CRISPR/Cas mediated gene inactivation of *acsA* failed for unknown reasons and there was insufficient time to attempt the generation of a new knockout mutant by using ClosTron mutagenesis or classical in-frame deletion.

5 Introduction of a soluble fumarate reductase into *C. autoethanogenum*

> It's the questions we can't answer that teach us the most. They teach us how to think. If you give a man an answer, all he gains is a little fact. But give him a question and he'll look for his own answers.
>
> Patrick Rothfuss, The Wise Men's Fear

5.1 Introduction

One of the original aims of the project was the enhancement of the succinate production in *C. autoethanogenum*, guided by a deeper understanding of the C_4 dicarboxylic acid metabolism of this organism. The following chapter describes an attempt of meeting this aim, by the introduction of a synthesised and codon optimised soluble fumarate reductase.

5.1.1 Fumarate reductases

Fumarate reductases (FRD) catalyse the reduction of fumarate to succinate using two electrons from various donors including quinol [177], reduced flavin adenine dinucleotide/mononucleotide ($FADH_2$/$FMNH_2$) [178], coenzyme M and B [179], or NADH [148][149].

Two major groups of fumarate reductases have been described [181]. Most typical FRDs belong to the first group, which are membrane bound enzymes and consist of three to four subunits: a catalytic subunit (FrdA) and an iron-sulfur subunit (FrdB). These are attached to the membrane by either one or two anchor subunits (FrdC/D). This specific type of FRD operates under anaerobic

conditions during fumarate respiration and in the maintenance of redox balancing [177].

The second, less common, type are soluble monomeric FRDs. They possess the conserved catalytic region of the subunit FrdA of the membrane-bound FRDs [181]–[183]. This kind of FRDs is found in several *Shewanella* species, *Saccharomyces cerevisiae*, *Trypanosoma brucei* and *Hydrogenobacter thermophilus* [134].

5.1.2 Expression of an optimised FRD from *Trypanosoma brucei* in *Aspergillus*

In 2016 Yang *et al.* [184] demonstrated succinate production could be enhanced in *Aspergillus saccharolyticus* by heterologous expression of the fumarate reductase from *T. brucei*. A truncated version of the FRD from *T. brucei* was created by omitting the putative glycosomal targeting sequence serine-lysine-isoleucine (SKI), and codon optimised, before expressing the gene on a plasmid in *A. saccharolyticus*. By doing so, the introduced FRD enzyme activity was increased up to 0.027 U/mg in the organism compared to the WT with no activity. This increased the organism's succinate production from 3.8 g l^{-1} up to 16.2 g l^{-1}.

That an amplified expression of a fumarate reductase can lead to an increase of succinate production could also be determined by Goldberg *et al.* who were able to show highly improved conversion of fumarate to succinate in recombinant plasmid *E. coli* strains [185]. Those strains contained amplified fumarate reductase and produced about 8-times more succinate compared to strains without recombinant plasmids [185].

In a recent patent application, very low levels of FRD activity have been reported for *C. autoethanogenum*. However, as stated in the previous chapters, under the conditions used, no activity was found in the current study. Furthermore, no convincing homologues for this enzyme were found to be encoded in the genome and addition of fumarate did not result in succinate formation, as might have been expected. Hence, it was of interest to introduce a heterologous FRD to (i) see whether succinate production could be achieved, and at what level and (ii) to study its general effect on fumarate fermentation. Due to the enhanced succinate production seen in *A. saccharolyticus*, it was decided to also use an optimised *T. brucei* FRD in *C. autoethanogenum*. The specific aims of the work described here were to

- Obtain a codon-optimised *T. brucei frd* gene and clone it into an expression vector.
- Introduce this vector into *C. autoethanogenum* and establish successful expression.
- Analyse the effect of FRD expression on succinate production and fumarate fermentation metabolism.

5.2 Results

5.2.1 Construction of an expression plasmid containing an optimised FRD gene

5.2.1.1 Generation of an optimised FRD gene

To generate a plasmid containing the gene for a soluble monomeric FRD, the amino acid sequence of the *T. brucei* enzyme (as used for *A. saccharolyticus*; [184]) was codon optimised for expression in *C. autoethanogenum* and synthesised in two fragments by ThermoFisher®, using GeneArt® gene synthesis (gene and amino acid sequences in Appendix b). This was due to the considerable length of the gene (3.7 kb). The codon-optimised FRD contained a natural BamHI side which was employed to combine the two fragments, as it formed the 3' end of the first and the 5' end of the second fragment.

Both fragments were amplified *via* PCR from the synthesised templates using the primers FRD_F1_NotI, FRD_R1_BamHI, FRD_F2_BamHI and FRD_R2_NheI, respectively (Table 2.4). After amplification both fragments were digested using BamHI, the first fragment additionally with NotI and second one additionally with NheI, as these sites had been incorporated at the 5' and 3' end of the optimised gene. The modular shuttle vector pMTL83151 (Table 2.3) was used for cloning. This vector was digested using NheI and NotI and antarctic phosphatase treated. After several attempts of a three-fragment ligation, no colonies, or only false positive colonies could be obtained. Due to this, SOE-PCR was attempted to combine the two FRD encoding fragments. Primer pairs FRD_F1_NotI/ FRD_R1_BamHI_overlap and FRD_F2_BamHI_overlap/FRD_R2_NheI were used to amplify each fragment in the first step of the SOE-PCR. In a second step, both fragments were

combined due to the created overlap in the first step, using the primer pair FRD_F1_NotI and FRD_R2_NheI. However, the PCR resulted in unspecific bands (data not shown). This SOE-PCR attempt was repeated several times, altering annealing and elongation temperatures, and using different polymerases. However, no PCR amplificate could be obtained.

A last attempt was the PCR amplification of the ligation product of both fragments after their digest with BamHI. This resulted in the expected gene band size of 3.7 kb (Figure 5.1).

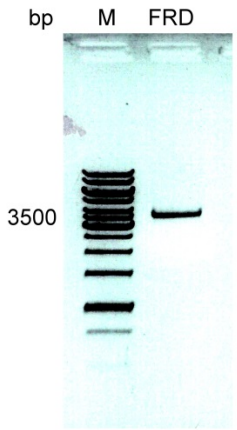


Figure 5.1: Combined FRD fragment after PCR using ligation mix as template.
Agarose gel (1 %) after PCR, using ligation mix of both FRD fragments as template. M: O'Gene Ruler, 1 kb DNA ladder; FRD: PCR product. Expected band size: 3.7 kb.

5.2.1.2 Construction of the pMTL83121 plasmid containing the *frd* gene

After the combined *frd* gene fragment had been generated, both the gene and the pMTL83151 plasmid were digested with NotI and NheI, ligated and then used to transform *E. coli* DH5α cells. However, even after several attempts and under different growth conditions of the *E. coli* cells (30 °C, 37 °C, aerobic and

37 °C anaerobic), no positive colonies were obtained. It was speculated that the gene might be toxic for *E. coli* cells. Therefore, the plasmid pMTL83121 was generated, which contained the low copy p15 Gram-negative origin of replication, instead of the high copy ColE1.

Using this backbone, ligation with the *frd* fragment and cloning into chemically competent *E. coli* DH5α cells, resulted in eight colonies. All colonies were inoculated into liquid LB medium containing chloramphenicol and grown over night at 30 °C. The plasmids were extracted and control digests undertaken using BamHI. Out of these eight screened colonies, only one showed the expected linearised plasmid size of 7.6 kb (Figure 5.2; lane 3).

The correct sequence of this one positive plasmid, termed pMTL8312_FRD was confirmed *via* Sanger sequencing.

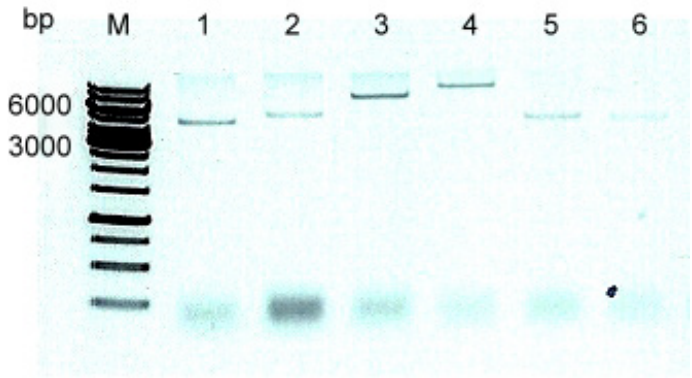


Figure 5.2: Control digest of putative pMTL8312_FRD clones.

Agarose gel (1 %) after BamHI digest of putative pMTL8312_FRD plasmids isolated from *E. coli* DH5α cells. M: O'Gene Ruler, 1 kb DNA ladder. The expected band size of the linearised plasmid was 7.6 kb. The clone on lane 3 showing the correct band size.

5.2.1.3 Construction of the pMTL8312_FRD plasmid including an N-terminal *Strep*-TagII

In order to not only analyse the protein and its activity in the cell free extract of both *E. coli* and *C. autoethanogenum*, but to also analyse the purified protein, an N-terminal *Strep*-tagged version of the FRD fragment was created. The primer pair FRD_F1_Not and FRD_R2_NheI_*Strep*TagII was used for PCR amplification of both synthesised BamHI digested and subsequently ligated *frd* fragments. The successfully generated tagged *frd* gene was cloned into the pMTL83121 plasmid and introduced into *E. coli* DH5α cells, grown at 30 °C. The sequence of positive clones was confirmed *via* Sanger sequencing. The generated plasmid was termed pMTL8312_FRD_*Strep*-TagII.

The vectors containing both FRD genes (with and without *Strep*-TagII) were additionally used to transform *E. coli* Sexpress cells for later conjugation into *C. autoethanogenum.*

5.2.2 Heterologous expression in *E. coli*

5.2.2.1 Expression in *E. coli* DH5α

Attempts were made to purify the produced FRD protein from the cell extracts of *E. coli* DH5α pMTL8312_FRD_*Strep*-TagII. Cells were grown, harvested and used to produce cell free extracts as described in 2.9.1. The generated cell extract was subjected to column-based *Strep*-Tag purification as outlined in 2.9.2.1. However, expression of the gene was very low, presumably due to the p15 replicon (low copy) used in the plasmid containing the *frd* gene. No protein was visible in the elution fraction after *Strep*-Tag purification and analysis *via* SDS-PAGE (Figure 5.3A). In the Western Blot, no bands of the

expected size of the protein (~124 kDa including 1 kDa tag) were visible, in the cell free supernatants, flow through and washing fraction 1. However, some smaller bands were very faint (Figure 5.3B). Those might have been unspecific bands or degenerated protein, which indicated protein toxicity.

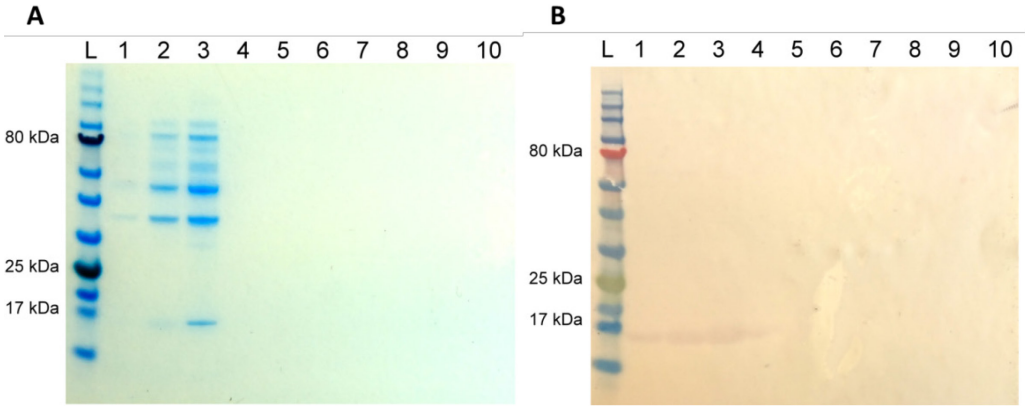


Figure 5.3: SDS PAGE gel (A) and Western Blot (B) after attempted purification of *T. brucei* FRD produced in *E. coli*.

(A) SDS PAGE gel (5-12 %) after staining with EasyBlue®, (B) Western Blot using *Strep*-Tactin® AP conjugate and NBT/BCIP colouring, of the via *Strep*-TagII affinity chromatography purified *T. brucei* FRD produced in *E. coli*. L: Colour pre-stained Protein Standard, Broad Range (NEB); 1: cell free extract; 2: flow through; 3: washing fraction 1; 4: washing fraction 5; 5-10: elution fractions 1-6.

5.2.2.2 Expression of the optimised *T. brucei frd* gene in an *E. coli* Δ*frd* strain

Due to the apparent toxicity of the *frd* gene in standard *E. coli* lab strains (DH5α, BL21DE3 and Top10 tested) it was decided to obtain an *E. coli frd* defective strain from the Coli Genetics Stock Center at Yale University (*E. coli* strain JW4114-1). The aim of this was to introduce the plasmid pMTL8312_FRD into an FRD deficient mutant and verify production of functional FRD through complementation. Chemically competent cells of the *E. coli frd* deficient strain, generated accordingly to 2.8.1, were thereby used for transformation. *E. coli* strains JW4114-1, JW4114-1 containing pMTL8312_FRD and DH5α were first grown anaerobically in enriched medium (LB and subsequently YTF) in the presence of the appropriate antibiotics. Kanamycin was added into the medium for the defect mutant, and, in case of the complementation, thiamphenicol was added to avoid plasmid loss. After 24 h of growth, the cells were streaked onto *E. coli* minimal medium (MM) agar plates (section 2.3.1) after Lambden and Guest [118]. Cells unable to grow anaerobically on MM with glycerol and fumarate (GF) or only fumarate (F) have been reported to be unable to use fumarate as an electron acceptor due to the lack of the *frd* gene [186].

Both, the DH5α positive control and JW4114-1 containing pMTL8312_FRD were able to grow on both MM plates, GF and F (Figure 5.4). The mutant without the plasmid, however, did not show growth on either, not even after 120 h of anaerobically incubation. This suggested that the pMTL8312_FRD encoded *frd* gene was functional and produced in *E. coli* at levels sufficient to allow growth under the employed selective conditions.

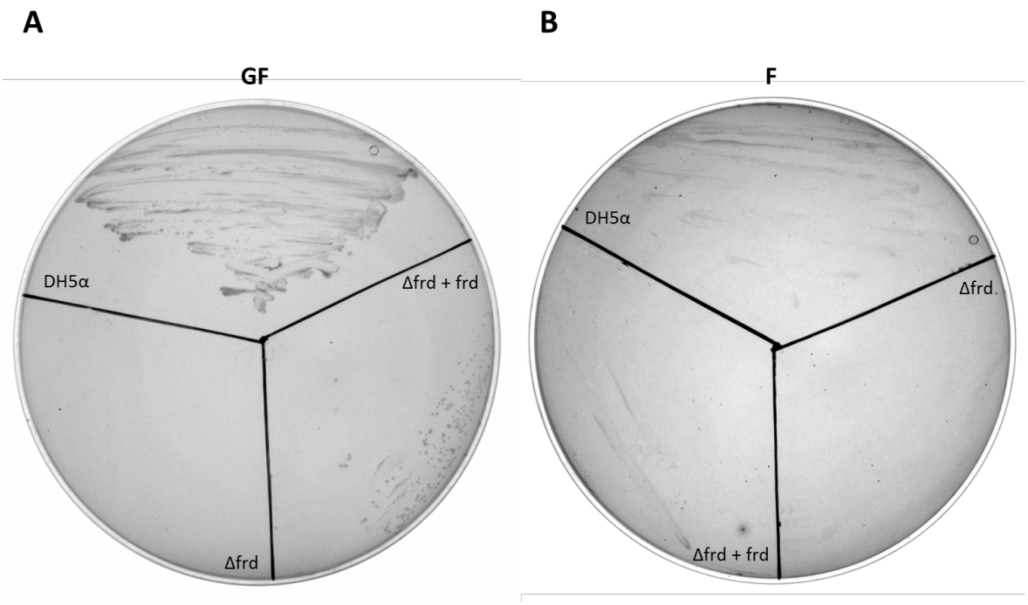


Figure 5.4: Anaerobic growth of *E. coli* DH5α, JW4114-1 and JW4114-1 pMTL8312_FRD on MM agar.

E. coli DH5α, *frd* knockout mutant *E. coli* JW4114-1 (Δfrd) and *E. coli* JW4114-1 plus pMTL8312_FRD (Δfrd + frd) grown anaerobically on minimal medium (MM) agar plates. A) MM plus 40 mM glycerol and 40 mM fumarate (GF); B) MM plus 40 mM fumarate (F).

5.2.3 Heterologous expression in *C. autoethanogenum*

5.2.3.1 Conjugation of pMTL8312_FRD into *C. autoethanogenum* cells

After the generation of the pMTL8312_FRD plasmid and its introduction into *E. coli* Sexpress cells, the plasmid was transferred into *C. autoethanogenum* cells *via* conjugation (section 2.8.2). Colonies able to grow on thiamphenicol (Tm) YTF plates were re-streaked and the presence of the *frd* gene verified *via* colony PCR. Positive bands were gel extracted and sent for Sanger sequencing. Additionally, promising colonies were inoculated into YTF liquid medium containing Tm to prevent plasmid loss. The plasmid was rescued *via* plasmid miniprep (section 2.7.2.2) and re-transformation of *E. coli* DH5α cells (section 2.8.1). Subsequently, the plasmid could be purified again from *E. coli* cells and

sent for sequencing. Only two out of 20 colonies showed the correct gene sequence. These two independent strains, termed here FRD1 and FRD2, were used for all further analyses.

To purify the FRD enzyme from *C. autoethanogenum*, the previously generated pMTL8312_FRD_*Strep*_TagII plasmid was introduced into WT cells *via* conjugation accordingly to section 2.8.2. Similar to pMTL8312_FRD, conjugation rate was very low and only one out of seven colonies showed the correct sequence.

5.2.3.2 Purification of *T. brucei* FRD produced in *C. autoethanogenum via* *Strep*-TagII

To analyse the properties of the purified enzyme, the *T. brucei* FRD was purified from *C. autoethanogenum* cell extracts (section 2.9.1) using the added N-terminal *Strep*-TagII *via* affinity chromatography (section 2.9.2.1). The obtained washing and elution fractions were used for SDS PAGE (section 2.9.2.3) and Western Blot (section 2.9.2.5). Again, unfortunately it was not possible to express a protein in the expected size of the FRD (~ 124 kDa, including *Strep*-Tag) (Figure 5.5A). The Western Blot (Figure 5.5B) shows faint bands of a much smaller size. Protein activity could be measured neither in the supernatant and flow through fractions, nor in cell free extracts of *C. autoethanogenum* pMTL8312_FRD. In all cases background reactions without substrate were seen and too high to obtain trustworthy data.

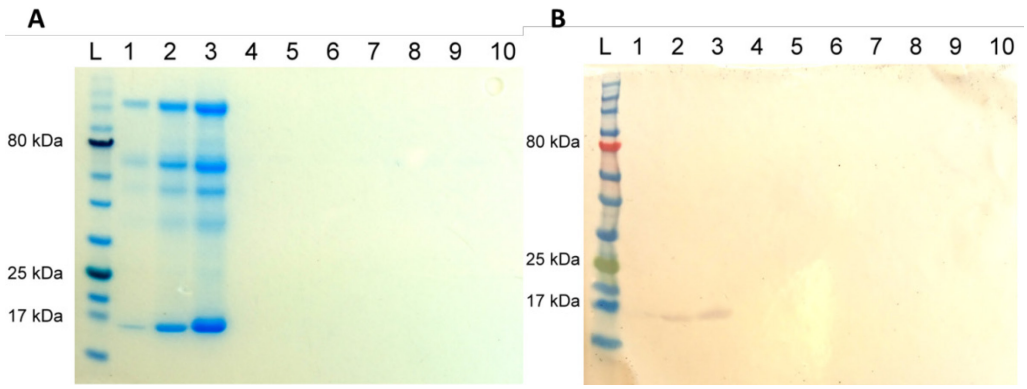


Figure 5.5: SDS PAGE gel (A) and Western Blot (B) after attempted purification of *T. brucei* FRD produced in *C. autoethanogenum*.

(A) SDS PAGE gel (5-12 %) after staining with EasyBlue®, (B) Western Blot using *Strep*-Tactin® AP conjugate and NBT/BCIP colouring, of the via *Strep*-TagII affinity chromatography purified *T. brucei* FRD produced in *C. autoethanogenum*. L: Colour pre-stained Protein Standard, Broad Range (NEB); 1: cell free extract; 2: flow through; 3: washing fraction 1; 4: washing fraction 5; 5-10: elution fractions 1-6.

5.2.3.3 Growth experiments

To analyse whether *C. autoethanogenum* can express the plasmid-borne soluble fumarate reductase gene and therefore show an increase in succinate production, growth experiments including fermentation product analysis (*via* NMR and HPLC) were conducted using the two pMTL8312_FRD carrying strains that were obatined. The carbon sources of these growth experiments were fructose, fumarate, fumarate plus hydrogen, carbon monoxide and carbon monoxide plus hydrogen. As control, both *C. autoethanogenum* with the introduced empty plasmid pMTL83121 and the wild type were used. To compare the data, both the wild type and plasmid control were grown under the same conditions and metabolites measured with the same methods as the FRD producing strains. All growth experiments were prepared and undertaken, unless otherwise stated, according to section 2.6.

Growth on fructose

To establish any metabolic effects of *frd* gene expression, FRD1, FRD2, WT and WT containing the empty pMTL83121 plasmid were grown in PETC-MES medium containing 40 mM fructose. Both FRD strains were showing very similar growth behaviour when grown on fructose with regards to OD_{600} and pH, compared to the WT and plasmid control (Figure 5.6). The WT reached the highest OD and a slightly lower pH, whereas FRD2 showed the lowest growth and pH change. The metabolic spectrum with focus on fructose consumption and succinate, lactate, ethanol and acetate production, was measured *via* HPLC.

As suggested by the growth profiles, the concentration of fructose decreased for all strains in a similar manner, even though the WT seemed to have consumed slightly more fructose compared to the mutants which may have caused the slightly increased OD (Figure 5.7).

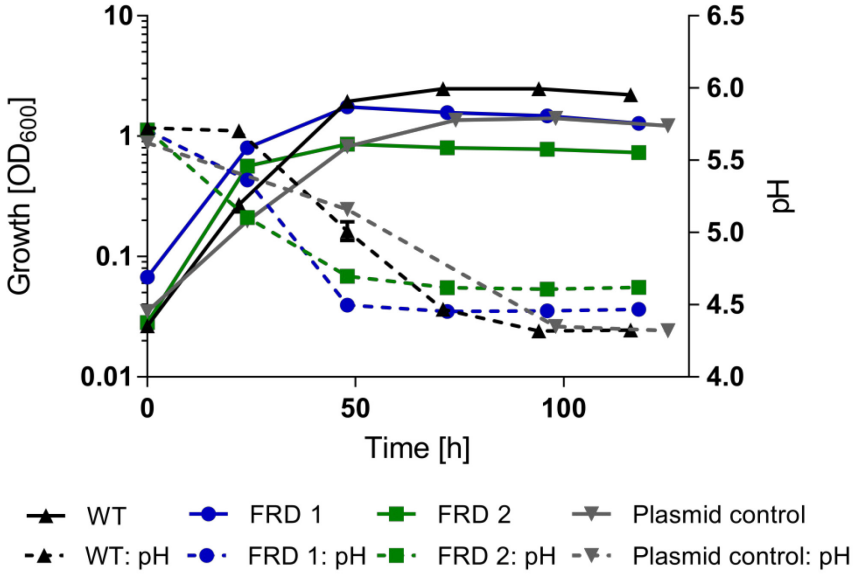


Figure 5.6: Growth and pH of *C. autoethanogenum* FRD strains, WT and plasmid control grown in PETC-MES on fructose.

Growth [OD_{600}] of *C. autoethanogenum* strains FRD1 and FRD2 harbouring the plasmid-borne soluble FRD compared to WT and WT plasmid control grown on fructose. FRD1: blue circles; FRD2: green squares; WT: black triangles; WT plasmid control: grey inverted triangles. OD_{600}: solid lines; pH: dashed lines. Data shown as mean ± SEM (n = 3).

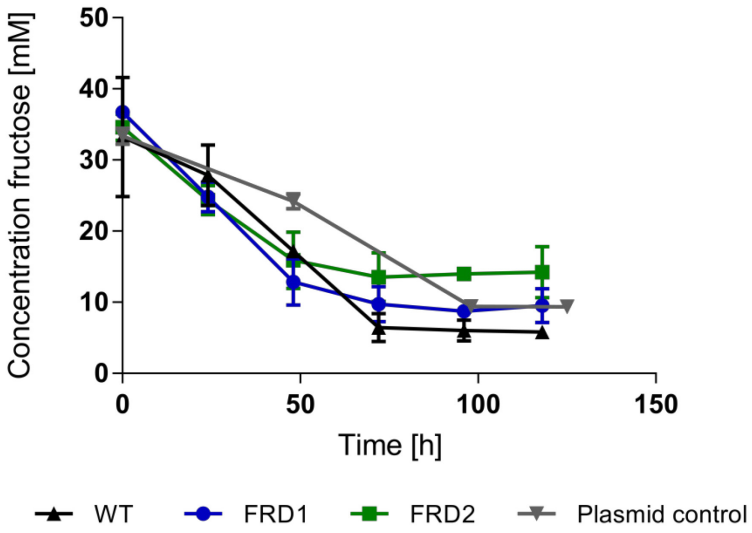


Figure 5.7: Fructose consumption of *C. autoethanogenum* FRD strains, WT and plasmid control grown in PETC-MES medium.

Fructose concentrations in the culture supernatant of FRD and WT strains grown in PETC-MES medium on 40 mM fructose were determined by HPLC. FRD1: blue circles; FRD2: green squares; WT: black triangles; WT plasmid control: grey inverted triangles. Data shown as mean ± SEM (n = 3).

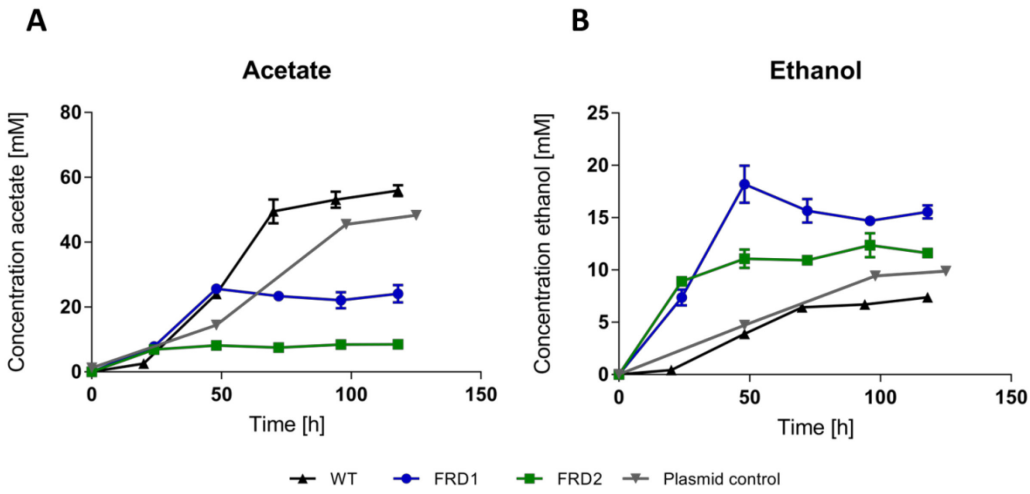


Figure 5.8: Acetate (A) and ethanol (B) production of FRD strains, WT and plasmid control grown in PETC-MES on fructose.

A) Acetate and B) ethanol production FRD and WT strains grown in PETC-MES medium on 40 mM fructose were determined by HPLC. FRD1: blue circles; FRD2: green squares; WT: black triangles; WT plasmid control: grey inverted triangles. Data shown as mean ± SEM (n = 3).

Both FRD strains showed considerably decreased acetate and increased ethanol production (Figure 5.8). The WT produced around 56 mM of acetate at its maximum (similar to the plasmid control), whereas FRD1 only produced 27 mM and FRD2 even less with 10 mM. With regards to ethanol, FRD1 shows increased ethanol production up to 20 mM, which is twice as much as the WT and plasmid control produced (~10 mM). However, FRD1 seems to metabolise some of the ethanol during the stationary growth phase as the concentration decreases by 4 mM.

FRD2 showed an even lower acetate concentration and a slightly less ethanol production compared to FRD1. It also did not grow to the same OD_{600} as FRD1.

As previously pointed out, the main interest was in potential succinate production by the FRD producing strains. Figure 5.9A demonstrates that,

indeed, both FRD mutants showed succinate production of up to 1.7 mM according to HPLC (and NMR, as first confirmation), which equates to 0.2 g l^{-1} and a yield of 0.03 g g^{-1} fructose.

In addition to the increase of ethanol and succinate production, a considerably increased amount of lactate was measured (Figure 5.9B). Lactate production of both FRD strains was significantly increased compared to the WT and plasmid control. FRD1 showed a maximum production of 11 mM lactate and FRD2 even 18 mM.

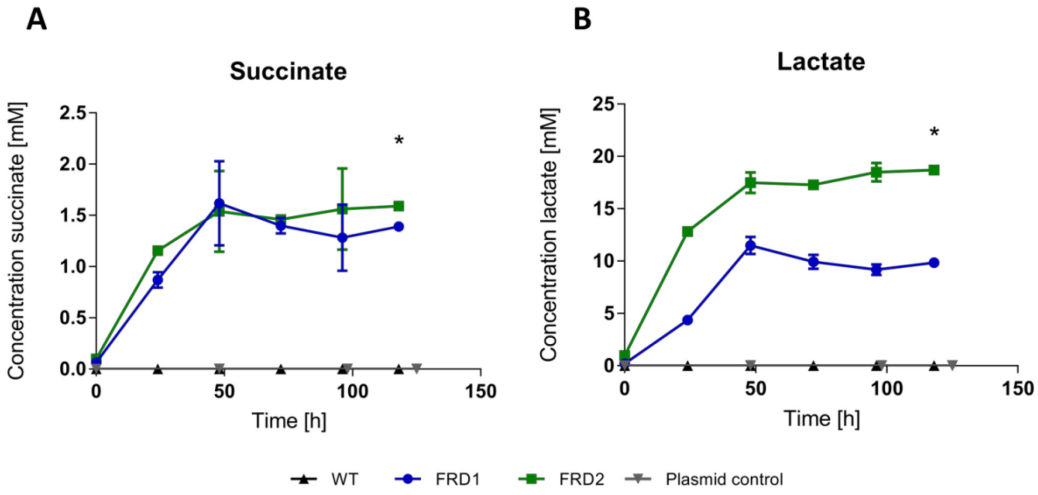


Figure 5.9: Succinate (A) and lactate (B) production of FRD strains, WT and plasmid control grown in PETC-MES on frcutose.

Succinate (A) and lactate (B) production of both FRD strains grown in PETC-MES medium on 40 mM fructose, measured *via* HPLC. FRD1: blue circles; FRD2: green squares; WT: black triangles; WT plasmid control: grey inverted triangles. Statistically significance is shown for one example each after 118 h. A) FRD1 to WT: paired t-test $t(4) = 43.13$, $p = 0.000$; FRD2 to WT: pared t-test $t(4) = 81.74$, $p = 0.000$. B) FRD1 to WT: paired t-test $t(4) = 38.93$, $p = 0.000$; FRD2 to WT: paired t-test $t(4) = 53.19$, $p = 0.000$. Data shown as mean ± SEM ($n = 3$).

Growth of fumarate and fumarate sparged with hydrogen

As shown in chapter 3, *C. autoethanogenum* is able to use fumarate as the only carbon and energy source. Fumarate is a pre-cursor for succinate and FRD the enzyme catalysing the formation of succinate from fumarate. Therefore, it was of interest to see whether (i) the FRD strains could still grow, or grow even better on fumarate (as the FRD reaction requires reducing equivalents in form of NADH for which a sink is needed) and (ii) which proportion of fumarate could be converted to succinate. Additionally, given the requirement of the FRD reaction for reducing equivalents, fumarate was to be used as carbon source in the presence of exogenous hydrogen (to be added in form of 100 % hydrogen in serum bottles at 1 bar overpressure). The formation of acetate and ethanol was measured using GC and the production of succinate and lactate was measured with HPLC.

Both FRD strains and the WT showed similar growth behaviour on both fumarate and fumarate sparged with hydrogen (Figure 5.10). Both pre-cultures were grown on fructose. That is why growth of the WT was slightly lower as previously measured (Chapter 3).

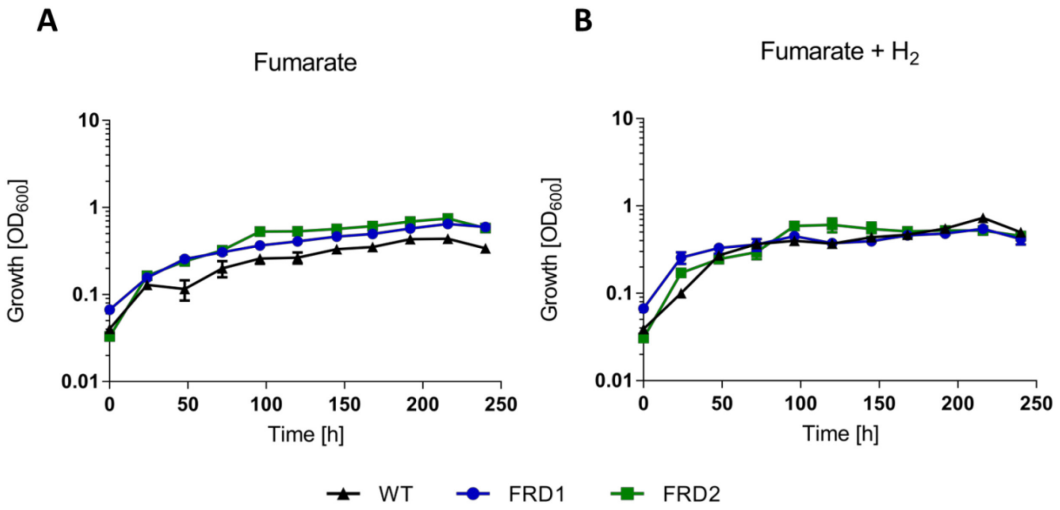


Figure 5.10: Growth of FRD strains and WT grown in PETC-MES on fumarate (A) and fumarate + H_2 (B).

Growth of *C. autoethanogenum* strains FRD1 and FRD2 harbouring the plasmid-borne soluble FRD compared to WT grown on A) fumarate and B) fumarate plus 1 bar 100 % H_2 overpressure. FRD1: blue circles, FRD2: green squares, WT: black triangles. Data shown as mean ± SEM (n = 3).

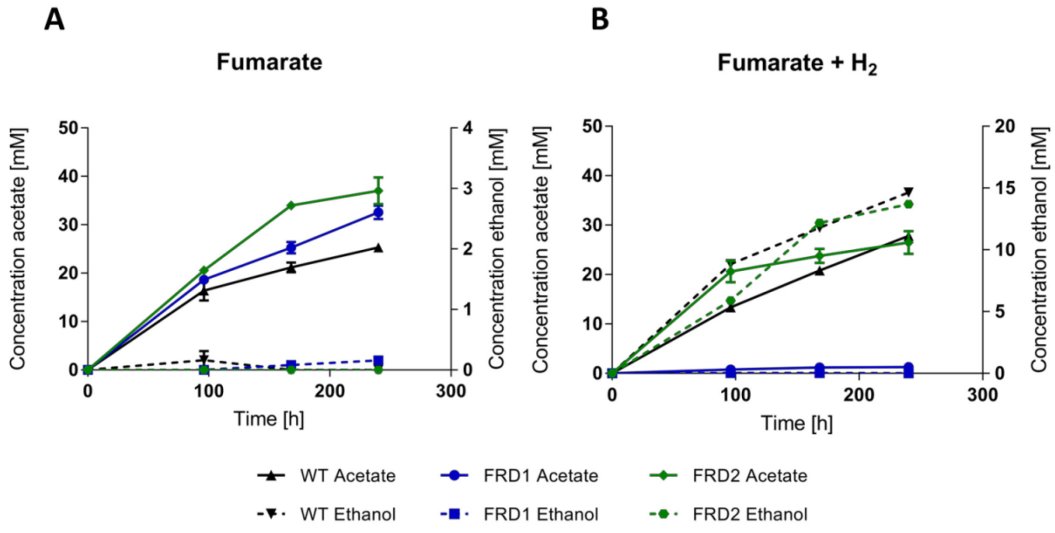


Figure 5.11: Acetate and ethanol production of FRD strains and WT in PETC-MES medium on fumarate (A) and fumarate + H_2 (B).

Acetate and ethanol production of *C. autoethanogenum* strains harbouring the plasmid-borne soluble FRD compared to WT grown on A) fumarate and B) fumarate plus 1 bar 100 % H_2 overpressure. FRD1: blue circles; FRD2: green squares; WT: black triangles. Solid lines: acetate, dashed lines: ethanol. Data shown as mean ± SEM (n = 3).

When grown on fumarate, in line with the observed lower growth, the WT showed a slightly decreased acetate production compared to the FRD1 and FRD2 strains. Again, the FRD strains differ, with FRD2 producing slightly more acetate (40 mM) than FRD1 (36 mM; Figure 5.11). With regards to the ethanol production, all strains showed the same behaviour. Barely any ethanol was produced, in line with the previously (chapter 3) established behaviour.

However, when grown on fumarate with additional provided hydrogen, acetate production appeared to be slightly decreased for FRD2, highly decreased for FRD1 and similar for the WT, when compared to fumarate only (Figure 5.11). With regards to the ethanol production, both FRD2 and the WT strain showed a considerably increased production compared to the growth on only fumarate. However, FRD1 produced hardly any ethanol when grown on fumarate plus hydrogen.

It was found that no lactate was produced for any of the strains (data not shown). However, succinate production for the FRD strains on fumarate/H_2 was significantly higher than observed for growth on fructose and fumarate only (Figure 5.12). The maximum production thus was 30 mM (3.54 g l^{-1}) of the strain FRD1 when grown on fumarate plus hydrogen. This results in the highest measured yield of succinate production for *C. autoethanogenum* of 0.76 g g^{-1} fumarate.

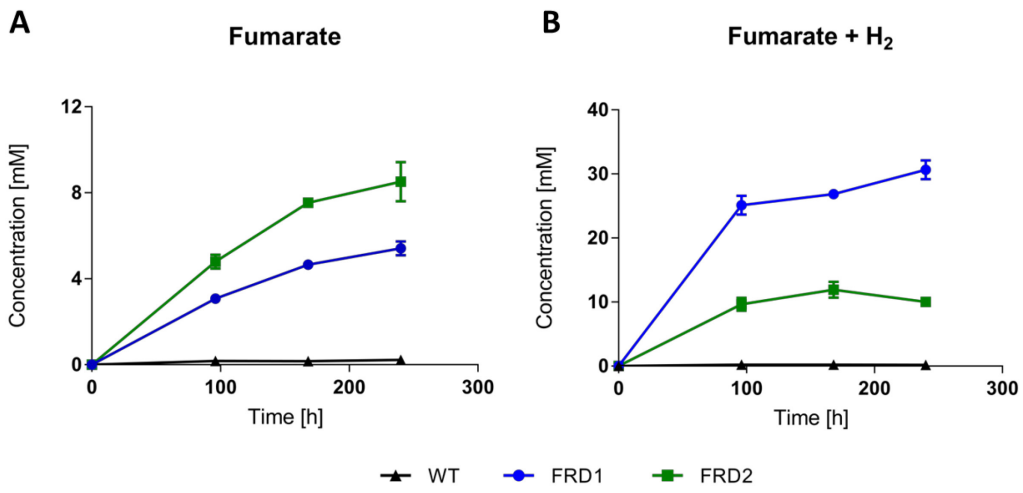


Figure 5.12: Succinate production of *C. autoethanogenum* FRD strains during growth on fumarate (A) and fumarate plus hydrogen (B).

Succinate production of *C. autoethanogenum* strains harbouring the plasmid-borne soluble FRD compared to WT grown on A) fumarate and B) fumarate plus 1 bar 100 % hydrogen overpressure. FRD1: blue circles; FRD2: green squares; WT: black triangles. Data shown as mean ± SEM (n = 3).

Growth on CO

Since one of the most interesting characteristics of *C. autoethanogenum* is the ability to grown under autotrophic conditions on carbon monoxide (CO), and the production of succinate under these conditions has not been observed until now, is was of high interest to establish whether the FRD strains continued to produce succinate on this carbon source.

Fructose grown cells were used to inoculate the main cultures in 250 ml serum bottles containing 50 ml PETC-MES medium under one bar CO overpressure (which thus only contained CO as carbon source apart from minor amounts of fructose carried over from the pre-cultures).

The following figures show growth (Figure 5.13), acetate, ethanol (Figure 5.14A) and succinate (Figure 5.14B) production of the FRD strains compared

to the WT during the growth on CO. Fermentation products were determined by HPLC.

As seen in Figure 5.13 the WT grew slightly faster compared to the FRD strains, however the maximum OD_{600} reached was the same (0.8). With regards to pH, for all strains the pH decreased over time, with the maximum decrease during the exponential growth phase.

Both FRD strains showed a very similar acetate and ethanol production profile, where the ethanol production peaked when the stationary phase was reached and then decreased again, whereas the acetate concentration showed its maximum at during the end of the exponential phase.

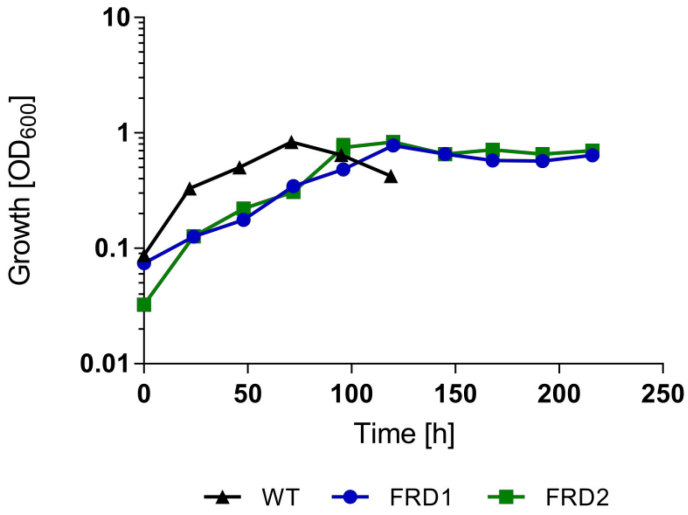


Figure 5.13: Growth of WT and FRD strains on CO.

Growth [OD_{600}] and pH was determined for *C. autoethanogenum* WT (black triangles) and strains FRD1 (blue circles) and 2 (green squares). Data shown as mean ± SEM (n = 3).

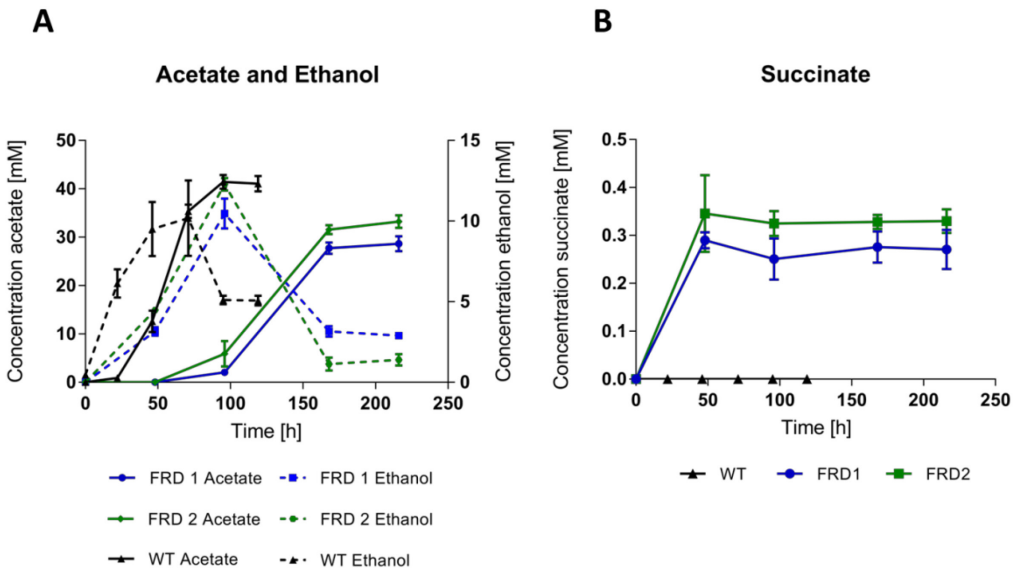


Figure 5.14: Acetate, ethanol (A) and succinate (B) production profile of WT and FRD strains in PETC-MES medium on CO.

HPLC measured concentrations of A) acetate: solid lines; left y-axis), ethanol: dashed lines; right y-axis) and B) succinate in the supernatants of *C. autoethanogenum* WT (black triangles) and FRD strains 1 (blue circles) and 2 (green squares) over time. Data shown as mean ± SEM (n = 3).

Despite the somewhat different amounts, the overall behaviour of the WT resembled that of the mutants. For the latter, ethanol production peaked once the stationary phase was reached, and was then re-assimilated. Acetate concentration showed its maximum at the end of the stationary phase. In general, the acetate production of the WT was slightly higher compared to the mutants, whereas the ethanol production was slightly lower.

With regards to succinate, production by the FRD strains was considerably lower compared to growth fructose, fumarate and fumarate with hydrogen (Figure 5.14B). Even though succinate was detected in the cultures of both FRD strains (maximum ~ 0.3 – 0.4 mM), this was most likely caused by the fructose that was left over in the medium from the pre-cultures (0.6 mM, data not shown). This can be assumed as the succinate concentration only increases

until 48 h (which is when the fructose is completely consumed) and then remains at the same level. From this it follows that that the *C. autoethanogenum* FRD strains did not produce succinate from carbon monoxide.

Growth on CO plus hydrogen

Since the addition of hydrogen in the growth experiments with fumarate increased the amount of produced succinate considerably, it was also added to cultures grown autotrophically on CO. For this, one bar of CO and additional 0.5 bar of H_2 (total of 1.5 bar overpressure) were applied to 250 ml serum bottles containing 50 ml PETC-MES medium, which were inoculated with WT, FRD1 and FRD2 strains.

The strains FRD1 and WT showed the same growth behaviour with respect to OD_{600} and pH profile, whereas FRD2 showed a slightly delayed and lower growth (Figure 5.15A). However, no succinate production could be measured for any of the strains (data not shown). Again, the FRD strains differed from each other and the WT in terms of acetate and ethanol production (Figure 5.15B), although direct comparison is difficult due to the different growth behaviour of FRD2. The FRD1 strain at least appeared to produce more ethanol (at peak concentration) than the WT, whereas acetate production for both strains was very similar.

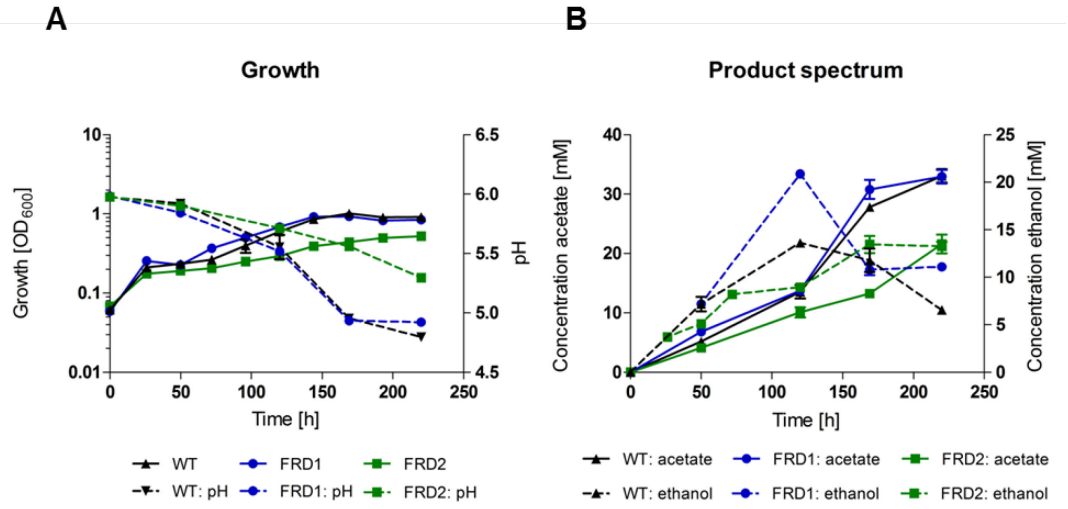


Figure 5.15: Growth (A) and product spectrum (B) of WT and FRD strains grown in PETC-MES on CO plus H_2.

A) OD_{600} (solid lines) and pH (dashed lines) of *C. autoethanogenum* strains on CO and H_2 with 1 and 0.5 bar overpressure. B) Acetate (solid lines) and ethanol (dashed lines) production measured by HPLC in the culture supernatant. FRD1: blue circles; FRD2: green squares; WT: black triangles. Data shown as mean ± SEM (n = 3).

5.3 Discussion

One of the aims of this PhD project was the improvement of the natural succinate production by *C. autoethanogenum via* reductive TCA pathway reactions, as the organism was said to produce a small amount of succinate (17 µM) as an overflow product [106][139]. However, as determined during the work on this project and as described in Chapter 3, *C. autoethanogenum* was found to lack the enzyme that converts the precursor fumarate into succinate in this pathway, the fumarate reductase (FRD). Thus, it was proposed to introduce a newly discovered soluble FRD, which had been found to improve succinate production in *Aspergillus saccharolyticus* [184], into the organism. As described previously, fumarate reductases and succinate dehydrogenases usually consist of a variable number of subunits and are mostly bound to the membrane. Thus, a soluble enzyme without additional subunits would simplify the work and cloning processes. In the following section, difficulties of the cloning process and the increase of succinate production observed are discussed.

5.3.1 Difficulties in the construction of the plasmid

The *T. brucei* fumarate reductase, proven to increase the succinate production in *Aspergillus saccharolyticus*, was codon optimised for *C. autoethanogenum* and synthesised in two parts by Invitrogen *via* GeneArt® (ThermoFisher). The company suggested an easy combination of those two fragments, due to existing BamHI restriction side, *via* digestion and ligation. However, the process of combining the two gene fragments was found to be more complicated than expected. The first method for combining the fragments was

performed according to the company's suggestions. Therefore, both fragments were digested and a three-component ligation of both the fragments and the plasmid backbone attempted. This, however, did not result in a positive outcome, despite various attempts including the change of the concentrations of the fragments and backbone, and incubation times. A next attempt was to combine both fragments by SOE-PCR before cloning. Therefore, primers including overlapping regions on the fragments were used and SOE-PCR (Figure 2.1) attempted. However, despite various changes in the PCR programme, a combined fragment of the *frd* gene could not be obtained. Therefore, the last obvious remaining method was to digest and ligate both fragments *via* their BamHI restriction side, and PCR amplify the ligation product. This, finally, resulted in a single combined *frd* gene sequence, which was verified *via* Sanger sequencing.

Furthermore, despite attempting the purification of the FRD in both *E. coli* and *C. autoethanogenum*, no purified FRD could be obtained. This led to the assumption that the tagged form was either instable as a protein, or, due to toxicity in *E. coli*, the vector/gene was not stably maintained and hence a truncated form transferred into *C. autoethanogenum*. Additionally, it was attempted to measure FRD enzyme activity for the tagged enzyme in cell free extracts, but without success. This is in line with the above interpretation of the finding made during the FRD purification in both *E. coli* and *C. autoethanogenum*.

5.3.2 Succinate production by *C. autoethanogenum*

After various attempts at cloning, the plasmid containing the *frd* gene sequence could be transferred into *C. autoethanogenum via* conjugation. However, only two out of 20 screened strains were confirmed to contain the correct plasmid, again hinting at stability issues. Therefore, both independently obtained strains were analysed in parallel. Indeed, the presence of the produced enzyme led to production of succinate during the growth on fructose as described in section 5.2.3.3. During the growth of the strains on fructose, up to 1.7 mM and therefore 0.2 g l^{-1} of succinate were produced. This is a 100 fold increase in comparison to the previously reported amount of 17 µM (0.017 mM) [108]. As stated in chapter 3, no evidence for native succinate production could be found under conditions employed in this study.

Overall, growth of the two FRD producing strains with regards to OD_{600} and pH was very similar compared to the WT when grown on fructose. As the cultures reduced the concentration of the provided fructose by about 30 mM, only around 3.7 % of the provided carbon was used for succinate production. Compared to the WT, both generated FRD strains showed an increased ethanol and lactate and decreased acetate production.

Due to the achievement of establishing the production of succinate during the growth on fructose, it was thought that growth on fumarate and especially the growth on fumarate with additional hydrogen supplementation, may lead to even higher production of succinate, as fumarate is the direct precursor of succinate and used by the introduced FRD enzyme. This assumption was proven to be true, as both FRD strains showed an increased succinate production when grown on fumarate (up to 5.5 mM and 8.7 mM for FRD1 and FRD2, respectively) and even higher in presence of exogenous hydrogen (up to

30 mM and 10 mM for FRD1 and FRD2, respectively). This might be due to the fact that reducing equivalents would be the limiting factor for the FRD reaction (in form of NADH) during the conversion of fumarate into succinate. For both strains, when grown on fumarate, no lactate could be measured. Additionally it was found, that even if comparable data for both strains could be achieved when growing only on fumarate (5.5 – 8.7 mM succinate; 36.8 – 40.5 mM acetate; constant low 3 mM ethanol), considerable differences were found when the strains were grown on fumarate in the presence of hydrogen. Here, the FRD1 strain produced very low amounts of acetate (5.4 mM) and ethanol (3.7 mM constant), whilst diverting most carbon into the production of succinate (30 mM) which equates 3.54 g l^{-1}. As the initial amount of fumarate provided was around 40 mM, it can be estimated that almost all the provided carbon, excluding the amount used for the biomass production, was converted into succinate. Unfortunately, the precise amount of fumarate used in this experiment could not be measured, as in the HPLC fumarate and acetate peaks overlay, and the LC-MS data resulted in inconclusive findings. Therefore the amount of metabolised fumarate was estimated using the theoretical amount of 40 mM that was initially provided. Using the numbers provided and the assumption that *C. autoethanogenum* has a biomass production of 0.34 g l^{-1} OD^{-1} (see 2.6), the yield of succinate during the growth on fumarate plus hydrogen for *C. autoethanogenum* FRD1 can be calculated as 0.76 g g^{-1} fumarate. Since only around 1.5 mM of acetate were produced, very little ATP could have been generated *via* the ACK reaction, which is the assumed pathway of energy generation in *C. autoethanogenum* on organic substrates [43].

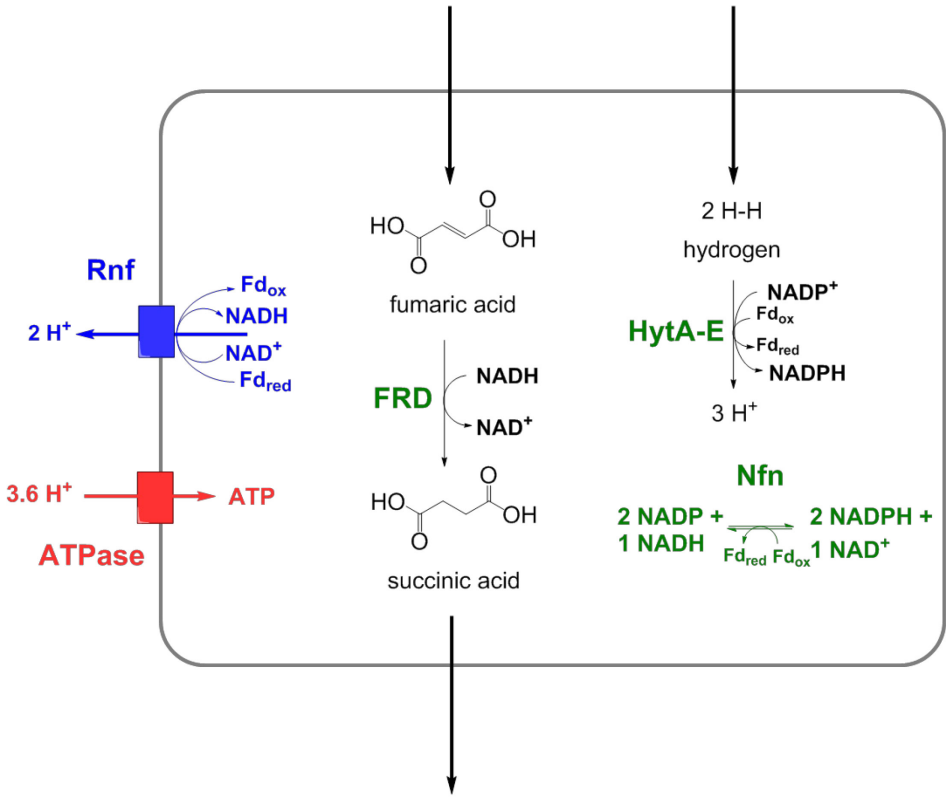


Figure 5.16: Proposed scheme of energy conservation during the production of succinate from fumarate and hydrogen by *C. autoethanogenum* FRD1.

Proposed energy conservation pathway for *C. autoethanogenum* when grown on fumarate plus hydrogen and overexpressing a soluble introduced fumarate reductase. Two H_2 provide the electrons and protons to generate 1 reduced ferredoxin, 1 NADPH and 3 H^+ by the HytA-E complex (an electron bifurcating and NADP dependent hydrogenase) **[31]**. The generated NADPH is converted to NADH by the Nfn complex **[31]**. Hereby generated NADH is used by the FRD to produce succinate. The NAD^+ and reduced ferredoxin generated during these processes are substrates of the Rnf complex **[32]** which forms a proton gradient whilst transferring electrons from ferredoxin to NAD^+. This generated proton motif force is used by an F_0F_1-type ATPase to generate ATP.

Therefore, the most likely way of energy conservation under these conditions, and therefore the fundament of growth, would be *via* the combinations of the Nfn and Rnf complex which generate a proton gradient across the cell membrane which then drives an ATPase and leads to ATP generation (Figure 5.16).

The FRD2 strain, in comparison, showed only a slightly increased production of succinate in presence of hydrogen (10.2 mM) but considerable acetate and ethanol production (26.5 mM and 13.7 mM, respectively). This suggests that the additionally provided hydrogen was rather used for the ethanol, than succinate production. This may indicate that expression of the *frd* gene in both strains differs. Alternatively, the metabolic changes observed for either strain may be further influenced by mutation(s) in chromosomally encoded genes. Next generation sequencing and RNA analyses may provide relevant information regarding the expression levels of FRD and other metabolic enzymes.

Previous studies of other bacteria have shown that the inactivation of the alcohol dehydrogenase, lactate dehydrogenase and formate lyase can lead to an improved succinate production [62] (section 1.6.2). Therefore, future attempts to improve succinate production might involve the inactivation of these genes in an *frd* expressing *C. autoethanogenum* background. However, the aforementioned bacteria all possess different metabolic networks. Thus, a potentially more promising approach would be to exploit the recently developed genome scale metabolic model of *C. autoethanogenum* (Rupert Norman, University of Nottingham; unpublished) for the development of novel metabolic engineering strategies.

One aim at the beginning of this work was to increase succinate production of *C. autoethanogenum* during its autotrophic growth on CO. Therefore both mutant strains and the WT were grown in serum bottles containing PETC-MES medium and 1 bar overpressure of CO. However, as stated in this chapter, the measured succinate production of 0.6 mM was likely produced by the remaining fructose in the pre-culture used for inoculation. Experiments with

CO grown pre-cultures would result in more definite data. It was attempted to wash cells before inoculation, but this led to no growth of the bacterium (data not shown). Slightly increased ethanol and decreased acetate production compared to the WT were measured for the FRD strains grown on CO, similar to the determined metabolic spectrum observed during the growth on fructose. Since the addition of hydrogen positively influenced the production of succinate, it was thought that growing the strains on CO plus hydrogen might show an effect to the succinate production. However, the results obtained here were similar to what was seen for growth on only CO. It was calculated that the production of succinate would be theoretically feasible (Rupert Norman, personal communication), but the conducted experiments suggest that autotrophic production of succinate is not favourable at least when relying on the existing metabolic network.

Future attempts to increase the production of succinate during the growth on CO or CO_2 and H_2 may therefore involve the inactivation of the ACK and ADH. This would prevent the organism from producing acetate and ethanol and therefore might steer the carbon and energy flux into succinate production. In 2015 Mock *et al.* proposed the possibility of energy production of *C. autoethanogenum* during the growth on CO_2 and H_2 without acetate production, but only ethanol production. Therefore, if both acetate and ethanol production are disabled and the FRD enzyme is expressed, it may be possible for the organism to generate succinate from CO, given that this would require the same input of NADH per molecule acetyl-CoA as the generation of ethanol.

5.3.3 Summary

The main aim of the work described in this chapter was the establishment and improvement of the succinate production by *C. autoethanogenum*. This was achieved by the introduction of a codon optimised soluble fumarate reductase on plasmid. This plasmid-borne gene could also be used to re-store the ability of an *E. coli frd* mutant to use fumarate anaerobically as electron sink.

During the growth on fructose a productivity of 0.2 g l^{-1} could be measured with a yield of 0.03 g g^{-1} fructose. When using fumarate as carbon source under the additional provision of 1 bar overpressure of H_2, succinate production was increased to 3.54 g l^{-1} with a yield of 0.76 g g^{-1} fumarate. However, when grown autotrophically, no succinate production could be measured.

6 Summary and general discussion

> The purpose of a storyteller is not to tell you how to think, but to give you questions to think upon
>
> Brandon Sanderson, Way of Kings

6.1 Key findings of this work

6.1.1 C_4 dicarboxylic acid metabolism of *C. autoethanogenum*

One of the original aims of this work was the improvement of the natural succinate production of *C. autoethanogenum*. However, in order to do so, the pathway(s) leading to said succinate production, needed to be understood. In this work it was found that *C. autoethanogenum* possesses a part of the branched TCA "cycle", the branch of which allows the use of fumarate, malate and oxaloacetate as carbon sources. However, this branch did not allow the utilisation of succinate, which is also a part of the TCA cycle.

C. ljungdahlii was, like *C. autoethanogenum*, found to have an incomplete TCA "cycle" and genes encoding for a malate dehydrogenase and fumarate hydratase, but no genes for a succinate dehydrogenase. Other acetogens, like *C. carboxidivorans* [187] and *M. thermoacetica* [188] also have a degenerated TCA "cycle". *M. thermoacetica* only lacks the gene encoding for a fumarate reductase [188], whereas *C. autoethanogenum* is missing a 2-oxoglutarate dehydrogenase. A 2-oxoglutarate dehydrogenase, however, was found in the closely related *C. ljungdahlii* [37]. A citrate synthase, even though not exactly described in the genome, was found to be most likely encoded by the gene with the locus tag Clau2674, which encodes for an (R)-citramalate synthase, but shows an 80 % similarity to the re-citrate synthase from *C. kluyveri* [189]. This

leads to the assumption that the branched pathways of the TCA cycle in anaerobic organisms evolved differently [188][190].

It was also established that *C. autoethanogenum* does not produce and excrete succinate, as previously stated [107][139], as this compound could be measured neither by HPLC nor LC-MS, at concentrations above the detection limit. The original claim that *C. autoethanogenum* naturally produces 17 µM of succinate could not be verified for the strain that was worked with. On the contrary, it was found that the yeast extract, an ingredient of PETC-ljungdahlii medium, contained succinate. As this resulted in a concentration of around 20 µM in the final medium, PETC-ljungdahlii was replaced with PETC-MES for all subsequent experiments. Furthermore, it was found that, the *C. autoethanogenum* WT strain JA1-1 (DSM10061) that was used for this study, does not contain genes encoding for a succinate dehydrogenase or fumarate reductase, meaning that the strain is theoretically not able to produce succinate *via* reactions of the reductive TCA pathway.

6.1.2 Fumarate metabolism of *C. autoethanogenum*

When *C. autoethanogenum* was first described by Abrini *et al.* [35], it was found that the organism was not able to use fumarate as sole carbon source, in contrast to the closely related *C. ljungdahlii* [36]. However, in this work, during early feeding experiments with fumarate in order to exclude a potential substrate limitation for a possible succinate production, it was found that the addition of fumarate led to an increased growth of the organism. By using 2,3-$^{13}C_2$-labelled fumarate, it was found that cysteine, provided as reducing agent and sulfur source, reacted spontaneously with the provided fumarate. Therefore

the sulfur source was changed to sodium sulfide. It was also possible to adapt *C. autoethanogenum* to growth on fumarate as sole carbon and energy source, which disproved Abrini's findings from 1994 [35]. It was therefore decided to analyse the fumarate fermentation pathway in more detail. NMR has become a powerful analytical tool and advantage was taken of local expertise and sophisticated equipment to establish *in vivo* growth analyses within an 800 MHz NMR machine. This provided the most interesting approach to solving the fumarate breakdown pathway and was, to the best of our knowledge, the first time an acetogenic bacterium was grown within the bore of an NMR machine spectrometer.

While *in vivo* NMR experiments have been conducted previously with bacterial and eukaryotic cells [167], [168], [191][192], including *Clostridium neopropionicum* [193], cells in those studies were grown outside of the NMR for these experiments, centrifuged and re-suspended in order analyse the resulting living cells within the NMR spectrometer. Therefore, analysing the product spectrum of bacteria during their growth within an NMR machine seems to be a new and useful method for future analyses.

By using both partially and fully labelled fumarate during these experiments, it was found that fumarate-derived CO_2, released *via* decarboxylation processes (oxaloacetate to pyruvate and pyruvate to acetyl-CoA) was partially re-assimilated *via* the WLP. Thus, the *in vivo* experiments were not only the first experiments conducted in this manner using an anaerobic bacterium, but also led to very conclusive data proving the involvement of the WLP in fumarate fermentation. Thus the following picture emerged for fumarate fermentation: fumarate is mainly converted to acetate, *via* the intermediates malate, oxaloacetate, pyruvate, acetyl-CoA and acetyl phosphate. CO_2, which is

formed as part of this process, is re-assimilated, making use of the generated reducing equivalents to form more acetate.

With the help of various enzyme assays it was found that overall alcohol dehydrogenase activity varied when the strain was grown on fumarate or fructose which was in agreement with the observation that ethanol is produced in small amounts during the growth on fumarate, but also re-assimilated according to GC and HPLC analysis. This was confirmed with the *in vivo* NMR experiments, which showed ^{13}C ethanol production during logarithmic growth, followed by a decrease after the cells had reached stationary phase. This led to the assumption that the ethanol is used to maintain the redox balance during the exponential growth phase: fumarate breakdown produces NADH, which is used in ethanol production to recycle NAD^+. It is possible that ethanol is later converted to acetate and the resulting NADH used for additional carbon fixation *via* the WLP.

Ethanol re-assimilation has been observed before in *Pichia stipitis* [194] and *Candita tropicalis* [195].

Further support for the proposed fumarate fermentation pathway was provided by the inactivation of the fumarate hydratase (FH) encoding gene, which was found to abolish the ability of *C. autoethanogenum* to utilise fumarate. Since the organism was still able to use malate as carbon source, it was therby proven that fumarate metabolism purely relies on the activity of the fumarate hydratase, catalysing its conversion to malate. As fumarate utilisation could be restored by introducing a plasmid-borne copy of the FH gene into the mutant, the dependency of fumarate breakdown on fumarate hydratase activity was unequivocally proven.

To prove the involvement of the WLP in fumarate metabolism, it was thought that inactivation of the acetyl-CoA synthase (AcsA subunit) (Clau1578/1579) might affect growth of *C. autoethanogenum* on fumarate. It was found by Liew *et al.* that the knockout of the *acsA* gene led to the inactivation of the WLP of *C. autoethanogenum* [171]. Therefore it was thought that inactivation of the WLP might disable the organism to use fumarate as carbon source, as about one third of the generated acetate is produced *via* this pathway. However, the generation of such a mutant was unfortunately not successful. Even though colonies were initially screened positive for a knockout of the gene complex, it was later found that the WT gene was still present in the genome. A second attempt of this experiment resulted in the same findings. A third attempt could unfortunately not be conducted, due to time issues.

6.1.3 Production of succinate by *C. autoethanogenum*

The improvement of the succinate production of *C. autoethanogenum via* the reductive TCA pathway was a major aim of this project. Since a gene encoding fumarate reductase could not be found in the genome after re-annotation by the GASCHEM group [42], it was thought that introduction of a heterologous fumarate reductase might lead to succinate formation. However, fumarate reductases are mostly consisting of several subunits and are usually attached to the cell membrane where they acquire electrons from an electron transport chain [177]–[181], which would make cloning and assembly of a functional FRD complex very difficult. However, as Yang *et al.* were able to increase succinate production in *Aspergillus saccharolyticus* by codon optimisation of a soluble FRD from *Trypanosoma brucei* [184], it was thought that introducing a

codon-optimised version of this gene into *C. autoethanogenum* might lead to similar results. Despite various cloning problems at first, it was possible to introduce a codon optimised version of this gene on a plasmid into *E. coli* and *C. autoethanogenum*. This gene proved to be functional in both organisms. The introduction of this gene into an *E. coli* FRD mutant, was found to enable the resulting strain to restore its ability to use fumarate as electron acceptor, in contrast to the defect strain [186]. This implies that the gene was active in this strain despite the *C. autoethanogenum* specific codon optimisation.

Additionally, when the plasmid-borne, codon optimised *frd* gene was introduced into *C. autoethanogenum*, it was found that the resulting strain was able to produce 1.7 mM, 0.2 g l^{-1}, of succinate during the growth on fructose. Additionally, when grown on the precursor fumarate, the production of succinate by *C. autoethanogenum* increased to up to 10 mM, 1.18 g l^{-1}. This titre could be even more increased when providing additional hydrogen to the fumarate. Under these conditions cells were able to produce up to 30 mM, 3.5 g l^{-1}, of succinate giving a yield of 0.76 g g^{-1} fumarate. Even though this is not close to the produced amounts of succinate by *Corynebacterium glutamicum* with 109 g l^{-1} [105], it is the highest amount of succinate produced, until now, by *C. autoethanogenum*, and very similar to the previously measured yield in *C. formicoaceticum* (0.67 g g^{-1} fumarate; [157]). However, even though *C. autoethanogenum* harbouring the plasmid-borne FRD was still able to grow autotrophically on CO, no improve of the succinate production could be observed. Due to time limitations no further experiments to improve these findings could be conducted. However, an important first step was made in the development of autotrophic succinate production by acetogenic bacteria.

6.2 Limitations of this study and future work

As part of a wider effort to analyse metabolic pathways of *C. autoethanogenum* and to improve the production of succinate by this organism, this study provided important information to the ongoing endeavour and further research. However, due to the time limitations of a PhD, some aspects of this study could not be sufficiently covered and might require further investigation.

6.2.1 Limitations and challenges

Work on *Clostridia*, and especially acetogenic *Clostridia*, is generally challenging due to their comparatively slow growth rates and, with regards to *C. autoethanogenum*, lack of sophisticated genetic tools available at the start of this study. During the first year of this project, many issues arose with respect to the transformation of the organism. Since electroporation into *C. autoethanogenum* proved to be unsuccessful using the protocols available for *C. ljungdahlii* and other *Clostridia* [196][197][198], conjugation provided the only form of transformation. However, until the change from *E. coli* CA434 to *E. coli* Sexpress as conjugation strain, the success rate of those conjugations was very low. This complicated the work with the organism with regards to its genetic modifications. However, due to the development and improvement of tools for this bacterium, including CRISPR (Peter Rowe, University of Nottingham; unpublished) and a new electroporation protocol [199], future work on this organism might be improved and become less challenging.

6.2.2 Further analyses of the fumarate metabolism

To determine how the WLP influences fumarate metabolism and if the inactivation of the WLP causes inactivation of the fumarate pathway or changes the spectrum of generated fermentation products, the attempted knockout of the AcsA subunit complex would need to be generated and growth characteristics to be completed. The generated *acsA* mutant could then be phenotypically characterised, in terms of its ability to ferment fumarate and other C_4 dicarboxylic acids.

It can be hypothesised that inactivation of the WLP may either lead to a reduced growth rate, or even inactivation of fumarate metabolism as a whole. Alternatively, part of the generated acetyl-CoA may be used for ethanol production, thus, serving as a sink for the generated reducing equivalents. Knockout attempts could be done *via* ClosTron, due to the previous successful ClosTron creation of this gene [171], Allelic Exchange [52] or another CRISPR attempt with a change of the Cas9 system.

6.2.3 Succinate production

With the demonstrated production of succinate by *C. autoethanogenum* FRD strains during the growth on fructose and fumarate, the achievement of succinate production during growth on CO or other C_1 waste gases is not out of sight.

The whole genome sequence of both FRD strains generated in this study (FRD1, FRD2), might provide further insight into the different behaviour of these strains during the growth on fumarate and hydrogen. It is possible that a mutation in one of the genomes is responsible for this difference. Genomic

DNA has already been isolated and is currently undergoing sequencing. Unfortunately, data were not available at the time of thesis submission.

Despite no (or very minor) succinate production during growth on CO and CO plus H_2, further mutations within the genome might enable the bacterium to favour the reductive TCA pathway. With the inactivation of the acetate and ethanol producing routes (mutation of *ack* and multiple *adh* genes) and *frd* over-expression, it might be possible to channel the carbon and energy flux into the production of succinate, using pyruvate (or oxaloacetate) and fumarate as electron sink (Figure 3.2).

A more sophisticated version of the above approach might involve the engineering of an FRD enzyme complex which operates similar to the bifurcating electron transferring flavoprotein/ butyryl-CoA dehydrogenase (ETF/BCD) complex. Using the latter, some *Clostridium* spp. are producing butyrate and gaining additional energy from the reaction of crotonyl-CoA to butyryl-CoA [200]. The ETF complex transfers electrons from NADH to the BCD which reduces crotonyl-CoA. Additionally, the ETF/BCD complex is bifurcating, which enables it to not only reduce crotonyl-CoA, but also ferredoxin using a second molecule of NADH [180][181]. This process is used by the bacteria to conserve energy. The redox potential ($E^{'}$) of the crotonyl-CoA/butyryl-CoA half reaction is -10 mV; the one of ferredoxin is -400 mV. The reduction potential of fumarate/succinate is +31 mV, which is even more positive than crotonyl-CoA/butyryl-CoA.

(4) $Fd_{ox} + 2\ NADH + crotonyl\text{–}CoA \rightarrow Fd_{red} + 2\ NAD^{+} + butyryl\text{–}CoA$ (ΔG° −44 kJ/mol) [201]

(5) $Fd_{ox} + 2\ NADH + fumarate \rightarrow Fd_{red} + 2\ NAD^{+} + succinate$

(ΔG° −52.41 kJ/mol)

(calculated using eQuilibrator, http://equilibrator.weizmann.ac.il/ and [31][32])

The calculated Gibb's free energy is very similar for both reactions (ΔG° = -44 kJ/mol and -52.41 kJ/mol; **(4)** and **(5)**). Therefore it might be feasible that the introduction of a synthetic, engineered ETF/FRD complex could lead to succinate production whilst conserving energy, even during autotrophic growth as schematically shown in Figure 6.1.

An alternative approach may involve the introduction of a classical energy conserving fumarate reductase complex. However, as *C. autoethanogenum* is devoid of electron transport chain components other than the Rnf complex [31], [32], [42], this would be a highly challenging undertaking.

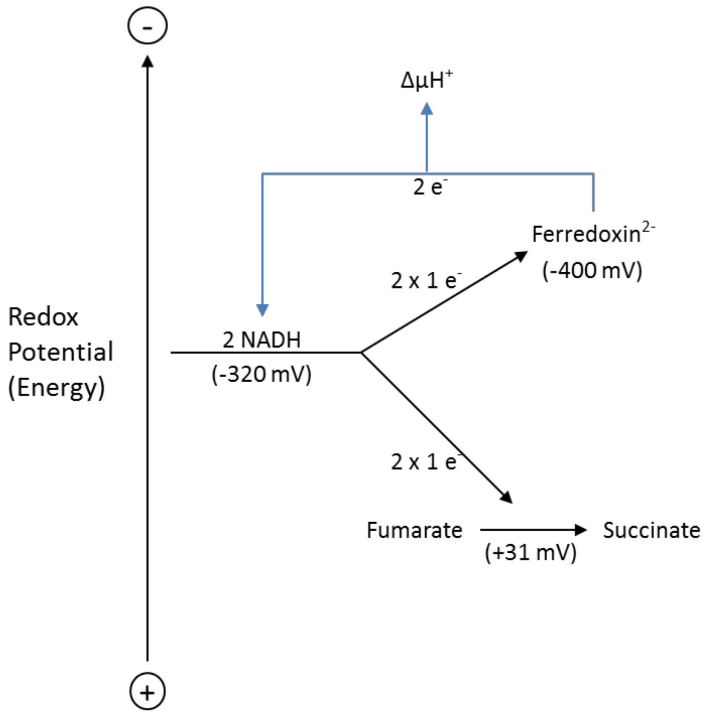


Figure 6.1: Proposed mechanism of electron bifurcation for a hypothetical ETF/FRD complex.

The approximate redox potentials E' are given in mV. Electrons provided by NADH are bifurcated, thereby reducing both ferredoxin (with a more negative redox potential) and fumarate (with a more positive redox potential). Two molecules of NADH are needed, providing four electrons in total. When ferredoxin is reduced, both electrons can be re-used to reduce NAD^+ (blue line). The herby generated proton motif force is used by an F_0F_1-type ATPase to generate ATP.

6.3 Concluding remarks

In this work the C_4 metabolism of *C. autoethanogenum* was investigated and the presence of a reaction sequence comprising TCA "cycle" reaction involved in C_4 dicarboxylic acid conversion was demonstrated. Furthermore, the growth of this organism on fumarate was studied thoroughly with the help of a new *in vivo* measurement technique using NMR analyses and ^{13}C-labelled compounds. Hereby the interaction of the WLP with the fumarate metabolism was verified. The inactivation of the fumarate hydratase gene of *C. autoethanogenum* led to the inactivation of the fumarate pathway. This was confirmed *via* complementation of the gene. A knockout of the WLP was attempted, but did not result in a successful gene inactivation.

The introduction of a soluble fumarate reductase, codon optimised from *T. brucei*, enabled *C. autoethanogenum* to produce succinate, using fructose and fumarate as carbon sources, in concentrations up to 3.5 g l^{-1} and yields of 0.76 g g^{-1} fumarate. This laid the foundation for succinate production from waste gases.

This study therefore presents an essential basis for the establishment of succinate production by *C. autoethanogenum* and a closer understanding of the C_4 dicarboxylic acid metabolism of the organism including the linkage between heterotrophic and autotrophic pathways.

7 Bibliography

[1] EIA, U.S. Energy Information Administration, 'Today in Energy'. 2017.

[2] U.S. Energy Information Administration Annual Energy Outlook 2014 Early Release Overview http://www.eia.gov/todayinenergy/detail.cfm?id=12251. (last acessed October 2017)

[3] EIA, U.S. Energy Information Administration, 'Today in Energy'. 2014.

[4] Ecotricity, 'The End Of Fossil Fuels'. https://www.ecotricity.co.uk/our-green-energy/energy-independence/the-end-of-fossil-fuels. (last accessed October 2017)

[5] I. Bechthold, K. Bretz, S. Kabasci, R. Kopitzky, and A. Springer, 'Succinic Acid: A New Platform Chemical for Biobased Polymers from Renewable Resources', *Chem. Eng. Technol.*, vol. 31, pp. 647–654, 2008.

[6] A. Bar-Even, E. Noor, and R. Milo, 'A survey of carbon fixation pathways through a quantitative lens', *J. Exp. Bot.*, vol. 63, pp. 2325–2342, 2012.

[7] J. E. Szulejko, P. Kumar, A. Deep, and K.-H. Kim, 'Global warming projections to 2100 using simple CO_2 greenhouse gas modelling and comments on CO_2 climate sensitivity factor', *Atmospheric Pollut. Res.*, vol. 8, pp. 136–140, 2017.

[8] LANZATECH, 'Carbon Capture in Fermentation', 2013/20130316424.

[9] H. G. Wood, S. W. Ragsdale, and E. Pezacka, 'The acetyl-CoA pathway: a newly discovered pathway of autotrophic growth', *TIBS*, vol. 11, pp. 14–18, 1986.

[10] T. Ezeji, 'Production of Bio-Derived Fuels and Chemicals', *Fermentation*, vol. 3, p. 42, 2017.

[11] M. Köpke *et al.*, '2,3-Butanediol Production by Acetogenic Bacteria, an Alternative Route to Chemical Synthesis, Using Industrial Waste Gas', *Appl. Environ. Microbiol.*, vol. 77, pp. 5467–5475, 2011.

[12] J. Becker, A. Lange, J. Fabarius, and C. Wittmann, 'Top value platform chemicals: bio-based production of organic acids', *Curr. Opin. Biotechnol.*, vol. 36, pp. 168–175, 2015.

[13] G. Fuchs, 'Alternative Pathways of Carbon Dioxide Fixation: Insights into the Early Evolution of Life?', *Annu. Rev. Microbiol.*, vol. 65, pp. 631–658, 2011.

[14] A. Bar-Even, E. Noor, and R. Milo, 'A survey of carbon fixation pathways through a quantitative lens', *J. Exp. Bot.*, vol. 63, pp. 2325–2342, 2012.

[15] B. Schiel-Bengelsdorf and P. Dürre, 'Pathway engineering and synthetic biology using acetogens', *FEBS Lett.*, vol. 586, pp. 2191–2198, 2012.

[16] H. L. Drake, A. S. Gößner, and S. L. Daniel, 'Old Acetogens, New Light', *Ann. N. Y. Acad. Sci.*, vol. 1125, pp. 100–128, 2008.

[17] M. J. Russell and W. Martin, 'The rocky roots of the acetyl-CoA pathway', *Trends Biochem. Sci.*, vol. 29, pp. 358–363, 2004.

[18] G. Diekert and G. Wohlfarth, 'Metabolism of homoacetogens', *Antonie Van Leeuwenhoek*, vol. 66, pp. 209–221, 1994.

[19] A. D. Adamse, 'New isolation of *Clostridium aceticum* (Wieringa)', *Antonie Van Leeuwenhoek*, vol. 46, pp. 523–531, 1980.

[20] G. Gottschalk and M. BRAUN, 'NOTES: Revival of the Name *Clostridium aceticum*', *Int. J. Syst. Evol. Microbiol.*, vol. 31, pp. 476–476, 1981.

[21] F. E. Fontaine, W. H. Peterson, E. McCoy, M. J. Johnson, and G. J. Ritter, 'A new type of glucose fermentation by *Clostridium thermoaceticum*', *J. Bacteriol.*, vol. 43, p. 701, 1942.

[22] M. D. Collins *et al.*, 'The phylogeny of the genus *Clostridium*: proposal of five new genera and eleven new species combinations', *Int. J. Syst. Bacteriol.*, vol. 44, pp. 812–826, 1994.

[23] V. Müller, 'Energy Conservation in Acetogenic Bacteria', *Appl. Environ. Microbiol.*, vol. 69, pp. 6345–6353, 2003.

[24] E. Rosenberg, E. F. DeLong, S. Lory, E. Stackebrandt, and F. Thompson, Eds., *The Prokaryotes*. Berlin, Heidelberg: Springer Berlin Heidelberg, 2013.

[25] R. Breitkopf, R. Uhlig, T. Drenckhan, and R.-J. Fischer, 'Two propanediol utilization-like proteins of *Moorella thermoacetica* with phosphotransacetlyase activity', *Extremophiles*, 2016.

[26] A. Das and L. G. Ljungdahl, 'Composition and primary structure of the F_1F_0 ATP synthase from the obligately anaerobic bacterium *Clostridium thermoaceticum*.', *J. Bacteriol.*, vol. 179, pp. 3746–3755, 1997.

[27] V. Müller, S. Aufurth, and S. Rahlfs, 'The Na^+ cycle in *Acetobacterium woodii*: identification and characterization of a Na^+ translocating F_1F_0-ATPase with a

mixed oligomer of 8 and 16 kDa proteolipids', *Biochim. Biophys. Acta BBA-Bioenerg.*, vol. 1505, pp. 108–120, 2001.

[28] L. G. Ljungdahl, 'The acetyl-CoA pathway and the chemostatic generation of ATP during acetogenesis', in *Acetogenesis*, New York, N.Y.: Chapman & Hall, pp. 63–87, 1994.

[29] F. Li, J. Hinderberger, H. Seedorf, J. Zhang, W. Buckel, and R. K. Thauer, 'Coupled Ferredoxin and Crotonyl Coenzyme A (CoA) Reduction with NADH Catalyzed by the Butyryl-CoA Dehydrogenase/Etf Complex from *Clostridium kluyveri*', *J. Bacteriol.*, vol. 190, pp. 843–850, 2008.

[30] H. Huang, S. Wang, J. Moll, and R. K. Thauer, 'Electron Bifurcation Involved in the Energy Metabolism of the Acetogenic Bacterium *Moorella thermoacetica* Growing on Glucose or H_2 plus CO_2', *J. Bacteriol.*, vol. 194, pp. 3689–3699, 2012.

[31] S. Wang, H. Huang, J. Kahnt, A. P. Mueller, M. Köpke, and R. K. Thauer, 'NADP-Specific Electron-Bifurcating [FeFe]-Hydrogenase in a Functional Complex with Formate Dehydrogenase in *Clostridium autoethanogenum* Grown on CO', *J. Bacteriol.*, vol. 195, pp. 4373–4386, 2013.

[32] J. Mock *et al.*, 'Energy Conservation Associated with Ethanol Formation from H_2 and CO_2 in *Clostridium autoethanogenum* Involving Electron Bifurcation', *J. Bacteriol.*, vol. 197, pp. 2965–2980, 2015.

[33] W. W. Metcalf, 'Classic Spotlight: Electron bifurcation, a unifying concept for energy conservation in anaerobes', *J. Bacteriol.*, vol. 198, p. 1358, 2016.

[34] J. W. Peters, A.-F. Miller, A. K. Jones, P. W. King, and M. W. Adams, 'Electron bifurcation', *Curr. Opin. Chem. Biol.*, vol. 31, pp. 146–152, 2016.

[35] J. Abrini, H. Naveau, and E.-J. Nyns, '*Clostridium autoethanogenum*, sp. nov., an anaerobic bacterium that produces ethanol from carbon monoxide', *Arch. Microbiol.*, vol. 161, pp. 345–351, 1994.

[36] R. S. Tanner, L. M. Miller, and D. Yang, '*Clostridium ljungdahlii* sp. nov., an acetogenic species in clostridial rRNA homology group I', *Int. J. Syst. Evol. Microbiol.*, vol. 43, pp. 232–236, 1993.

[37] M. Köpke *et al.*, '*Clostridium ljungdahlii* represents a microbial production platform based on syngas', *PNAS*, vol. 107, pp. 13087–13092, 2010.

[38] Project description, 'GASCHEM project, University of Nottingham'. 2013.

[39] European Commission, 'Horizon 2020, Monitoring Report 2015', 2015.

[40] J. M. Bruno-Barcena, M. S. Chinn, and A. M. Grunden, 'Genome Sequence of the Autotrophic Acetogen *Clostridium autoethanogenum* JA1-1 Strain DSM 10061, a Producer of Ethanol from Carbon Monoxide', *Genome Announc.*, vol. 1, pp. e00628-13-e00628-13, 2013.

[41] S. D. Brown *et al.*, 'Comparison of single-molecule sequencing and hybrid approaches for finishing the genome of *Clostridium autoethanogenum* and analysis of CRISPR systems in industrial relevant *Clostridia*', *Biotechnol Biofuels*, vol. 7, p. 40, 2014.

[42] C. M. Humphreys *et al.*, 'Whole genome sequence and manual annotation of *Clostridium autoethanogenum*, an industrially relevant bacterium', *BMC Genomics*, vol. 16, p. 1085, 2015.

[43] K. Schuchmann and V. Müller, 'Autotrophy at the thermodynamic limit of life: a model for energy conservation in acetogenic bacteria', *Nat. Rev. Microbiol.*, vol. 12, pp. 809–821, 2014.

[44] N. P. Minton *et al.*, 'A roadmap for gene system development in *Clostridium*', *Anaerobe*, vol. 41, pp. 104–112, 2016.

[45] J. T. Heap, O. J. Pennington, S. T. Cartman, G. P. Carter, and N. P. Minton, 'The ClosTron: A universal gene knock-out system for the genus *Clostridium*', *J. Microbiol. Methods*, vol. 70, pp. 452–464, 2007.

[46] L. Shao *et al.*, 'Targeted gene disruption by use of a group II intron (targetron) vector in *Clostridium acetobutylicum*', *Cell Res.*, vol. 17, p. 963, 2007.

[47] P. Gupta and Y. Chen, 'Chromosomal engineering of *Clostridium perfringens* using group II introns', *Chromosom. Mutagen.*, pp. 217–228, 2008.

[48] G. Mohr *et al.*, 'A Targetron System for Gene Targeting in Thermophiles and Its Application in *Clostridium thermocellum*', *PLoS ONE*, vol. 8, p. e69032, 2013.

[49] S. A. Kuehne and N. P. Minton, 'ClosTron-mediated engineering of *Clostridium*', *Bioengineered*, vol. 3, pp. 247–254, 2012.

[50] P. J. Enyeart, G. Mohr, A. D. Ellington, and A. M. Lambowitz, 'Biotechnological applications of mobile group II introns and their reverse transcriptases: gene targeting, RNA-seq, and non-coding RNA analysis', *Mob. DNA*, vol. 5, p. 2, 2014.

[51] C. L. Frazier, J. San Filippo, A. M. Lambowitz, and D. A. Mills, 'Genetic Manipulation of Lactococcus lactis by Using Targeted Group II Introns:

Generation of Stable Insertions without Selection', *Appl. Environ. Microbiol.*, vol. 69, pp. 1121–1128, 2003.

[52] J. T. Heap *et al.*, 'Integration of DNA into bacterial chromosomes from plasmids without a counter-selection marker', *Nucleic Acids Res.*, vol. 40, pp. e59–e59, 2012.

[53] Y. K. Ng *et al.*, 'Expanding the Repertoire of Gene Tools for Precise Manipulation of the *Clostridium difficile* Genome: Allelic Exchange Using pyrE Alleles', *PLoS ONE*, vol. 8, p. e56051, 2013.

[54] R. Barrangou and L. Marraffini, 'CRISPR-Cas Systems: Prokaryotes Upgrade to Adaptive Immunity', *Mol. Cell*, vol. 54, pp. 234–244, 2014.

[55] K. S. Makarova *et al.*, 'Evolution and classification of the CRISPR–Cas systems', *Nat. Rev. Microbiol.*, vol. 9, pp. 467–477, 2011.

[56] Y. Zhang, A. Grosse-Honebrink, and N. P. Minton, 'A universal mariner transposon system for forward genetic studies in the genus *Clostridium*', *PLoS One*, vol. 10, p. e0122411, 2015.

[57] T. Werpy and G. Petersen, 'Top Value Added Chemicals from Biomass, Volume I', US Department of Energy, 2004.

[58] H. Zoebelein and V. Böllert, Eds., *Dictionary of renewable resources*, 2nd rev. and enl. ed. Weinheim : New York: Wiley-VCH, 2001.

[60] J. J. Beauprez, M. De Mey, and W. K. Soetaert, 'Microbial succinic acid production: Natural versus metabolic engineered producers', *Process Biochem.*, vol. 45, pp. 1103–1114, 2010.

[61] Global Succinic Acid Market Analysis & Trends 2013 - 2017 - Industry Forecast to 2025. https://ceo.ca/@newswire/global-succinic-acid-market-analysis-trends-2013-2017 (last accessed September 2017)

[62] N. Nghiem, S. Kleff, and S. Schwegmann, 'Succinic Acid: Technology Development and Commercialization', *Fermentation*, vol. 3, p. 26, Jun. 2017.

[63] O. L. Polly, 'Production of succinic acid', Patent number 2533620, 1950.

[64] K. Lohbeck, H. Haferkorn, W. Fuhrmann, and N. Fedtke, 'Maleic and Fumaric Acids', in *Ullmann's Encyclopedia of Industrial Chemistry*, Wiley-VCH Verlag GmbH & Co. KGaA, Ed. Weinheim, Germany: Wiley-VCH Verlag GmbH & Co. KGaA, 2000.

[65] K.-K. Cheng, G.-Y. Wang, J. Zeng, and J.-A. Zhang, 'Improved Succinate Production by Metabolic Engineering', *BioMed Res. Int.*, vol. 2013, pp. 1–12, 2013.

[66] M. Carvalho, M. Matos, C. Roca, and M. A. M. Reis, 'Succinic acid production from glycerol by *Actinobacillus succinogenes* using dimethylsulfoxide as electron acceptor', *New Biotechnol.*, vol. 31, pp. 133–139, 2014.

[67] C. R. Malloy, A. D. Sherry, and F. M. H. Jeffrey, 'Carbon flux through citric acid cycle pathways in perfused heart by ^{13}C NMR spectroscopy', *FEBS Lett.*, vol. 212, pp. 58–62, 1987.

[68] Y. Arikawa *et al.*, 'Isolation of Sake Yeast Strains Possessing Various Levels of Succinate- and/or Malate-Producing Abilities by Gene Disruption or Mutation', *J. Biosci. Bioeng.*, vol. 87, pp. 333–339, 1999.

[69] J. M. Otero, D. Cimini, K. R. Patil, S. G. Poulsen, L. Olsson, and J. Nielsen, 'Industrial Systems Biology of *Saccharomyces cerevisiae* Enables Novel Succinic Acid Cell Factory', *PLoS ONE*, vol. 8, p. e54144, 2013.

[70] A. M. Raab, G. Gebhardt, N. Bolotina, D. Weuster-Botz, and C. Lang, 'Metabolic engineering of *Saccharomyces cerevisiae* for the biotechnological production of succinic acid', *Metab. Eng.*, vol. 12, pp. 518–525, 2010.

[71] D. N. Kamra, 'Rumen microbial ecosystem', *Curr. Sci.*, vol. 89, pp. 125–135, 2005.

[72] M. V. Guettler, D. Rumler, and M. K. Jain, '*Actinobacillus succinogenes* sp. nov., a novel succinic-acid-producing strain from the bovine rumen', *Int. J. Syst. Bacteriol.*, vol. 49, pp. 207–216, 1999.

[73] C. P. Davis, D. Cleven, J. Brown, and E. Balish, '*Anaerobiospirillum*, a new genus of spiral-shaped bacteria', *Int. J. Syst. Bacteriol.*, vol. 26, pp. 498–504, 1976.

[74] N. P. Nghiem, B. H. Davison, B. E. Suttle, and G. R. Richardson, 'Production of succinic acid by *Anaerobiospirillum succiniciproducens*', *Appl. Biochem. Biotechnol.*, vol. 63, pp. 565–576, 1997.

[75] P. Lee, S. Lee, S. Hong, H. Chang, 'Isolation and characterization of a new succinic acid-producing bacterium, *Mannheimia succiniciproducens* MBEL55E, from bovine rumen', *Appl. Microbiol. Biotechnol.*, vol. 58, pp. 663–668, 2002.

[76] J. G. Zeikus, M. K. Jain, and P. Elankovan, 'Biotechnology of succinic acid production and markets for derived industrial products', *Appl. Microbiol. Biotechnol.*, vol. 51, pp. 545–552, 1999.

[77] D. H. Park, M. Laivenieks, M. V. Guettler, M. K. Jain, and J. G. Zeikus, 'Microbial utilization of electrically reduced neutral red as the sole electron donor for growth and metabolite production', *Appl. Environ. Microbiol.*, vol. 65, pp. 2912–2917, 1999.

[78] J. J. Beauprez, M. De Mey, and W. K. Soetaert, 'Microbial succinic acid production: Natural versus metabolic engineered producers', *Process Biochem.*, vol. 45, pp. 1103–1114, 2010.

[79] P. Kim, M. Laivenieks, J. McKinlay, C. Vieille, and J. Gregory Zeikus, 'Construction of a shuttle vector for the overexpression of recombinant proteins in *Actinobacillus succinogenes*', *Plasmid*, vol. 51, pp. 108–115, 2004.

[80] Y.-S. Jang *et al.*, 'Construction and Characterization of Shuttle Vectors for Succinic Acid-Producing Rumen Bacteria', *Appl. Environ. Microbiol.*, vol. 73, pp. 5411–5420, 2007.

[81] S. J. Lee, H. Song, and S. Y. Lee, 'Genome-Based Metabolic Engineering of *Mannheimia succiniciproducens* for Succinic Acid Production', *Appl. Environ. Microbiol.*, vol. 72, pp. 1939–1948, 2006.

[82] Y. S. Jang, S. Y. Lee, J. W. Lee, and H. Song, 'Gene encoding malic enzyme and method for preparing succinic acid using the same', Patent number US7470770B2, 2008.

[83] S. Y. Lee and S. J. Lee, 'Rumen bacteria variants and process for preparing succinic acid employing the same', Patent number US7470530B2, 2008.

[84] N. S. Samuelov, R. Datta, M. K. Jain, and J. G. Zeikus, 'Whey fermentation by *Anaerobiospirillum succiniciproducens* for production of a succinate-based animal feed additive', *Appl. Environ. Microbiol.*, vol. 65, pp. 2260–2263, 1999.

[85] N. S. Samuelov, R. Lamed, S. Lowe, and J. G. Zeikus, 'Influence of CO_2-HCO_3- levels and pH on growth, succinate production, and enzyme activities of *Anaerobiospirillum succiniciproducens*', *Appl. Environ. Microbiol.*, vol. 57, pp. 3013–3019, 1991.

[86] M. Laivenieks, C. Vieille, and J. G. Zeikus, 'Cloning, sequencing, and overexpression of the *Anaerobiospirillum succiniciproducens*

phosphoenolpyruvate carboxykinase (pckA) gene.', *Appl. Environ. Microbiol.*, vol. 63, pp. 2273–2280, 1997.

[87] R. Chatterjee, C. S. Millard, K. Champion, D. P. Clark, and M. I. Donnelly, 'Mutation of the ptsG Gene Results in Increased Production of Succinate in Fermentation of Glucose by *Escherichia coli*', *Appl. Environ. Microbiol.*, vol. 67, pp. 148–154, 2001.

[88] R. De Anda *et al.*, 'Replacement of the glucose phosphotransferase transport system by galactose permease reduces acetate accumulation and improves process performance of *Escherichia coli* for recombinant protein production without impairment of growth rate', *Metab. Eng.*, vol. 8, pp. 281–290, 2006.

[89] N. Flores *et al.*, 'Growth Recovery on Glucose under Aerobic Conditions of an *Escherichia coli* Strain Carrying a Phosphoenolpyruvate:Carbohydrate Phosphotransferase System Deletion by Inactivating *arcA* and Overexpressing the Genes Coding for Glucokinase and Galactose Permease', *J. Mol. Microbiol. Biotechnol.*, vol. 13, pp. 105–116, 2007.

[90] J. J. Beauprez *et al.*, 'Influence of C_4-dicarboxylic acid transporters on succinate production', *Green Chem.*, vol. 13, p. 2179, 2011.

[91] C. S. Millard, Y.-P. Chao, J. C. Liao, and M. I. Donnelly, 'Enhanced production of succinic acid by overexpression of phosphoenolpyruvate carboxylase in *Escherichia coli*', *Appl. Environ. Microbiol.*, vol. 62, pp. 1808–1810, 1996.

[92] R. R. Gokarn, M. A. Eiteman, and E. Altman, 'Expression of pyruvate carboxylase enhances succinate production in *Escherichia coli* without affecting glucose uptake', *Biotechnol. Lett.*, vol. 20, pp. 795–798, 1998.

[93] L. Stols, G. Kulkarni, B. G. Harris, and M. I. Donnelly, 'Expression of *Ascaris suum* malic enzyme in a mutant *Escherichia coli* allows production of succinic acid from glucose', in *Biotechnology for Fuels and Chemicals*, Springer, pp. 153–158, 1997.

[94] M. I. Donnelly, 'Expression of *Ascaris suum* Malic Enzyme in a Mutant *Escherichia coli* Allows Production of Succinic Acid from Glucose', in *Biotechnology for Fuels and Chemicals: Proceedings of the Eighteenth Symposium on Biotechnology for Fuels and Chemicals Held May 5–9, 1996, at Gatlinburg, Tennessee*, vol. 63, p. 153, 1997.

[95] M. I. Donnelly, C. S. Millard, M. J. Chen, J. W. Rathke, and D. P. Clark, 'A novel fermentation pathway in an *Escherichia coli* mutant producing succinic

acid, acetic acid, and ethanol', in *Biotechnology for Fuels and Chemicals*, Springer, pp. 187–198, 1998.

[96] G. N. Vemuri, M. A. Eiteman, and E. Altman, 'Succinate production in dual-phase *Escherichia coli* fermentations depends on the time of transition from aerobic to anaerobic conditions', *J. Ind. Microbiol. 38 Biotechnol.*, vol. 28, pp. 325–332, 2002.

[97] G. N. Vemuri, M. A. Eiteman, and E. Altman, 'Effects of Growth Mode and Pyruvate Carboxylase on Succinic Acid Production by Metabolically Engineered Strains of *Escherichia coli*', *Appl. Environ. Microbiol.*, vol. 68, pp. 1715–1727, 2002.

[98] H. Lin, R. V. Vadali, G. N. Bennett, and K.-Y. San, 'Increasing the Acetyl-CoA Pool in the Presence of Overexpressed Phosphoenolpyruvate Carboxylase or Pyruvate Carboxylase Enhances Succinate Production in *Escherichia coli*', *Biotechnol. Prog.*, vol. 20, pp. 1599–1604, 2004.

[99] H. Lin, K.-Y. San, and G. N. Bennett, 'Effect of Sorghum vulgare phosphoenolpyruvate carboxylase and *Lactococcus lactis* pyruvate carboxylase coexpression on succinate production in mutant strains of *Escherichia coli*', *Appl. Microbiol. Biotechnol.*, vol. 67, pp. 515–523, 2005.

[100] H. Lin, G. N. Bennett, and K.-Y. San, 'Metabolic engineering of aerobic succinate production systems in *Escherichia coli* to improve process productivity and achieve the maximum theoretical succinate yield', *Metab. Eng.*, vol. 7, pp. 116–127, 2005.

[101] K. Jantama, X. Zhang, J. C. Moore, K. T. Shanmugam, S. A. Svoronos, and L. O. Ingram, 'Eliminating side products and increasing succinate yields in engineered strains of *Escherichia coli* C', *Biotechnol. Bioeng.*, vol. 101, pp. 881–893, 2008.

[102] J. Kalinowski *et al.*, 'The complete *Corynebacterium glutamicum* ATCC 13032 genome sequence and its impact on the production of l-aspartate-derived amino acids and vitamins', *J. Biotechnol.*, vol. 104, pp. 5–25, 2003.

[103] B. Litsanov, M. Brocker, and M. Bott, 'Toward Homosuccinate Fermentation: Metabolic Engineering of *Corynebacterium glutamicum* for Anaerobic Production of Succinate from Glucose and Formate', *Appl. Environ. Microbiol.*, vol. 78, pp. 3325–3337, 2012.

[104] S. Okino, R. Noburyu, M. Suda, T. Jojima, M. Inui, and H. Yukawa, 'An efficient succinic acid production process in a metabolically engineered

Corynebacterium glutamicum strain', *Appl. Microbiol. Biotechnol.*, vol. 81, pp. 459–464, 2008.

[105] N. Zhu, H. Xia, J. Yang, X. Zhao, and T. Chen, 'Improved succinate production in *Corynebacterium glutamicum* by engineering glyoxylate pathway and succinate export system', *Biotechnol. Lett.*, vol. 36, pp. 553–560, 2014.

[106] M. Köpke, S. Nagaraju, W. Chen 'Recombinant microorganisms and methods of use thereof', Patent number WO 2013/115659 A2.

[107] LANZATECH, 'Fermentation Process', Patent number 2013/20130260429.

[108] LANZATECH, 'Fermentation and Simulated Moving Bed Process', Patent number 2013/20130316412.

[109] M. Köpke *et al.*, '2,3-Butanediol Production by Acetogenic Bacteria, an Alternative Route to Chemical Synthesis, Using Industrial Waste Gas', *Appl. Environ. Microbiol.*, vol. 77, no. 15, pp. 5467–5475, Aug. 2011.

[110] M. Köpke, C. Mihalcea, J. C. Bromley, and S. D. Simpson, 'Fermentative production of ethanol from carbon monoxide', *Curr. Opin. Biotechnol.*, vol. 22, pp. 320–325, 2011.

[111] F. W. Studier and B. A. Moffatt, 'Use of bacteriophage T7 RNA polymerase to direct selective high-level expression of cloned genes', *J. Mol. Biol.*, vol. 189, pp. 113–130, 1986.

[112] D. Hanahan, 'Studies on transformation of *Escherichia coli* with plasmids', *J. Mol. Biol.*, vol. 166, pp. 557–580, 1983.

[113] T. Baba *et al.*, 'Construction of *Escherichia coli* K-12 in-frame, single-gene knockout mutants: the Keio collection', *Mol. Syst. Biol.*, vol. 2, 2006.

[114] H. Dong, Y. Zhang, Z. Dai, and Y. Li, 'Engineering *Clostridium* strain to accept unmethylated DNA', *PLoS One*, vol. 5, p. e9038, 2010.

[115] J. T. Heap, O. J. Pennington, S. T. Cartman, and N. P. Minton, 'A modular system for *Clostridium* shuttle plasmids', *J. Microbiol. Methods*, vol. 78, pp. 79–85, 2009.

[116] G. Bertani, 'Studies on Lysogenesis I.: The Mode of Phage Liberation by Lysogenic *Escherichia coli*', *J. Bacteriol.*, vol. 62, p. 293, 1951.

[117] G. Bertani, 'Lysogeny at Mid-Twentieth Century: P1, P2, and Other Experimental Systems', *J. Bacteriol.*, vol. 186, pp. 595–600, 2004.

[118] P. R. Lambden and J. R. Guest, ‘A novel method for isolating chlorate-resistant mutants of *Escherichia coli* K12 by anaerobic selection on a lactate plus fumarate medium’, *Microbiology*, vol. 93, pp. 173–176, 1976.

[119] J. A. Breznak and R. N. Costilow, ‘Working with Anaerobes’, *Physochemical Factors Growth*, vol. P. Gerhard (ed.), Methods for general and molecular bacteriology, no. American Society for Microbiology, Washington, pp. 137–154, 1994.

[120] A. Grosse-Honebrink, ‘Forward and Reverse Genetics in Industrially Important *Clostridia*’, University of Nottingham, 2017.

[121] F. Widdel, ‘Theory and Measurement of Bacterial Growth’, in *Grundpraktikum Mikrobiologie, Universität Bremen*, 2007.

[122] E. T. Papoutsakis, ‘Equations and calculations for fermentations of butyric acid bacteria’, *Biotechnol. Bioeng.*, vol. 26, pp. 174–187, 1984.

[123] N. Chester and D. R. Marshak, ‘Dimethyl Sulfoxide-Mediated Primer Tm Reduction: A Method for Analyzing the Role of Renaturation Temperature in the Polymerase Chain Reaction’, *Anal. Biochem.*, vol. 209, pp. 284–290, 1993.

[124] J. Perutka, W. Wang, D. Goerlitz, and A. M. Lambowitz, ‘Use of Computer-designed Group II Introns to Disrupt Escherichia coli DExH/D-box Protein and DNA Helicase Genes’, *J. Mol. Biol.*, vol. 336, pp. 421–439, 2004.

[125] W. J. Dower, J. F. Miller, and C. W. Ragsdale, ‘High efficiency transformation of *E. coli* by high voltage electroporation’, *Nucleic Acids Res.*, vol. 16, pp. 6127–6145, 1988.

[126] M. M. Bradford, ‘A rapid and sensitive method for the quantitation of microgram quantities of protein utilizing the principle of protein-dye binding’, *Anal. Biochem.*, vol. 72, pp. 248–254, 1976.

[127] U. K. Laemmli, ‘Cleavage of Structural Proteins during the Assembly of the Head of Bacteriophage T4’, *Nature*, pp. 680–685, 1970.

[128] W. N. Burnette, ‘“Western Blotting”: Electrophoretic transfer of proteins from sodium dodecyl sulfate-polyacrylamide gels to unmodified nitrocellulose and radiographic detection with antibody and radioiodinated protein A’, *Anal. Biochem.*, vol. 112, pp. 195–203, 1981.

[129] M. D. Hatch, ‘A simple spectrophotometric assay for fumarate hydratase in crude tissue extracts’, *Anal. Biochem.*, vol. 85, pp. 271–275, 1978.

[130] H. U. Bergmeyer, 'Neue Werte für die molaren Extinktions-Koeffizienten von NADH und NADPH zum Gebrauch im Routine-Laboratorium', *Z Klin Chem Klin Biochem*, vol. 13, pp. 507–508, 1975.

[131] P. Hillmer and G. Gottschalk, 'Particulate nature of enzymes involved in the fermentation of ethanol and acetate by *Clostridium kluyveri*', *FEBS Lett.*, vol. 21, pp. 351–354, 1972.

[132] H. U. Bergmeyer, *Methods of enzymatic analysis*, vol. I–III. Weinheim: Chemie, 1983.

[133] D. P. Clark and J. E. Cronan, 'Acetaldehyde Coenzyme A Dehydroganse of *Escherichia coli*', *J. Bacteriol.*, vol. 144, pp. 179–184, 1980.

[134] A. Miura, M. Kameya, H. Arai, M. Ishii, and Y. Igarashi, 'A Soluble NADH-Dependent Fumarate Reductase in the Reductive Tricarboxylic Acid Cycle of *Hydrogenobacter thermophilus* TK-6', *J. Bacteriol.*, vol. 190, pp. 7170–7177, 2008.

[135] H. Nakajima, K. Suzuki, and K. Imahori, 'Purification and properties of acetate kinase from *Bacillus stearothermophilus*', *J. Biochem. (Tokyo)*, vol. 84, pp. 193–203, 1978.

[136] D. S. Wishart *et al.*, 'HMDB: the Human Metabolome Database', *Nucleic Acids Res.*, vol. 35, pp. D521–D526, 2007.

[137] S.A. Richards and J.C.Hollerton, *Essential Practical NMR for Organic Chemistry*. Wiley, 2011.

[138] T.D.W. Claridge, *High-resolution NMR techniques in Organic Chemistry*, vol. 2nd edition. Elsevier, 2009.

[139] E. Marcellin *et al.*, 'Low carbon fuels and commodity chemicals from waste gases – systematic approach to understand energy metabolism in a model acetogen', *Green Chem*, vol. 18, pp. 3020–3028, 2016.

[140] A. B. Lowe, 'Thiol-ene "click" reactions and recent applications in polymer and materials synthesis', *Polym Chem*, vol. 1, no. 1, pp. 17–36, 2010.

[141] Y. Liu *et al.*, 'Thio-Michael addition of α,β-unsaturated amides catalyzed by Nmm-based ionic liquids', *RSC Adv*, vol. 7, pp. 43104–43113, 2017.

[142] L. E. Erickson, 'Biomass elemental composition and energy content', *Biotechnol. Bioeng.*, vol. 22, pp. 451–456, 1980.

[143] I. G. Minkevich and V. K. Eroshin, ‘Productivity and heat generation of fermentation under oxygen limitation’, *Folia Microbiol. (Praha)*, vol. 18, pp. 376–385, 1973.

[144] M. J. Johnson, W. H. Peterson, and E. B. Fred, ‘Oxidation and reduction relations between substrate and products in the acetonebutyl alcohol fermentation’, *J. Biol. Chem.*, vol. 91, pp. 569–591, 1931.

[145] D. M. Greenberg, *Metabolic Pathways Vol-1*. Academic Press: New York, 1960.

[146] H. A. Krebs, ‘The History of the Tricarboxylic Acid Cycle’, *Perspect. Biol. Med.*, vol. 14, pp. 154–172, 1970.

[147] J. E. Cronan, Jr. and D. Laporte, ‘Tricarboxylic Acid Cycle and Glyoxylate Bypass’, *EcoSal Plus*, vol. 1, 2005.

[148] M. C. Evans, B. B. Buchanan, and D. I. Arnon, ‘A new ferredoxin-dependent carbon reduction cycle in a photosynthetic bacterium’, *Proc. Natl. Acad. Sci.*, vol. 55, pp. 928–934, 1966.

[149] M. Hugler, C. O. Wirsen, G. Fuchs, C. D. Taylor, and S. M. Sievert, ‘Evidence for Autotrophic CO_2 Fixation via the Reductive Tricarboxylic Acid Cycle by Members of the Subdivision of Proteobacteria’, *J. Bacteriol.*, vol. 187, pp. 3020–3027, 2005.

[150] S. W. Ragsdale and E. Pierce, ‘Acetogenesis and the Wood–Ljungdahl pathway of CO_2 fixation’, *Biochim. Biophys. Acta BBA - Proteins Proteomics*, vol. 1784, pp. 1873–1898, 2008.

[151] J. R. Andreesen, A. Schaupp, C. Neurauter, A. Brown, and L. G. Ljungdahl, ‘Fermentation of glucose, fructose, and xylose by *Clostridium thermoaceticum*: effect of metals on growth yield, enzymes, and the synthesis of acetate from CO_2’, *J. Bacteriol.*, vol. 114, pp. 743–751, 1973.

[152] C. D. Smolke, *The Metabolic Pathway Engineering Handbook*. CRC Press, 2010.

[153] E. Stackebrandt, I. Kramer, J. Swiderski, and H. Hippe, ‘Phylogenetic basis for a taxonomic dessection of the genus *Clostridium*’, *FEMS Immunol. Med. Microbiol.*, pp. 253–258, 1999.

[154] S. F. Altschul *et al.*, ‘Gapped BLAST and PSI-BLAST: a new generation of protein database search programs’, *Nucleic Acids Res.*, vol. 25, pp. 3389–3402, 1997.

[155] J. L. Cotter, M. S. Chinn, and A. M. Grunden, 'Ethanol and acetate production by *Clostridium ljungdahlii* and *Clostridium autoethanogenum* using resting cells', *Bioprocess Biosyst. Eng.*, vol. 32, pp. 369–380, 2009.

[156] G. Cecchini, I. Schröder, R. P. Gunsalus, and E. Maklashina, 'Succinate dehydrogenase and fumarate reductase from *Escherichia coli*', *Biochim. Biophys. Acta BBA-Bioenerg.*, vol. 1553, pp. 140–157, 2002.

[157] M. Dorn, J. R. Andreesen, and G. Gottschalk, 'Fermentation of fumarate and L-malate by *Clostridium formicoaceticum*', *J. Bacteriol.*, vol. 133, pp. 26–32, 1978.

[158] G. Diekert and R. K. Thauer, 'Carbon Monoxide Oxidation by *Clostridium themroaceticum* and *Clostridium formicoaceticum*', *J. Bacteriol.*, vol. 136, pp. 597–606, 1978.

[159] M. M. Karl, A. Poehlein, F. R. Bengelsdorf, R. Daniel, and P. Dürre, 'Complete Genome Sequence of the Autotrophic Acetogen *Clostridium formicaceticum* DSM 92 ^{T} Using Nanopore and Illumina Sequencing Data', *Genome Announc.*, vol. 5, pp. e00423-17, 2017.

[160] D. Ikeda, T. Karasawa, K. Yamakawa, R. Tanaka, M. Namiki, and S. Nakamura, 'Effect of isoleucine on toxin production by *Clostridium difficile* in a defined medium', *Zentralblatt Für Bakteriol.*, vol. 287, pp. 375–386, 1998.

[161] N. Fonknechten *et al.*, '*Clostridium sticklandii*, a specialist in amino acid degradation: revisiting its metabolism through its genome sequence', *Bmc Genomics*, vol. 11, p. 555, 2010.

[162] K. Winzer, K. Lorenz, and P. Dürre, 'Acetate kinase from *Clostridium acetobutylicum*: a highly specific enzyme that is actively transcribed during acidogenesis and solventogenesis', *Microbiology*, vol. 143, pp. 3279–3286, 1997.

[163] M. Straub, M. Demler, D. Weuster-Botz, and P. Dürre, 'Selective enhancement of autotrophic acetate production with genetically modified *Acetobacterium woodii*', *J. Biotechnol.*, vol. 178, pp. 67–72, 2014.

[164] E. M. Green, Z. L. Boynton, L. M. Harris, F. B. Rudolph, E. T. Papoutsakis, and G. N. Bennett, 'Genetic manipulation of acid formation pathways by gene inactivation in *Clostridium acetobutylicum* ATCC 824', *Microbiology*, vol. 142, pp. 2079–2086, 1996.

[165] W. Kuit, N. P. Minton, A. M. López-Contreras, and G. Eggink, 'Disruption of the acetate kinase (ack) gene of *Clostridium acetobutylicum* results in delayed acetate production', *Appl. Microbiol. Biotechnol.*, vol. 94, pp. 729–741, 2012.

[166] R. Breitkopf, 'Expression von Genen des Acetatmetabolismus in *Moorella thermoacetica*', Masterarbeit, Universität Rostock, 2013.

[167] A. Neves, W. Pool, J. Kok, O. Kuipers, and H. Santos, 'Overview on sugar metabolism and its control in – The input from in vivo NMR', *FEMS Microbiol. Rev.*, vol. 29, pp. 531–554, 2005.

[168] Z. Serber, A. T. Keatinge-Clay, R. Ledwidge, A. E. Kelly, S. M. Miller, and V. Dötsch, 'High-Resolution Macromolecular NMR Spectroscopy Inside Living Cells', *J. Am. Chem. Soc.*, vol. 123, pp. 2446–2447, 2001.

[169] C. M. Cooksley, Y. Zhang, H. Wang, S. Redl, K. Winzer, and N. P. Minton, 'Targeted mutagenesis of the *Clostridium acetobutylicum* acetone–butanol–ethanol fermentation pathway', *Metab. Eng.*, vol. 14, pp. 630–641, 2012.

[170] P.-L. Tremblay, T. Zhang, S. A. Dar, C. Leang, and D. R. Lovley, 'The Rnf Complex of *Clostridium ljungdahlii* Is a Proton-Translocating Ferredoxin:NAD^+ Oxidoreductase Essential for Autotrophic Growth', *mBio*, vol. 4, pp. e00406-12-e00406-12, 2012.

[171] F. Liew, A. M. Henstra, K. Winzer, M. Köpke, S. D. Simpson, and N. P. Minton, 'Insights into CO_2 Fixation Pathway of *Clostridium autoethanogenum* by Targeted Mutagenesis', *mBio*, vol. 7, pp. e00427-16, 2016.

[172] J. Mock *et al.*, 'Energy Conservation Associated with Ethanol Formation from H_2 and CO_2 in *Clostridium autoethanogenum* Involving Electron Bifurcation', *J. Bacteriol.*, vol. 197, pp. 2965–2980, 2015.

[173] H. N. Abubackar, M. C. Veiga, and C. Kennes, 'Carbon monoxide fermentation to ethanol by *Clostridium autoethanogenum* in a bioreactor with no accumulation of acetic acid', *Bioresour. Technol.*, vol. 186, pp. 122–127, 2015.

[174] S. A. Kuehne, S. T. Cartman, J. T. Heap, M. L. Kelly, A. Cockayne, and N. P. Minton, 'The role of toxin A and toxin B in *Clostridium difficile* infection', *Nature*, vol. 467, pp. 711–713, 2010.

[175] J. T. Heap *et al.*, 'The ClosTron: Mutagenesis in *Clostridium* refined and streamlined', *J. Microbiol. Methods*, vol. 80, pp. 49–55, 2010.

[176] B. Meinecke, J. Bertram, and G. Gottschalk, 'Purification and characterization of the pyruvate-ferredoxin oxidoreductase from *Clostridium acetobutylicum*', *Arch. Microbiol.*, vol. 152, pp. 244–250, 1989.

[177] J. J. Van Hellemond and A. G. Tielens, 'Expression and functional properties of fumarate reductase.', *Biochem. J.*, vol. 304, p. 321, 1994.

[178] K. Enomoto, Y. Arikawa, and H. Muratsubaki, 'Physiological role of soluble fumarate reductase in redox balancing during anaerobisis in *Saccharomyces cerevisiae*', *FEMS Microbiol. Lett.*, vol. 215, pp. 103–108, 2002.

[179] S. Heim, A. Künkel, R. K. Thauer, and R. Hedderich, 'Thiol: fumarate reductase (Tfr) from *Methanobacterium thermoautotrophicum*', *FEBS J.*, vol. 253, pp. 292–299, 1998.

[180] S. Besteiro *et al.*, 'Succinate Secreted by *Trypanosoma brucei* Is Produced by a Novel and Unique Glycosomal Enzyme, NADH-dependent Fumarate Reductase', *J. Biol. Chem.*, vol. 277, pp. 38001–38012, 2002.

[181] V. Coustou *et al.*, 'A Mitochondrial NADH-dependent Fumarate Reductase Involved in the Production of Succinate Excreted by Procyclic *Trypanosoma brucei*', *J. Biol. Chem.*, vol. 280, pp. 16559–16570, 2005.

[182] H. Muratsubaki and K. Enomoto, 'One of the Fumarate Reductase Isoenzymes from *Saccharomyces cerevisiae* is encoded by the OSM1 gene', *Arch. Biochem. Biophys.*, vol. 352, pp. 175–181, 1998.

[183] S. L. Pealing, A. C. Black, F. D. Manson, F. B. Ward, S. K. Chapman, and G. A. Reid, 'Sequence of the gene encoding flavocytochrome c from Shewanella putrefaciens: a tetraheme flavoenzyme that is a soluble fumarate reductase related to the membrane-bound enzymes from other bacteria', *Biochemistry (Mosc.)*, vol. 31, pp. 12132–12140, 1992.

[184] L. Yang, M. Lübeck, B. K. Ahring, and P. S. Lübeck, 'Enhanced succinic acid production in *Aspergillus saccharolyticus* by heterologous expression of fumarate reductase from *Trypanosoma brucei*', *Appl. Microbiol. Biotechnol.*, vol. 100, pp. 1799–1809, 2016.

[185] I. Goldberg, K. Lonberg-Holm, E. I. Bagley, and B. Stieglitz, 'Improved Conversion of Fumarate to Succinate by *Escherichia coli* strains Amplified for Fumarate Reductase', *Appl. Environ. Microbiol.*, vol. 45, pp. 1838–1847, 1983.

[186] P. R. Lambden and J. R. Guest, 'Mutants of *Escherichia coli* K12 unable to use fumarate as an anaerobic electron acceptor', *Microbiology*, vol. 97, pp. 145–160, 1976.

[187] D. Paul *et al.*, 'Genome Sequence of the Solvent-Producing Bacterium Clostridium carboxidivorans Strain P7T', *J. Bacteriol.*, vol. 192, pp. 5554–5555, 2010.

[188] M. A. Islam, K. Zengler, E. A. Edwards, R. Mahadevan, and G. Stephanopoulos, 'Investigating *Moorella thermoacetica* metabolism with a genome-scale constraint-based metabolic model', *Integr Biol*, vol. 7, pp. 869–882, 2015.

[189] F. Li, C. H. Hagemeier, H. Seedorf, G. Gottschalk, and R. K. Thauer, 'Re-Citrate Synthase from *Clostridium kluyveri* Is Phylogenetically Related to Homocitrate Synthase and Isopropylmalate Synthase Rather Than to Si-Citrate Synthase', *J. Bacteriol.*, vol. 189, pp. 4299–4304, 2007.

[190] A. Becerra, M. Rivas, C. García-Ferris, A. Lazcano, and J. Peretó, 'A phylogenetic approach to the early evolution of autotrophy: the case of the reverse TCA and the reductive acetyl-CoA pathways', *Int Microbiol*, vol. 17, pp. 91–97, 2014.

[191] W. Li, 'Multidimensional HRMAS NMR: a platform for *in vivo* studies using intact bacterial cells', *The Analyst*, vol. 131, p. 777, 2006.

[192] E. M. Lohmeier-Vogel, D. D. McIntyre, and H. J. Vogel, 'Phosphorus-31 and carbon-13 nuclear magnetic resonance studies of glucose and xylose metabolism in cell suspensions and agarose-immobilized cultures of *Pichia stipitis* and *Saccharomyces cerevisiae*.', *Appl. Environ. Microbiol.*, vol. 62, pp. 2832–2838, 1996.

[193] J. L. Tholozan, J. P. Touzel, E. Samain, J. P. Grivet, G. Prensier, and G. Albagnac, '*Clostridium neopropionicum* sp. nov., a strict anaerobic bacterium fermenting ethanol to propionate through acrylate pathway', *Arch. Microbiol.*, vol. 157, pp. 249–257, 1992.

[194] K. Skoog, B. Hahn-Hägerdal, H. Degn, J. P. Jacobsen, and H. S. Jacobsen, 'Ethanol reassimilation and ethanol tolerance in *Pichia stipitis* CBS 6054 as studied by ^{13}C nuclear magnetic resonance spectroscopy', *Appl. Environ. Microbiol.*, vol. 58, pp. 2552–2558, 1992.

[195] E. Lohmeier-Vogel and B. Hahn-Hägerdal, 'The utilization of metabolic inhibitors for shifting product formation from xylitol to ethanol in pentose

fermentations using *Candida tropicalis*', *Appl. Microbiol. Biotechnol.*, vol. 21, pp. 167–172, 1985.

[196] C. Leang, T. Ueki, K. P. Nevin, and D. R. Lovley, 'A Genetic System for *Clostridium ljungdahlii*: a Chassis for Autotrophic Production of Biocommodities and a Model Homoacetogen', *Appl. Environ. Microbiol.*, vol. 79, pp. 1102–1109, 2013.

[197] M. E. Pyne, M. Moo-Young, D. A. Chung, and C. P. Chou, 'Development of an electrotransformation protocol for genetic manipulation of *Clostridium pasteurianum*', *Biotechnol. Biofuels*, vol. 6, p. 50, 2013.

[198] J. D. Oultram, M. Loughlin, T.-J. Swinfield, J. K. Brehm, D. E. Thompson, and N. P. Minton, 'Introduction of plasmids into whole cells of *Clostridium acetobutylicum* by electroporation', *FEMS Microbiol. Lett.*, vol. 56, pp. 83–88, 1988.

[199] B. Molitor, K. Kirchner, A. W. Henrich, S. Schmitz, and M. A. Rosenbaum, 'Expanding the molecular toolkit for the homoacetogen *Clostridium ljungdahlii*', *Sci. Rep.*, vol. 6, 2016.

[200] G. Herrmann, E. Jayamani, G. Mai, and W. Buckel, 'Energy Conservation via Electron-Transferring Flavoprotein in Anaerobic Bacteria', *J. Bacteriol.*, vol. 190, pp. 784–791, 2008.

[201] W. Buckel and R. K. Thauer, 'Energy conservation via electron bifurcating ferredoxin reduction and proton/Na^+ translocating ferredoxin oxidation', *Biochim. Biophys. Acta BBA - Bioenerg.*, vol. 1827, pp. 94–113, 2013.

[202] L. Girbal *et al.*, 'Homologous and Heterologous Overexpression in *Clostridium acetobutylicum* and Characterization of Purified Clostridial and Algal Fe-Only Hydrogenases with High Specific Activities', *Appl. Environ. Microbiol.*, vol. 71, pp. 2777–2781, 2005.

[203] A. R. Archibald, J. Baddiley, and G. A. Shaukat, 'The glycerol teichoic acid from walls of *Staphylococcus epidermidis* I2', *Biochem. J.*, vol. 110, pp. 583–588, 1968.

[204] W. Andersch, H. Bahl, and G. Gottschalk, 'Level of enzymes involved in acetate, butyrate, acetone and butanol formation by *Clostridium acetobutylicum*', *Eur. J. Appl. Microbiol. Biotechnol.*, vol. 18, pp. 327–332, 1983.

Appendix

a. Plasmid maps

Maps for the most important plasmids used in this study are shown below.

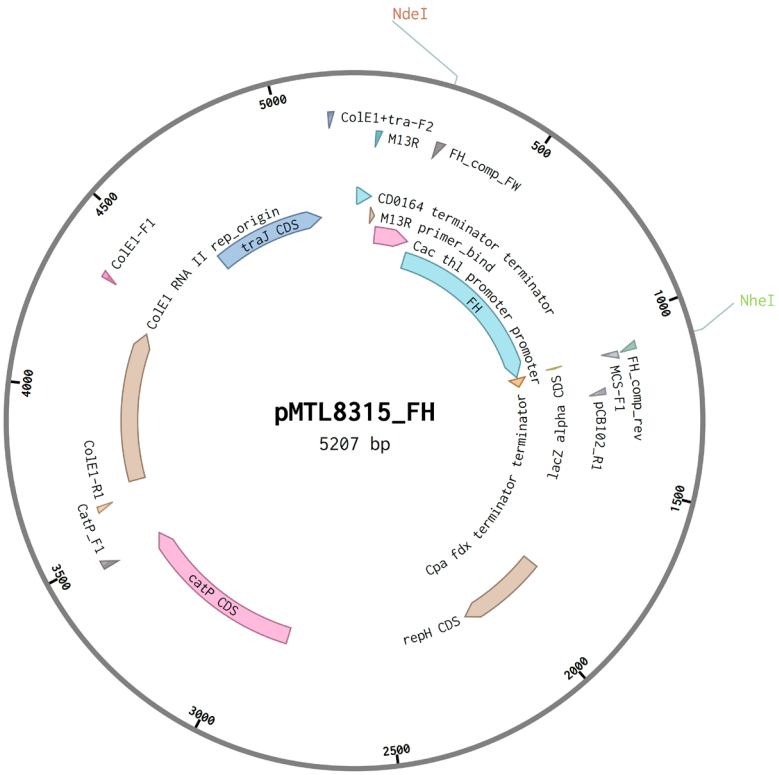


Figure A.1: Plasmid map pMTL8315_FH

Plasmid used for fumarate hydratase complementation. FH: fumarate hydratase gene from *C. autoethanogenum* (Clau1855); catP: chloramphenicol resistance cassette; P_{thl}: thiolase promoter from *C. acetobutylicum*.

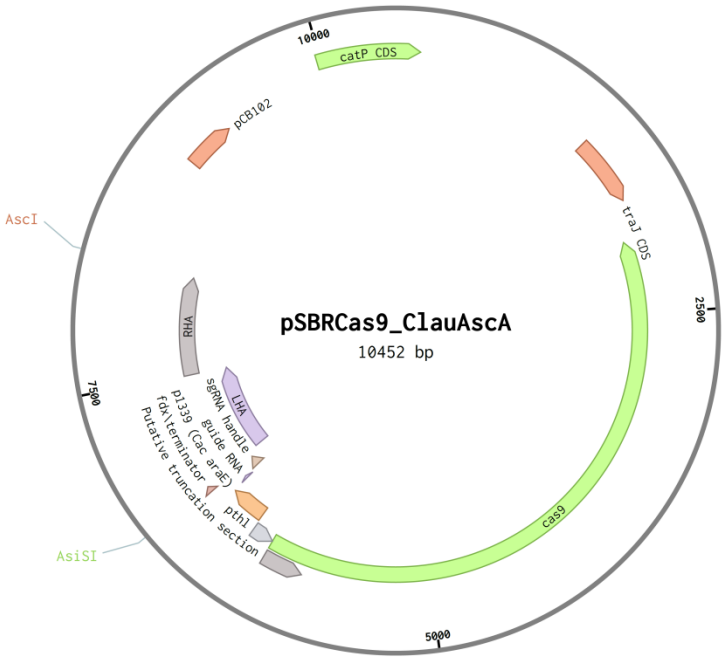


Figure A.2: Plasmid map for pSBRCas9_ClauAscA

Plasmid map for the plasmid used for CRISPR knockouts. RHA: Right homology arm; LHA: left homology arm; P_{thl}: thiolase promoter from *C. acetobutylicum*; catP: chloramphenicol resistance cassette. The guide RNA varied as three different guide RNAs were used.

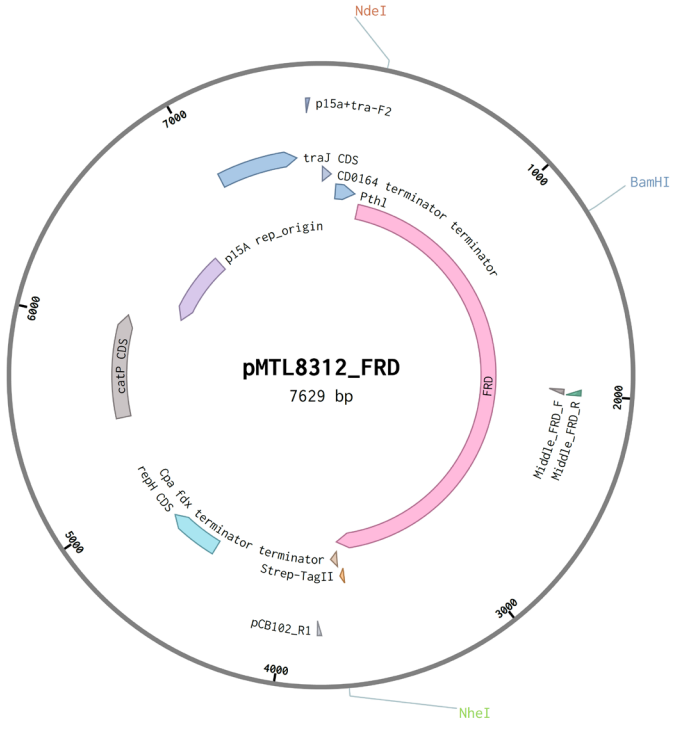


Figure A.3: pMTL8312_FRD.

Plasmid used for the introduction of a codon optimised fumarate reductase into *C. autoethanogenum*; FRD: fumarate reductase gene; P_{thl}: thiolase promoter from *C. acetobutylicum*; catP: chloramphenicol resistance cassette.

b. Codon optimised *frd* gene and protein sequence

The following shows the codon optimised gene and protein sequence for the introduced *T. brucei* FRD synthesised by Invitrogen *via* GeneArt® (ThermoFisher). The gene was synthesised in two fragments, gene 1 and gene 2. The genes were combined into the final, complete *frd* by restriction with BamHI, ligation and PCR.

Gene sequence ordered following codon optimisation:

Yellow marked sequence: Thiolase promoter from *C. acetobutylicum.*
Green marked sequences: Restriction enzyme sides; first to last: NotI, NdeI, BamHI, NheI.
The actual optimised gene starts after the NdeI and ends before the NotI restriction side.

GCGGCCGCACTAGCCCGCTTTTTAACAAAATATATTGATAAAAATAATAATAGTGGGTATAAT
TAAGTTGTTAGAGAAAACGTATAAATTAGGGATAAACTATGGAACTTATGAAATAGATTGAAA
TGGTTTATCTGTTACCCCACTAGTGTATCAAAATTTAGGAGGTTAGTTCATCATATGGTAGAT
GGAAGAAGTAGTGCAAGCATAGTAGCAGTAGATCCTGAAAGAGCAGCAAGAGAAAGAGATGCA
GCAGCAAGAGCATTATTACAAGATAGTCCTTTACATACTACTATGCAATATGCAACTAGTGGA
TTAGAATTAACTGTACCTTATGCATTAAAAGTAGTAGCAAGTGCAGATACTTTTGATAGAGCA
AAAGAAGTAGCAGATGAAGTACTTAGATGTGCATGGCAATTAGCAGATACTGTACTTAATAGT
TTTAATCCTAATAGTGAAGTAAGTTTAGTAGGAAGATTACCTGTAGGACAAAAACATCAAATG
AGTGCACCTTTAAAAAGAGTAATGGCTTGTTGTCAAAGAGTATATAATAGTTCTGCAGGATGT
TTTGATCCTAGCACTGCACCTGTAGCAAAAGCATTAAGAGAAATAGCACTTGGAAAAGAAAGA
AATAATGCATGTTTAGAAGCATTAACTCAAGCATGTACTTTACCTAATAGTTTTGTAATAGAT
TTTGAAGCTGGAACTATAAGTAGAAAACATGAACATGCAAGTCTTGATCTTGGAGGTGTAAGT
AAAGGATATATAGTAGATTATGTAATAGATAATATAAATGCAGCAGGATTTCAAAATGTATTT
TTTGATTGGGGAGGTGATTGTAGAGCAAGTGGAATGAATGCAAGAAATACTCCTTGGGTAGTA
GGAATAACTAGACCTCCTAGTTTAGATATGCTTCCTAATCCTCCTAAAGAAGCAAGTTATATA
TCTGTAATAAGTTTAGATAATGAAGCATTAGCAACTAGTGGTGATTATGAAAATTTAATATAT
ACTGCAGATGATAAACCTTTAACTTGTACTTATGATTGGAAAGGTAAAGAATTAATGAAACCT
AGTCAAAGTAATATTGCACAAGTAAGTGTAAAATGTTATAGTGCAATGTATGCAGATGCATTA
GCAACAGCATGTTTTATTAAACGGGATCCGGCAAAAGTAAGACAATTACTTGATGGTTGGAGA

TATGTAAGAGATACAGTAAGAGATTATAGAGTATATGTTAGAGAAAATGAAAGAGTAGCAAAA
ATGTTTGAAATAGCAACTGAAGATGCAGAAATGAGAAAAAGAAGAATATCTAATACTTTACCT
GCAAGAGTAATAGTAGTTGGAGGTGGATTAGCAGGATTAAGTGCAGCAATAGAAGCAGCAGGA
TGTGGTGCACAAGTAGTATTAATGGAAAAAGAAGCAAAACTTGGAGGAAATAGTGCAAAAGCA
ACTAGTGGAATAAATGGATGGGGAACTAGAGCACAAGCAAAAGCAAGTATAGTAGATGGTGGA
AAATATTTTGAAAGAGATACTTATAAATCTGGAATAGGTGGAAATACTGATCCTGCATTAGTA
AAAACTTTAAGTATGAAAAGTGCAGATGCAATAGGATGGCTTACTAGTCTTGGAGTACCTCTT
ACAGTACTTAGTCAACTTGGAGGACATTCTAGAAAAAGAACTCATAGAGCACCTGATAAAAAA
GATGGAACTCCTTTACCTATAGGATTTACTATAATGAAAACTTTAGAAGATCATGTAAGAGGA
AATTTATCTGGAAGAATAACTATAATGGAAAATTGTAGTGTAACTAGTTTATTAAGTGAAACT
AAAGAAAGACCTGATGGAACTAAACAAATAAGAGTAACTGGTGTAGAATTTACTCAGGCAGGA
TCTGGAAAAACTACTATTTTAGCAGATGCAGTAATACTTGCAACTGGTGGATTTAGTAATGAT
AAAACTGCAGATTCTTTATTAAGAGAACATGCACCTCATTTAGTAAATTTTCCAACTACTAAT
GGACCTTGGGCAACTGGTGATGGTGTAAAATTAGCACAAAGACTTGGAGCACAGCTTGTAGAT
ATGGATAAAGTACAACTTCATCCTACTGGACTTATAAATCCTAAAGATCCTGCAAATCCTACT
AAATTTCTTGGACCTGAAGCACTTAGAGGATCTGGTGGTGTATTACTTAATAAACAGGGAAAA
AGATTTGTAAATGAATTAGATTTAAGAAGTGTAGTAAGTAAAGCAATAATGGAACAAGGTGCA
GAATATCCTGGAAGTGGTGGAAGTATGTTTGCATATTGTGTACTTAATGCAGCAGCACAAAAA
CTTTTTGGAGTAAGTAGTCATGAATTTTATTGGAAAAAAATGGGATTATTTGTAAAAGCAGAT
ACTATGAGAGATTTAGCAGCATTAATAGGATGTCCTGTAGAAAGTGTACAGCAAACATTAGAA
GAATATGAAAGATTAAGTATAAGTCAAAGAAGTTGTCCTATAACTAGAAAAAGTGTATATCCT
TGTGTATTAGGAACTAAAGGACCTTATTATGTAGCATTTGTAACTCCTAGTATACATTATACT
ATGGGAGGATGTTTAATAAGTCCTAGTGCAGAAATACAAATGAAAAATACTAGTAGTAGAGCA
CCTTTAAGTCATAGTAATCCTATATTAGGACTTTTTGGAGCTGGAGAAGTAACTGGTGGTGTA
CATGGTGGAAATAGATTAGGTGGAAATTCTTTATTAGAATGTGTAGTATTTGGAAGAATAGCT
GGTGATAGAGCAAGCACTATATTACAAAGAAAAAGTAGTGCATTATCTTTTAAAGTATGGACT
ACTGTAGTACTTAGAGAAGTAAGAGAAGGTGGTGTTTATGGTGCAGGATCTAGAGTATTAAGA
TTTAATCTTCCTGGTGCATTACAAAGAAGTGGACTTAGTCTTGGACAATTTATAGCAATAAGA
GGTGATTGGGATGGACAGCAGCTTATAGGATATTATAGCCCTATAACTTTACCTGATGATTTA
GGAATGATAGATATATTAGCAAGAAGTGATAAAGGTACTTTAAGAGAATGGATAAGTGCATTA
GAACCTGGTGATGCAGTAGAAATGAAAGCATGTGGTGGACTTGTAATAGAAAGAAGATTATCT
GATAAACATTTTGTATTTATGGGACATATAATAAATAAATTATGTTTAATAGCTGGAGGAACT
GGTGTAGCACCTATGCTTCAAATAATAAAAGCAGCATTTATGAAACCTTTTATAGATACTTTA
GAATCTGTACATTTAATATATGCAGCAGAAGATGTAACTGAATTAACTTATAGAGAAGTATTA
GAAGAAAGAAGAAGAGAATCTAGAGGAAAATTTAAAAAAACTTTTGTACTTAATAGACCTCCT
CCTTTATGGACTGATGGTGTAGGATTTATAGATAGAGGAATATTAACTAATCATGTACAACCT
CCAAGTGATAATTTACTTGTAGCAATATGTGGACCTCCTGTAATGCAAAGAATAGTAAAAGCA
ACTTTAAAAACTTTAGGATATAATATGAATTTAGTAAGAACTGTAGATGAAACTGAACCTAGT
GGAAGTTAAGCTAGC

Protein sequence of the introduced *T. brucei* FRD:

MVDGRSSASIVAVDPERAARERDAAARALLQDSPLHTTMQYATSGLELTVPYALKVVASADTF
DRAKEVADEVLRCAWQLADTVLNSFNPNSEVSLVGRLPVGQKHQMSAPLKRVMACCQRVYNSS
AGCFDPSTAPVAKALREIALGKERNNACLEALTQACTLPNSFVIDFEAGTISRKHEHASLDLG
GVSKGYIVDYVIDNINAAGFQNVFFDWGGDCRASGMNARNTPWVVGITRPPSLDMLPNPPKEA
SYISVISLDNEALATSGDYENLIYTADDKPLTCTYDWKGKELMKPSQSNIAQVSVKCYSAMYA
DALATACFIKRDPAKVRQLLDGWRYVRDTVRDYRVYVRENERVAKMFEIATEDAEMRKRRISN
TLPARVIVVGGGLAGLSAAIEAAGCGAQVVLMEKEAKLGGNSAKATSGINGWGTRAQAKASIV
DGGKYFERDTYKSGIGGNTDPALVKTLSMKSADAIGWLTSLGVPLTVLSQLGGHSRKRTHRAP
DKKDGTPLPIGFTIMKTLEDHVRGNLSGRITIMENCSVTSLLSETKERPDGTKQIRVTGVEFT
QAGSGKTTILADAVILATGGFSNDKTADSLLREHAPHLVNFPTTNGPWATGDGVKLAQRLGAQ
LVDMDKVQLHPTGLINPKDPANPTKFLGPEALRGSGGVLLNKQGKRFVNELDLRSVVSKAIME
QGAEYPGSGGSMFAYCVLNAAAQKLFGVSSHEFYWKKMGLFVKADTMRDLAALIGCPVESVQQ
TLEEYERLSISQRSCPITRKSVYPCVLGTKGPYYVAFVTPSIHYTMGGCLISPSAEIQMKNTS
SRAPLSHSNPILGLFGAGEVTGGVHGGNRLGGNSLLECVVFGRIAGDRASTILQRKSSALSFK
VWTTVVLREVREGGVYGAGSRVLRFNLPGALQRSGLSLGQFIAIRGDWDGQQLIGYYSPITLP
DDLGMIDILARSDKGTLREWISALEPGDAVEMKACGGLVIERRLSDKHFVFMGHIINKLCLIA
GGTGVAPMLQIIKAAFMKPFIDTLESVHLIYAAEDVTELTYREVLEERRRESRGKFKKTFVLN
RPPPLWTDGVGFIDRGILTNHVQPPSDNLLVAICGPPVMQRIVKATLKTLGYNMNLVRTVDET
EPSGS

c. Intron sequences used for ClosTron mutants

Table A.1: Intron sequences used for ClosTron mutants

Orf name	Intron sequence	Intron position	bp gene	putative function
Clau_1855_1	TTATCCTTAGTTAGCAATCTCGTG CGCCCAGATAGGGTGTTAAGTCAA GTAGTTTAAGGTACTACTCTGTAA GATAACACAGAAAACAGCCAACCT AACCGAAAAGCGAAAGCTGATACG GGAACAGAGCACGGTTGGAAAGCG ATGAGTTACCTAAAGACAATCGGG TACGACTGAGTCGCAATGTTAATC AGATATAAGGTATAAGTTGTGTTT ACTGAACGCAAGTTTCTAATTTCG ATTCTAACTCGATAGAGGAAAGTG TCTGAAACCTCTAGTACAAAGAAA GGTAAGTTACAGAGATTGACT	48s	843	Fumarate Hydratase alpha subunit
Clau_1855_2	TTATCCTTAGTAGGCCAGGGGGTG CGCCCAGATAGGGTGTTAAGTCAA GTAGTTTAAGGTACTACTCTGTAA GATAACACAGAAAACAGCCAACCT AACCGAAAAGCGAAAGCTGATACG GGAACAGAGCACGGTTGGAAAGCG ATGAGTTACCTAAAGACAATCGGG TACGACTGAGTCGCAATGTTAATC AGATATAAGGTATAAGTTGTGTTT ACTGAACGCAAGTTTCTAATTTCG ATTCCTACTCGATAGAGGAAAGTG TCTGAAACCTCTAGTACAAAGAAA GGTAAGTTATACCCCTGGACT	300s	843	Fumarate Hydratase alpha subunit

d. Additional work during this thesis

Whilst working on the main thesis projects, additional work was done in cooperation with different departments inside and outside of the university. This work is briefly described in the following section.

i. Inhibition of the acetate kinase of *C. autoethanogenum*

One part of the GASCHEM project, undertaken by Alexander T. Wichlacz, was to synthesise and test acetate kinase activity inhibiting chemicals. For this, the acetate kinase (ACK) of *C. autoethanogenum* was purified and its enzyme activity analysed. For this, help was provided during the generation of the plasmid, cloning, enzyme purification and enzyme assays. Due to previous positive experience in overexpression and enzyme purification, it was decided to use the pT plasmid system [25][202]. The acetate kinase gene (Clau3275) of *C. autoethanogenum* was PCR amplified using the primers FW_ACK 5'-ccccGGATCCATGAAAATATTAGTAGTAAACTGT-3' and Rev_ACK 5'-GGGGCCCGGGTTTATTTTCAACTATTTCTTTTG-3'.

The *Strep*-TagII which was used for the purification was already available at the C-terminal end of the sequence in the pT plasmid. Therefore, during the design of the reverse primers, the stop codon TAA was deleted in order to attach the tag onto the tag encoding sequence.

The pT_ACK plasmid map is shown in Figure A.4. The PCR amplified gene was cloned into pT*HydA* (obtained from Girbal *et al.* [202]) using the restriction sides BamHI and Cfr9I. The purification of the protein was conducted *via Strep*-tagII affinity chromatography as described in 2.9.2.1. To

demonstrate successful protein purification, SDS-PAGE and Western Blot were performed. The purified protein was then used for later ACK enzyme assay analyses (2.9.3.5). However, only during cloning and the first protein purification and enzyme assays, help was given. The rest of the work, the synthesis and analysis of the specific inhibitors, was done by A.T. Wichlacz.

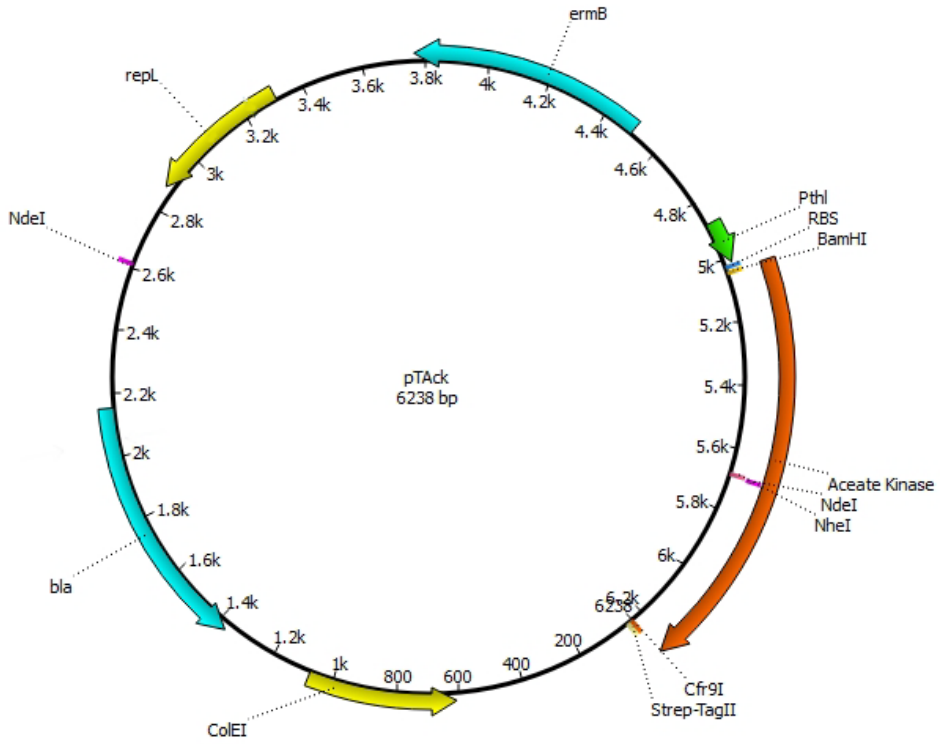


Figure A.4: Plasmid map of pTAck.

Plasmid map used for the expression in *E. coli* cells and overexpression of the *ack* gene. Bla: ampicillin resistance cassette; ermB: erythromycin resistance cassette; P_{thl}: Thiolase promoter from *C. acetobutylicum*; RBS: Ribosome binding side.

ii. Isolation of teichoic acid from *C. autoethanogenum* cells

In order to support the GASCHEM project and to get more accurate mathematical and genome scale models for *C. autoethanogenum*, the bacterium was analysed with respect to its protein, genomic DNA, RNA, lipid, polysaccharide and teichoic acid content by various members of the GASCHEM group. This work also provided a value for biomass production for *C. autoethanogenum* of 0.34 g l^{-1} OD^{-1} which was used for biomass and carbon balance calculations in this study.

For analysis of the teichoic acid content of *C. autoethanogenum*, the method after Archibald was used [203]. For this, 250 ml of *C. autoethanogenum* culture were centrifuged at 4000 rpm for 15 min at 4 °C. The gained cells were then lysed using 5 ml of 1 x BugBuster solution and 1 mg lysozyme. The mix was left shaking at RT for 20 min at 25 rpm. Afterwards, the lysed cells were centrifuged at 4 °C, 7000 rpm for 20 min, the gained pellet was washed with 100 mM sodium phosphate buffer (pH 7) and freeze dried over night. This resulted in 186 mg of cell wall material. The material was dissolved in 20 ml of 10 % (w/v) trichloracetic acid and stirred at 4 °C for 24 h. The mix was afterwards centrifuged at 7000 rpm, 4 °C for 15 min and the supernatant immediately mixed with 20 ml ice-cold ethanol. The resulting mixture was kept at 4 °C until later use. Further 20 ml of 10 % trichloracetic acid were used to dissolve the pellet and stirred at 4 °C for 48 h. Then, the mix was centrifuged again at 7000 rpm and 4 °C for 20 min and the resulting supernatant added to 20 ml ice cold ethanol. Both supernatants mixes were joined together and their precipitants dissolved in 5 ml of 10 % trichloracetic acid. The insoluble material was removed *via* centrifugation and 20 ml ice cold ethanol added to the supernatant. This mix was then centrifuged

again for a last time for 15 min at 4 °C and 7000 rpm. The teichoic acid precipitated as a fine powder which was weighted. Out of 186 mg of cell wall material, 1.4 mg of teichoic acid could be isolated. This result, amongst the other biomass information, is used for a publication regarding biomass and metabolic models of *C. autoethanogenum* (by Rupert Norman, University of Nottingham, in progress).

iii. Crystallisation of the PduL protein of *Moorella thermoacetica*

During studies for the degree of Master of Science at the University of Rostock it was found that the gene moth1181 encodes for an enzyme with phosphotransacetylase (PTA) activity, even though no similarities to confirmed PTAs were found for its protein sequence. These finding resulted in the 2016 published paper "Two propanediol utilization-like proteins of *Moorella thermoacetica* with phosphotransacetylase activity" by Breitkopf *et al.* [25]. Due to the start of the PhD project at the University of Nottingham in November 2013, further interesting analyses regarding this protein were done by a successor. However, since the University of Nottingham and more specifically, the Centre for Biomolecular Science building, has a group which is specialised in analysing protein structures, it was agreed that some additional work, in order to obtain more facts about this protein, could be done in Nottingham. Therefore, the protein PduL2, which is encoded by moth1181, was expressed in *E. coli* BL21(DE3) cells and purified *via Strep*-tagII purification. The protein then was freed from salts and concentrated to 11 mg/ml in order to undertake protein crystallisation. Protein crystals of PduL protein in *apo* form were obtained in 2.0 M ammonium sulfate and 0.1 M Bis-

Tris buffer, pH 5.5. Protein crystals with bound substrate (CoA) were formed in 0.2 M Lithium-acetate, 2.2 M ammonium sulfate buffer. The crystals were analysed by Dr. Purushotham Selvakumar and Dr. Ingrid Dreveny from the University of Nottingham.

Furthermore, the involvement of specific amino acid residues in the active side of the enzyme was studied by the analysis of the enzyme activity of a set of proteins with site specific mutations. Mutants were generated at the University of Rostock, the enzyme activity measured at the University of Nottingham.

Enzyme activities of both the wild type and the mutated proteins, were measured in the physiological direction according to Andersch *et al.* (1983) as described in Breitkopf *et al.*, 2016. In brief, generation of acetyl phosphate was measured by monitoring the release of free coenzyme A as an increase in absorbance at 412 nm caused by the formation of a thiolate anion out of 5,5′-dithiobis(2-nitrobenzoic acid) (DTNB) after reaction with a sulfhydryl group of coenzyme A. Reaction mixtures contained 0.1 M potassium phosphate (KP) buffer (pH 7.6), 10 µl 6 mM acetyl-CoA, 4 µl 1 M DTNB (working concentration 40 mM) and purified protein. The extinction coefficient (ε) used for calculating the specific activity was 13.6 cm2/µmol [204].

Figure A.5 shows the obtained crystal structure of the protein. The following tables state the mutated enzymes with one altered amino acid residue (Table A.2) and the obtained PTA enzyme activities for the respective mutated enzymes (Table A.3).

The stated results are about to be published.

Table A.2: Mutated enzymes with one altered amino acid residue.

Amino acid and position in *Moth1181* gene	Codon in *M. thermoacetica*	Amino acid substitution to…	Codon in *E. coli*
His_{16}	CAT	Ala_{16}	GCG
His_{18}	CAC	Ala_{18}	GCG
Arg_{65}	CGT	Ala_{65}	GCG
Arg_{71}	CGG	Gln_{71}	CAG
Glu_{77}	GAA	Ala_{77}	GCG
Ser_{95}	TCT	Ala_{95}	GCG
His_{127}	CAC	Ala_{127}	GCG
His_{172}	CAC	Ala_{172}	GCG

Table A.3: PTA enzyme activities of mutated enzymes.

Amino acid change in *Moth1181* gene	Relative PTA activity [%]
No change (WT)	100
$His_{16}Ala$	0
$His_{18}Ala$	0
$Arg_{65}Ala$	21.12
$Arg_{71}Gln$	0.16
$Glu_{77}Ala$	0.14
$Ser_{95}Ala$	72.5
$His_{127}Ala$	0.21
$His_{172}Ala$	0.04

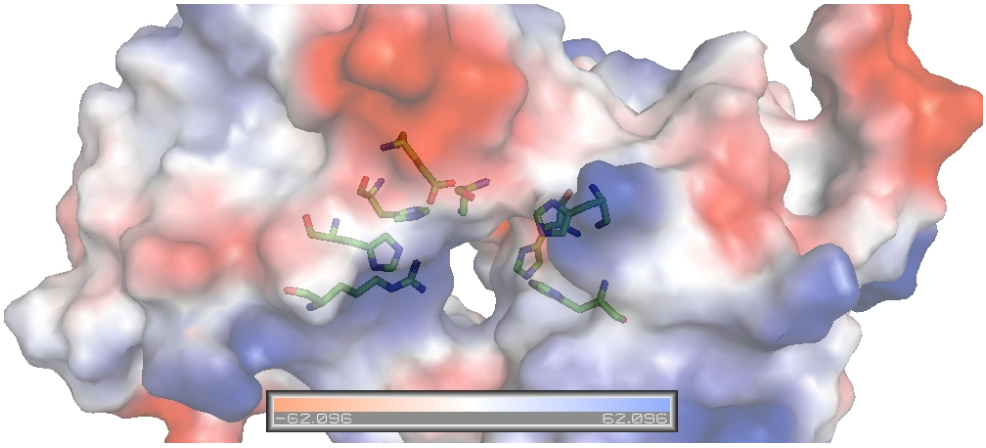


Figure A.5: Crystal structure of PduL2.

Crystal structure of PduL2 (Moth1181) analysed by Dr. Purushotham Selvakumar.